SKB

TECHNICAL REPORT

92-31

The Äspö Hard Rock Laboratory: Final evaluation of the hydrogeochemical pre-investigations in relation to existing geologic and hydraulic conditions

John Smellie[1], Marcus Laaksoharju[2]

[1] Conterra AB, Uppsala, Sweden
[2] GeoPoint AB, Stockholm, Sweden

November 1992

THE ÄSPÖ HARD ROCK LABORATORY: FINAL EVALUATION OF
THE HYDROGEOCHEMICAL PRE-INVESTIGATIONS IN RELATION
TO EXISTING GEOLOGIC AND HYDRAULIC CONDITIONS

John Smellie[1], Marcus Laaksoharju[2]

1   Conterra AB, Uppsala, Sweden
2   GeoPoint AB, Stockholm, Sweden

November 1992

THE ÄSPÖ HARD ROCK LABORATORY: FINAL EVALUATION OF THE HYDROGEOCHEMICAL PRE-INVESTIGATIONS IN RELATION TO EXISTING GEOLOGIC AND HYDRAULIC CONDITIONS.

John Smellie,
Conterra AB,
Uppsala.

Marcus Laaksoharju,
GeoPoint AB,
Stockholm.

Foreword

This report represents a detailed on-going complement to earlier hydrogeochemical studies carried out at Äspö. Although not all data were then available, the overall hydrogeochemical trends, classifications and interpretations reported, in particular by Laaksoharju (1988, 1990a), Tullborg and Wallin (1991) and Wikberg et. al. (1991), have been largely supported and confirmed by this present evaluation. The general picture has only become more focused. Hydrogeochemical predictions at depth (Wikberg et. al. 1991), prior to construction of the Äspö Hard Rock Laboratory (HRL), have also been shown to be largely valid, at least based on present information. Excavation of the laboratory will be the ultimate arbitrary as to the success of these predictions.

The main thrust of this present evaluation, in addition to supporting earlier results and predictions, has been to assess the quality of the groundwaters and their chemistry. In order to evaluate and model the hydrogeochemistry of any system and to distinguish between natural variation and unnatural deviation, the quality and unbiased nature of the sampling, the natural hydraulic conditions, the geological surroundings and the analytical accuracy and precision etc., must all be addressed. This need for a multidisciplinary approach to groundwater evolution and modelling is demonstrated. The evaluated data are used to describe groundwater evolution, to describe the origin of the groundwater, to construct a conceptual groundwater flow model for Äspö, and to relate the Äspö studies to the wider perspective of other similar site investigations in Fennoscandia.

The report has been organised to compile existing and new analytical data and to provide an updated status on hydrogeochemical analysis and interpretation for Äspö. However, since Äspö is a large on-going research project, new data have become available during the writing of the report. To distinguish between the various data already reported and interpreted elsewhere, all sources are referenced where possible.

CONTENTS.

EXECUTIVE SUMMARY.

Introduction.

The Swedish Nuclear Fuel and Management Company (SKB) is currently excavating the access tunnel to an underground experimental laboratory, the Äspö Hard Rock Laboratory, planned to be located some 500 m below the island of Äspö which is located in the Simpevarp area, southeast Sweden. The construction of an underground laboratory forms part of the overall SKB strategy to test, not only the construction techniques for deep excavation, but also the various methods and protocols required to obtain a three-dimensional model of the geology and groundwater flow and chemistry, within a fractured crystalline bedrock similar to that envisaged for the final disposal of spent fuel. Äspö was chosen because it geologically represents a variety of typical crystalline bedrock environments.

The hydrogeochemical activities described and interpreted in this report form part of the initial Pre-investigation Phase (from the surface to around 1000 metres depth) aimed at siting the laboratory, describing the natural hydrogeological and hydrogeochemical conditions in the bedrock and predicting the changes that will occur during excavation and construction of the laboratory. Hydrogeochemical interpretation has therefore been closely integrated with the hydrogeological investigations and other disciplines of major influence, in particular, bedrock geology and geochemistry and fracture mineralogy and chemistry.

A large section of this report has been devoted to the detailed investigation of each individual zone hydraulically selected, tested and sampled for hydrogeochemical characterisation. The main objective was to establish the reliability or representativeness of each groundwater collected, in relation to the bedrock level sampled. Only by achieving a set of representative groundwater samples and hence a reliable set of chemical analyses, can some of the detailed hydrogeochemical studies be carried out.

The data have been used to describe the chemistry and origin of the Äspö groundwaters, models have been developed to illustrate groundwater mixing and standard geochemical modelling approaches have been employed to understand rock/water interaction processes. An attempt has been made to integrate the hydrogeochemical information with known geological and hydrogeological parameters to construct a conceptual groundwater flow model for the island.

General geology and hydrogeology.

The island of Äspö comprises a slightly undulating topography (10 m a.s.l) of well exposed rock. The geology is characterised by a red to grey porphyritic granite-granodiorite of Småland type, containing microcline megacrysts up to 1 to 3 cm in size. To the south of the island a redder granite variety, the Ävrö "true" granite, outcrops, containing small (<1 cm) sparsely distributed microcline megacrysts. Within the granite are east-west trending lenses/sheets of fine-grained greenstone (metabasalt) which are usually strongly altered. Subordinate lenses of fine-grained grey metavolcanites (of dacitic composition) also occur. Both of these rock types predate the Småland granite. Finally, small occurrences of pegmatite commonly occur as very narrow dykes (decimetres in size).

Structurally, the island is divided into two main blocks by an NE-trending regional shear zone (EW-1). In both blocks the Småland granite, with associated greenstones and fine-grained granite/aplite varieties, dominates, although in the southern block below 300 m, more basic dioritic varieties of the Småland granite begin to dominate.

The EW-1 shear zone, which is vertical to subvertical to the north, consists of strongly foliated heterogeneous Småland granite containing a large number of mylonitic lenses and greenstone xenoliths. Highly fractured zones (5-10 m wide), alternating with more normally fractured rock, complicate the shear structure which has also undergone substantial weathering, seen as oxidation of magnetite to hematite and Fe-oxyhydroxides. This explains the negative aeromagnetic anomally.

The northern block is more fractured than its southern counterpart; in both cases the fractures are vertical to sub-vertical in orientation. One important group of discontinuous subhorizontal zones occurs at depths of 300-500 m.

The main fracture filling mineral phases consist of, in decreasing order of frequency: group A (chlorite, calcite), group B (hematite, Fe-oxyhydroxides, epidote, fluorite), and group C (pyrite, magnetite, laumonite/prehnite, gypsum).

The aerial distribution of hydraulic conductivity at Äspö on the site scale is heterogeneous. Generally the fine-grained granite/aplite tends to be the most conductive unit, probably because it is the most competent rock type and is therefore inclined to fracture easily in response to tectonic movement. The increased fracture frequency in the northern block of Äspö reflects a correspondingly higher hydraulic conductivity. Furthermore, there is also a general decrease in the variability of hydraulic conductivity with depth. There is a significant increase in conductivity at depths between 100-200 m and 400-500 m, which may correspond to the vertical distances separating gently dipping subhorizontal hydraulic fracture zones.

Recharge/discharge and groundwater flow through Äspö is controlled by the major

tectonic fractures and discontinuities with a general groundwater flow trend, at least in the upper 500 m or so, from south to north, facilitated by the NNW-trending vertical to subvertical fractures. The major E-W trending shear zone is a strong recharge feature.

Groundwater Quality.

The Äspö groundwaters are classified as "representative" or "not representative" based on the presence or absence of tagged borehole activity water and tritium, and on the groundwater extraction pump rates used (Table A). In some borehole sections the extraction pump rate, chosen to conduct downhole hydraulic interference tests, was based on hydraulic rather than hydrogeochemical criteria. Consequently, and depending on the hydraulic properties of the interconnected conductive zones, groundwaters are being removed which are a mixture of waters from varying levels and origins in the bedrock. The correlation between high extraction rates and a non representative groundwater sample is of no great surprise at Äspö. From the hydraulic investigations several large-scale water conducting fractures control the groundwater flow through the island. Interference tests have shown the interconnection between these zones, some recharging (e.g. EW-1 and the NNW-trending vertical to subvertical fracture zones), some discharging (e.g. subvertical zone NE-1). In addition, at high flow rates it is not possible to accurately measure important parameters such as the redox potential.

Treated individually, the data evaluated from these Äspö studies may not appear too promising. However, from the detailed borehole section studies reported, it is possible to know with reasonable certainty the origin of the groundwaters especially at lower extraction rates (<500 mL/min), that have been short-circuited from other bedrock levels. This has played an important role in establishing the levels of groundwater mixing and also in explaining some of the discrepancies (i.e. pH and Eh) in the water/rock and chemical equilibrium modelling. At high extraction rates (>500 mL/min) this detective work is more difficult, but nevertheless the major ion fluctuations have been extremely useful in helping to construct the conceptual groundwater flow model of the island.

This study helps to underline the difficulty in having to judge the quality of a sample. An anomalous value can indicate contamination, but depending on the initial concentration and the hydrogeochemical environment, the disturbance may have been nullified by natural chemical reactions in the bedrock prior to sampling. Of the many variables measured, elements at low concentration and particularly the redox sensitive values, tend to be the most sensitive to perturbations, whilst other variables show little change. A degree of uncertainty always hangs over samples collected for analysis; the only way to increase the level of reliability and confidence is to minimise any disturbance to the natural groundwater system prior to, and during, groundwater sampling.

Table A: Classification of sampled groundwaters from Äspö.

Borehole /section (m)	Representative		Not Representative			
	A	B	C	D	E	F
KAS02						
202–214.5	x					
308–344	x					
314–319		x				
463–468			x			
530–535	x					
802–924		x				
860–924		x				
KAS03						
129–134	x					
196–223				x	x	
248–251		x				
347–374		x				
453–480				x	x	
609–623					x	
690–1002				x	x	
860–1002	x				x	
KAS04						
226–235			x			x
334–343	x					
440–481			x			
KAS06						
204–277				x		x
304–377	x					
389–406				x		
439–602				x		x
HAS13						
0–100				x		x

A= Representative groundwater for the sampled isolated level (Assumed limited sampling radius because of the low extraction pump rates: <200 mL/min).

B= Representative groundwater for the sampled isolated level (Assumed large sampling radius because of the high extraction pump rates: 1500 to 18800 mL/min).

C= Non-representative groundwater at low extraction pump rates.

D= Non-representative groundwater at high extraction pump rates.

E= Containing borehole activity water (>1% uranine).

F= Containing a young (<45 a) groundwater component (>2 TU).

Hydrogeochemical evolution of the groundwaters.

Considerable effort has been made to ensure an acceptable level of quality control for groundwater analysis. All reported data, unless otherwise stated, have charge imbalance errors within 4%, the majority lying within 2-3%. All hydrogeochemical data, together with data from all related disciplines, are stored in the GEOTAB database and are easily accessible.

<u>Major Chemical Trends.</u>

The Äspö groundwaters are shown to be mainly reducing (available Eh data record values of -250 to -320 mV; nearly all the total iron is in the ferrous state; sulphide is mostly present in small quantities from 0.02 to 1.10 mg/L; total dissolved uranium is very low ranging from 0.08-0.58 µg/L), moderately alkaline (pH from 7.3-8.3 units), and changing from a Na-Ca(Mg) HCO_3-Cl type at the near-surface (0-150m), through a Na-Ca(Mg) Cl-HCO_3 type at depths of 150-300 m, to a Na-Ca(Mg) Cl-SO_4 type at depths of 300-800 m, and finally the deepest, most saline waters are of Ca-Na(Mg) Cl-SO_4 type occurring from below approx. 800 m (Fig. A).
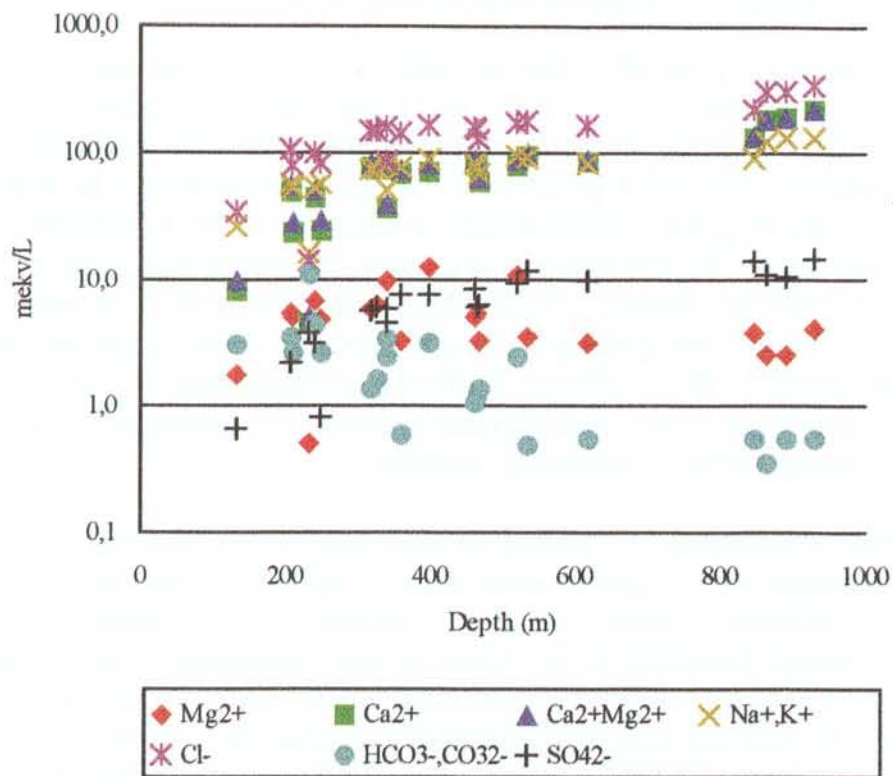
Figure A: Modified Shoeller plot showing major ion trends with depth.

Increasing with depth are Cl, Br, Na, Ca, SO_4, Sr and Li, i.e. constituents which can be derived from water/rock interaction during long residence times in the bedrock. Decreasing are HCO_3, Mn, Mg, $Fe_{(tot)}$, $Fe_{(II)}$ and TOC, i.e. constituents influenced by reactions occurring in the soil cover and in the upper part of the bedrock where conditions are oxidising and the pH is low. Decreasing $Fe_{(tot)}$ and $Fe_{(II)}$ with depth is caused by changes in the overall redox system. A pH increase may also result in oversaturation and co-precipitation of iron minerals. Finally, those constituents which are considered more or less constant, include SiO_2, Al, K, F, PO_4, I, NO_2 and NO_3.

It is important, however, to bear in mind that these depth-dependent subdivisions are only approximate; in reality highly saline groundwaters can be found within 50 m from the bedrock surface, whilst in other cases waters with a recognisable near-surface component can be detected at least down to 300 m. The distribution of groundwater chemistry is very heterogeneous when Äspö is considered as a whole. If only the conducting fracture zones are considered, i.e. where the majority of water samples have been sampled, then the groundwaters tend to have more uniform compositions because they obtain their character through mixing along fairly rapid conductive flow paths, i.e. mainly determined by the hydraulic gradient, rather than by chemical rock/water interaction. Thus, in the knowledge that most of the samples have been taken from water conducting fractures, the above general subdivisions are broadly true.

Redox Conditions and the Geochemical Behaviour of Uranium.

The groundwaters are generally reducing with maximum values ranging from -250 to -320 mV and pH ranges from 7.3 to 8.3 units; the reducing conditions are supported by almost all the iron being in the ferrous state and often only small amounts of detectable sulphide. The redox potential of the Äspö groundwaters is largely determined by the $Fe_{(III)}$-$Fe_{(II)}$ redox couple. Using this couple to calculate theoretical redox potential values for the groundwaters, and comparing them with the in situ field Eh measurements, showed a reasonably good correlation. Low redox potentials appear to be achieved very quickly in the groundwaters, which indicates that even at very shallow depths (~50 m) efficient buffering reactions must be occurring within the conducting fracture zones (and adjacent bedrock?) to ensure such a rapid drop in the redox potential during groundwater recharge.

The geochemical behaviour of uranium is very much redox dependent, in addition to the total concentrations of ligands which form complexes of relative strength with uranium in its different oxidation states, i.e. carbonate, biophosphate etc. Further to the Eh redox trends described above, there are also consistently low uranium contents (apart from two samples) in the groundwaters, where values range from 0.08-0.72 µg/L. These low contents also support reducing conditions. Low dissolved uranium usually relates to high $^{234}U/^{238}U$ activity ratios, the latter often reflecting near stagnant conditions required to allow the build-up of excess ^{234}U from recoil effects. At Äspö the $^{234}U/^{238}U$ activity ratios are high to very high, ranging from 2.6-7.2.

Calculations to show the relationship between the measured Eh and uranium geochemistry show that the main solubility limiting phases are crystalline uraninite (UO_2) and the more amorphous U_4O_9 phase. These uranium oxide phases are very difficult to identify mineralogically in the fracture zones; they exist probably as very small discrete crystals (uraninite) and as surface coatings (the more amorphous types) probably in close association with the micaceous (chlorite) and hematite/Fe-oxyhydroxide phases.

Groundwater Evolution.

Fracture mineral studies within the upper 0-350 m of Äspö partly support the premise that hydrogeochemical changes appear to follow the normal evolutionary trend in fractured conductive Swedish crystalline rocks, i.e. an uppermost horizon with a paucity of calcite, a lower horizon characterised by the precipitation of calcite, and finally the lowermost horizon where calcite is by and large absent. These horizons generally correspond to depths of approx. 0-40 m, 40-250 m and finally 250m downwards. This depth penetration of near-surface derived groundwater is clearly supported by comparing other surface-sensitive parameters such as pCO_2, TOC, HCO_3 and tritium.

At greater depths, however, normal evolutionary chemical trends become less clear. This is mostly a function of increasing salinity which commonly exceeds 10 000 mg/L at and below 800 m. These saline waters are interpreted as representing a separate, deep, possibly regional groundwater system, which is almost stagnant except when intercepted by deeply penetrating conducting fracture zones, which locally encourage partial mixing with upper, near-surface derived more dynamic groundwater systems. Groundwater mixing, and the associated hydrogeochemical repercussions, was therefore a major process addressed in order to interpret the chemical evolution of the Äspö groundwaters. The large-scale recharging EW-1 shear zone, because of its well constrained geometry, available hydraulic data and the fact that the hydrogeochemistry is well known from several intersecting percussion drilled boreholes, proved an ideal location to carry out these mixing calculations.

Mixing of the groundwaters is relatively simple to model with regards to the chloride content, the most conservative ion present and the most concentrated, as demonstrated by applying a simple two-component Cl mixing model for each borehole. For the other major ions present in smaller amounts, such as Na, Ca, HCO_3 and SO_4, the model indicates some marked deviations from ideal mixing, which suggests that other processes must be contributing to the chemistry within this mixing interval to account for the elemental deviations registered. These ionic distribution patterns underline, once again, the three main hydrogeochemical categories: shallow mixed (0-250 m), intermediate mixed (250-600 m) and deep (>800 m).

According to the mixing model, the interface between shallow and intermediate is characterised, in particular, by an increased relative deviation from ideal mixing for

Ca, K and SO_4 and a decreased relative deviation for HCO_3; Na usually shows an antipathetic relationship to Ca. The interface between intermediate and deep shows a continued increase in the relative deviation for Ca, but no change in SO_4 or K. In contrast with the previous interface, however, HCO_3 shows a marked increase, whilst both Na and Mg decrease. To explain these deviations, two main water/rock mechanisms are generally invoked, mineral precipitation/dissolution and ion exchange.

To address the precipitation/dissolution hypothesis, mineral equilibrium calculations (using PHREEQE) were carried out using a realistic mineral database founded on actual mineralogical observations. These calculations show that positive mineral saturation indices indicate close saturation or a slight oversaturation with respect to quartz, fluorite, laumonite and calcite; this essentially reflects the phases identified from the fractures. In contrast gypsum is always undersaturated, which supports the small amounts recorded from the fractures, and that pyrite (only sporadically present) is generally (but not always) oversaturated. Evaluation of the hematite and Fe-oxyhydroxide phases (locally highly represented), which can be either strongly over- or under-saturated, is complicated by their sensitivity to the Eh input (i.e. reliability of the field measurements) and/or inadequacies in the thermodynamic database.

In conclusion, the data do not clearly correlate with a systematic sequence of mineral dissolution/precipitation necessary to explain the observed chemical trends down to 1 000 m. Calcite instability can explain some of the Ca trends in the uppermost 300 m or so, but the steady increase of Ca and sympathetic decrease of Na with depth needs an alternative mechanism. The hydrothermal breakdown of plagioclase, associated with albite recrystallisation is a mechanism favoured to explain the present day increase in Ca and depletion of Na with increasing depth in other areas of Fennoscandia. Mineral chemistry (microprobe) and textural relationships at Äspö support this reaction, where plagioclase of oligoclase composition has been progressively altered to albite with subsidiary muscovite/sericite and calcite.

To address the ion exchange hypothesis, the relevant exchange ions (Na, Ca, K and Mg) were compared to chloride to try and obtain a clear picture of trends in the water chemistry related to seawater dilution, and to limit the number of possible options open for interpretation. Sodium, the most dominant ion after Cl, shows close similarities with the seawater dilution line in the upper 200-250 m but is markedly depleted relative to seawater at greater depths. Calcium shows a strong enrichment relative to seawater and Mg and K show depletion. These trends thus infer the possibility that when seawater enters a freshwater aquifer, ion exchange processes remove Na, K and Mg from the seawater in exchange for Ca.

Sulphate, when compared to Cl, initially shows a congruent trend with seawater at shallower depths and depletion relative to seawater dilution at greater depth. This depletion would suggest that bacterial sulphate reduction might be occurring in the saline groundwaters. Sulphur isotope studies (and the detectable odour of H_2S)

conducted in groundwater samples from Laxemar, located adjacent to Äspö, would appear to support this process. Since the saturation index for gypsum is undersaturated in all samples, gypsum precipitation does not play a role in affecting the sulphate concentrations.

In summary, whilst the application of both mineral dissolution/precipitation and ion exchange processes to explain the observed hydrochemical trends at Äspö have been partly successful, some important areas of uncertainty still remain. In common with other Fennoscandian environments, model calculations indicate that cation exchange is insufficient to account for the change in water chemistry, assuming that there is an intrusion of seawater into freshwater aquifers. In addition, the general lack of widespread clay mineral occurrences in the bedrock at Äspö (usually only represented locally) would tend to reduce the ion exchange capacity of the system. In contrast, there is some evidence that mineral stabilities may possibly explain the increasing Ca/Na ratio with depth. These reactions, however, which incorporated meteoric-derived waters, occurred deep in the bedrock under hydrothermal conditions during much younger periods in the geological history of the granite. Subsequent mixing with additional meteoric groundwaters (and fluids derived from other sources) may have resulted in present day compositions and Ca/Na signatures.

Isotope geochemistry and origin of the groundwaters.

Stable and Radioisotope Features.

Stable isotope plots of the Äspö groundwaters, and comparison with near-surface waters from both Äspö and Laxemar and present day Baltic seawater, show that all samples plot below the global meteoric line and there is a large spread of isotopic values ($\delta^{18}O$ from -15.8 to -7.2‰ and δD from -124 to -62‰). The groundwaters are clearly meteoric related in origin; the position of the samples below the meteoric line, i.e. indicating small enrichments in $\delta^{18}O$, or depletions in δD, is usually interpreted as indicating surface water evaporation effects, for example, in enclosed basins or inland seas. Similar isotopic trends have been reported from other areas in Fennoscandia.

Initially, the Äspö stable isotopic data appear to lack any kind of overall consistency. Some samples show a degree of affinity with modern Baltic waters, others with near-surface fresh/brackish waters, and of the remainder, the highly saline varieties tend to cluster around the -13.2 to -12.5‰ $\delta^{18}O$ interval and somewhat closer to the global meteoric line. Another feature is the quite regular trend to heavier isotope values with increasing depth along the recharging EW-1 zone. This trend has been interpreted as indicating an ancient marine/glacial melt water.

In terms of relative age, the Baltic seawater/near-surface waters should represent the most recent, youngest water component, the deep saline waters should be among the oldest, and the remainder should be of intermediate age due to the natural hydraulic and imposed mixing processes. Although not many radiocarbon data are available, there are enough to generally support these trends.

The $^{234}U/^{238}U$ activity ratios for the Äspö groundwaters are high to very high (2.6 to 7.2) showing widespread isotopic disequilibrium in the groundwaters due to excess ^{234}U caused by rock/water interaction processes. This ^{234}U excess is caused by the ingrowth of ^{234}U due to the solution of alpha-recoil ^{234}Th at the rock/water interfaces during the permeation of groundwater through the bedrock. The inference, therefore, is that the groundwaters are moving sufficiently slowly through the bedrock so as to allow a ^{234}U excess to accumulate. The high activity ratio values which characterise the Äspö groundwaters, are an indication that long residence times are occurring, thus supporting very low groundwater flow rates.

In summary, the Äspö stable isotopic data indicate five different groupings: a) modern Baltic seawater (0-50 m; recent), b) fresh/brackish near-surface water (0-200 m; recent), c) deep saline water (>800 m; ancient), d) brackish water collected at low extraction rates from less conductive, more massive rock units (100-250 m; ancient), e) water representative of the "fracture matrix" (>250 m; intermediate to ancient), and f) various mixing components (0-500 m; intermediate age), especially between type (e) and type (b), caused by excessive extraction rates coupled with short-circuiting between the sampled borehole section and the surface bedrock horizons. This is in close accordance with the hydrogeochemical data and supported by the groundwater mixing models.

Saline Groundwater.

Most reported samples of saline groundwaters seem to represent mixtures of meteoric water with a highly concentrated brine, which may be an ancient relict seawater or fluids genetically linked to geochemical processes occurring over long periods of geological time in the bedrock (e.g. rock/water interaction). This description best describes the major groundwater types found in much of the Fennoscandia Shield area peripheral to the Baltic Sea.

Two major types of saline water occur at Äspö; marine-derived (0-500 m) and deep Ca-rich brines (>800 m). The geochemistry and stable isotope signatures of the former type have been compared to other investigated areas located peripheral to the Baltic sea, e.g. Hästholmen, Forsmark, Finnsjön, where influence from both modern Baltic water and ancient Litorina water (7 400-2 500 BP) might be expected. With regard to the Äspö (i.e. those waters characterised by a dominant marine signature), it is postulated that the majority of the waters to depths of 500 m are similar to those of Finnsjön. These Finnsjön waters, although still considered to be coastal marine in origin (i.e. lying within the maximum extent of the Litorina Sea

transgressions), have been significantly modified by water/rock interactions and by other salt water sources. Younger waters, of greater marine signature and similar to Hästholmen and Forsmark, also occur, but are subordinate.

The origin of saline waters prior to the Weichselian glacial period of ca. 20 000 BP is unknown, but the salinity may have derived from many possible sources which include accumulated residual igneous/metamorphic fluids, limited water/rock interactions, fluid inclusions and other unknown saline sources. These saline waters were then modified by dilution and mixing with infiltrating rain/glacial melt waters prior to, during, and subsequent to the Weichselian ice sheet, and to the more recent Yoldia and Litorina Sea transgressions ca. 10 000 and 7 500 BP ago. Perhaps some subordinate seawater freezing has also contributed to increasing salinity during these glacial epochs. In any case, these processes have resulted in a continuous change of groundwater isotopic signatures such as $\delta^{18}O$ and percentage modern carbon. Following isostatic uplift and exposure of Äspö, the near-surface marine water was gradually replaced/flushed out by fresher water, mostly precipitation, together with some present Baltic Sea water component. The local hydraulic system characterising Äspö is an important control to this mixing and flushing, which are on-going processes occurring coevally with isostatic recovery in the Baltic Shield.

Meteoric-derived saline groundwaters at Äspö from low conductive bedrock environments or from discharging zones at depth, lack any significant marine signatures and have a general chemistry reflecting water/rock interaction in a near-stagnant environment. Recent mixing and dilution processes (within the last 10 000 BP) have not been a major influence on these groundwaters, unless they have been hydraulically transported upwards into a mixing environment. This mixing and dilution is occurring at Äspö where the interface between the discharging saline waters and the recharging shallower groundwaters lies around 400-600 m. It is believed that these Ca-rich saline waters orginate deep in the bedrock (>1000 m) and chemically represent the large-scale, sub-horizontal regional groundwater flow which is flowing eastwards.

Conceptual groundwater flow model of Äspö.

The conceptual flow model (Fig. B) is mainly based on borehole geochemical trends and detailed observations from individual borehole sections investigated in this study.

Regionally, the Äspö area probably lies within a dominant WNW-ESE trending hydraulic gradient at greater depths determined by the topography of the mainland, along a profile extending several kilometres to the WNW. This regional groundwater flow gradient accesses Äspö mainly by two major EW-trending fracture or shear zones (EW-1 and NE-1) which extend westwards to the mainland. Other less important EW-trending fracture zones include NE-2, EW-3 and NE-3,4. Cross-cutting these fractures, and producing a grid-type fracture pattern, is a series of gently dipping discontinuous fractures (20-30°N) which comprise the EW-5/EW-X fracture

Figure B: Conceptual groundwater flow model for Äspö.
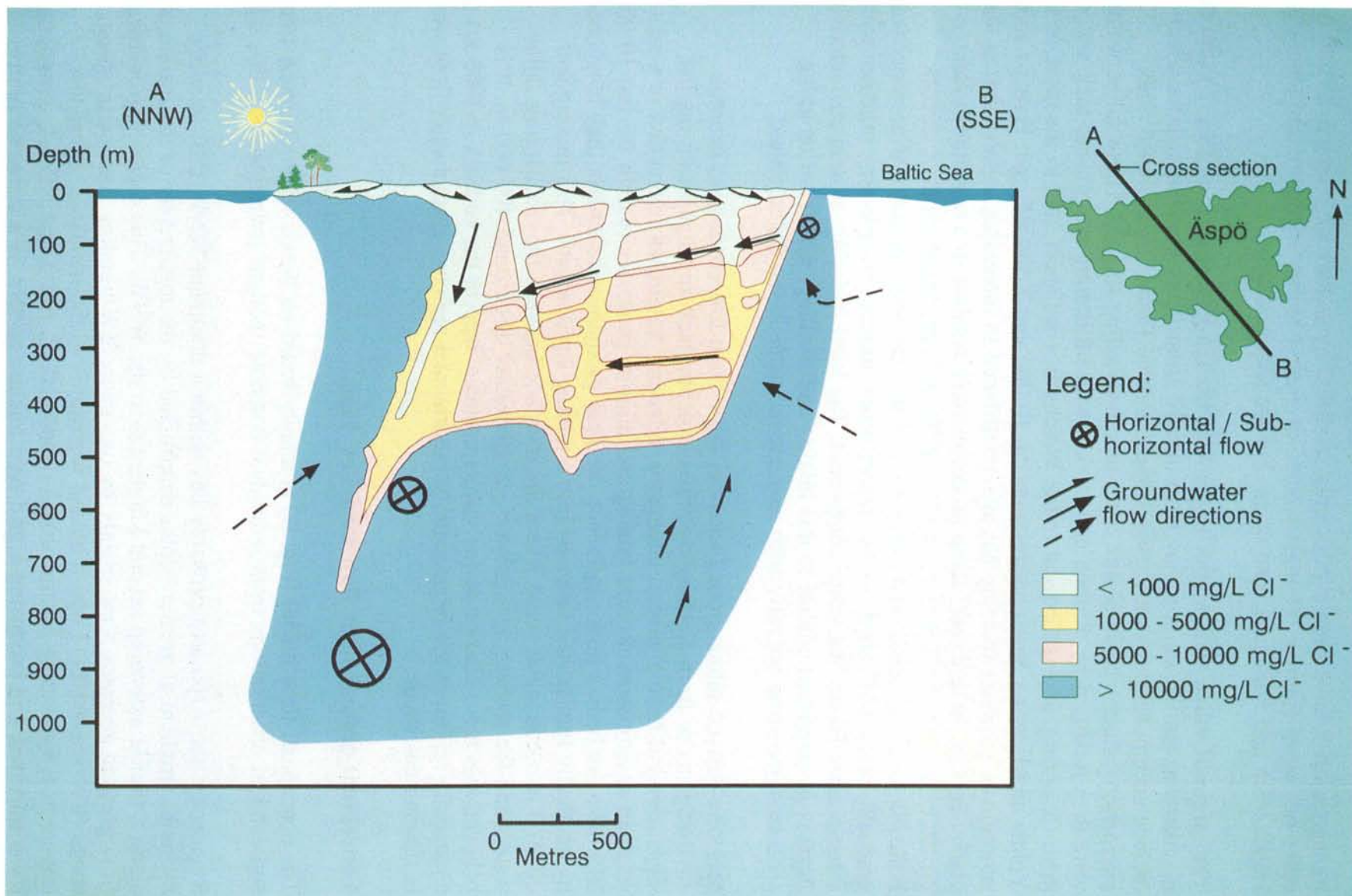
zones. Located behind the constructed vertical profile are a series of vertical to subvertical NNW-SSE-trending fractures.

Essentially, as this regional groundwater flow gradient approaches Äspö, subsidiary flow directions are established up, down, around and through the fracture grid system, the local directions being determined by the hydraulic properties of the individual fractures, but with the dominant regional groundwater flow continuing eastwards. Because of the topography at Äspö, and assuming steady state and porous conditions, two water bodies exist superimposed on the deep regional groundwaters. These consist of a marine-derived water and a floating lens of fresh (to brackish) water, with a narrow dispersion zone at the interface. In reality, however, conditions are not steady state and porous, but rather more dynamic and fracture controlled. As a result, the aerial extent and thickness of the fresh water layer is variable and greatly influenced by the local hydrology of the upper 100-150 m of bedrock.

Figure B illustrates a diagramatic representation of possible groundwater flow directions and a series of isohalines obtained from Cl values recorded from the sampled borehole sections. Four groundwater types have been selected; <1 000 mg/L, 1 000-5 000 mg/L, 5 000-10 000 mg/L and >10 000 mg/L Cl. It can be readily seen that a "fresh" or brackish water lens occupies most of the upper 50 m of the island, and that more saline waters (marine-derived) extend to some considerable depth, on average to 300-500 m, but extending further to around 400-500 m in zone EW-1.

Educated estimates of salinity characterising the low conductive bedrock mass are also indicated. These were made assuming that some migration/diffusion of saline pore water has occurred since uplift in order to differentiate the central part of Äspö (5-10 000 mg/L Cl) from the surrounding bedrock (>10 000 mg/L Cl) which generally represents more closed, stagnant groundwater conditions.

It should be pointed out that the absence of detail under the Baltic Sea surrounding Äspö is due to a lack of hydrogeochemical data; no attempt has therefore been made to indicate any groundwater mixing trends or to establish the influence of zones NE-3 and NE-4.

Groundwater flow in the upper brackish layer is mainly influenced by local recharge in the central part of Äspö and corresponding discharge at the periphery of the island. More minor groundwater circulation is caused by small topographic variations in the island. Within the central, 50-500 m part of the bedrock, large scale hydraulic gradients exist between points of major discharge (zones NE-1 and NE-2) and recharge (zones EW-1 and EW-3). Groundwater flow, facilitated by the geometry of the gently dipping EW-5/EW-X zones, therefore occurs transverse to the regional gradient in this central part of Äspö.

In terms of the hydrogeochemical studies, all of which point to groundwater mixing and chemical heterogeneity in the upper 500 m of the island, the presented

conceptual model illustrates quite convincingly the role fracture frequency and hydraulics play in in the upper 500 m (especially zones EW-5/EW-X and the interconnecting NNW-SSE zones). Effectively, this three dimensional fracture grid system results in the active mixing, circulation and redistribution of groundwater originating from different sources, especially within the upper 100-200 m, but locally also down to 400 m, and even deeper when hydraulic conditions are favourable.

Conclusions.

<u>Specific.</u>

The Äspö hydrogeochemical studies show the following conclusions:

* There are at least three sources of meteoric water which are entering and mixing within the upper 500 m of the Äspö site: a) recent fresh to brackish near-surface waters (mostly precipitation), b) modern Baltic Sea water, and c) deep saline waters. Subordinate amounts of ancient seawater and glacial melt water probably also contribute.

* The major hydrogeochemical character of the groundwaters can be explained by the mixing of waters from two major sources; shallow fresh/brackish vs. deep saline.

* Groundwater samples collected from highly conducting fractures tend to have more unifrom compositions because they obtain their character through mixing along fairly rapid conductive flow paths, i.e. mainly determined by the groundwater flow rather than by rock/water interaction.

* There is no single, evolutionary flow path extending uninterrupted from surface to depths greater than 1 000 m convenient for interpretation and modelling.

* The trends in the upper 250-300 m are dominated by the downward movement of potentially aggressive surface-derived waters, where mineral dissolution/precipitation and ion exchange processes have to some extent contributed to the groundwater chemistry. However, this water also contains a significant component of both modern and ancient Baltic seawater.

* At greater depths highly saline groundwaters, which are welling up very slowly from depth, also mix to limited degrees. A mixing interface between these deep saline and the more surface-derived varieties extends approximately from 400-500 m depth.

* Field redox measurements are reasonably reliable and the redox potential is largely determined by the $Fe_{(III)}$-$Fe_{(II)}$ redox couple.

* Low redox potentials appear to be achieved very quickly in the groundwaters, which indicates that even at very shallow depths (~50 m) efficient buffering reactions must be occurring within the conducting fracture zones (and adjacent bedrock?) to ensure such a rapid drop in the redox potential during groundwater recharge.

* The hydrogeochemical and isotopic heterogeneity in the upper 500 m is attributed to:

> a) natural hydraulic mixing whereby the three-dimensional fracture grid system (especially zones EW-5/EW-X and the interconnecting NNW zones) results in an active mixing, circulation and redistribution of groundwater originating from different sources, particularly within the upper 100-200 m, but also down to 400 m, and

> b) perturbations caused by excessive groundwater extraction rates (and even sometimes at lower rates in low conducting environments) used for the interference pump tests, coupled with short-circuiting between the sampled borehole positions and the near-surface bedrock horizons.

* There are two types of saline groundwater: marine derived and non-marine derived. The former characterises most of the groundwater down to 500 m, where it is mostly derived from the Litorina/Yoldia transgressions (with fresh and modern Baltic components) modified by rock/water interaction, and the latter at depths greater than 800 m is of meteoric derivation with a general chemistry reflecting rock/water reactions in a near-stagnant environment.

General.

The study has emphasised the following:

* The necessity to plan well in advance the sampling and hydraulic testing programmes so that groundwater sampling achieves enough priority to ensure unperturbed conditions.

* The requirement of a multidisciplinary and integrated approach to hydrogeochemical interpretation. By integrating as many parameters as possible, it is still quite possible to come near to understanding the true system.

* Traditional geochemical modelling programs should be used to test ideas rather than generate new ones.

THE ÄSPÖ HARD ROCK LABORATORY: FINAL EVALUATION OF THE HYDROGEOCHEMICAL PRE-INVESTIGATIONS IN RELATION TO EXISTING GEOLOGIC AND HYDRAULIC CONDITIONS.

John Smellie
Conterra AB

Marcus Laaksoharju
GeoPoint AB

1. Introduction.

The Swedish Nuclear Fuel and Management Company (SKB) is currently excavating the access tunnel to an underground experimental laboratory, the Äspö Hard Rock Laboratory, planned to be located some 500 m below the island of Äspö which is located in the Simpevarp area, southeast Sweden, about 20 km NNE of Oskarshamn (Fig. 1.1).

The construction of an underground laboratory forms part of the overall SKB strategy to test, not only the construction techniques for deep excavation, but also the various methods and protocols required to obtain a three-dimensional model of the geology and groundwater flow and chemistry, within a fractured crystalline bedrock similar to that envisaged for the final disposal of spent fuel. To demonstrate and quantify many of the site-dependent parameters that will ultimately control the safety of a final repository, together with evaluating the functions of the various engineered barriers in a realistic environment, should go a long way to help validate some of the models and assumptions included in an overall performance safety analysis.

Äspö was chosen because it geologically represents a variety of typical crystalline bedrock environments. In addition, it is an easily accessible region and already forms part of the OKG-owned complex which hosts two nuclear utilities and the spent fuel intermediate storage facility, CLAB.

The activities described and interpreted in this report (some preliminary results have already been presented by Smellie and Laaksoharju (1991)) form part of the initial Pre-investigation Phase (from the surface to around 1000 metres depth) aimed at siting the laboratory, describing the natural hydrogeological and hydrogeochemical conditions in the bedrock and predicting the changes that will occur during excavation and construction of the laboratory. Phase 2, the construction phase, is expected to be operative from 1990-1994 followed by the Final Phase 3, the operation phase, which may continue from 1994 to 2050.
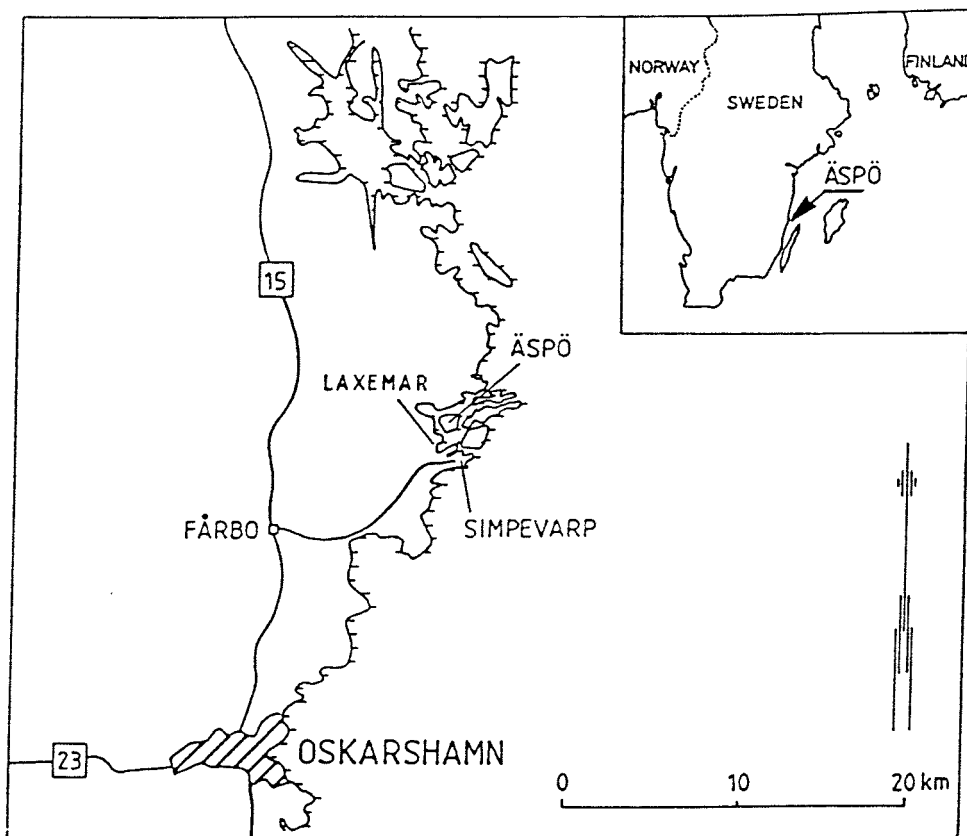
Figure 1.1. Location map showing the position of Äspö.

Phase 1 is extremely important in that it will provide the only opportunity to study the natural groundwater conditions in the bedrock. In particular, the present groundwater chemistry will provide the reference source point for all subsequent hydrogeochemical investigations carried out during phases 2 and 3. Without these primary reference groundwater data, future interpretation of chemical changes may be based more on extrapolation rather than fact. This is not a desireable situation. A major part of this report is therefore devoted to the quality assurance of the groundwater samples already collected and analysed.

In this respect, each groundwater sample is evaluated on the basis of: a) the potential contamination effect of borehole activities prior to sampling, b) the possibility of induced contamination during sampling, c) the hydrogeology of the borehole sections sampled, and d) possible uncertainties in some of the analytical protocols. As a result of this quality assurance, only groundwater samples considered to be representative, i.e. here defined as those which show no evidence of mixing with other water sources, whether from drilling water, younger, near-surface water, or from deeper groundwaters (Smellie et al., 1985), have been selected for detailed interpretation. Hydrogeochemical interpretation has been closely integrated with the hydrogeological investigations and other disciplines of major influence, in particular, bedrock geology and geochemistry and fracture mineralogy and chemistry.

Because of the apparent simplicity of the hydrology and groundwater chemical evolution at Äspö (Laaksoharju, 1988; A-C. Nilsson, 1989), in contrast with many of the earlier site-specific investigations (e.g. Smellie et al., 1985, 1987; Smellie and Wikberg, 1989, 1991), these waters provide a good opportunity to experiment with some new modelling approaches (Laaksoharju and Nilsson, 1989; Laaksoharju, 1990a) aimed at characterising the present groundwater chemistry and predicting changes expected to occur at greater depths.

2. Parameters Considered.

The major hydrologic and chemical parameters considered have been already outlined and discussed in detail by Smellie et al. (1985, 1987) in connection with earlier site-specific studies conducted in Sweden. The interested reader is referred to these reports and the references listed therein. However, as the Äspö project has also been the proving ground for some new techniques and improvements in groundwater characterisation, both hydrologically and chemically (see Almén and Zellman, 1991), some of these techniques, together with the testing of different modelling approaches, are outlined in more detail below and serve to complement the earlier reports of Smellie et al. (op.cit.).

At Äspö the following major parameters have been considered:

- hydraulic conductivity and head
- groundwater flow
- borehole geology/fracture mineralogy
- borehole geophysics
- hydrogeochemical parameters
- groundwater redox-sensitive parameters
- uranium geochemistry
- environmental isotopes
- the role of microbes, colloids and organic material
- major element geochemical rock/water equilibrium modelling
- groundwater mixing models
- multivariant analysis and groundwater classification
- modelled predictions of groundwater chemistry

2.1. Hydraulic conductivity and head.

Because of changes in emphasis within the SKB programme since the earlier site-specific studies carried out from 1982-1987, the same detail of hydraulic pressure head data to characterise the borehole sections sampled for groundwater at Äspö are unfortunately not available. However, educated estimates and qualitative extrapolations have nevertheless proved to be very helpful.

The hydrogeological data available from the Äspö region are presented in several reports, e.g. a compilation of available hydrogeological data (Rhén, 1987), hydraulic tests at Laxemar and Äspö (L. Nilsson, 1988, 1989, 1990; Rhén et al., 1991), transient interference tests at Äspö (Rhén, 1988), an integrated evaluation of hydrogeological and geophysical data (Liedholm, 1989), and a predictive groundwater flow model from long-term pump testing (Grundfelt et al., 1990).

Further to the earlier methods described in Smellie et al. (1985), an additional technique has been employed at Äspö with specific reference to measuring natural groundwater flow in rock. The point dilution technique (Ogilvi, 1958; Gustafsson, 1984, 1986) provides a semi-quantitative method for the in situ measurement of groundwater flow in fractures and fracture zones under natural hydraulic gradient conditions, and in the natural flow direction. This method was used with considerable success at Finnsjön (Gustafsson and Andersson, 1989, 1991). It has an obvious advantage when measuring the total flow compared to the traditional borehole hydraulic tests (single-hole injections tests and interference tests) whereupon the groundwater flow can only be calculated by assuming a natural gradient value.

Äspö has also provided the opportunity to test the downhole flowmeter which can measure directly the "natural" groundwater flow into a borehole from a conducting fracture zone and hence calculate the conductivity of the tested borehole section.

2.1.1 Borehole Measurement of Groundwater Flow Using the Point Tracer/dilution Method.

This method relies upon the use of a tracer, which is introduced as a homogeneous pulse into a borehole test section sealed off by rubber packers. The tracer will be diluted due to non-labelled groundwater from the fracture zone flowing through the borehole. The dilution of the tracer introduced is proportional to the water flow through the borehole section, and thus to the groundwater flow in the fracture zone. Within the borehole section the tracer must always be completely mixed and the concentration is measured as a function of time.

Groundwater flow rate through the borehole test section is calculated from the water volume in the test section and the dilution as a function of time according to Equation (1), which is the solution of the equation of continuity for the dilution of a homogeneously distributed tracer solution in a constant volume V at steady-state groundwater flow.

$$Q_w = - V \ln(C/C_o)/t \qquad (1)$$

where
Q_w = groundwater flow rate through the borehole test section (m^3/s)

V = water volume in the borehole test section (m^3)

t = time (s)

$$C_o \quad = \text{initial tracer concentration}$$
$$C \quad = \text{tracer concentration at time t}$$

Dilution as a function of time is obtained from a semi-logarithmic diagram of normalised tracer concentration versus time. In the ideal case the relation between time and logarithmic concentration is linear according to Equation (1).

As the dilution measurements aim in relating the measured groundwater flow rate through the borehole section to the rate of the undisturbed groundwater flow in the fracture zone, the flow field distortion must be taken into consideration, i.e. the degree to which the groundwater flow converges and diverges in the vicinity of the borehole test section. The groundwater specific discharge (Darcy-velocity), defined as the discharge per unit cross-sectional area perpendicular to groundwater flow, is denoted by v_f. With a correction factor, â, which accounts for the distortion of the flow lines owing to the presence of the borehole it is possible to calculate the specific discharge according to equations (2) and (3). If the groundwater flow not is perpendicular to the borehole-axis this also has to be accounted for (Gustafsson, 1986).

The cross-sectional area used to calculate the specific discharge is

$$A = 2 \; r \; L \; â \qquad (2)$$

Hence, the specific discharge is given by

$$v_f = Q_w/A \qquad (3)$$

The quotient Q_w/A may thus also be expressed as a volumetric flux density, Q_f, $(m^3/m^2 yr)$.

Determination of the groundwater flow rate in each individual fissure requires either isolation of the single fissures in short test sections or knowledge about the number of flowing fissures in the test section. Calculations of the velocity in the fissures also requires knowledge about the fissure apertures.

If the drilling has not caused any disturbances outside the borehole radius the correction factor â is 2.0 at laminar flow in a plane parallel fissure, if the flow is perpendicular to the borehole, or a homogeneous porous medium (Ogilvi, 1958). According to the formula of Ogilvi the value of â will however at least vary within â $= 2 \pm 1.5$ in fractured rock (Gustafsson, 1986). Hence, the groundwater specific discharge measured in one point of a fracture zone is determined with an accuracy of ±75%, according to the flow field distortion. The accuracy in flow determination is however not only due to the factor â. The tracer is also diluted due to changed

physical and chemical properties of the labelled water in the test section compared to the native groundwater. The downhole equipment itself may also cause disturbances and in borehole sections of considerable length vertical currents may be found. The equipment, tracers and concentrations used eliminates most of these disturbances. Molecular diffusion of the tracer into the fractures always exists, but it can often be neglected at considerable groundwater flow in short test sections.

At Äspö groundwater flow has been measured both under disturbed hydraulic gradient conditions, i.e. by pumping, and under natural gradient conditions.

2.1.2. Borehole Measurement of Hydraulic Conductivity Using the Flowmeter in Conjunction with Pumping.

The downhole flowmeter has been developed to measure axi-symmetrical water flow at selected points along a borehole. It works on the principle that fluid passing a downhole probe will activiate a flow velocity meter in the probe. The registered velocity is transfered as signals through the logging cable to the module (Fig. 2.1). Using a calibration data table, based on measurements taken at different flow rates under controlled conditions, the recorded data can be converted into flow units (litres/min.).
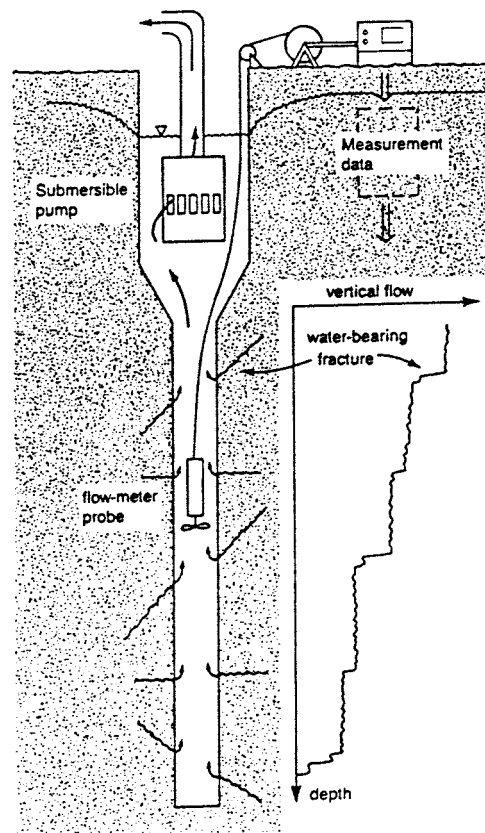
Figure 2.1. Downhole flowmeter measurement equipment (Almén and Zellman, 1991).

The procedural sequence is as follows:

1) The water pump is lowered to the required location in the borehole.
2) The borehole is pumped until the flow rate equals borehole recharge, thereby maintaining a constant groundwater level.
3) The probe is then lowered to a predetermined depth below the pump where measurements are to be taken.
4) Measurements are recorded at even distances (usually 1 m) down the borehole for a specific time interval from which the mean registered counts/sec. values are calculated.
5) Measurements are made whilst lowering the probe down the borehole to minimise groundwater perturbations (e.g. turbulence).

The smallest flow detected by the probe is equivalent to the minimum force that has to be overcome before the propeller revolves. This corresponds to approx. 15 litres/min. in a 56 mm diameter borehole. In practice, therefore, this threshold force must be exceeded, and this is normally done by increasing the flow-rate into the borehole by pumping. The total pumped volume of water must therefore be carefully monitored over some time, and an average measure of flow calculated, so that variations in pumped flow-rate are not misinterpreted as an anomalous groundwater flow into the borehole from the bedrock.

Sources of error include: a) defects around the axis of the propeller resulting in the recording of erroneous pulses, and b) calibration of the instrument; this should be carried out in a tube of specific diameter and not the borehole as the diameter is often variable.

This method may soon be superceded by the UCM-Flowmeter which is based on acoustic principles. Both up- and down-hole, variations in groundwater flow into the borehole can be detected and quantified. Although still in prototype form, test results from Laxemar and Äspö are promising.

2.2. Borehole geology/fracture mineralogy.

Detailed drillcore information exists for the major rock units encountered (Wikman, et al., 1988; Stanfors, 1988), for the frequency and type of fractures and the major mineral infillings (Stråhle, 1988, 1989; Stråhle and Fridh, 1989; Sehlstedt et al., 1990), and for the separation and analysis of mineral fillings (mineral identification, chemistry and isotopic signatures) selected from sealed and open fracture zones (Tullborg in Wikman et al., 1988; Tullborg, 1989; Tullborg et al., 1990). Furthermore, rock stress measurements are available for selected boreholes (Bjarnason et al., 1989).

2.3. Borehole geophysics.

As a direct complement to the geological and hydrogeological investigations, a considerable amount of geophysical data are available. Geophysical logging of the cored boreholes (Sehlstedt and Triumf, 1988; Sehlstedt et al., 1990) has generally comprised the following methods: a) borehole deviation, b) caliper, c) sonic, d) natural gamma, e) single point resistance, f) self-potential, g) magnetic susceptibility, h) normal resistivity (1.6 m), i) lateral resistivity (1.6 - 0.1 m), j) temperature, and k) borehole fluid resistivity. Logging of the percussion boreholes was restricted to a, d, and g-k. For example, such methods greatly increase our knowledge of fracturation (conductive vs. non-conductive) and groundwater salinity, in addition to aiding packer positioning and emplacement. A correlation of geology and geophysics has subsequently been carried out by Sehlstedt and Stråhle (1989), and a combined evaluation of geology, geophysics and hydrogeology more recently presented by Leidholm (1989).

Borehole radar measurements to help locate the position and lateral extent of the fracture zones have been carried out at both Laxemar and Äspö (Niva and Gabriel, 1988) and later at Äspö (Carlsten, 1989, 1990). A correlation between radar data and geophysical, geological and hydrological borehole parameters using multivariate analysis has been presented by Carlsten et al. (1989). In this report, only the radar reflectors used for interpretation of zones between boreholes and the surface have been included (S. Carlsten, written comm., 1992).

Limited to one hole (KAS07), a Vertical Seismic Profiling (VSP) survey was conducted to detect zones of fracturation and other anomalies in the structure of the Äspö rockmass, ultimately to construct a three-dimensional model showing major fracture positions and orientations (Cosma et al., 1990).

Geophysical laboratory measurements (density, magnetic susceptibility, remanent magnetization, resistivity, induced polarisation and porosity), and natural gamma (uranium, thorium and potassium), have been carried out on core material from two boreholes (one at Laxemar and the other at Äspö) and the results detailed by Nisca (1988). These data provide a valuable complement to the geological mapping of the drillcore, e.g. in providing additional information on rock types, their composition and genesis, and on the location of potential zones or horizons of hydraulic character.

2.4. Chemical parameters.

The long-term integrity of the waste packaging for high-level radioactive waste is stongly influenced by the hydrochemical properties of the surrounding groundwaters. The most important chemical parameters for determining the extent of copper corrosion and radionuclide mobility are the redox condition, pH, and the concentrations of metal complexing ligands such as carbonate-, fluoride-, chloride,

sulphide and phosphate-ions, and fulvic acids etc. Contact with unsuitable groundwater compositions may accelerate corrosion of the copper canister, lead to increased dissolution of the spent fuel, and finally result in an increase in transport rate of released actinides through the geological barriers to the biosphere.

Copper is thermodynamically stable under reducing conditions when sulphide is absent. The solubility and mobility of most actinides are expected to be low in a naturally reducing groundwater environment. Sulphide, on the other hand, will react with copper thus making copper oxidation with water possible, despite the reducing conditions. In addition, complexation with carbonates can, for instance, increase the solubility of uranium especially under oxidising conditions, which may be present, for example, during radiolysis.

Integrating groundwater chemistry with the hydrogeological data offers the possibility to improve the prediction of groundwater flow patterns in the bedrock. This information is used to model the past history of the groundwaters (evidence of ion-exchange; long/short residence times etc.) and also to predict future changes in composition and flow pattern. Surface and near-surface groundwaters tend to have uniform compositions because they obtain their character through mixing along fairly rapid conductive flow paths, i.e. mainly determined by the hydraulic gradient rather than by chemical rock/water interaction. At greater depths, groundwater tends to permeate slowly through the rock with increased exposure to rock/water ion-exchange processes. In this environment the bedrock/fracture mineral chemistry becomes important in determining the groundwater compositions.

Surface, near-surface and deep ground waters are best distinguished from each other by pH, total salt and carbonate contents. Shallow waters are rather dilute with high calcium and bicarbonate contents due to the dissolution of calcite, and neutral pH. Deeper groundwaters have a much higher pH, higher sodium and chloride contents (i.e. contributions from slowly dissolving minerals such as feldspar) but lower carbonate contents (even though calcium remains an important component) due to calcite precipitation. The carbonate content of the water is important as the CO_3^{2-} ion is a very strong complexing agent for the actinides, resulting in soluble carbonate complexes in the groundwater. The total carbonate content is highest in the near-surface waters and decreases with depth, i.e. as the water becomes older.

The salt content of very old groundwater is sometimes extremely high; the source is debatable with seawater, fluid inclusions, rock/water interaction and residual igneous/metamorphic fluids all having been proposed as possible sources.

2.5. Groundwater redox-sensitive parameters.

The redox condition of the groundwater is one of the most important parameters for estimating the safety of a nuclear waste repository. For example, if the actinides (i.e.

released through canister corrosion) are assumed for modelling considerations to migrate in a reduced form (e.g. Pu(VI), Pu(V), Pu(IV), Pu(III)) through the geosphere, the radiation dose released to the biosphere will be two orders of magnitude lower than in the case where the actinides are transported in an oxidised form.

The redox condition of the groundwater is reflected by the measured redox potential, the amount of dissolved oxygen, and by the contents and oxidation states of the elements iron, sulphur and uranium. From all the various redox couples present in the groundwater it is possible to calculate a redox potential. However, these calculations would give us as many different results as the number of redox couples used in the calculations (Lindberg and Runnels, 1984). This simply indicates that no true redox equilibrium exists in the water. Work by Wikberg et al. (1987) and Wikberg (1987) has shown that the redox properties are largely determined by the Fe(II)/Fe(III) system, (e.g. relevant to much of the reported groundwater data in Smellie et al. (1985, 1987)), and recently Grenthe et al. (1992) have shown that stable and reproducible redox potentials can be measured with an accuracy of ± 25 mV and are in close agreement with theoretical expectations (Langmuir and Wittemore, 1971). However, much of the measurement and interpretation of field redox data from borehole investigations tend to be complicated by the mixing of waters of different origins.

Oxygen is a very strong oxidant in the Eh-region of interest for the groundwaters. Small amounts of oxygen dissolved in water will drastically affect the Eh measurements (e.g. Smellie and Wikberg, 1991). Oxygen reacts rapidly with sulphide which means that these components should not be expected to be found in the same water sample. The existence of measureable amounts of sulphide in the water is an indicator of very reducing conditions. The sulphide is oxidised to sulphate by dissolved oxygen whereas the opposite reaction only occurs in the presence of bacterial activity.

Previous hydrogeochemical investigations mostly employed surface redox potential measurements; at Äspö, both surface and downhole measurements have been carried out when possible. Downhole measurements are considered not only to be more stable, but are much more practical when monitoring over long periods of time. Technical difficulties, such as pump failure, have only a marginal effect, which contrasts with the surface equipment whereupon electrodes are strongly affected due to oxygen diffusion into the surface cell which in turn influences the redox processes on the electrode and in solution. The downhole electrodes are virtually unaffected because of the total absence of oxygen in the surrounding groundwater (Wikberg, 1987). A further advantage of the downhole method is that after the initial calibration process, the electrodes are stable without drift for periods of several months. With surface equipment drift commonly occurs, and every time the cells are opened for calibration, subsequent Eh measurements are disturbed for periods of several days before all the atmospheric oxygen is removed and stabilisation is possible.

2.6. Uranium geochemistry.

The degree of uranium dissolution and mobility in groundwaters can be used as an important redox-sensitive parameter, in addition to being of particular interest in the context of high-level waste safety assessment considerations because its chemical behaviour resembles closely the more harmful actinides such as neptunium and plutonium in the +6 and +4 oxidation states. The hydrochemical behaviour of uranium in the geosphere and under laboratory conditions renders it very instructive in helping to predict long-term actinide behaviour in the far-field in the event of canister corrosion and subsequent radionuclide leakage.

Uranium studies reveal an extremely complex picture of the many parameters that can influence the behaviour of uranium in narural groundwaters. Based on Langmuir (1978) and Giblin et al. (1981), the major influencing parameters are listed below:

a) the uranium content in the source rocks and its leachability,

b) the proximity of groundwater to uranium-bearing rocks and minerals,

c) concentrations in the groundwaters of carbonate, phosphate, vanadate, fluoride, sulphate, calcium, potassium and other species which can form uranium complexes or insoluble uranium minerals,

d) the sorptive properties of materials such as organic compounds, oxyhydroxides of iron, manganese and titanium, and clays,

e) pH and Eh states of the groundwater environment,

f) redox state of the uranium species,

g) kinetics of uranium speciation reactions, and

h) rates of groundwater mixing and circulation,

However, for modelling purposes the most important parameters are pH, Eh and the total concentrations of the ligands which form strong complexes with uranium in its different oxidation states, i.e. carbonate and phosphate.

2.7. The role of microbes, colloids and organic material.

Since the early site-specific studies (KBS-3, 1983) the potential role of microbes, colloids and organic material in the mobilisation of actinides, particularly in the far-field, has been increasingly recognised and studied. Since then, microbiological studies have been carried out at three test-sites, one of which was at Ävrö (Pedersen,

1988), and this was followed up by further studies (Pedersen, 1989, 1990) at Laxemar (LX01), Ävrö (AV01) and Äspö (KAS02), and more recently (Pedersen and Albinsson, 1990) also from Äspö (KAS02).

A general review of colloidal systems and their potential relevance to nuclear waste disposal is presented by Vuorinen (1987). Specifically, the role of colloidal/organic material in ionic binding equilibria using polyelectrolyte solutions has been studied by Marinsky et al. (1988), and on a more practical note, the isolation (Allard et al., 1990), characterisation (Swedish sites including KAS02, Äspö; Pettersen et al., 1990; Laaksoharju, 1990b) and complex forming properties of humic acids (Ephraim et al., 1990), have been recently described. A state of the art document summarising the concentrations of particulate matter and humic substances in deep Swedish groundwaters, and the estimated effects on the adsorption and transport of radionuclides, is presented by Allard et al. (1991).

The dispersed phase in a natural groundwater sample consists mainly of inorganic colloids (e.g. clays, metal oxides and hydroxides, metal carbonates), organic colloidal material (dominantly humic acids with subordinate fulvic acids; most of the TOC is complex and unknown) and microbial populations. In Swedish deep water samples colloidal concentrations range from 0.01 to 400 mg/m^3, humic and fulvic substances from 0.01 to 500 mg/m^3 and microbial components from 0.1 to 50 mg/m^3.

The presence of these substances in groundwaters can play an important role in the far-field transport of trace metals (e.g. radionuclides) within the geosphere and ultimately to the biosphere. The potential for transport is suggested because the micrometre particles are far smaller than the pores in permeable and fractured media, and their high surface area per unit mass means that they will be effective sorption substrates.

The mobility and distribution of trace metals in the aqueous environment are naturally related to the hydrogeological and hydrochemical nature of the system. The most important hydrochemical parameters of the system are: a) the pH (at a specific redox potential), which determines the degree of hydrolysis and charge properties of many of the relevant radionulides, b) the presence of inorganic complexing agents (primarily carbonate; occasionally sulphate, fluoride and phosphate), c) the presence of complexing natural organics (humic and fulvic acids), and d) to some extent the salinity.

Complexation with humic material is one of the most important mechanisms for many of the divalent transition elements at low or intermediate pH in typical surface waters (> 1 mg/L humic material). Trivalent elements (e.g. the lanthanides and actinides) tend to hydrolyse at a fairly low pH and form very strong complexes with humic substances, even in groundwaters of low humic content (0.01-0.1 mg/L).

Specifically, the presence of humics will influence trace element mobility by:

1. Changing the sorption properties due to the formation of metal humates.
2. Due to the formation of an organic film on inorganic particles, new surfaces will be created with different sorption properties.
3. The formation of macro molecular aggregates of a colloidal nature.

Radionuclide species in solution will tend to sorb onto solid media (e.g. exposed geological surfaces along conducting fractures and fissures) and onto mobile solid particulate matter (inorganic colloids, microbes) present in the groundwater. The former mechanism will therefore retard radionuclide mobility whilst the latter will increase mobility. The sorption mechanisms on particulate material can be reversible or irreversible, but the mechanisms are still not well enough understood to quantify and model. Irreversible sorption presents the greatest threat; such particles would be able to transport the sorbed nuclide fraction at the same velocity as the groundwater flow-rate through the conductive fracture systems, and may not therefore have the same opportunity for decay as the dissolved fraction (Allard et al. 1991).

Certain difficulties are encountered in the study of colloidal/organic material mainly due to reasons of a practical nature, for example, groundwater contamination by drilling debris, the difficulties of ultrafiltrating the different colloidal fractions (i.e. coagulation effects) and sometimes the difficulty of extracting sufficient amounts of material from restricted volumes of borehole groundwater. Because of the limited amount of material, the identification and analysis of such small-sized particles (commonly from 0.05-0.45 microns) is both time consuming and difficult.

Relatively few studies have documented the role of colloid/organic substances in the mobilisation and transportation of trace elements, although Buddemeier and Hunt (1988) have recently demonstrated radionuclide transport by colloids flowing through a fractured media at the Nevada test-site; Miekeley et al. (1990), on the other hand, found that even though radionuclides had sorbed onto colloidal material, there was little or no evidence of colloidal transport through subsurface media.

Microbial organisms are known to be important factors in many geochemical processes, and studies have shown that microbial contamination (e.g. introduced during drilling, excavation and ultimately the sealing of the repository) of nuclear waste repositories is inevitable, and therefore cannot be precluded from even a very deep repository for high-level waste. In fact, it is only fairly recently that near-field safety analysis calculations have considered the possibility of microbial activity which may affect the integrity of the total waste package and the subsequent release and migration of the radionuclides.

Microbial organisms will only come into contact with the radioactive waste once the complete integrity of the system of engineered barriers has been breached. At present, however, the exact mechanism of radionuclide uptake by the microbes is not known.

They may be either actively taken up into the oganisms interior, or remain sorbed onto the exterior surface. Radionuclide transportation will depend on both the microbial population size and their mobility. Certain microbes, possessing flagella, will be more mobile along 'free' flowing fractures/fissures. Microorganisms that are not self-propelling will tend to be more influenced by their morphology and the nature of the fracture surfaces over which they are passing. Retardation of microbial mobility may occur where nutrients or energy sources are located, thus causing a coagulating effect.

In general, therefore, microbes could thus have both positive effects (e.g. inhibition by fissure/pore blockage) and negative effects (e.g. sorption onto mobile groups moving towards a nutrient source, or simply flowing with the water) (McKinley et al., 1985).

2.8. Environmental isotopes.

Within the Swedish hydrogeochemical programme, the major environmental isotopes have been routinely measured. These consist of tritium (^{3}H), radiocarbon (^{14}C) and the stable isotopes deuterium (^{2}H) and oxygen (^{18}O); use is also made of the uranium decay series radionuclide ratios ^{234}U/^{238}U. Using such isotopic data groundwaters can be characterised in terms of:

a) identification of areas of static groundwater where regional migration of radionuclides should be minimal,
b) estimation of water velocities in circulating hydrologic systems
c) groundwater source(s),
d) degrees of mixing of groundwaters from different sources, and
e) as an aid in predicting future natural changes in the chemistry of the groundwater,

As most ^{3}H (half-life 12.43 a) and ^{14}C (half-life 5730 a) present to-day in the atmosphere have resulted from thermonuclear contamination, both methods (especially ^{3}H) are of particular use in distinguishing between recent water (recharge after 1952) and older water (recharge prior to 1952) thus providing important information on, for example, groundwater recharge velocities. The ^{14}C data are here presented as % modern carbon with less onus on radiocarbon age determinations, although these are still very useful as qualitative indicators. ^{14}C-dating can strictly speaking be done only if the atmospheric production of ^{14}C has remained constant in the past, and that the zero age concentration of ^{14}C in the materials to be analysed, preferably prior to 1952, is known. These requirements, plus the fact that groundwater systems are usually dynamic and open, and the geology often complex, can make quantitative age determinations laborious and uncertain.

The stable isotopes, ^{18}O and ^{2}H, occur naturally in water and are stable to radioactive decay. For practical purposes these isotopes are used to distinguish water originating

from different sources (through isotopic fractionation each source has a distinct isotopic signature) in the assumption that they remain unchanged from recharge to groundwater flow conditions. Variations in isotopic abundance is not thought to be adversely influenced by presently occurring atmospheric radiogenic production. The initial stable isotope concentration of water is basically controlled by:

1. Condensation stages resulting in precipitation; this tends to result in isotopic fractionation and depends on changes of temperature and pressure.

2. Subsequent evaporation stages; this tends to result in an increase in isotopic content of the residual water and depends on the relative humidity.

The isotopic values are plotted on a δ^2H (‰) vs. $\delta^{18}O$ (‰) diagram and interpreted relative to present day oceanic precipitation which is characterised by a deuterium excess (d) of 10 ‰. This is presented graphically by a linear relationship expressed by $\delta^2H = 8\ \delta^{18}O + 10$ (Craig, 1961). In general, a slope less than 8 (i.e. relative deuterium enrichment) is indicative of water resulting from evaporation in an enclosed basin environment, whilst a slope greater than 8 (i.e. relative deuterium depletion) indicates changes in palaeoclimate.

Certain complications can arise, however, such as an enrichment of $\delta^{18}O$ from rock/water geothermal interaction, enrichment of $\delta^{18}O$ and depletion of δ^2H resulting from feldspar alteration to clays, and gaseous exchange of CO_2 and H_2S from charged groundwaters can result in a depletion of $\delta^{18}O$ and an enrichment of δ^2H respectively.

2.9. Chemical equilibrium modelling.

The early reported hydrogeochemical studies (Smellie et al., 1985) of groundwater data made little use of computer codes to model the geochemical parameters of the water samples obtained. This was somewhat rectified for the Klipperås groundwater data (Smellie et al., 1987) where the modelling work fell naturally into two categories: redox groundwater characterisation and geochemical interpretation of the analytical data (aqueous speciation and solution-mineral equilibria). A similar approach has been adopted for the Äspö groundwater data.

A large number of computer programs are available and reported in the literature (Nordstrom and Ball, 1984). The computer program used in this report is PHREEQUE (Parkhurst et al., 1980) and was selected for the quality and documentation of its thermodynamic database.

The PHREEQUE model uses as input the chemical analysis of the sampled waters, and using the pertinent parameters and equations included in the database, it determines the equilibrium state of the sampled groundwaters. The results of the

calculations include the concentrations of all species in the aqueous solution and the mineral saturation indices.

To model the geochemical reactions occurring along a flow path, coupled to the mixing of groundwaters from different sources, the program NETPATH (Plummer et al., 1991) was used. This program uses WATEQFP (modified after WATEQF; Plummer et al., 1976) to calculate the distribution of aqueous species and construct the input file to NETPATH. Essentially, NETPATH is used to "interpret net geochemical mass-balance reactions between an initial and final water along a flow path. The net geochemical mass-balance reaction consists of the masses (per kg of water) of plausible minerals and gases that must enter or leave the initial water along a flow path to define the composition of a selected set of chemical and isotopic constraints observed in the final water. If initial waters mix and subsequently react, NETPATH computes the mixing proportion of two initial waters, and net geochemical reactions that can account for the observed composition of the final water".

2.10. Multivariant analyses and groundwater classification.

Multivariate analyses (MV) are used to identify or model the character of analytical data; the strength of this approach is that several or all variables in a data matrix can be examined simultaneously. The character of the data in a general data matrix is therefore more easily identified than using univariate analysis, where only one variable is compared at a time (Wold, 1987). With multivariate analysis, data can be explored, minimised, structured, classified and correlated. This technique is especially designed for evaluation and interpretation.

MV deals with Objects (samples) described by Variables (chemical quantities), and searches to establish the relationship between objects, between variables, and between objects and variables.

Objects can be: equal   Variables can be: equal
                 similar   similar
                 dissimilar   dissimilar
                 proportional   proportional
                 mixtures   linear comb

MV attempts to address the following: that objects 1, 2 and 3 are equal or similar, that objects 4 and 5 are equal or similar, but dissimilar from objects 1, 2 and 3. These objects can be assigned to various categories and this is accomodated by using classification analyses. Linear or complex relationships are possible between one variable and some other variables, or between some variables and some other variables; these relationships are expressed by a Correlation analysis. The variables need not all to be of the same type, for example, variables Cl, Na, Ca, K are

continuous variables, water flow is a discrete variable and the sampling method and rock type are considered discrete variables.

At Äspö, some early modelling used multivariant analysis to classify or categorise the groundwaters by simplifying the available analytical data (Laaksoharju and A-C. Nilsson, 1989 and Laaksoharju, 1990a). The questions posed (Mardia et al., 1979) were: a) which are the most useful chemical variables?, b) which variables are insignificant?, c) can the groundwaters be correctly/realistically classified?, and d) can unknown categories of groundwater chemistry be predicted? Furthermore, can the method be used as a quality control of groundwater samples?

In terms of quality control, classifying a groundwater as being representative or otherwise of the depth sampled, particularly in crystalline bedrock were groundwater movement is controlled by fracture flow, is a trying exercise. Many variables play an important part, e.g. borehole activities and any associated contamination, groundwater extraction rates, borehole and bedrock hydraulics etc. In order to try and arrive at a simplified, constrained approach, mathematically and therefore objectively based, a study was carried out comparing normal classifying procedures, which often require a familiarity and a "feel" for the data, with a "cold" multivariant analytical approach. The approach and results of this exercise are outlined in Section 6.1 and details of the multivariant analyses performed are presented in Appendix 1.

2.11. Groundwater mixing models.

At Äspö the measured groundwater composition is a product of water/rock interaction and mixing processes. In order to examine reactions and hence understand the groundwater evolution taking place in natural systems, these processes must be separated. This is a first attempt to reduce the effect on the chemical composition due to mixing. The mixing process is often complex and can involve several end-members. In this study a simple two component mixing model was tested; the construction of multi-member mixing models are presently being studied. The model used certainly oversimplify a system which would be more realistically described by including a third component, seawater.

Constituents such as Cl, Br, Sr and Li are water conservative elements and can therefore be used in the mixing calculations (Laaksoharju, 1990a). Here, the Cl composition is used as an inert tracer. As native end-members, the groundwater compositions of KAS03: 802-1002 m (deep component) and HAS05: 45 m (shallow component) were used. The Cl content from each of these two end-members was then mixed in portions necessary to achieve the measured Cl contents of the other samples being studied (see Section 5.1.8).

The following steps were followed: mixing ratio calculations followed by deviation calculations. The former describe the necessary portions of water needed from both

end-members to achieve the Cl content measured in the new sample. The latter are used to predict new values for Na, Ca, HCO$_3$, SO$_4$, Cl and K etc. The predicted values are then compared to the measured values expressed in mg/L or a relative deviation expressed in %. Little or no deviation from the model predictions indicates that the concentration can be adequately explained by mixing; large deviations indicate sources or sinks for a particular element that are not accounted for by the mixing model. The reason for the deviation may be reactions or other influences from unknown end-members.

The mixing ratio is calculated according to the formula:

$$\text{Mixing Ratio} = (X-A)/(B-A)$$

where:

X = measured Cl concentration
A = measured Cl concentration of end-member 1 (shallow)
B = measured Cl concentration of end-member 2 (deep)

The deviation from the mixing model for respective elements is calculated according to the formula:

$$\text{Deviation} = A-(B*C + D*E)$$

where:

A = measured element concentration
B = mixing ratio for end-member 1 (shallow)
C = measured element concentration for end-member 1 (shallow)
D = mixing ratio for end-member 2 (deep)
E = measured concentration for end-member 2 (deep)

3. Groundwater Sampling and Analysis.

3.1. General.

Results from previous groundwater evaluation studies (Smellie et al., 1985, 1987), carried out as part of the Swedish site characterisation programme, recommended several suggestions to improve the quality and representative character of the groundwaters sampled. These studies showed that the greatest disturbances to groundwater quality are caused by:

* borehole drilling
* gas-lift pumping
* hydraulic injection tests
* water sampling
* open-hole effects
* drilling debris/rock flour

As a result, the provision of a borehole specifically for hydrochemical purposes was included in the Finnsjön study to test various methods and techniques to improve groundwater quality (Smellie et al., 1987; Smellie and Wikberg, 1989, 1991). This involved the use of booster air-flush drilling and taking "first-strike" groundwaters during a stepwise sampling/drilling protocol.

Booster air-flush drilling was expected to effectively avoid contamination of the hydro-environment often caused by the flushing water medium during rotary drilling. Booster drilling, in combination with a stepwise drilling/sampling protocol, would therefore have the advantage of: a) locating fairly precisely the intersection depth of the hydraulically conductive horizons, b) obtaining representative groundwaters for the level sampled, free of contamination from any hydraulic connection with a deeper, water-filled borehole section, and c) avoiding groundwater contamination from any long-term open-hole effects (Smellie and Wikberg, op. cit.). Furthermore, the presence of conducting fracture zones along the borehole sections should be initially located using geophysical logging techniques, and then sampled prior to the hydraulic injection tests which are usually a source of contamination.

The Finnsjön study clearly showed the limitations of only using the booster air-flush percussion method. Its efficiency is limited by the amount of accumulating water entering the borehole, which in turn is governed by the bedrock hydraulics. Often, as at Finnsjön, such effects are not important down to relatively shallow depths (200-250 m); at greater depths, however, a considerable air pressure is required to continually clear the hole from the accumulating water. Increasing the air pressure at such depths only serves to extend the radius of groundwater contamination (i.e. oxygen/groundwater dissolution) further out into the host rock along hydraulically susceptible horizons (i.e. high conductivity coupled with a negative piezometric head, i.e. excess pressure in the borehole compared to the surrounding rock). Long

pumping times are therefore necessary to remove these effects which have been demonstrated to significantly influence pH and redox-sensitive parameters such as Eh, uranium and Fe(II). At depths greater than 250 m rotary water-flush techniques, although still introducing contaminating fluids, were preferred.

3.2. Groundwater quality at Äspö.

The groundwater quality at Äspö is discussed under three main headings: drilling, the period following drilling but prior to sampling, and finally the main sampling period itself. It should be borne in mind that the general groundwater chemistry at Äspö shows a sharp contrast between near-surface fresh water (0 to approx. 100 m) and highly saline deeper (>500 m) groundwaters (Laaksoharju, 1990a). Groundwater mixing during borehole activities is therefore a distinct possibility.

3.2.1. Drilling.

The site-specific programme at Äspö introduced a new modified core-drilling technique which went some way in satisfying the criteria set out for groundwater quality improvement. The borehole (telescopic borehole) is designed with a larger diameter (155 mm) in the uppermost 100 m which during drilling houses an air-lift pumping system, and a smaller diameter (56 mm) at depths below 100 m (Fig. 3.1). The objective of this system is create a pressure draw-down in the borehole during drilling, so that the formation water and flushing fluids collecting in the hole are pumped rapidly to the surface carrying the various rock debris. Rapid removal of these components should prevent their penetration into the bedrock via conductive fracture zones. Furthermore, as the first 100 m of the hole is by air-flush percussion, the required air pressure is reasonably low and should not therefore unduly affect the bedrock hydrogeochemistry.

In practice, however, the first 100 m were drilled by the rotary diamond core method using water flushing (mainly to secure a drillcore profile) and this may have resulted in groundwater contamination in the upper part of the bedrock. However, the present drilling campaign (both percussion and rotary core methods) have shown that the upper approx. 100 m of bedrock in the northern part of Äspö appears to be "dry". As the groundwater levels for the area average around 6-8 m depth, the inference is that at least the first 100 m of bedrock is tight and not particularly conductive and little flushing water should have been lost to the bedrock. This is supported by the drilling logs which record little water loss. In the southern part of the island, however, the bedrock seems to be more conductive at these higher levels and groundwater contamination cannot therefore be totally ruled out.

According to the technique described above, drilling from 100 m to greater depths should theoretically ensure a contamination-free environment. Although no quantitative measurements were carried out, estimates of water/drilling debris loss to

the bedrock were as low as 2% (borehole KAS02) but as high as 45% (borehole KAS04). This was partly illustrated during the stepwise drilling/sampling protocol. Sampling for "first-strike" groundwaters was carried out systematically at packed-off intervals of 100 m during drilling. Two samples were taken, the first when one section volume of borehole water was removed, and the second when approx. 1.2 m³ of water had been removed. Analysis of the samples showed that the percentage of drilling water (tagged by a uranine tracer; 0.5 mg/L initially added to the drilling water) present in the early samples was high, ranging from 0.6-68% with a mean value of 28% (boreholes KAS02-08). In some boreholes the percentage dropped during repeated chemical sampling (e.g. KAS08 from 23.6 to 0.6 %), in others there was little difference (e.g. KAS03 from 52 to 42 to 41%). These variations will very much depend on the hydraulic character of each individual borehole. In general, therefore, at the cessation of drilling, some residual drilling water probably still remains in the boreholes and in the immediate surrounding bedrock prior to the final chemical characterisation sampling.
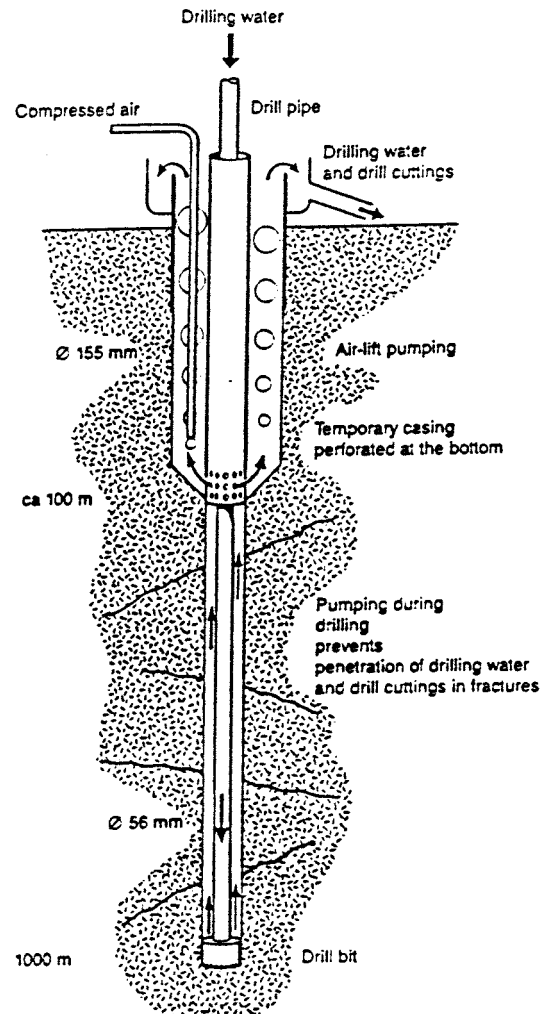
Figure 3.1. Details of the telescope borehole drilling technique (Almén and Zellman, 1991.

3.2.2. Subsequent to Drilling.

Subsequent to drilling, the following sequence of borehole activities have been carried out at the Äspö sites:

* borehole clearance, test pumping of the entire borehole and spinner surveys,

* geophysical logging of the entire borehole,

* hydraulic injection tests along 3 and 30 m sections (only KAS02-KAS08),

* based on the above test results, specific conductive borehole sections were selected for transient interference tests, and dilution tests were performed on some boreholes sections, and

* groundwater sampling from isolated sections of approx. 3-10 m length,

The sequence of activities from drilling to groundwater sampling are not always systematic; groundwater sampling (sometimes only limited to uranine monitoring of the flushing water contents) has been carried out at various occasions in association with drilling (described above), borehole clearance and pump tests etc. An example of the sequence of activities for boreholes KAS02 and KAS03 are given in Tables 3.1 and 3.2.

As referred to above, and discussed in detail by Smellie et al. (1985), borehole activities, when carried out prior to groundwater sampling, can have a detrimental effect on the water quality. Raising and lowering of geophysical probes results in groundwater perturbation, and injection testing, carried out by introducing clean formational water (i.e. from HAS05 in the northern part of Äspö; partly from HAS13 and KAS11 in the southern part) between two packers positioned 3 and 30 m apart respectively, can result in direct contamination. Contamination need not relate to major compositional changes of the formational groundwaters, but may mean introducing waters which have undergone pH and Eh changes through degassing and oxidation etc. This, however, relates mostly to the upper 100 m of bedrock where the introduced waters are derived from the same bedrock depth. At greater depths, where the formational groundwaters are highly saline, hydraulic testing effectively introduces a fresh, non-saline component into the most conductive zones intercepted by the boreholes, which may subsequently be detected by a change in salinity.

The injection water pressure is chosen to exceed the hydrostatic pressure in the section by 200 kPa. The injection time varies from 10 to 120 minutes (most commonly 10 min.), and the total volume of water has been measured using a flowmetre. From this information the hydraulic conductivity can be calculated (L. Nilsson, 1989). The degree of contamination will depend very much on the borehole

hydraulics; this will be discussed for each borehole section sampled in the next chapter.

Table 3.1: Sequence of some activities carried out in borehole KAS02

Borehole Activity	Date	Section (m)	Drilling water (%)	Tritium (TU)
Drilling	871102 - 880126	0 - 924		
Injection Test	880203 - 880207	102 - 672		
Injection Test	880207 - 880207	102 - 924		
Injection Test	880207 - 880505	102 - 159		
Pump Test 1 (+DWS)	880315 - 880317	0 - 924	1.60-0.5	
Chemical Sampling	880325 - 880412	314 - 319	1.00-0.61	<8.45
Chemical Sampling	880413 - 880425	463 - 468	0.76-0.38	<8.45
Chemical Sampling	880428 - 880505	530 - 535	0.41-0.28	<8.45
Spinner Survey	880608 - 880608	0 - 924		
Chemical Sampling	880826 - 880828	248 - 251		
Pump Test 2	880917 - 880920	802 - 924		
Chemical Sampling	880918 - 880920	802 - 924	0.48-0.22	<8.45
Pump Test 3	880924 - 880927	308 - 344		
Chemical Sampling	880925 - 880927	308 - 344	0.71	<8.45
Pump Test 4	880929 - 880929	117 - 126		
Injection Test	881026 - 881026	405 - 420		
Injection Test	881026 - 881026	672 - 702		
Injection Test	881108 - 881109	702 - 801		
Injection Test	881121 - 881204	474 - 801		
Injection Test	881205 - 881205	423 - 474		
Injection Test	881205 - 881205	423 - 426		
Injection Test	881205 - 881205	552 - 555		
Chemical Sampling	881216 - 890111	202 - 214.5	3.00-0.81	0.3
Chemical Sampling	890113 - 890131	860 - 924	0.28-0.22	0.2
Tracer Test (B4)	890807 - 890818	309 - 345		
Tracer Test (B2)	890807 - 890818	800 - 854		
Chemical Sampling	900503 - 900613	309 - 345		
Chemical Sampling	900503 - 900613	800 - 854		

DWS = Drilling water sample for analysis.

Open hole effects may contribute to a general mixing of groundwater types in the borehole, in the case of Äspö the mixing of non-saline with saline would appear to pose the greatest problem. The degree of mixing will depend on the hydraulic properties of the borehole and possibly on groundwater density variations. As shown in Table 3.1. testing and sampling from borehole KAS02 lasted from November 1987 to May 1990, a period of two and a half years. However, the near continuous perturbation of the borehole waters during this time may well have prevented any open hole equilibration of groundwater flow in the bedrock that could have resulted in long-term mixing.

3.2.3. During Sampling.

Sampling from conductive borehole sections (selected on the basis of drillcore mapping, geophysical logging, spinner surveys and hydraulic testing) is carried out by isolating the desired section using an inflation packer system; straddle lengths of 3 to 15 m were used. The procedure is well established and the packer systems should be accurately positioned without any major problem. Nevertheless, short-circuiting along fracture networks can lead to borehole water (upper and lower levels) being forced around the packers via the bedrock, or groundwater from higher or lower horizons being brought into the sampling section. These problems can arise when the conductivity of the section being sampled is insufficient and/or the pump flow rate is excessively high. When possible, one tried to minimise such occurrences at Äspö using very low pump flow rates, in the order of 60 to 200 mL/min (A-C Nilsson, 1989).

3.2.4. Conclusions.

In general, the methodology used at Äspö has been such that groundwater contamination during borehole activities could, in some cases, be problematic (e.g. the fact that most of the borehole logging and hydraulic testing was carried out prior to groundwater sampling) but was minimised in others (e.g. in some cases with the implementation of low pump flow rates). Furthermore, the large variation in salinity with depth may, during borehole activities, result in some enhanced salinity of the higher level groundwaters and a corresponding dilution of deeper level groundwaters. The extent of any contamination will depend to a large degree on the borehole hydraulics.

Tables 3.1. and 3.2 illustrate the series of borehole activities, some of which might be expected to result in groundwater contamination. Unfortunately the data for the two most sensitive indicators for near-surface water contamination, the percentage of tagged activity water (i.e. drilling water and hydraulic injection test water) and tritium, are incomplete, especially for tritium. However with those data available, tritium was plotted against percentage tagged activity water (Fig. 3.2) in order to test qualitatively whether the tagged activity water could be the main source of contamination. The figure shows no correlation, even allowing for dilution of the original tritium content in the HAS05-derived activity waters. This indicates that other groundwaters from different levels and sources (i.e. untagged) are also present.

Available data for borehole KAS02 indicate minimal contamination. The tagged activity water component, apart from the initial stages of the pump test at 0-924 m (March '88) and the groundwater sampling at 202-214.5 m (December '88), is consistently under 1%, considered an acceptable level (A-C. Nilsson, 1989), and the tritium values are near the level of detection. The tritium content for the drilling water, i.e. from borehole HAS05, is not known, but HAS13, one of the drilling water sources in the southern part of Äspö, records only 1.2 TU. In general, therefore,

without considering the major ion chemistry and the redox parameters which are detailed in section 5, it would appear that by the time the groundwaters were sampled from KAS02, little residual borehole water remained in most of the borehole sections tested and sampled.

Table 3.2: Sequence of some activities carried out in borehole KAS03

Borehole Activity	Date	Section (m)	Drilling water (%)	Tritium (TU)
Drilling	880104 - 880407	0 - 1002		
Air-lift Test	880302 - 880302	540 - 640		
Air-lift Test	880321 - 880321	640 - 780		
Pump Test 1 (DWS)	880418 - 880420	0 - 1002	21-4	
Spinner Survey	880418 - 880420	0 - 1002		
Injection Test	880429 - 880429	103 - 373		
Injection Test	880429 - 880429	673 - 1002		
Injection Test	880518 - 880518	103 - 932		
Injection Test	880519 - 880520	103 - 163		
Injection Test	880520 - 880603	163 - 484		
Injection Test	880821 - 880823	373 - 673		
Injection Test	880628 - 880630	484 - 550		
Pump Test 2	880807 - 880810	196 - 223		
Chemical Sampling	880807 - 880810	196 - 223	8.43-2.70	
Pump Test 3	880813 - 880816	347 - 374	7.89-0.83	
Pump Test 4	880819 - 880822	453 - 480		
Chemical Sampling	880819 - 880822	453 - 480	3.62-2.13	
Pump Test 5 (DWS)	880825 - 880828	248 - 251	2.68-1.04	
Pump Test 6	880831 - 880803	609 - 623		
Chemical Sampling	880831 - 880903	609 - 623	3.92-2.23	
Pump Test 7	880906 - 880909	690 - 1002		
Chemical Sampling	880906 - 880909	690 - 1002	2.92-2.57	
Chemical Sampling	890212 - 890222	129 - 134	0.08-0.06	0.15
Chemical Sampling	890308 - 890316	860 - 1002	3.92-2.23	0.40
Chemical Sampling	900509 - 900613	533 - 636		
Tracer Test (C2)	900718 - 900726	107 - 252		
Tracer Test (C5)	900718 - 900730	537 - 626		

DWS = Drilling Water Sample.

For borehole KAS03, with the exception of section 129-134 m, all sections for which data are available indicate higher than acceptable levels of drilling water (>1%); the single tritium value (0.15 TU) indicates no surface or near-surface water component. The absence of tagged activity water in the shallowest section supports the ascertion above that the initial approx. 100 m of bedrock is of low conductivity and very little drilling water has penetrated along the sampled zone. In general contrast with KAS02, therefore, there still remains residual tagged activity water in the bedrock immediate to borehole KAS03.

4,5

4,0

3,5

3,0

2,5

3H(TU)

2,0

1,5

1,0

0,5

0,0

0,0   0,1   0,2   0,3   0,4   0,5   0,6   0,7   0,8   0,9   1,0

DrillWater (%)
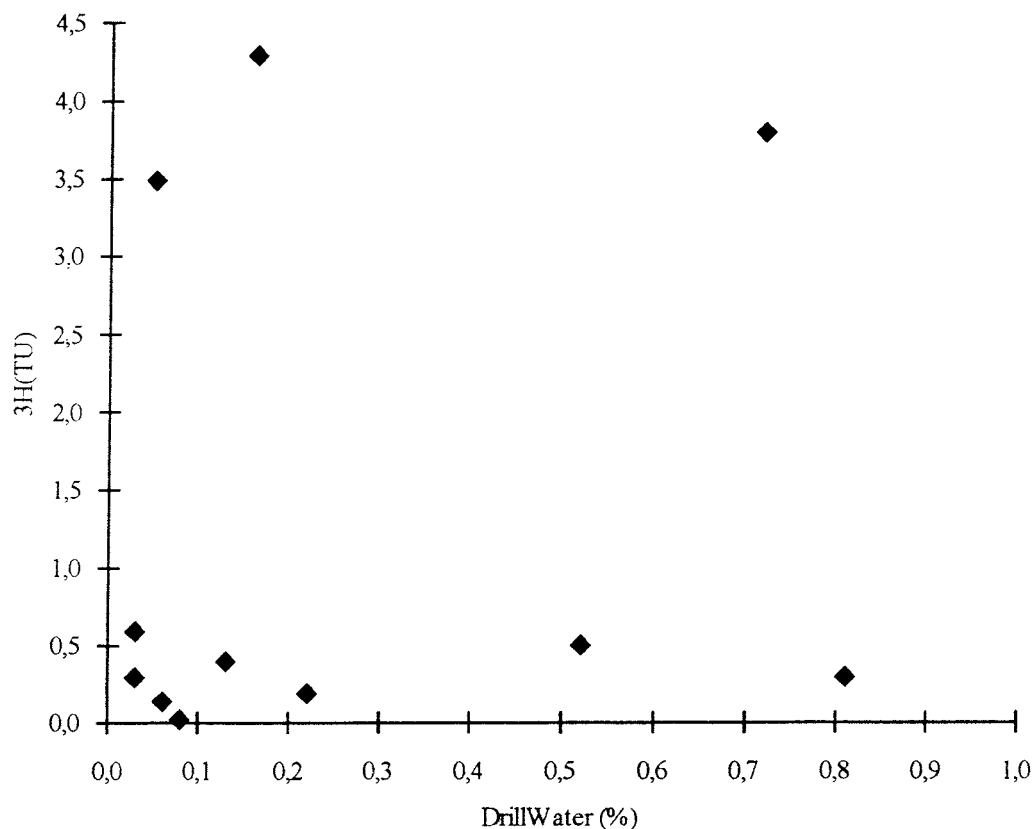
Figure 3.2. Plot of tritium (TU) vs. tagged (uranine) activity water (%)
    for the Äspö groundwaters.

In both boreholes the question still remains whether untagged groundwaters from other sources have been completely removed. This is is more difficult to determine, particularly bearing in mind the presumed low initial tritium content of the HAS05 groundwaters used in the borehole activities. This is partly illustrated in boreholes KAS04 and KAS06 (Table 3.3). From one horizon in KAS04 (226-235 m) and two horizons in KAS06 (204-277 m and 439-602 m respectively) the percentage of tagged activity water is very low to negligible (0.05-1.19%). Tritium, on the other hand, shows values ranging from 3.50-4.30 TU. This would explain some of the lack of correlation in Figure 3.2 and also support the previous assertion that groundwaters from other bedrock levels are also a potential source of contamination.

Table 3.3: Chemical sampling carried out in boreholes KAS04 and KAS06.

Borehole Activity	Date	Section (m)	Drilling water (%)	Tritium (TU)
Borehole KAS04.				
Drilling	880317 - 880501	0 - 481		
Chemical Sampling	890329 - 890403	440 - 481	0.08-0.04	0.03
Chemical Sampling	890409 - 890418	226 - 235	0.19-0.15	4.30
Chemical Sampling	890420 - 890427	334 - 343	0.63-0.52	0.50
Borehole KAS06.				
Drilling	881212 - 890129	0 - 602		
Chemical Sampling	890612 - 890615	389 - 406	0.24-0.03	0.60
Chemical Sampling	890605 - 890608	304 - 377	0.33-0.04	0.30
Chemical Sampling	890529 - 890601	204 - 277	1.19-0.72	3.80
Chemical Sampling	890619 - 890622	439 - 602	0.15-0.05	3.50
Tracer Test (F5)	890820 - 890824	191 - 249		
Tracer Test (F1)	890820 - 890824	431 - 500		
Tracer Test (F5)	890926 - 891010	191 - 249		
Tracer Test (F1)	890926 - 891010	431 - 500		

3.3. Groundwater sampling and analysis.

An outline of the sampling protocol, sample treatment and the analysis carried out, is given by A-C. Nilsson, (1989; 1991). In general, sampling was conducted on three occasions: during drilling (as described above), sampling for complete chemical characterisation using specified packed-off borehole sections, and sampling during pumping tests. The basic sampling and analytical equipment is essentially similar to that described by Almén et al. (1986), Axelsen et al. (1986) and Wikberg, (1987). The integrated equipment system used is schematically illustrated in Figure 3.3.

3.3.1. Sampling and Sample Preparation.

For complete hydrochemical characterisation the groundwater is essentially pumped up from chosen water-conducting sections in the bedrock sealed off by inflatable rubber packers with an adjustable straddle length. The hydraulic conductivity of these sections averaged between 10^{-8} ms^{-1} and 10^{-6} ms^{-1}. A hydraulically operated piston pump is placed in connection to the packers giving a maximum flow of about 250 mL/min. It has the capacity of reducing the pressure within the sampled section by more than 1 MPa. The Eh and pH values were monitored both at the bedrock

surface, when the water is pumped through a flow-through cell located in the mobile laboratory, and by a downhole probe (Eh and pH) located within the sampling interval of the packer system. Three different types of Eh probe were used: gold, platinum and glassy carbon.

ANALYSED PARAMETERS

FIELD LABORATORY

1. Flow meter
2. Surface chemical probe (pH, Eh, pS, pO$_2$ conductivity)
3. Calibration unit
4. In line filter 0.45μm
5. Carbon-14 sampler
6. Sampling for:
   A. Field analysis
   B. External analysis
   C. Backup storage

DRILLING WATER CONTENT:
Uranine
DISSOLVED ELEMENTS:
Na K Ca Mg Si O$_2$ Mn
Fe (tot) Fe (II) HCO$_3$ F Cl
Br SO$_4$ S(-II) NO$_2$ NO$_3$
NH$_4$ PO$_4$

DISSOLVED ELEMENTS:
Na K Ca Mg Si Mn
Fe (tot) HCO$_3$ F Cl S(-II)
NO$_2$ NO$_2$+NO$_3$ NH$_4$ PO$_4$ Al
Sr Li I Ra Th U Rn
FILTER RESIDUES:
Ca Al Fe Mn S Si
ISOTOPES:
^{2}H ^{3}H ^{18}O ^{13}C ^{14}C ^{234}U
ORGANICS:
TOC Fulvic and humic acids

DOWNHOLE CHEMICAL PROBE: pH, Eh

GAS SAMPLER

PUMP

GASES:
N$_2$ O$_2$ H$_2$ CO CO$_2$ Ar He
CH$_4$...C$_4$H$_{10}$

Figure 3.3. Schematic representation of the water-flow system from borehole to analysis (Almén et al., 1986).

Following installation of the packers and the downhole equipment the pump is started and the capacity is adjusted to give as high a water flow as possible without exceeding a pressure drawdown of 0.5 MPa (= 50 mwc). Pumping is continued until a stable groundwater composition is achieved, on average after at least two days. When stability is achieved, it is often the continuous change in composition of the main constituents that determines the length of the ensuing sampling period. At Äspö 2-4 weeks were sufficient for each section at flowrates which varied between 60-120 mL/min.

In contrast to the low pump extraction rates used in the complete chemical characterisation protocol, groundwaters sampled during pump testing have resulted from high extraction rates (anything from 4 000 to 115 000 mL/min) which in some cases may have exceeded the pump pressure drawdown.

The groundwater pumped up into the mobile laboratory normally passes through an in-line 0.45 micron filter before it is collected for analyses. However, when samples for iron and manganese determinations are collected, a 0.45 micron single-use poly carbonate filter is used. This kind of filter is also used under special circumstances for the determination of particle fractions in the water. In this case the water passes through a series of filters with a range of pore sizes grading from 0.45 to 0.2 to 0.05 microns. The particle fractions collected on these filters are analysed for Fe, Al, Mn, S, Ca, Mg and Si. The filtrate is analysed for total and ferrous iron.

The groundwater is constantly pumped up into the mobile laboratory and samples for different analyses are taken when required (immediately prior to the actual determination). Collected water samples during a one day period receive the same sample number. Generally no preservation is needed, except for samples to be sent for external analyses or stored for reference.

Samples collected for analysis in the mobile laboratory.

The sample volumes needed for the main constituent analysis are 1 litre untreated and 1 litre acidified by hydrochloric acid. Some samples require to be collected in specially prepared vessels, for example:

- Hydrochloric acid is added to the empty volumetric flasks prior to sampling for iron determinations.

- The samples for sulphide determinations are collected in glass bottles (so called Winkler bottles with a ground glass stopper), with a calibrated volume close to 150 ml, and analysed immediately.

Samples collected for control analyses or special analyses.

These samples are collected at the same occasion, once a week or once per sampled borehole section.

- The control sample for sulphide is preserved by the addition of sodium hydroxide and zinc acetate.

- Samples used for cation analyses by ICP-AES or AAS in external laboratories are preserved by addition of hydrochloric acid up to 1 % by volume.

- A 5 litre unfiltered sample is needed for the uranium, radium, radon and thorium analyses performed at Studsvik Energiteknik.

- A 5 litre acidified sample is needed for the determination of the uranium isotope ratios at the Avdelningen för radiofysik, Lasarettet i Lund.

- A 1 litre unfiltered sample is needed for tritium and an unfiltered 100 mL for ^{18}O and deuterium; determinations are carried out at the "Institut för Energi Teknik", Kjeller, Norway.

- A 1 litre sample is needed for tritium determination at the IAEA, Vienna.

- Sample collected for radiocarbon (^{14}C). In this case the carbonate content of 130 litres of water is required to be reduced to a volume of 1 litre by acidifying the water with hydrochloric acid, expelling the CO_2 by nitrogen, and trapping it in a bottle containing sodium hydroxide through which the gas passes. If a tandem accelerator is available, this pre-concentration process is not necessary.

As mentioned above, the groundwater pumped up into the mobile laboratory passes through an in-line 0.45 micron filter before it is collected for analysis. In special cases the water is filtered through a series of filters with a range of pore sizes grading from 0.45 through 0.2 to 0.05 microns. The particle fractions collected on these filters are analysed for Fe, Al, Mn, S, Ca, Mg and Si. The filtrate is analysed for total and ferrous iron.

3.3.2. Analysis and Quality Assurance.

For the analysis of deep groundwaters great care has to be taken to avoid changing redox conditions during sampling and analysis. The elements analysed are those considered most important for the safety assessmnet of a nuclear waste repository. The main constituents, Na, K, Ca, Mg, Cl, HCO_3 and SO_4 indicate the groundwater residence time in the rock by showing the extent of the rock/water interaction.

The anions of this group are potential complexing agents and are thus important for the calculation of waste canister corrosion, dissolution and transport of the nuclides comprising the waste, assuming a worse case scenario. F, Br, PO_4 and SiO_2 are useful for identifying the origin of the water and the state of equilibrium. Fe(II), $Fe_{(tot)}$ and S(-II) are primarily analysed in order to describe the redox conditions and thus to support the Eh measurements. They also give information on the buffer capacity of the water.

In the field laboratory the contents of the main constituents and redox sensitive elements are continuously analysed to achieve an immediate feed-back of the groundwater composition and stability. This allows the analytical protocol to be constantly modified during sampling and analysis. Furthermore, this system enables

the redox sensitive elements to be analysed immediately without atmospheric contamination.

The field analysis are carried out using an ion chromatograph, by spectrophotometry and by titration. Uranium, radium and radon are determined by neutron activation; alpha spectrometry is also used to determine uranium in addition to measuring the $^{234}U/^{238}U$ activity ratios. Tritium and the stable isotopes ^{18}O and deuterium are anslysed by natural decay counting and mass spectrometric methods respectively. Most components are analysed regularly and by more than one method. For example, one sample per pumping day was analysed both in the field laboratory and by inductively-coupled plasma (ICP) at the Royal Institute of Technology, Stockholm. Control analyses were carried out weekly, or, once at each sampled level at the pumping period, by separate laboratories, namely the "Institut för Vatten- och Luftvårdsforskning" (IVL) or Miljöanalytiska Laboratoriet AB (MILAB). The laboratories involved, the analytical methods employed, and the ionic species analysed, are listed in Table 3.4. Since 1990, the control analyses have been carried out by the Swedish Geological Company (SGAB) in Luleå.

An integral part of the analytical protocol has been devoted to quality assurance evaluation of the analytical methods, the reliability of the analytical data and the storage and accessibility of the database.

Table 3.4: Methods, laboratories and detection limits of analyses performed in the laboratory and in the field. (Modified after A-C. Nilsson, 1989).

Method	Element	Laboratory	Detection limit (mg/l)
IC	Na	MFL	0.1
ICP-AES	"	KTH	0.04
AAS (Flame)	"	IVL	0.005
Titr. (SIS 028119)	Ca	MFL	2
ICP-AES	"	KTH	0.006
AAS (Flame)	"	IVL	0.02
IC	K	MFL	0.1
ICP-AES	"	KTH	0.04
AAS (Flame)	"	IVL	0.005
Titr. (SIS 028121)	Mg	MFL	0.4
ICP-AES	"	KTH	0.0001
AAS (Flame)	"	IVL	0.001
Spect. (P-H Tamm)	Si	MFL	1
ICP-AES	"	KTH	0.004
AAS (Flame)	"	IVL	0.2

Table 3.4. contd.

Method	Element	Laboratory	Detection limit (mg/l)
Spect. (P-H Tamm)	Mn	MFL	0.01
ICP-AES	"	KTH	
AAS[1]	"	IVL	
Spect. (Ferrozine)	$Fe_{(tot)}$	MFL	0.005
ICP-AES	"	KTH	0.002
AAS (Furnace)	"	IVL	0.001
AAS (Flame)	"	IVL	0.05
Spect. (Ferrozine)	$Fe_{(II)}$	MFL	0.005
ICP-AES	Sr	KTH	0.0001
AAS (Flame)	"	IVL	0.05
ICP-AES	Li	KTH	0.001
AAS (Flame)	"	IVL	0.001
ICP-AES	Al	KTH	0.009-0.03
AAS (Furnace)	"	IVL	0.001
Titr. (SIS 028120)	Cl	MFL	10
FIA/Spect.(SIS 028133)"		IVL	1
Pot. (SIS 028135)	F	MFL	0.1
Pot. (SIS 028135)	"	IVL	0.1
Titr. (SS 028139)	HCO_3	MFL	0.5
Titr. (SS 028139)	"	IVL	0.5
Spect. (SIS 028115)	S^{2-}	MFL	0.01
Spect. (SIS 028115)	"	MILAB	0.01
IC	SO_4	MFL	0.05
ICP-AES	S_{tot}	KTH	0.02
Spect. (SS 028126)	$P-PO_4$	MFL	0.002
Spect. IVL Method	"	IVL	0.001
Pot. (Orion Method)	I	MILAB	0.05
IC	Br	MFL	0.05
Spect. (SIS 028132)	$N-NO_2$	MFL	0.001
Spect. (SIS 028134)	$N-NH_4$	MFL	0.005
Indust. Method No. 329-74 W/A	"	IVL	0.01

Table 3.4. contd.

Method	Element	Laboratory	Detection limit (mg/l)
FIA./Spect. (SIS 028133) Tecator ASN 62-01/83	$N-NO_2 + N-NO_3$	IVL	0.005
Astro. M. 2001	TOC	IVL	0.5
Neutron Activation	Natural U	Studsvik	-
	Ra	"	$8.5E^{-3}$ Bq/L
	Rn	"	-
	Th	"	$5.0E^{-4}$ μq/L
Alpha Spectrometry	$^{235}U/^{238}U$ $^{234}U/^{238}U$	Radiofysik Lund	
Natural Decay Counting Mass Spectrometry	^3H ^2H ^{18}O	Energi Teknik Kjeller "	8 TU - -
Natural Decay Counting	^3H	IAEA, Vienna	<0.1 TU

MFL	- Mobile Field Laboratory
IVL*	- Institut för Vatten- och Luftvårdsforskning
MILAB	- Miljöanalytiska Laboratoriet AB
IC	- Ion Chromatography
ICP-AES	- Inductively-Coupled Plasma Atomic Emissiom Spectroscopy
AAS	- Atomic Absorption Spectroscopy
Titr.	- Titrimetric Method
Spect.	- Spectrophotometric Method
Pot.	- Potentiometric Measurement
FIA./Spectr.	- Flow Injection Analyses followed by Spectrophotometric Detection.
Astro. M.	- Carbon Analyser (ASTRO trademark)
* SGAB since 1990	

3.3.2.1. The GEOTAB database.

A considerable volume of field and analytical data have been collected since SKB commenced site-specific investigations in 1977. It was therefore considered expedient to store all data in a single, integrated database easily accessible to the general scientific community. The database, knwn as GEOTAB, is a relational database based on a concept from Mimer Information Systems and further modified by Ergodata. The hardware consists of a VAX computer located at KRAB (Kraftverksbolagens Redovisningsavdelning AB) in Stockholm, and data are stored on-line. Several reports are available describibg GEOTAB, most recently summarised by Eriksson and Sehlstedt (1991) and Eriksson et al. (1992).

The groundwater hydrogeochemical investigations at Äspö generated three different types of chemical data (A-C. Nilsson, per.comm. 1991):

* Computer controlled (automated) measurements of pH, Eh etc.

* Analyses of the water composition, major and trace components

* Special analyses, i.e. determination of isotopes, dissolved gases and particulate matter in the groundwaters

Before filing, the chemical data were subjected to quality control and an overview of the data treatment is illustrated schematically in Figure 3.4. Furthermore, all primary data are stored separately on tape making it possible to trace different types of data and allow reevaluation if necessary.
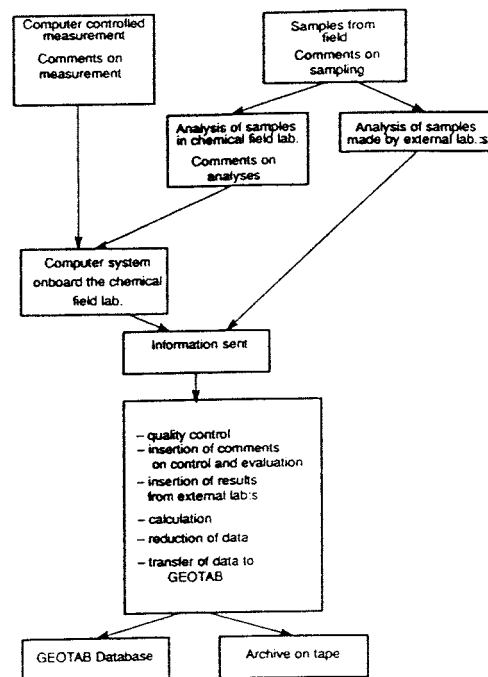

Figure 3.4. Schematic illustration of the data quality control treatment.

3.3.2.2. Quality control of groundwater analyses.

As listed in Figure 3.4, the major part of the groundwater analyses have been
performed in the mobile field laboratory (MFL). Control analyses by independent
laboratories (mostly IVL), and a direct on-going comparison of the analytical data,
have been considered the best approach to check the reliability of the results. There
have been changes in the laboratories involved and the analytical techniques
employed during the four years that the Äspö investigations have been in progress. A
breakdown of the quality control protocol since 1987 is as follows:

* Prior to 1989 one sample was analysed daily in the field (MFL) and one sample
  was dispatched weekly to IVL for analysis

* From 1989 to 1990 the cations were analysed by ICP-AES at KTH in addition to
  in the field (MFL). The number of control samples sent to IVL was reduced to
  one, taken from each sampled level at the end of each sampling period.

* From 1990 to 1991 the weekly monitoring of the groundwater chemistry in a
  number of borehole sections was performed without the field laboratory. In these
  cases the samples were analysed at KTH by ICP-AES, and the anions by standard
  methods. Control samples, sent to SGAB for ICP-AES major ion analysis, were
  also analysed for some trace elements by ICP-MS (not included in Table 3.4).

Generally over the last four year period the ionic concentrations determined by the
various laboratories have agreed within 10%, although this is to large extent
dependent on the element in question and its concentration. When a large disparity
was noted, the analyses were repeated. As an example of interlaboratory analytical
control, Table 3.5 shows a typical comparison of ICP analyses from borehole KAS03
carried out by KTH (ICP-AES) and SGAB (ICP-AES). When the analytical sets from
the various laboratories were considered to be in good agreement the data were
compiled and further evaluated to produce a final dataset of representative
concentration values for each sample.

Table 3.5. Borehole KAS03 (level 533-636 m): interlaboratory comparison of ICP
groundwater analysis.

ICP	Na mg/L	K mg/L	Ca mg/L	Mg mg/L	Sr mg/L	Mn mg/L	Li mg/L	Fe_{tot} mg/L	S mg/L
KTH	1700	7.5	1340	42.0	23.6	0.32	0.72	0.08	116.0
SGAB	1700	7.8	1330	40.1	24.2	0.28	0.82	0.06	116.3

Charge imbalance errors can be a very sensitive indication to the analytical quality of the analysis. The following equation was used:

$$100 \times \frac{(\text{cation equivalent/litre} - \text{anion equivalent/litre})}{(\text{cation equivalent/litre} + \text{anion equivalent/litre})}$$

As inferred above, the charge balance errors for the Äspö samples rarely exceeded 5% which is considered acceptable. Figure 3.5 illustrates the distribution of charge balance errors for 53 groundwater analyses from the Äspö area. The charge balance errors all lie within 4%.

Number of samples
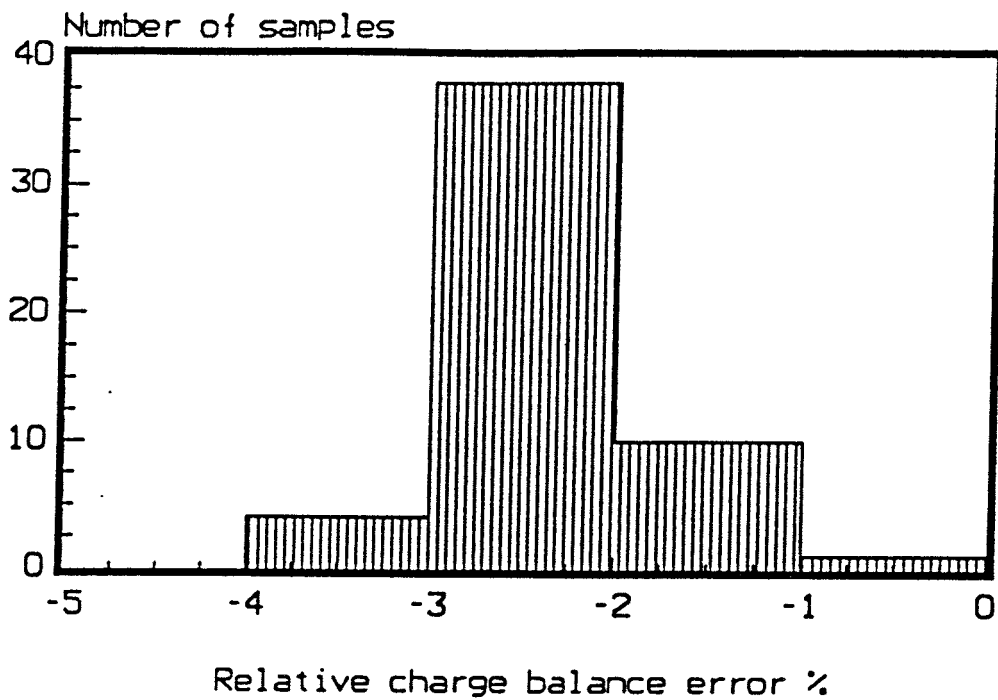
Relative charge balance error %

Figure 3.5. Distribution of charge balance errors for 53 groundwater analyses for the Äspö area (after A-C Nilsson, 1991)

3.3.2.3. Performance control of the mobile field laboratory (MFL).

Water analyses

All the primary analytical data are computerised and stored daily in the field laboratory. These data include instrument readings, dilution factors, control standards, control factors, calibration etc. The raw data are checked and than saved separately on data files in the Vax computer at SKB. This type of information can be used to detect changes in the analytical performance with time. For the spectrophotometric methods, as an example, calibration factors (abs/µg) are calculated from the calibration curves. A control standard, with a concentration close to the sample, is analysed at each analytical occasion, and a control factor (abs/µg) is calculated. If the control factor and the calibration factor disagree, a new calibration is carried out. The control factor is also a useful indicator for the long-term assessment of instrument performance.

Computer controlled measurements.

The performance of the electrodes and probes used in the computer controlled measurements are checked by means of calibrations and calibration constants. Calibrations are carried out at least once before, and once after, the measurements in the borehole section. If the measurement period is longer than two weeks additional calibrations have to be performed. The calibration data from the field laboratory are saved separately in the Vax computer. Stable readings between the electrodes involved in the redox and pH measurements are usually a good indication that the measurements have been successful. A plot of Eh against pH can be a useful tool to check the plausibility of the results.

3.3.2.4. Quality control on ICP-measurements at KTH.

Quality control of the analytical results provided by ICP-AES at KTH has been on-going since the beginning of 1989. Initially, the only actual control was the comparison of these results with those carried out by IVL, SGAB Analys and the Mobile Field Laboratory. Subsequently, control samples were introduced in the analytical protocol. Two certified artificial water samples were used as control blanks, and analysed at least once a day. Long-term statistics are obtained by plotting the analytical results of the control samples onto control charts.

4. General Features of the Äspö Hard Rock Laboratory (HRL) Site.

The following abbreviated account of the general features is based mainly on the reported studies of Almén et al. (1991), and Wikberg et al. (1991), and references cited therein. The Äspö HRL site is located in the Simpevarp area, southeast Sweden, about 20 km NNE of Oskarshamn. The island itself (approx. 1 km^2) is triangular-shaped with an irregular, serrated coastline and a mildly undulating topography. The northern coastline, in addition to the northern slopes in general, are steep. The central part of the island, which has the highest topography (13-15 m a.s.l.), is transected by an open east-west trending valley. Outcrop exposure is good (approx. 90%); otherwise only a thin moraine/soil cover exists mostly located within and along small depressions and valleys, thus facilitating surface geological mapping and ground geophysical surveys.

Investigations in the Simpevarp/Äspö area started in 1986 with an airborne geophysical survey of the of the Simpevarp region (approx. 25x35 km) followed up by ground geophysical surveys in the Laxemar area and on the islands of Ävrö and Äspö. Using landsat and digital models, in conjunction with aeromagnetic expressions, the regional lineament pattern was determined and related to the bedrock geology. Mapping of outcrop structures helped to describe the geometry of the major fracture sets and their relationship to the regional lineaments. Using available archive groundwater data, and relating these to the regional topography, an evaluation of the regional precipitation, evaporation, runoff and groundwater recharge was carried out. Some idea as to the regional groundwater flow pattern was also obtained.

This was followed by detailed studies focussing in on the island of Äspö. Surface studies included the mapping, geochemistry and petrography of the bedrock, ground geophysical surveys (e.g. VLF, resistivity, magnetic, radiometric, seismic refraction/reflection) and the analysis of ductile and brittle fracturation. An impression of the three-dimensional geology and hydrogeology of the area was obtained by drilling 20 percussion boreholes (total length of 2200 m) and 14 rotary cored boreholes (total length of 6600 m). Borehole investigations covered the areas of geology (rock units, fracture frequency, fracture mineralogy - identification and chemistry etc.), geophysics (identification and location of conducting fracture zones, different rock units, temperature/density measurements of the borehole water etc.) and hydrogeology (spinner surveys and hydraulic testing by injection and pumping to determine groundwater flow directions, bedrock conductivity and transmissivity etc.).

4.1. Geological features.

The geology of the Simpevarp region has been compiled and studied by Kornfält and Wikman (1987a and b) and Wikström (1989). The bedrock is dominated by granites and granitoids associated with the Småland-Värmland batholith and dated to within the range of 1760-1840 Ma (Jarl and Johansson, 1988). These granites are generally classified as being post-orogenic in relation to the Svecofennian, and should,

therefore, transect the dominant regional structures in the region. According to Wikström (1984) and Wikström and Aaro (1986) this is only partly true; many cases can be cited where the marginal rocks are observed to be conformably folded and deformed with the older bedrock. This has been presented as evidence that the granitoid intrusions have taken place coevally with on-going regional deformational processes producing, in places, high-grade metamorphism coupled with partial melting of the country rock (e.g. formation of high-amphibolite facies gneisses). The mafic enclaves and dykes in the granites have probably formed by a continuous magma-mixing and magma-mingling process, producing a very inhomogeneous rock mass ranging in composition from true granites to dioritic and gabbroic rocks.

The Småland granites exhibit a general foliation trending N70°E to E-W, mostly steeply dipping. These are often intruded by fine-grained, grey to red granites or aplites (as dykes and smaller massifs of 0.5 to 5 m in dimension) which may be a later post-orogenic magma differentiation phase, although an anorogenic origin cannot be excluded. A foliation can also be observed in this rock type.

Greenstones occur as large massifs (diorite-gabbroid composition) and as small lenses and sheets in the Småland granites. A finer-grained, homogeneous greenstone type, which is thought to be a metabasalt, can be observed to be transected by the fine-grained granite/aplite mentioned above. An intermediate group of grey, medium-grained rocks have been designated as a tonalite. This is massive, homogeneous, contains xenoliths of metavolcanics, and is also intruded by the Småland porphyry granites.

The Götemar, Uthammar and Virbo granites, dated to be some 300 Ma younger than the surrounding Småland granites, occur as diapiric intrusions in the area and are an important influence on the local geological and tectonic setting of Äspö area. Aeromagnetic anomalies surrounding some of these granites (i.e. positive Bouger anomalies and negative magnetic anomalies) suggest that most of the granite mass exists at depth. Many of the fine-grained granite/aplite dykes and smaller massifs mentioned above may be associated with these anorogenic diapirs.

The island of Äspö is characterised by a porphyritic granite-granodiorite with microcline megacrysts up to 1 to 3 cm in size. To the south of the island a redder granite variety, the Ävrö "true" granite, outcrops, containing small (<1 cm) sparsely distributed microcline megacrysts. Contained within the granite are east-west trending lenses/sheets of fine-grained greenstone (metabasalt) which are usually strongly altered. Subordinate lenses of fine-grained grey metavolcanites (of dacitic composition) also occur. Both of these rock types predate the Småland granite. Finally, small occurrences of pegmatite commonly occur as very narrow dykes (decimetres in size).

4.2. Tectonic features.

4.2.1. Regional Interpretation.

Regional lineament interpretation (Tirén et al., 1987) in the Simpevarp region (Fig. 4.1) points to the intersection of four main lineament sets, NW-SE and E-W (older) and N-S and NE-SW (younger), forming an orthogonal pattern, and presumed to reflect fracture zones in the area. Of the four lineament sets, the N-S and E-W sets dominate producing a suborthogonal first order system of lineaments. These can extend for some 20-50 km and often coincide with zones of low magnetic character some hundred or so metres wide; central to these zones, fracture zones of up to some tens of metres wide can also occur. The other lineament sets, the NW-SE and NE-SW trending features, represent second order zones of another almost orthogonal system. These are mostly 100-200 m wide and extend from 1 to 20 km. In general, the northern part of the region is characterised more by the NW-SE set and the southern part by the NE-SW; Äspö is located precisely at the intersection of two lineament pairs (E-W and NW-SW).

Aeromagnetic surveys (Fig. 4.2) indicate that well defined N-S fracture zones are about 100 to 200 m wide with vertical to subvertical dips; E-W trending fractures are more difficult to characterise but evidence shows them to include relatively shallow dips, often to the north, and achieving widths of up to 500 m (Nisca, 1987). Lateral displacements are thought to be small (100-300 m) for the former, and somewhat larger for the latter. In addition to being the most recently reactivated, there were indications to suggest that the N-S trending fracture zones are more likely to be water-bearing than the E-W variety. Finally, a conjugate shear system, comprising a set of fracture zones oriented NNE-SSW and NNW-SSE, was also observed.

Mapping of fracture zones from outcrop and road-cuttings etc. in the Simpevarp region supported many of the regional geophysical and landsat lineament interpretations. The most conspicuous pattern shows evident strike directions around NS and N50W, and also a strong E-W strike. Less marked, but nevertheless coinciding with the regional foliation, is a fracture set in a sector falling between N40°W and N65°E. Dips are mostly vertical to near-vertical although sub-horizontal structures have been observed in association with the the anorogenic granite diapirs (e.g. Götemar granite). Low-angled shear zones probably also exist, most likely associated with EW lineaments.

Fracture lengths for the different rock types were measured on outcrops; fractures were longest in the tonalite and porphyritic granite and shortest in the greenstones; the geometric mean value ranged from 0.6 to 1.2 m. Fracture density distribution was found to be log-normal and the median values were almost equal. The main rock types, i.e. the Småland granite and granodiorite, dominate, and the confidence interval (95%) for the mean value for these rocks was a density of 1.4 to 1.7
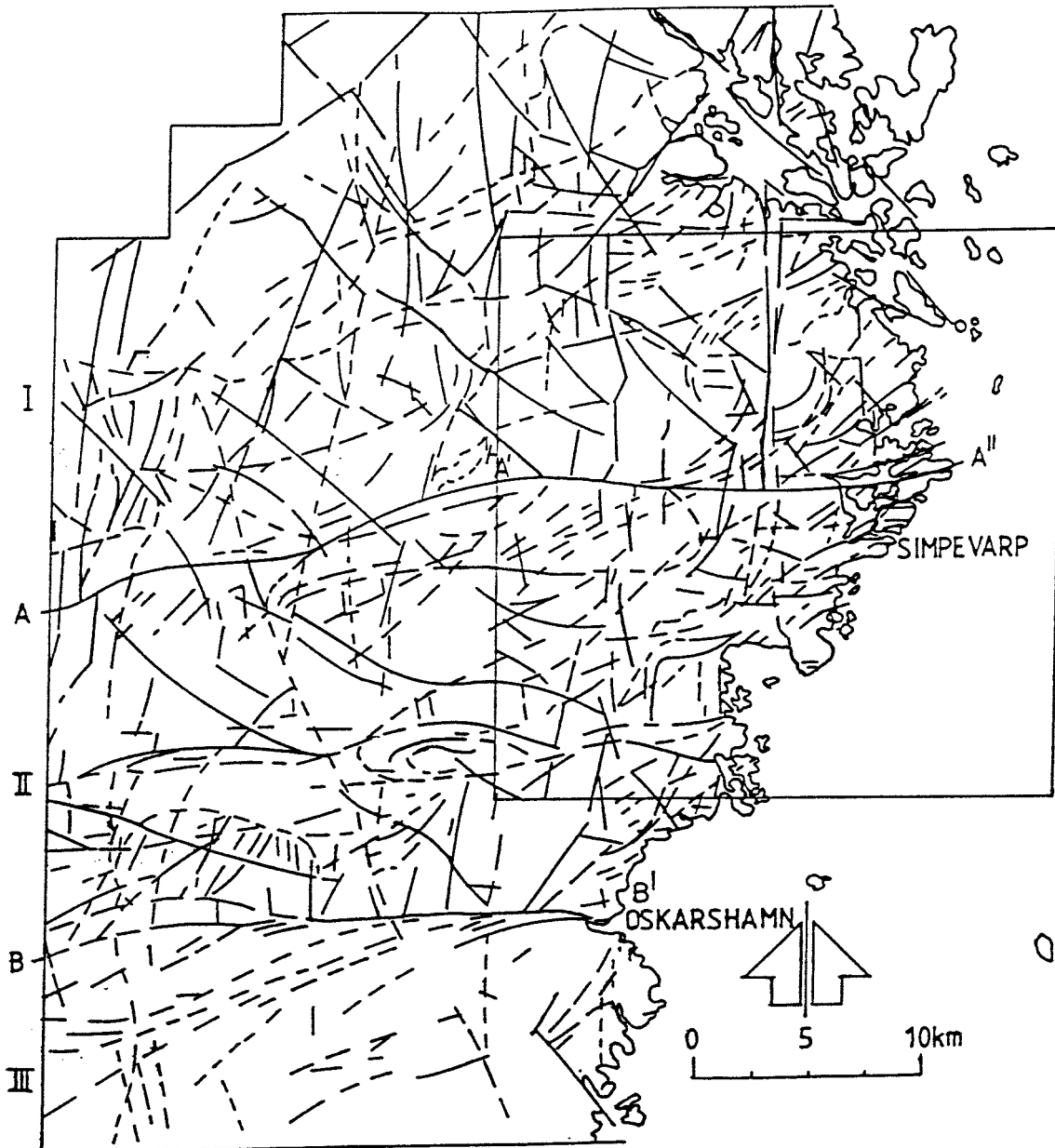
Figure 4.1. Relief map lineament interpretation of the Oskarshamn region
(after Tirén et al., 1987).

fractures per square metre. The main deformation mechanism giving rise to the observed structures in the Simpevarp region has probably been tensional and due to uplift.

4.2.2. Local Interpretation.

In general, the lineament pattern on Äspö is similar to the regional pattern interpreted from the adjacent mainland. According to Tirén and Beckholmen (1987), the island of Äspö is located within a triangular local block which is transected by three regional discontinuities. In the centre of Äspö two of these discontinuities (EW and NE trending) intersect, dividing the island into four blocks. The third discontinuity (N80°E trending) coincides with the northern shore line and is thought to be a shear zone. The most frequent lineament directions on the island are N5°W, followed by N45°W and N80°E, and the southern part of the island appears to be less deformed.

From outcrop mapping of two uncovered and cleaned NS rock profiles, a total of 25 fracture zones were recorded, mostly trending EW reflecting the Äspö shear zone direction (N55°E). Related to bedrock type, the longest fractures were associated with the porphyritic granite and the shortest with the mylonite; the fracture density of the fine-grained granite/aplite type was greater then the porphyritic variety. Geophysical logging of the drillcores (e.g. Sehlstedt et al. 1990) supports the high fracture density of the fine-grained granite/aplite.

The majority of the fractures on Äspö represent reactivated older structures and present patterns very much depend on the nature of the older structures being reactivated. For example, EW gneissic zones, NE or EW trending mylonites and gently dipping alteration zones etc. Fracture zones trending N, NE or EW normally had ductile precursors whereas those trending NW apparently did not.

4.2.3. Fracture Mineralogy.

The compiled geochronology of the Simpevarp region and the fracture mineral paragenesis is schematically presented in Figure 4.3 (Wikberg et al., 1991). Of major importance for the geology and tectonic setting of the region are the diapiric anorogenic intrusions of the Götemar and Uthammar granites some 1400 Ma ago. Furthermore, these intrusions have, by postmagmatic circulation of hydrothermal fluids, contributed significantly to the fracture mineralogy observed in outcrop and in the drillcore material.

From borehole investigations (Tullborg, in Wikman et al., 1988; Tullborg, 1989) the fracture mineralogy is dominated by chlorite, calcite, hematite and epidote; quartz, muscovite, laumonite, prehnite, fluorite and pyrite are also frequent together with low-temperature minerals such as Fe-oxyhydroxides; clay minerals are generally rare at Äspö.
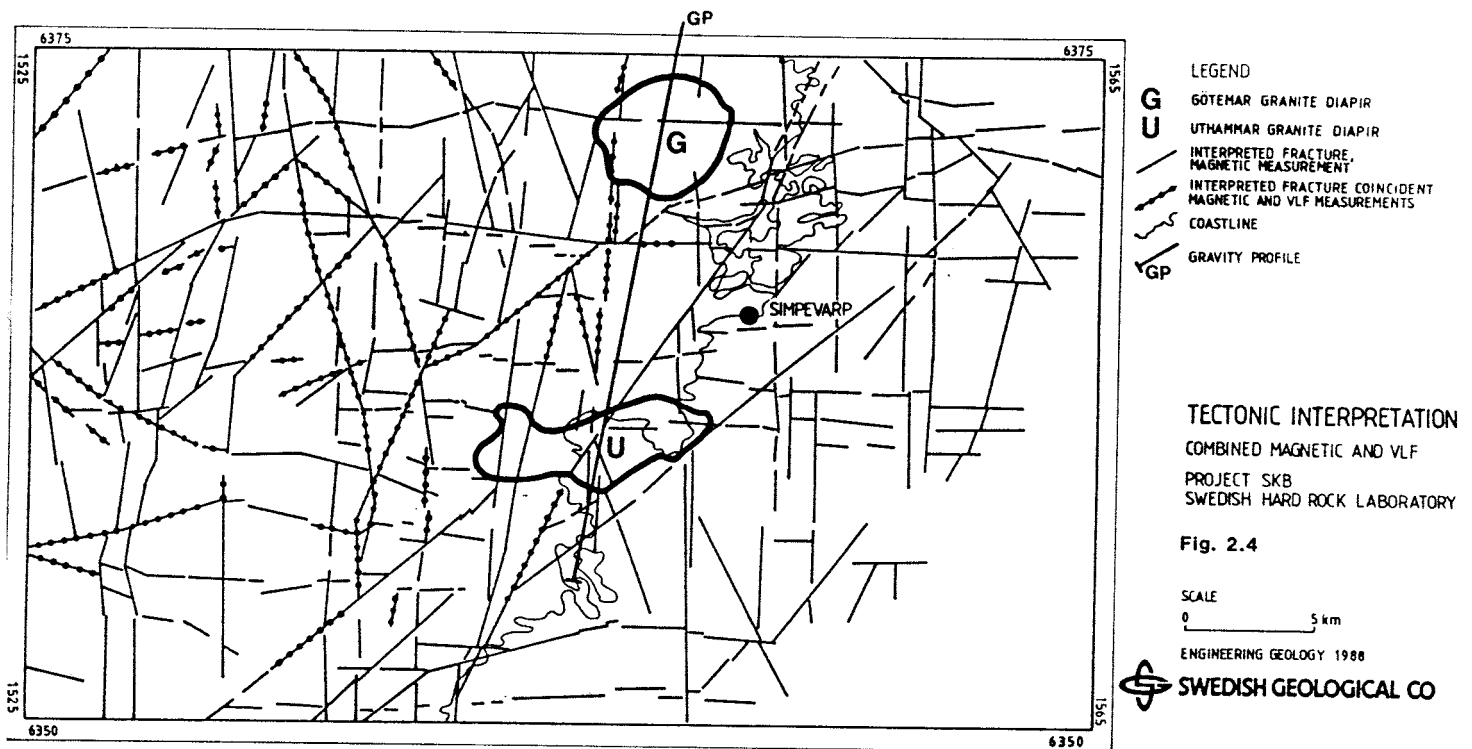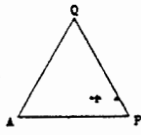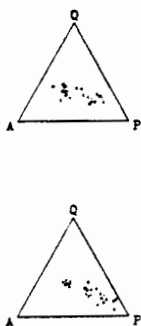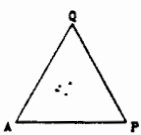
Figure 4.2. Basic fracture analysis of the Simpevarp area based on magnetic
and VLF measurements (after Nisca, 1987).

4.3. Generalised tectonic model of the Äspö HRL site.

Based on all available aerial, outcrop and borehole data, Wikberg et al. (1991) have presented generalised models for Äspö (Figs. 4.4 and 4.5). The island is divided into two main blocks by an NE-trending regional shear zone. In both blocks the Småland granite, with associated greenstones and fine-grained granite/aplite varieties, dominates, although in the southern block, below 300 m, more basic, dioritic varieties of the Småland granite begin to dominate.

The shear zone, which is vertical to subvertical to the north, consists of strongly foliated, heterogeneous Småland granite, containing a large number of mylonitic lenses and greenstone xenoliths. Highly fractured zones (5-10 m wide), alternating with more normally fractured rock, complicate the shear structure which has also undergone substantial weathering, seen as oxidation of magnetite to hematite and Fe-oxyhydroxides. This explains the negative aeromagnetic anomally.

CHRONOLOGIC SCHEME OF THE MAIN ROCK UNITS AND EVENTS IN THE SIMPEVARP AREA.

TIME SCALE, Ma (1)	ROCK UNIT (1)	MODAL CLASSIFICATION	ROCK TYPE (1) STRUCTURES (4, 5)	SEQUENCE OF EVENTS (2,3,4)	FRACTURE FILLINGS (2)
2000-1850	Oldest supracrustals		Metaandesites		
1925-1800	Primorogenic rocks		Gneissic granites Granodiorites		
1840-1760	Postorogenic Småland-Värmland granitoids		Porphyritic granite-granodiorite-diorite. Fine-grained granite. Mafic dykes and enclaves. Greenstone.	Continuos magmamingling and magma-mixing process. Regional deformation. Folding E-W to ENE-WSW foliation. Mylonitic shear zones.	Mylonites or "shear-bands" containing fine-grained epidote, muscovite and recrystallized quartz
1400-1350	Anorogenic rocks		Coarse-grained granite (Götemar-granite) Fine-grained granite Dolerite Chlorite veins.	Tension Post-magmatic hydrothermal circulation of the anorogenic granite	Fe-rich, idiomorphic epidote. One generation of fluorite. Growth of idiomorphic quartz, muscovite, hematite, fluorite, calcite and spherulic chlorite.
~1100				Burial metamorphism.	Prehnite, hematite-stained laumontite, calcite and fluorite.
600-300			Clastic dykes. Cambrian (?) sandstone. Post-chlorite veins. Fault scarps?	Burial metamorphism. Reactivation of older structures?	Gypsum, chlorite, illite, probably calcite and possibly Fe-oxyhydroxides.
Synglacial-present time			Fault scarps? Fractures?	Fracturing? Reactivation of older structures?	Calcite, Fe-oxyhydroxides and clay-minerals like kaolinite. Present groundwater circulation?

1 Kornfält-Wikman (1987) 2. Tullborg (1989) 3. Wikström (1989) 4. Talbot-Munier (1989) 5. Mörner (1990)

Figure 4.3. Geochronological summary of the major events in the Simpevarp area (compiled by Wikberg et al., 1991).

Outcrop and drillcore investigations clearly show that the northern block is more fractured than its southern counterpart; this is also reflected in the measured hydraulic conductivities which are lower in the southern block. Two subhorizontal zones, indicated by seismic reflection measurements (Fig. 4.5) at depths of 300-500 m and 950-1150 m respectively, have not been completely confirmed by drilling nor by hydraulic interference pump testing.

4.4. Surficial hydrological features.

4.4.1. Regional Features.

The Simpevarp region, characterised by thin layers of Quaternary deposits covered by overlying peat bogs in the depressions, is dominated by the Marströmmen and Virboån drainage basins which flow, respectively, into the Baltic Sea to the north and south of Simpevarp (Fig. 4.6); both cover distances of up to 40 km (Svensson, 1987). Between these two discharge points the eastern part of the coast is drained by a large number of small streams into the Baltic Sea. Of these, the Fighultebäcken, Släthultebäcken, Laxemarån and Gerseboån are the most important. The Virboån basin, the largest with a drainage area of 601 km^2, has a lake portion of 8.0% (the largest lake is Hummeln at 6.3 km^2). Marströmmen, with a drainage area of 486 km^2, has a lake portion of 7.0% with Sliss-sjön at 2.4 km^2 being the largest lake included. The Äspö site is located just off the coast near the discharge point of the Laxemarån into the Baltic Sea.

The water balance of the site area during the period 1951-1960, based on data from SE Sweden, has been roughly calculated to:

Adjusted precipitation:	675 mm/year
Potential evaporation:	616 mm/year
Actual evaporation:	490 mm/year
Run-off:	150-200 mm/year

Most of the precipitation falls during the late summer (July- 64 mm; August- 62 mm) and decreases slightly from autumn to spring. Of the annual precipitation 18.2 % falls as snow and the snow cover exists on average 91 days of the year (Nov. 30 to April 7); the annual mean temperature at Oskarshamn is approx. 6.4°C with February being the coldest month with a mean temperature of -2.9°C.

The run-off varies considerably over the year and patterns for both the Virboån and Marströmmen basins are similar. The main water volume is discharged during the spring snow thaw and during the late autumn rains; this results in discharge peaks in April and in Dec./Jan. respectively.
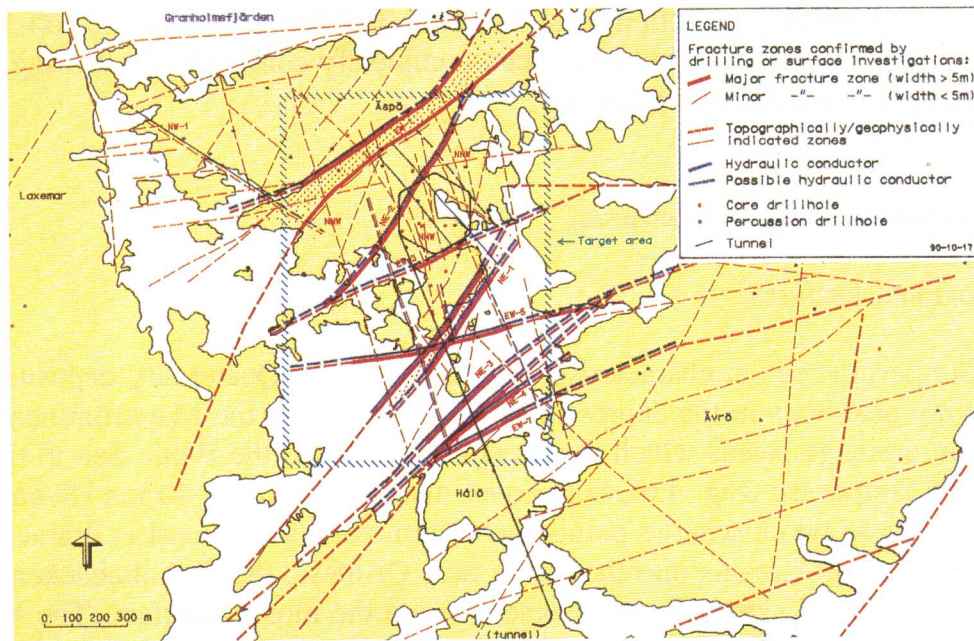
Figure 4.4. Generalised hydrogeotectonic model for the Äspö region (Wikberg, 1991).
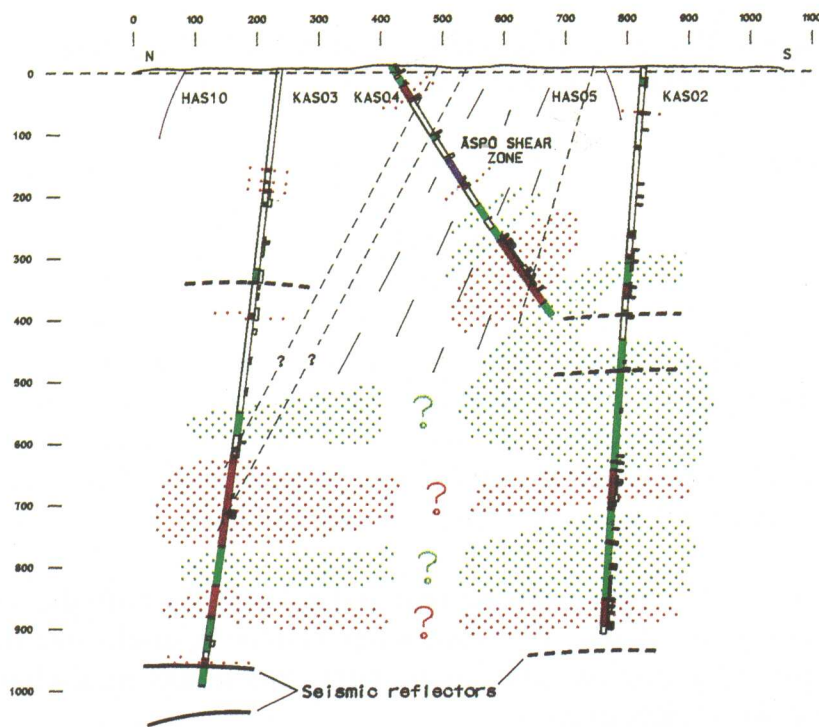
Figure 4.5. Generalised profile across Äspö island (Wikberg et al., 1991).
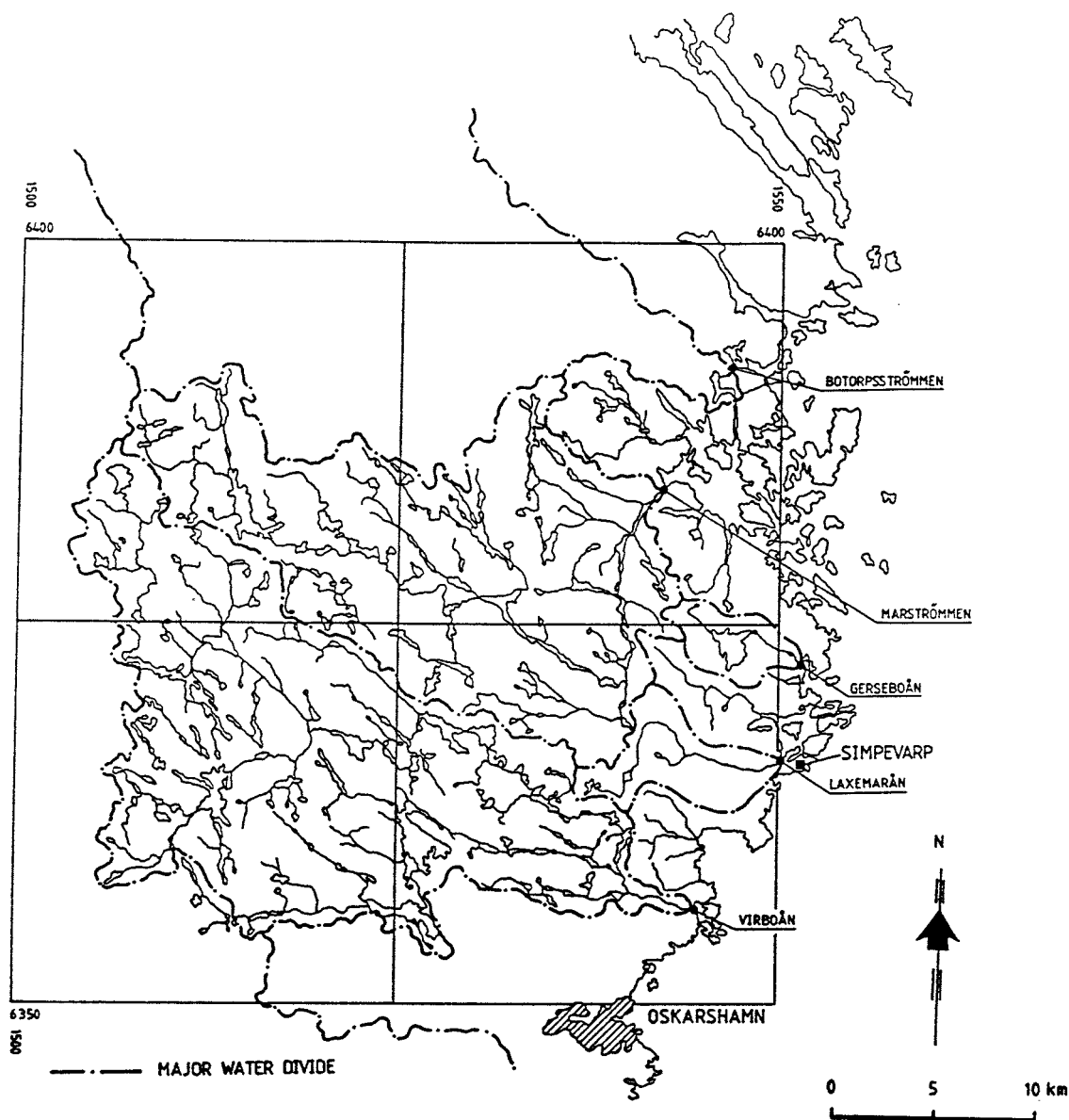
Figure 4.6. Regional drainage patterns influencing the Simpevarp area
(after Svensson, 1987).

The seasonal variation of the groundwater level in this part of Sweden generally shows a single minimum and maximum value during the year. The minimum value coincides with late summer and the main period of groundwater recharge is during the autumn; this is prolonged by the short mild winter so that the maximum levels occur in spring; sometimes there is a secondary winter minimum. The changes in pressure head are fast and show relatively large amplitudes. Groundwater recharge estimates for the region range from 128-218 mm/year in pervious terrain.

4.4.2. Local Features.

Äspö mostly comprises a slightly undulating topography (max. height of 10 m) of bare rock with an absence of perennial streams (Lindahl, 1989). Valleys and depressions tend to be filled with till and any surface drainage to the sea is indicated by marsh areas; some surface accumulations of water occur in the spring and autumn (Fig. 4.7).

Based on the limited topography a series of water divides describing the surface drainage conditions show that some local groundwater recharge probably occurs in the central part of Äspö (Fig. 4.8). From the regional evaluation described above, a precipitation surplus of around 185 mm/year is available for recharge/run-off processes following evapotranspiration. It has been estimated that the annual recharge at Äspö is approx. 3 mm/a.
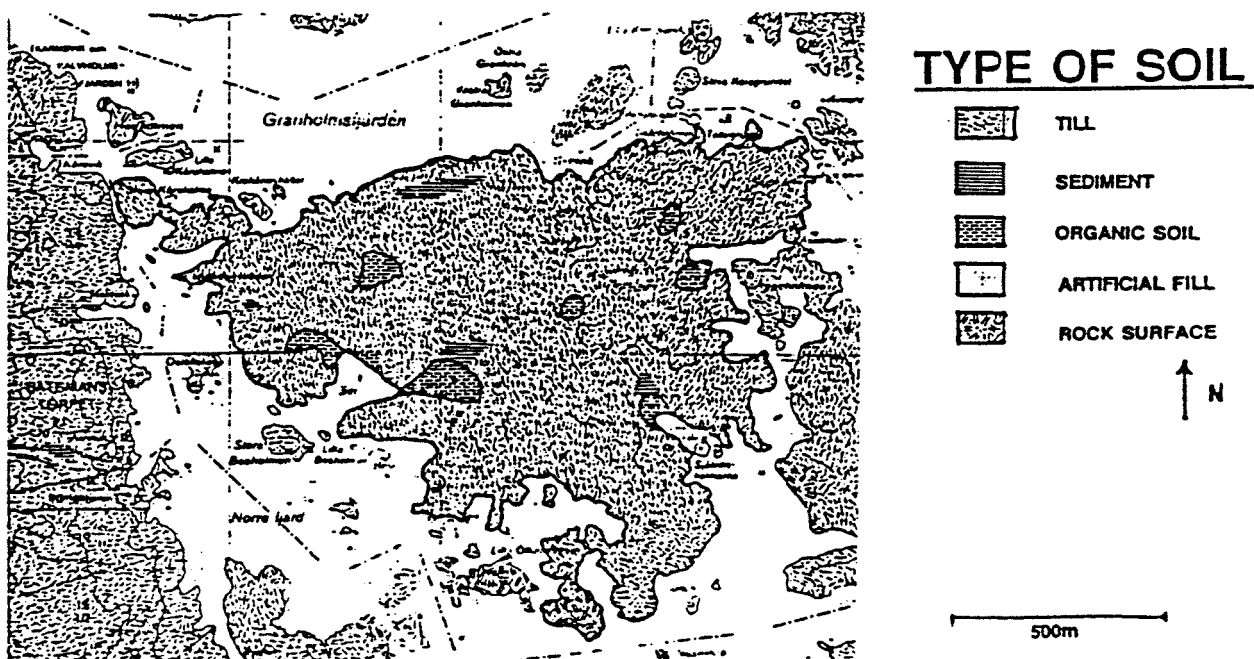

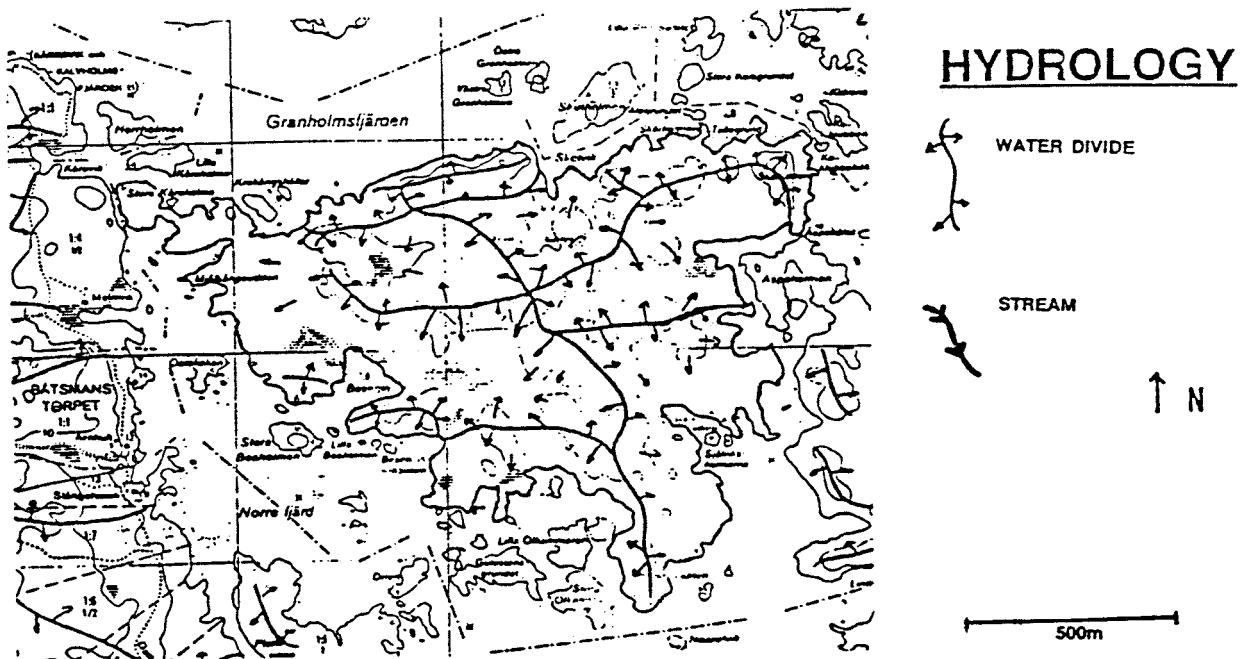Figure 4.7. Surface exposure and soil cover on Äspö (Lindahl, 1989).

Figure 4.8: Surface topography and drainage conditions on Äspö (Lindahl, 1989).

4.5. Bedrock hydrogeological features and groundwater flow.

4.5.1. The Conceptual Model.

Based mainly on surface and downhole geological and hydrogeological criteria, a conceptual structural subdivision of Äspö has been presented by Wikberg et al. (1991). This subdivision is illustrated in Figure 4.9. The hydraulic connection or transmissivity, if any, between the various zones, has been established using airlift and/or downhole interference pump tests, and recording groundwater level drawdowns in other adjacent strategically placed boreholes, drilled to intersect the major fracture or shear zones at different depths and angles. These structures, which are considered to be the main conductive pathways through Äspö, have been classified by Wikberg et al. (1991) as certain (EW-1, NE-2, EW-3, NE-1, NE-3 and NE-4), probable (NNW and EW-7) and possible (NNW, EW-5 and EW-X).

The areal distribution of hydraulic conductivity on the site scale at Äspö is heterogeneous as it depends on many interrelated variables such as rock type, fracture coating material and the length of the borehole section measured (Liedholm, 1990). Generally, the fine-grained granite/aplite tends to be the most conductive, probably because it is the most competent rock type and is therefore inclined to fracture easily in response to tectonic movement. In an analysis of conductivity vs. fracture coating mineralogy, Liedholm (op. cit.) found a correlation between higher conductivity and

hematite and Fe-oxyhydroxide coatings, lower conductivity and calcite coatings, and chlorite coatings gave intermediate ratings. Calcite and chlorite are by far the most common fracture coating phases in the open fractures.
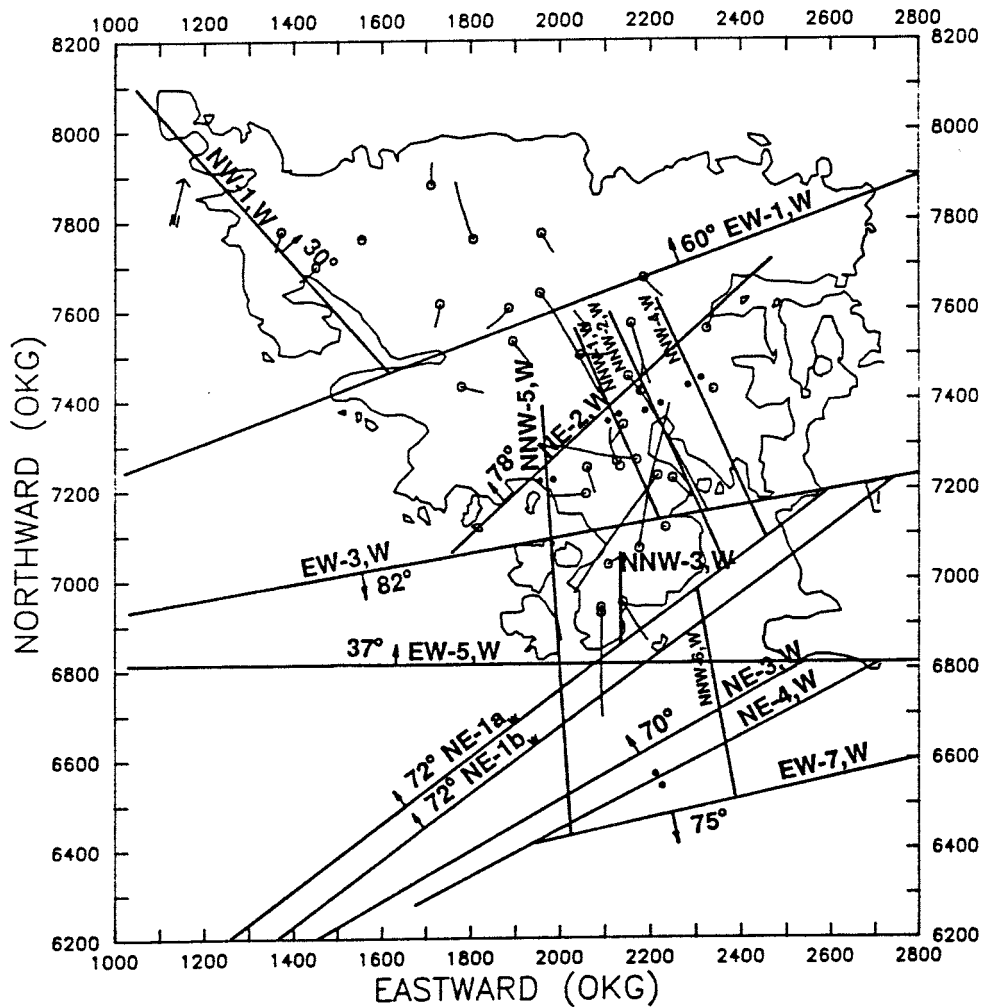
Figure 4.9. Conceptual structural subdivision of Äspö (from Wikberg et al., 1991).

Some large-scale hydraulic properties can, however, be acertained for Äspö, for example, in the upper 100 m the hydraulic conductivity tends to increase to the west, but is still lower than the mainland further to the west. In addition, there is an apparent weak correlation with depth whereupon the conductivity decreases, but this is only based on one borehole (KAS02) where diorite dominates. Other boreholes, if treated individually, may show an inverse relationship. In general the southern Äspö block is considered less pervious than its northern counterpart. Furthermore, there are indications from several boreholes (e.g KAS02, 5, 7 and 8) of a decrease in the

variability of hydraulic conductivity with depth, and that there is a significant increase in conductivity at depths between 100-200 m and 400-500 m, which may correspond to the vertical distances separating gently dipping hydraulic fracture zones in the area.

In terms of a two or three dimensional conceptual model showing the major groundwater flow directions at Äspö, there is, unfortunately, no published detailed information. The nearest approach to estimating relatively shallow groundwater flow directions is presented by Wikberg et al. (1991) where each major conducting fracture and shear zone are addressed individually, and available geological, hydrogeological and hydrochemical data are used as support for their existence. Potential groundwater flow associated with these zones were summarised by Wikberg et al. (op. cit.) as follows:

* Zone EW-1 exhibits a low hydraulic conductivity (estimated transmissivity of $2.0x10^{-5}$ m^2s^{-1}) in its central part; hydrochemical evidence indicates an inflow or recharge of fresh water in the upper part of the zone, extending to a deeper level than the surrounding bedrock.

* Zone NE-2 is characterised as being moderately hydraulically conductive (estimated transmissivity of $0.4x10^{-5}$ m^2s^{-1}); hydrochemical evidence suggests a slight discharge of water through the zone.

* Zone EW-3 is considered to be an unimportant hydraulic conductor (estimated transmissivity of $0.05x10^{-5}$ m^2s^{-1}); no available hydrochemical data.

* Zone NE-1 is highly conductive and there is a strong hydraulic connection with Ävrö (estimated transmissivity of $2.0x10^{-4}$ m^2s^{-1}; upper 300 m is considered to be somewhat higher). High, near-surface contents of chloride and carbonate support groundwater discharge in this zone.

* Zone EW-5 is geologically complex with an estimated transmissivity of $2.0x10^{-5}$ m^2s^{-1}. Similarly high, near-surface chloride and carbonate contents, in common with NE-1, also suggest groundwater discharge in this zone.

* Zones EW-7, NE-3 and NE-4 are not well investigated; estimated transmissivities are $1.4x10^{-4}$, $3.0x10^{-5}$ and $3.5x10^{-4}$ m^2s^{-1} respectively. Hydrochemical data show high salinity and high carbonate contents indicating discharge conditions.

* Zones comprising NNW; estimated transmissivities for these NNW-trending zones range from 1.5 to $4.0x10^{-5}$ m^2s^{-1}. Hydrochemical evidence points to fresh water inflow or recharge along these zones to depths greater than the surrounding bedrock.

Some of these hydraulic concepts have been recently reviewed and tested by Ittner et al. (1991), Andersson (1991) and Gustafsson et al. (1991). Essentially tracer tests, and evaluation of the pump test at LPT-2, have supported the hydraulic fracture conceptual model of Wikberg et al. (1991). In particular, zones NNW-1, NNW-2 and NE-1 are the dominating hydraulic structures, consisting of a few highly conductive fractures with high flow rates; there is a good hydraulic connection between zone NE-2 and these NNW-trending structures. However, zone NE-1, having higher conductivities in the component fractures and therefore lower dispersivities, is a more distinct conductor than NE-2. Zone EW-5 is judged to be a good but complex conductor with many widely spread yet interconnected low conductive flow paths. Dispersivities are therefore correspondingly high.

4.5.2. The Numerical Model.

Numerical simulations of the saline/fresh water interface and groundwater flow at Äspö have been reported by Svensson (1988, 1990a,b, 1991) and summarised in Wikberg et al. (1991).

As part of the early generic studies to locate a suitable site for the Äspö underground laboratory, Svensson (1988) used a numerical model to simulate the intrusion of seawater into a fractured porous rock medium to predict the salinity stratification and flow field in order to explain the groundwater salinity distributions in and around Äspö.

The reference case, derived from groundwater measurements conducted at Äspö and using assumed hydraulic parameters, is presented in Figure 4.10 and the modelled homogeneous reference case in Figure 4.11. Waters of three differing salinities (and therefore different densities) were used in the reference case. The pressure boundary generates an inflow of fresh water (recharge) at the top-left boundary, and an outflow of brackish water (discharge) at the top-right boundary to the sea. Meanwhile the high salinity beneath the outflow boundary results in a hydrostatic pressure distribution which generates an inflow gradient, thus bringing in water with a salinity of 1% and causing an upward movement of highly saline water, a) under the recharge inflow boundary, and b) under the outflow boundary towards the sea. Degrees of mixing will occur at the fresh/saline groundwater interface.

The predicted salinity and flow field, using the porosity, dispersion coefficient and hydraulic conductivity in Figure 4.10, is shown in Figure 4.11. The saline water found at 300-400 m depth at the left boundary represents the centre of the island. By varying the dispersion coefficient (e.g. to be proportional to the Darcy velocity) and the hydraulic conductivity (causing it to decrease with depth) gave a similar result for the former case; in the latter case the flow is forced closer to the surface, but the fresh/saline interface is forced to greater depths.
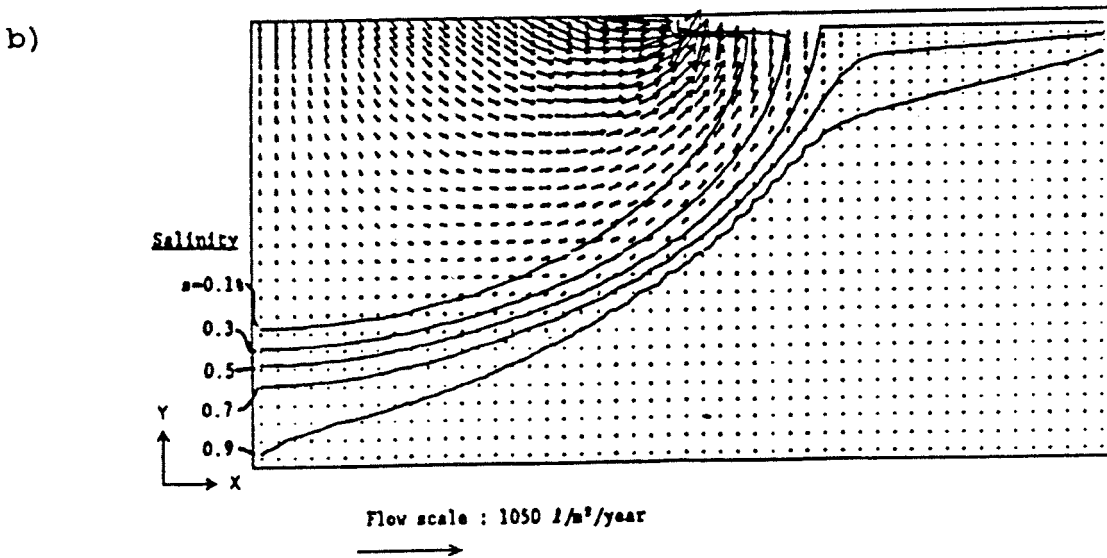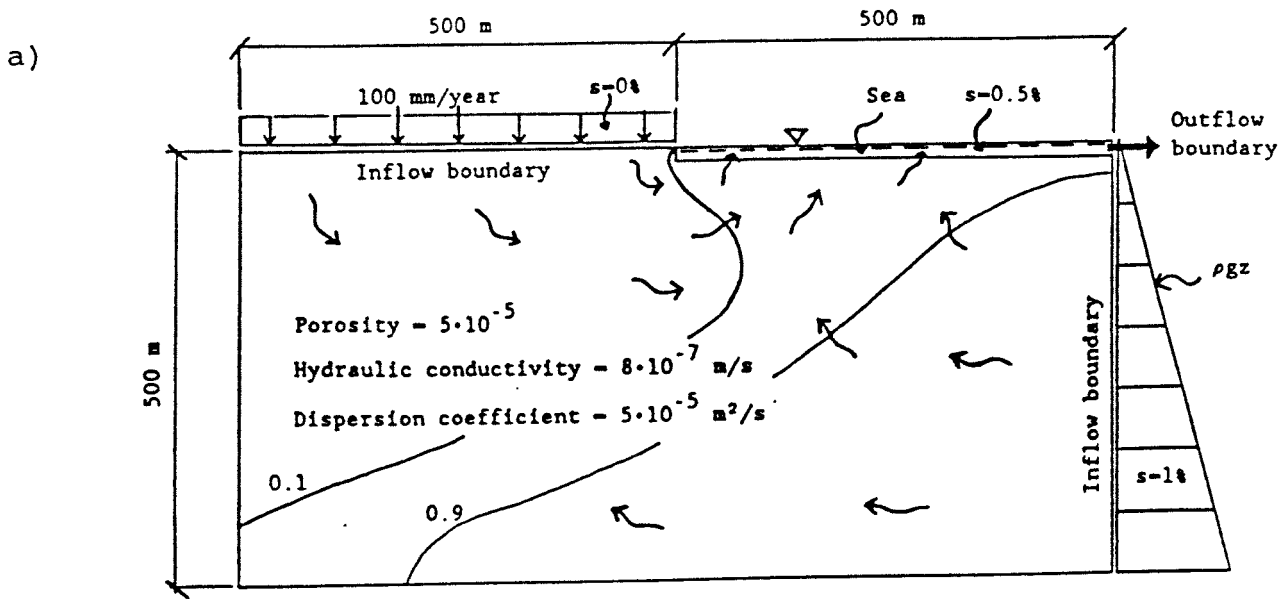
Figure 4.10. The reference case with assumed parameters (a) and the homogeneous reference case (b). (After Svensson, 1988).

A more realistic picture is obtained by modelling a fractured rock medium and coupling stochastically generated hydraulic conductivities (Fig. 4.11). This shows how the highly saline water (bottom right-hand sector) "seeks" its way through the fractured medium (Svensson, 1988).
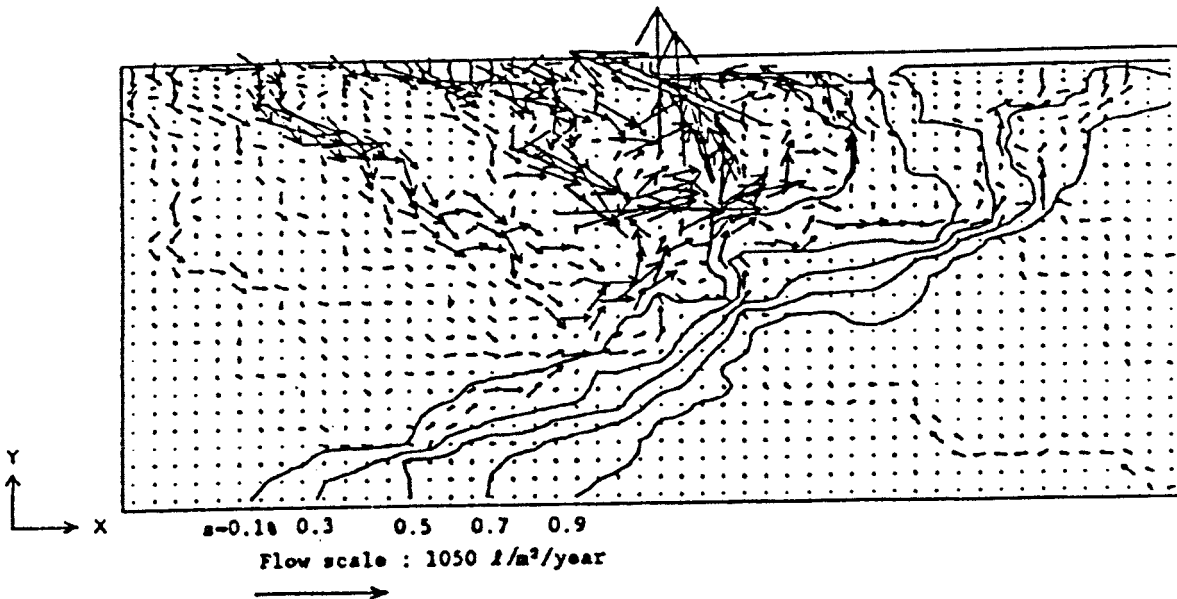
c) Standard deviation, lnK = 4

Figure 4.11. Simulations with stochastically generated hydraulic conductivities (After Svensson, 1988).

Numerical simulations of the groundwater flow at Äspö have also been carried out by Svensson (1990b, 1991). The model essentially: a) confirmed the vertical salinity distribution as measured at Äspö, b) indicated that the depth of the fresh water aquifer is found at 200 m, somewhat deeper than measurements show, and c) predicted steady state conditions thus giving rise to the speculation that the fresh water aquifer can represent a transient stage, and maybe even increasing its depth. Unfortunately no details or discussion of the groundwater flow directions shown in in his figures have been presented.

However, a qualitative visual interpretation of the groundwater flux path directions along a NW-NE section through Äspö (Fig. 5.4 in Wikberg et al., 1991) suggests that zone NE-1 is a strong point of discharge, EW-3 is weakly recharging, possibly also NE-2; EW-1 is uncertain but some upward flux may be indicated. In the NE sector of Äspö there is a clear subhorizontal groundwater flux from around the EW-1 shear zone towards the NNW.

5. Borehole Hydrogeochemical Investigations: Results and Discussion.

The borehole results from the Äspö site are presented in Tables 5.1 to 5.14 and Figures 5.1 to 5.56. The hydrogeological data used for calculation purposes are based on hydraulic measurements carried out along 3 m and 30 m sections of the boreholes, except for the total volume of water removed during the sampling period which is measured directly. Usually there is a wide distribution of fracture type and frequency within such a 30 m section, and as only a small percentage of these fractures will be sampled for water (i.e. double packer straddle lengths varied between approx. 5 and 10 m), the question arises as how representative are the hydrogeological data for the actual fracture or fracture zones being sampled for groundwater. Furthermore, the integrity of the geochemical rock/water equilibrium modelling depends greatly on correctly selecting the main conducting fracture and identifying quantitatively the fracture mineral phases in contact with the groundwater sampled and analysed.

5.1. Borehole KAS02.

Borehole KAS02 (Fig. 5.1), located in the SE sector of Äspö, has an upper diameter of about 155 mm (down to 100 m) and a lower diameter of 56 mm (to the full length of 924 m). The borehole was drilled at an inclination of 85° to investigate the bedrock geology, hydrogeology and hydrogeochemistry.

The most common rocks encountered are dark-grey, fine- to medium-grained intrusive rocks of dioritic composition. Many are heterogeneous due to the influence of younger granitoid intrusions; this activity may have resulted in the prominence of red microcline megacrysts which characterise the diorites. These rock types dominate the lower part of the core from around 315 m to the hole bottom. The top part of the hole is characterised mostly by granite/aplite of fine- to medium-grained texture and colour variations from reddish-grey to greyish-red. Here the microcline megacrysts tend to be somewhat smaller. Greenstone horizons (1-10 m thick), which are mainly metavolcanic in origin, sporadically occur within the upper 400 m of the hole. Along the total length of the drillcore the Småland granite accounts for 40% followed by diorite (42%), fine-grained granite/aplite (14%) and finally greenstone (4%).

KAS02 intersects two major tectonic zones (Fig. 5.2), that of NE-2 at around 800-920 m, and the shallow dipping (20-30° to the NNW) EW-5/EW-X zones which intersect KAS02 at the upper and lower portions of the borehole respectively. Zone NE-2 trends NE/75°NW to 85°SE and is estimated to be some 5-10 m in width; its extent at the bedrock surface is 500-600 m. It can be regarded as the southern part of the main Äspö shear zone (EW-1). Zones EW-5/EW-X, associated with a thrust, outcrop approx. 300 m east of southern Äspö. Two major mylonitic zones, associated with 1-2 m wide crush zones, occur at 455-485 m and 550-570 m respectively (perhaps associated with EW-X); high fracture frequencies not associated with mylonitisation also occur throughout the core, particularly from 300-400 m (EW-5?) and 800-900 m (NE-2).

Statistical evaluation of all the fractures (Liedholm, 1989) shows a tendency for the fracture intensity to decrease from the surface to about 400-600 m. Even though the variation is rather low, borehole sections from 300-400 m and 675-725 m can be regarded as primary fracture high frequency anomalies, and the sections around 200, 475, 550 and 775 m as secondary high frequency anomalies. Because of their greater competence, the aplitic rocks are more prone to fracturing than the other rock types since the region became increasingly brittle as it cooled down (Talbot, et al., 1988). For example, the mean total number of fractures per 3 metres in aplite is 26.4 compared to 17.6 for granite (Liedholm, 1989).

Some of the fracture zones have been interpreted from drillcore mapping to be horizontal to subhorizontal in orientation (i.e. 0-20° dip) and may represent intersections with zones EW-5 and EW-X; potential zones occur at 10-150, 370, 870 and 910 m. However, borehole radar indicates somewhat higher angles, for
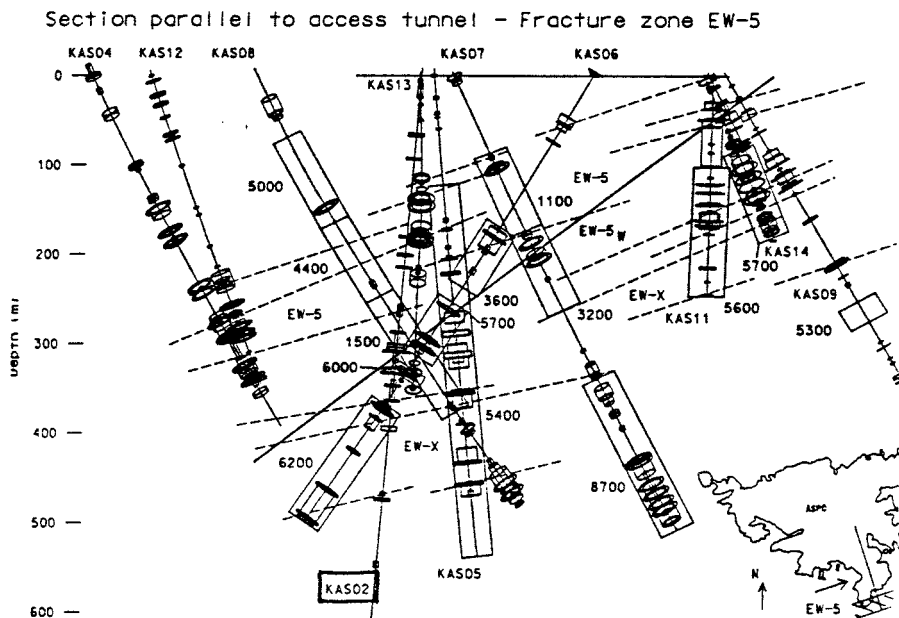
a)

ÄSPÖ
TOP VIEW
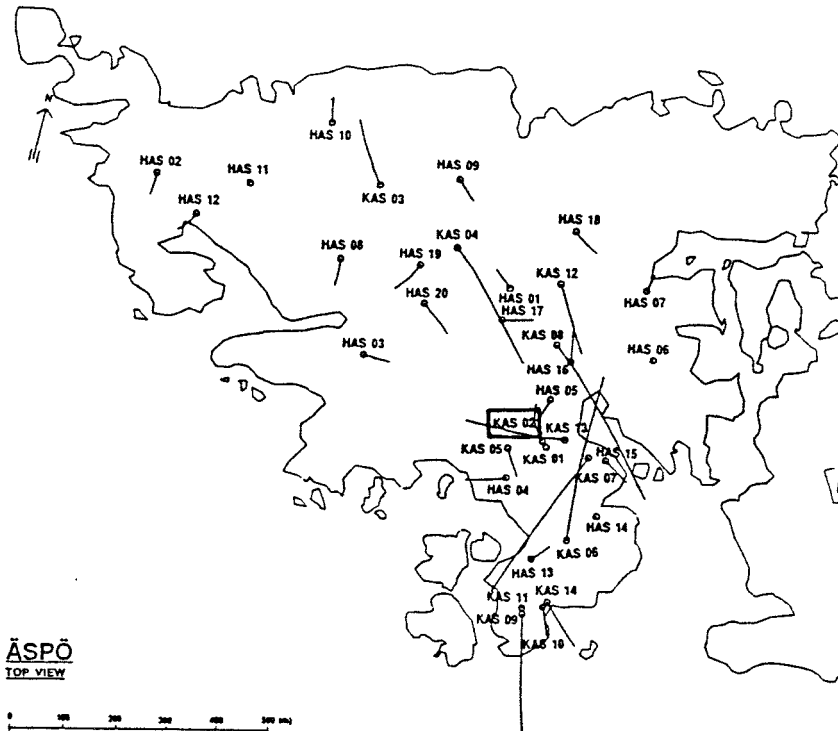
b)

Figure 5.1. Location of borehole KAS02 (a) and its relationship to the EW-5/EW-X gently dipping shear zones (b). (Water-bearing fractures are indicated by the transverse elipsoids along the borehole and the boxed sections the sampled borehole length; the Cl contents are marked. For further details see Wikberg et al., 1991).

example, fracture/borehole intersections of 25-40° between 316-376 m and of 35-50° between 800-900 m have been noted. Also indicated at various points along the borehole are vertical to subvertical fracture systems aligned roughly parallel to the borehole axis.

Relating drillcore mapping to borehole geophysical methods (Fig. 5.2) reveals fracturing at nine major sections (100, 215, 315, 375, 535, 630, 675, 770, 810-900 m). There is a clear correlation between high fracture frequency and aplite dykes, zones of alteration, bedrock contacts and intermediate to basic volcanics. The aplitic zones are easily denoted by higher than background levels of uranium and, in this case, also potassium (Nisca, 1988). The zones at 100, 215, 315 and 810-900 m correlate with borehole water temperature fluctations; Sehlstedt (1988) has interpreted, particularly the zones at 315 m and 770 m, as being open and water conducting. The salinity is very high throughout the borehole ranging from 3 000 to 8 000 mg/L equivalent NaCl in the upper 300 m of the borehole to 10 000 to 15 000 mg/L from 400 m to the hole bottom; a maximum of 20 000 mg/L occurs at 676-691 m corresponding to an aplitic zone.

Throughout the drillcore length the average total distribution of natural vs. sealed fractures present (excluding the mylonitic crush zones) are 3.65 and 0.47 fractures/metre respectively. Major fracture filling minerals are quartz, calcite, epidote, chlorite, fluorite, hematite, Fe-oxyhydroxides and clay minerals such as illite, montmorillonite and kaolinite; prehnite and zeolites such as laumontite also occur more sporadically (Tullborg, 1988; Tullborg et al., 1990). Sehlstedt and Triumf (1988) have plotted the fracture coating occurrence of hematite and Fe-oxyhydroxide with depth. Hematite (mostly of hydrothermal origin) is present in small amounts from within 10 m of the bedrock surface to the bottom of the drillcore; major amounts are present from 810-920 m. Fe-oxyhydroxides, commonly formed from the oxidation of hematite and other Fe-bearing phases at shallow depths by oxidising groundwaters, also occur throughout the drillcore. Whether these Fe-oxyhydroxides represent: a) an artefact from late-stage hydrothermal processes, b) more recent low temperature groundwater oxidation reactions along highly conducting recharge fractures, or c) precipitation caused byba decrease in solubility of Fe(III) at the high pH values and low carbonate concentrations encountered at greater depths (Grenthe et al., 1992), has not been completely resolved.

Plotting the percentage of calcite coated fractures in relation to the total number of fractures versus depth has traced the surface-related dissolution "front" of calcite to about 10 m depth (Tullborg, 1988).

From hydraulic injection testing (approx. 100-800 m; 3 m intervals from 102-801 m and 35 m intervals from 102-782 m) and spinner surveys (approx. 100-880 m at 1 metre intervals) the areas of high hydraulic conductivity largely conform with the geophysical results (Fig. 5.2). Down to 100 m, the extent of the casing, the drilling log data show that little formational water was intercepted and there was minimal
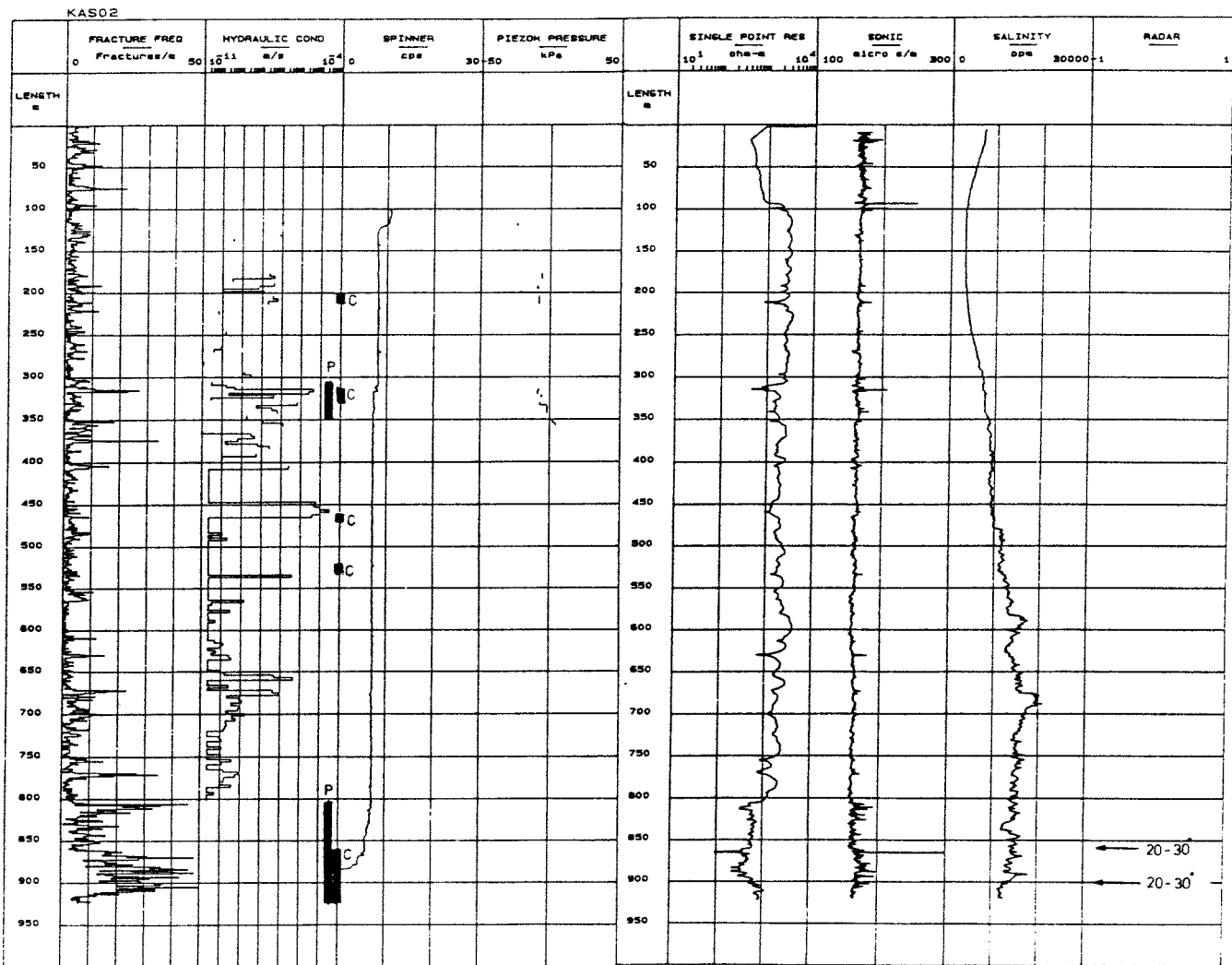
Figure 5.2. Composite log of borehole KAS02.
Bars placed between the hydraulic conductivity and spinner log columns
indicate the borehole section lengths sampled for groundwater chemistry;
(P = pump test sampling; C = complete chemical characterisation)

loss of flushing water; this indicates a very low hydraulic conductivity in this shallow bedrock zone. General conductivities measured along the rest of the borehole are irregular and respond to both marked and more discrete fracture zones; maximum conductivity values range from 10^{-7} to 10^{-5} ms^{-1} and correspond to sections 330, 410, 460, 540 and 660 m. The spinner survey recorded a relatively uniform profile apart from three major anomalies located at approx. 120 m, from 310-330 m and below 800 m. More detailed evaluation (Gentzschein and Andersson, 1988a) has shown that 5 intervals represent almost the total hydraulic conductivity of the borehole. These occur at 118-125, 309-318, 336-343, 803-848 and 868-887 m respectively, with transmissivity values ranging from 0.4×10^{-5} to 7.9×10^{-5} m^{2}s^{-1} (Fig. 5.3b).

Estimated piezometric head data mostly show negative values (Figs. 5.2 and 5.3c) corresponding particularly to fracture zones at 215, 336-343, 463-468 and 802-924 m. Two methods are presented: VIAK and SGAB. The former are mainly based on estimations derived during the initial pressure from injection testing in packed-off sections, and the latter are based on direct measurement.

Major water-bearing conductors of shallow (100 m) and deep (>800 m) origin are supported by the pump test which showed hydraulic contact from KAS02 to KAS01 and HAS04 (see Fig. 5.1 for locations), resulting in calculated transmissivities of 1.5×10^{-4} and 2.2×10^{-4} m^{2}s^{-1} respectively.

In summary, these various data would suggest that in borehole KAS02 groundwater flow occurs at various depths, with greatest influence at around 125 m and >800 m. This is to some extent supported by the temperature log which shows observable temperature increases at these two locations; a further important location may be 310-330 m. Groundwaters sampled from this borehole appear to be relatively free from contamination resulting from borehole activities; this is supported by the absence of tagged drilling and injection test waters discussed under Section 3.2.4 and illustrated in Figure 5.3a. However, there may be an increased risk that groundwaters collected from shallow depths (0-300 m) may not be representative, as inferred from Figure 5.3d, which attempts to integrate all the sources of potential disturbance to groundwater quality.

5.1.1. Level 202-214.5 m.

The selected borehole length (Fig. 5.2) comprises grey to red, fine- to medium-grained Småland granite with red megacrysts of microcline. Close to end of the section (214-215 m) occurs a thin aplite horizon. The fracture frequency is generally fairly low (average of 5 fractures/metre) with a maximum (up to 10 fractures/metre) occurring between 211-214 m near the granite/aplite junction.
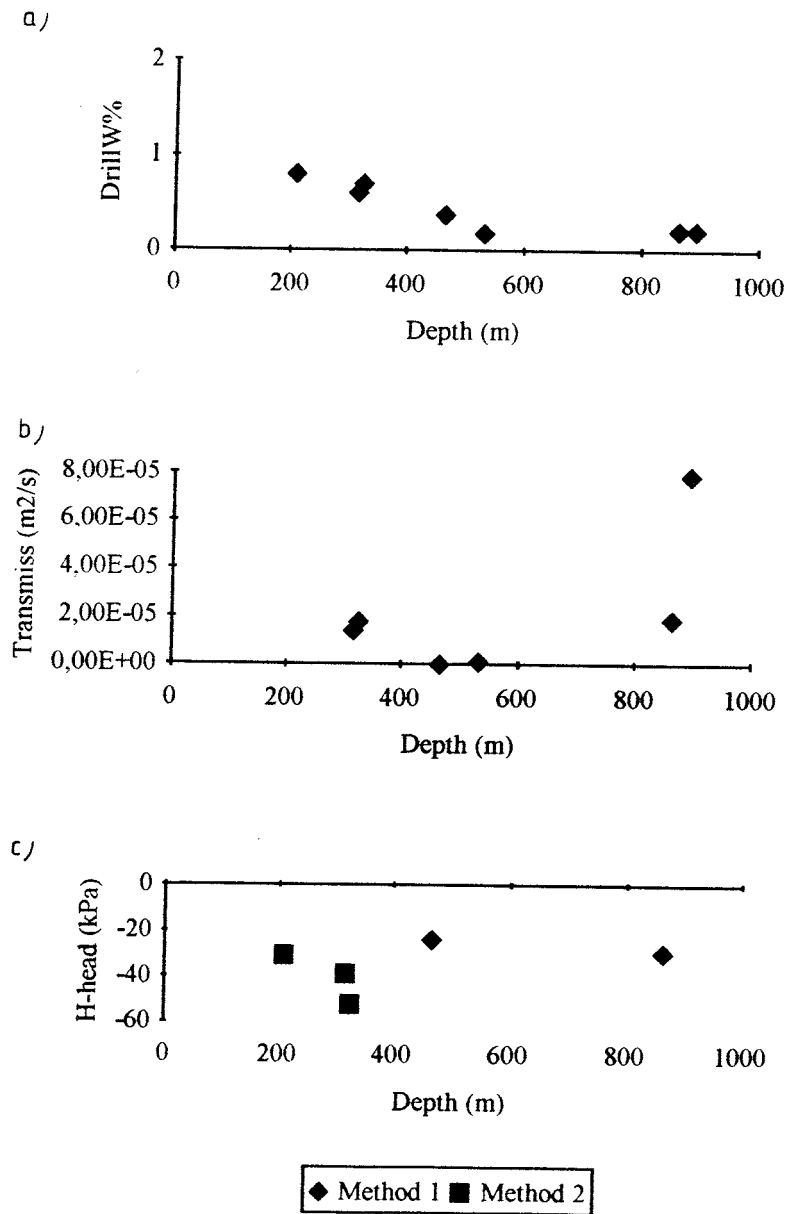
Figure 5.3. Summary of borehole measurements: a) uranine tagged activity water (from drilling and hydraulic injection tests), b) transmissivity, and c) piezometric head (Method 1 = VIAK; 2 = SGAB).

Hydrology.

The sampled section includes a series of five tested borehole lengths of 3 m; the highest conductivities relate to 204-210 m ($3.1x10^{-8}$-$6.0x10^{-8}$ ms^{-1}) compared to a general background of $3.1x10^{-13}$ ms^{-1}. The higher conductivity probably reflects the greater fracture frequency from 211-214 m. The 30 m length pump test (192-222 m) gave an average conductivity of $6.7x10^{-10}$ ms^{-1}.

Water Chemistry.

The sampled water (Table 5.1.) has a mean pH value of 7.4 and is extremely saline (3820 mg/L Cl) when compared with a normal Swedish groundwater from crystalline bedrock (e.g. 4-15 mg/L Cl). Furthermore the alkalinity (71 mg/L HCO_3) is quite low. The water is Na-Ca(Mg) Cl-HCO_3 in type, i.e. equivalent to Äspö Type B of Laaksoharju (1990a).

Redox-sensitive Parameters.

A strongly reducing groundwater environment is indicated by negative Eh values (-260 mV), the presence of sulphide (0.5 mg/L) and that most of the iron is in the ferrous state.

Isotopic Geochemistry.

The stable isotope values plot just under the meteoric water line (Fig. 5.4); tritium is less than detection (<8 TU) and the percentage modern carbon is 23% (apparent radiocarbon age of 10 435 BP). Even though the sampling level is in the upper bedrock levels, the groundwater is old and there is no evidence of mixing with a younger near-surface derived component.

Uranium Geochemistry.

The uranium values (Table 5.2) are low (0.15 μg/L) and the $^{234}U/^{238}U$ activity ratio is high (3.16). This would suggest a groundwater of reducing character which has been subject to long bedrock residence/reaction times in order to accumulate sufficient ^{234}U from recoil mechanisms to result in a high activity ratio.

Summary.

The groundwater chemistry supports the hydrogeological and drilling activity observations in that the sampled groundwater is representative for this bedrock horizon. This is further supported from the sampling log which shows that at low extraction rates (61 mL/min) there was little change in the measured and analysed parameters during the 26 day period. The groundwater is not recent in origin, as indicated by the isotopic data, although the alkaline content (71 mg/L) and TOC

value (6.0 mg/L) indicates significant near-surface influence, presumably occurring over long time-scales, at least more than 50 years as shown by the absence of tritium.
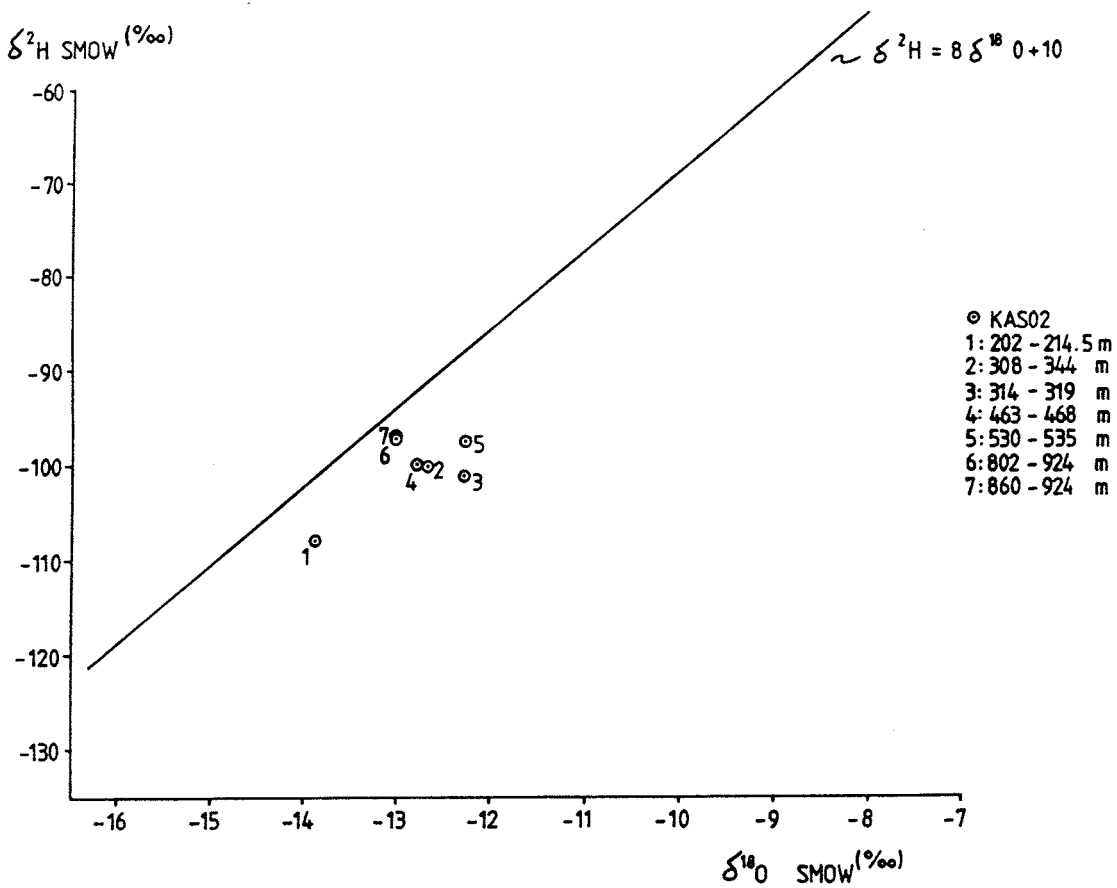

Figure 5.4. Stable isotope composition of borehole KAS02 groundwaters, Äspö, compared to the Global Meteoric Water Line.

5.1.2. Level 308-344 m.

The sampled section (Fig. 5.2) comprises three rock types; fine- to medium-grained Småland granite occasionally with microcline megacrysts (approx. 316-344 m), fine-grained greenstone (approx. 308-316 m) and an aplitic horizon approx. 70 cm wide (at 315 m). The core length on average contains around 6 fractures/metre with a maximum of 26 fractures/metre (mostly open) located from 311-317 m centred around the aplite. These fractures, which show up clearly from the borehole radar measurements, intersect the borehole axis at 35° and probably form part of EW-5/EW-X zone. The mineral infilling phases are dominated by calcite, quartz and pyrite with subordinate chlorite, laumontite and hematite with minor Fe-oxyhydroxides.

Hydrology.

Hydraulic measurements at 3 m intervals along the sampled section clearly demarcate the open fracture zone (314-318 m recording an average conductivity of 2.4-4.3x 10^{-6} ms^{-1}) compared to a general background conductivity of around 10^{-10} ms^{-1}. Other sections of higher average conductivity occur at 321-324 m ($3.9x10^{-8}$ ms^{-1}) and at 330-333 m ($6.4x10^{-7}$ ms^{-1}). The average hydraulic conductivity measured along the 30 m section (312-342 m) recorded $3.6x10^{-7}$ ms^{-1}. Spinner responses occur at 309-318 m and 336-343 m (transmissivities of $1.4-0.4x10^{-5}$ m^2s^{-1}); no piezometric head data are available.

The absence of residual tagged activity water (<1%) and low tritium (<8 TU), together with the lack of groundwater chemical variation observed during the high extraction rate in progress for 4 days (5 000 mL/min.), would support a representative sample being collected from this relatively high conductive location. The stability of the groundwater chemistry is further demonstrated from Table 5.3 which shows that after an absence of 14 months, the groundwater composition eventually approaches similar values, although six weeks of pumping were required at low extraction rates.

Water Chemistry.

The sampled water (Table 5.1) records a pH of 7.6; the major ions Na, K, Ca, Mg, Cl and SO_4 are present in greater amounts than the previous level, whilst HCO_3 is somewhat lower. The groundwater is Na-Ca(Mg) Cl-SO_4 in type, equivalent to Äspö Type C after Laaksoharju (1990a).

Trace element compositions (not tabulated) show significant amounts of Cr (7 ppm), Ni (18 ppm), Pb (8 ppm) and Zn (18 ppm). This may be a reflection on bedrock composition, i.e. the fine-grained metabasic greenstone which lies close to the most conductive zone.

Redox-sensitive Parameters.

No redox potential measurements are available; iron contents are high ($Fe_{(tot)}$= 0.715 mg/L) but most is is in the ferrous state (0.622 mg/L), and sulphide is lower (0.16 mg/L) than in the previous level. This may indicate that conditions here are marginally more oxidising.

Isotope Geochemistry.

The stable isotope data ($\delta^{18}O$ = -12.7 ‰; δ^2H = -99.8 ‰), in common with the preceding level, plot just under the meteoric water line (Fig. 5.4). Tritium is very low (<8 TU); no radiocarbon data are available.

Uranium Geochemistry.

Uranium content and activity ratio (Table 5.2) are similar to the previous level; reducing conditions and long groundwater bedrock residence/reaction times are again indicated.

Summary.

This borehole section has been sampled during a pump test at an extraction rate of 5 000 mL/min. Even so, the groundwater chemistry has generally remained remarkably stable during the 4 days of pumping which reflects the highly conductive nature of the zone (possible zone EW-5). However, small trends are observable such as decreases in Ca, K, and Mn and increases in Mg and SO_4; continued pumping may have shown a progressive increase in saline groundwater from greater depths which may be derived from the most conductive zone at 314-318 m which is known to intersect the borehole axis at 30-40°.

5.1.3. Level 314-319 m.

The geology, fracture characteristics and hydrogeology of this borehole length has been described under Level 308-344 m; the chosen interval straddles the most conductive section at 314-318 m (Fig. 5.2).

Summary.

There is very little overall difference between this groundwater and that sampled from the longer borehole section discussed above, even though the extraction rate was restricted to 180 mL/min. Exceptions include a higher pH (8.2 vs. 7.6), higher total iron (0.794 vs. 0.715 mg/L), uranium (0.34 vs. 0.15 ug/L) and sulphide (0.16 vs. <0.01 mg/L) contents, and a lower uranium activity ratio (3.06 vs. 4.11). Perhaps in

general a less reducing groundwater environment than the previous borehole section is suggested by these chemical data.

There is no significant evidence of a younger, near-surface derived groundwater component (e.g. <8 TU tritium and <1% tagged activity water); long bedrock residence/reaction times are indicated by the small amount of modern carbon (i.e. 21 % indicating an apparent radiocarbon age of 12 670 BP) and the uranium isotopic data.

The similarity in composition between these two measured sections essentially confirms the suitability of the water sampled, and that most of the water sampled from the 308-344 m section has originated from the most highly conductive fracture zone at 314-318 m.

5.1.4. Level 463-468 m.

This section (Fig. 5.2) is contained completely within the dark-grey, fine- to medium-grained diorites containing occasional megacrysts of microcline. One small open fracture zone (some centimetres in width) is located at 466 m; the section is characterised by a background of 4-5 fractures/metre. Apart from the occurrence of hematite, there is no additional information on the fracture filling mineral phases.

Hydrology.

From the 3 m measured sections (462-468 m) the average recorded conductivity is very low (2.2×10^{-11} ms^{-1}); this is reflected in the 30 m section (462-492 m) with a range of conductivity from 3.4×10^{-8} to 1.7×10^{-11} ms^{-1}. Transmissivity within the sampled section is also low (8.4×10^{-9} m^{2}s^{-1}) and the hydraulic head negative (-23.71 m). The spinnner survey (Fig. 5.2) indicates no significant conductivity. It would thus appear that this is a very unsuitable section to sample groundwater; there is the danger that the generally low conductivity of the borehole section may cause short-circuiting around the packer system, thus accessing water from the borehole above or below the packers.

Water Chemistry.

The groundwater chemistry (Table 5.1) shows no significant difference from the previous level. This fact, together with the hydrogeological parameters discussed above, indicates that it is, in fact, essentially the same water which has been short-circuited to the pump from the open borehole above the packer system.

Redox-sensitive Parameters.

See above.

Isotope Geochemistry.

See above.

Uranium Geochemistry.

See above.

Summary.

See above.

5.1.5. Level 530-535 m.

In common with the previous level (Fig. 5.2), the dominant rock type here consists of diorite with microcline megacrysts. The general fracture frequency is low (3-5 fractures/metre); one open fracture (approx. 50 cm wide) is located at 534 m which may represent part of zone EW-X. Hematite has been observed as an infilling phase.

Hydrology.

Hydraulic testing in the 3 m sections from 528-537 m records a very low average background hydraulic conductivity of 2.2×10^{-11} ms^{-1} from 528-534 m, but considerably higher from 534-537 m (3.7×10^{-7} ms^{-1}) coinciding with the open fracture at 534 m. A response at this location was also noted from the single point resistivity and sonic logs, but not from the spinner survey (Fig. 5.2). Along the 30 m measured section from 522-552 m an average conductivity of 3.6×10^{-8} ms^{-1} was recorded. Transmissivity along the 530-535 m section was calculated to be 1.1×10^{-6} m^{2}s^{-1}; no piezometric head values are available.

During the pump extraction period (8 days) all measured physico-chemical parameters remained constant after the initial day. This suggests that at the low flow extraction rate of 117 mL/min the hydraulic conductivity of the packed off section was adequate to sample representative groundwaters from this general depth.

Water Chemistry.

This level (Table 5.1) represents a continued transition to a more saline groundwater. The pH remains similar (8.3) to the previous two levels but further increases in Cl (to 6370 mg/L), SO$_4$ (to 550 mg/L) and Br (to 42 mg/L), and in Na and Ca (Mg, alkalinity and TOC on the other hand continued to decrease), point to an even more evolved Na-Ca(Mg) Cl-SO$_4$ type groundwater, equivalent to Type D (Ca-Na-Cl) of Laaksoharju (1990a).

Redox-sensitive Parameters.

The total iron contents also continue to drop (0.505 vs. 0.226 mg/L); almost all is present in the ferrous state (0.226 mg/L). Reducing conditions are also indicated by the measured negative Eh values (-310 mV) and detectable amounts of sulphide (0.18 mg/L).

Isotope Geochemistry.

Following the same trend for the shallower groundwaters, the stable isotope values plot just below the meteoric water line (Fig. 5.3). Tritium is low, around <8 TU; no radiocarbon data are available.

Uranium Geochemistry.

Uranium contents (Table 5.3) are low (0.13 µg/L) and $^{234}U/^{238}U$ actvity ratios continue to be moderately high (3.25), suggesting reducing conditions and long bedrock groundwater residence/reaction times.

Summary.

The hydraulic properties of this section appear to be conducive for the sampling of representative uncontaminated groundwater, the major and possibly only groundwater source point is via the open conducting fracture zone at 534 m. Little tagged activity water has remained in the adjacent bedrock, and any that may have, has been quickly removed during the initial stages of pumping. The groundwater chemistry indicates long residence times and a generally reducing environment. The waters are becoming increasingly more saline and of deeper origin; this sampled level thus probably represents a mixing zone between deep and very deep saline groundwaters.

5.1.6. Level 802-924 m.

This packed-off section (Fig. 5.2) extends from 802 m to the hole bottom. To 862 m the bedrock consists of diorite containing occasional microcline megacrysts; the rock is finely foliated from 820-862 m. From 862 m the fine-grained granites or aplites become increasingly dominant (via a short transition horizon) and persist to 909 m whereupon once again the diorite occurs, extending to the hole bottom.

Fracturing is intense throughout the section with a background frequency from 802-860 m of around 10 fractures/metre and from 860-910 m of 20 fractures/metre. Areas of maximum fracturing occur at approx. 815 m (45 fractures/metre), 868, 879 and 884 m (45-48 fractures/metre) and 905 m (50 fractures/metre). Borehole radar has identified one major fracture zone at 865 m (35-50° to borehole axis).

The fractures are considered to be open and the main fracture filling mineral phases are quartz, chlorite/montmorillonite, plagioclase, muscovite, kaolinite, Fe-oxyhydroxides and ± pyrite, with subordinate amounts of calcite, epidote and K-feldspar and minor amounts of illite, prehnite, phengite, anthopholite and hematite.

Hydrology.

No 3 m or 30 m hydraulic testing was conducted deeper than 798 m. Spinner surveys, however, carried out down to 890 m (Fig. 5.2), reveal two hydraulically conductive zones: a) 803-848 m with maximum water inflow at 823 m and 835 m, and b) 868-887 m with maximum water flow at 868 m, 879 m and 884 m. Transmissivities for the two zones have been calculated to 1.9×10^{-5} m^2s^{-1} and 7.9×10^{-5} m^2s^{-1} respectively. A piezometric head of -29.31 m has been calculated for the 803-848 m section (Fig. 5.3c).

Zones of high conductivity coupled with high negative head values may be expected to result in contamination from the tagged activity waters, provided that they have not been quickly flushed out of the system. Examination of the monitoring log during the four days of pumping show consistent tagged water values (<1%) after the initial day; tritium values are low (<8 TU). Any groundwater contamination rersulting from borehole activities would therefore appear to have been flushed out of this highly conductive system prior to pumping, monitoring and sampling. In any case, the absence of any hydraulic injection testing along this section would automatically preclude at least one potential source of contamination

Water Chemistry.

The sampled water (Table 5.1), extracted at a rate of 15 200 mL/min, is characterised by a pH of 8.2, a low alkalinity of 7.1 mg/L HCO_3 and a highly saline composition of Ca-Na(Mg) Cl-SO_4 type whereupon Ca dominates over Na (equivalent to Type D of Laaksoharju, 1990). The TOC content is predictably very low (0.5 mg/L).

Redox-sensitive Parameters.

Compared to the previous levels the total iron content has decreased (to 0.027 mg/L) and virtually all is in the ferrous state (0.023 mg/L); the sulphide content is also very low (0.01 mg/L). No redox potential measurements are available.

Isotope Geochemistry.

The stable isotope data plot near to the meteoric water line (Fig. 5.4); tritium is low, around 8 TU (detection limit) and no radiocarbon data are available.

Uranium Geochemistry.

Dissolved uranium values (Table 5.3) have increased slightly from the previous levels (0.64 vs. 0.13-0.34 µg/L) and the activity ratios have correspondingly decreased (3.16 vs. mean of 3.45). This may be a function of the greater conductivity in this section; for example, because residence times are less, the build-up of ^{234}U will be limited and the $^{234}U/^{238}U$ activity ratio will decrease accordingly.

Summary.

A considerable borehole length of high hydraulically conductivity has been pumped using a large extraction rate of 15 200 mL/min. The groundwater originates deep in the bedrock (via NE-1?), is therefore highly saline, and little chemical variation occurs during the extraction period. It is therefore assumed that any tagged activity water contamination has been flushed out of the system prior to pumping, and that the sampled water is representative of the general depth pumped. The fact that the uranium contents have increased and the activity ratios decreased may be an artefact from the high pump rates used to extract the water. The very low sulphide concentration might also suggest the incursion of marginally oxidising conditions.

Long-term stability of the groundwater chemistry is shown by resampling during monitoring of borehole section 800-854 m after a break of over two years. The analyses (compare Tables 5.1 and 5.4) showed little change.

5.1.7. Level 860-924 m.

This level (Fig. 5.2) forms part of the larger borehole section already described above and was selected for complete groundwater sampling (at 130 mL/min) because of the more regional importance of the dominant fracture zone (NE-1) located around 865 m.

Water Chemistry.

Very little difference in the major groundwater chemistry exists between this borehole section and the larger section described above (Table 5.1).

Redox-sensitive Parameters.

The total iron, although still present in only small quantities, is slightly higher in concentration in this section (0.051 vs. 0.027 mg/L); sulphide is also higher (0.72 vs. 0.01 mg/L).

Isotope Geochemistry.

Stable isotopes (Fig. 5.4) are identical to the above-described level; a tritium value of 0.2 TU indcates a total absence of any youger, near-surface derived groundwater component at this level. No radiocarbon data are available.

Uranium Geochemistry.

No significant difference exists between this section and that described above.

Summary.

The hydraulic character of this borehole section shows that the groundwater extracted for analysis mostly originates from the highly conductive zone at around 865 m. Furthermore, the fact that there is very little difference when compared with the complete 802-824 m section, either suggests that all the water originates from 865 m or, the complete 802-924 m section is so conductive that the same water resevoir is tapped along the complete borehole length. The water orginates at great depth, is reducing and there is no trace of contaminants from borehole activities. The collected samples from this section are therefore considered to be representative for the highly conductive zone (NE-1).

5.1.8. Borehole summary and discussion.

Geological Setting.

From geological, geophysical and hydrogeological considerations, seven horizons were chosen in borehole KAS02 (Fig. 5.2) to hydrogeochemically characterise the southern part of Äspö. Borehole KAS02 is thought to intersect two major tectonic zones, that of NE-2 at around 800-920 m, which trends NE60-70°N and outcrops beneath the sea just south of Äspö, and the shallow dipping (20-30°NNW) EW-5/EW-X zones which intersect KAS02 in the upper and lower borehole levels respectively. Ductile structures, sometimes heavily foliated and sheared, and some more intensively sheared and mylonitised, occur at 455-485 m and 550-570 m. General fracturing of the borehole is common and lies around 3-5 fractures/metre, with intensified horizons up to 10-20 fractures/metre and very intensified horizons up to 35-45 fractures/metre. Fracturing is very often associated near or at lithological contact zones and particularly associated with the more competent, brittle, aplitic horizons which occur throughout the borehole length. Areas of least fracturing mostly occur within the more massive Småland granitoids and the diorites between 100-300 m and 420-650 m respectively.

Hydraulic Character and Water Quality.

Generally in Äspö the upper 100 m of bedrock records low hydraulic conductivities (estimated median of $K^{100} = 1 \times 10^{-8}$ ms^{-1}), and the SE sector (where KAS02 is located) is less permeable than the NW sector. In borehole KAS02, because of the dominance of diorite, the hydraulic conductivities tend to be low and there is an overall trend of decreasing conductivity with depth. Hydraulic injection tests (3 m lengths from 102-801 m and 30 m lengths from 102-782 m) show that potentially conductive zones correspond to the most intensively fractured areas; these were further supported and quantified by the spinner surveys (100-890 m at 1 metre intervals; Fig. 5.2).

Prior to sampling for hydrogeochemical characterisation a considerable number of borehole activities were carried out in borehole KAS02 (Table 3.1). However, considering both the uranine (tagged activity water) and tritium contents, the amount of residual water from borehole activities (and/or incursion of younger, near-surface derived groundwaters) remaining in the borehole and immediate bedrock vicinity was found to be minimal. This is supported by the water loss statistics which show that the loss of flushing water was only in the order of 4 m^3 (i.e. 286 m^3 flushing water retrieved at the surface from a total of 290 m^3). Furthermore, there was little change in the groundwater physico-chemical parameters monitored during the large-scale pump tests, during sampling for hydrogeochemical characterisation and also at levels 309-345 m and 800-854 m which were resampled during monitoring after a break of 14 months (compare Table 5.1 with Tables 5.3 and 5.4).

Most indications therefore show, with one exception, that the groundwaters collected are representative for the general depths sampled and that contamination was minimal. The exception occurs at 463-468 m where water was short-circuited during pumping, causing a hydraulic connection through the bedrock from the borehole water above the packer system to the isolated borehole section being sampled. Consequently, and bearing in mind that two of the levels were subject to both the complete hydrogeochemical sampling and pump testing, only four levels now exist for hydrogeochemical evaluation.

Chemical and Isotopic Features.

The general chemical features of the KAS02 groundwaters are summarised in Figures 5.5 to 5.8. Based on physico-chemical parameters, the groundwaters are without exception generally reducing (available Eh data vary from -260 to -310 mV; almost all the total iron is in the ferrous state; total dissolved uranium is very low ranging from 0.13 to 0.64 μg/L; sulphide is present in measureable amounts from <0.01 to 0.72 mg/L) and that a continuous change from less saline groundwaters of Na-Ca(Mg) Cl-HCO$_3$ type to very saline groundwaters of Ca-Na(Mg) Cl-SO$_4$ type occurs from near the surface (to within 200 m at least) to the deepest extent of the
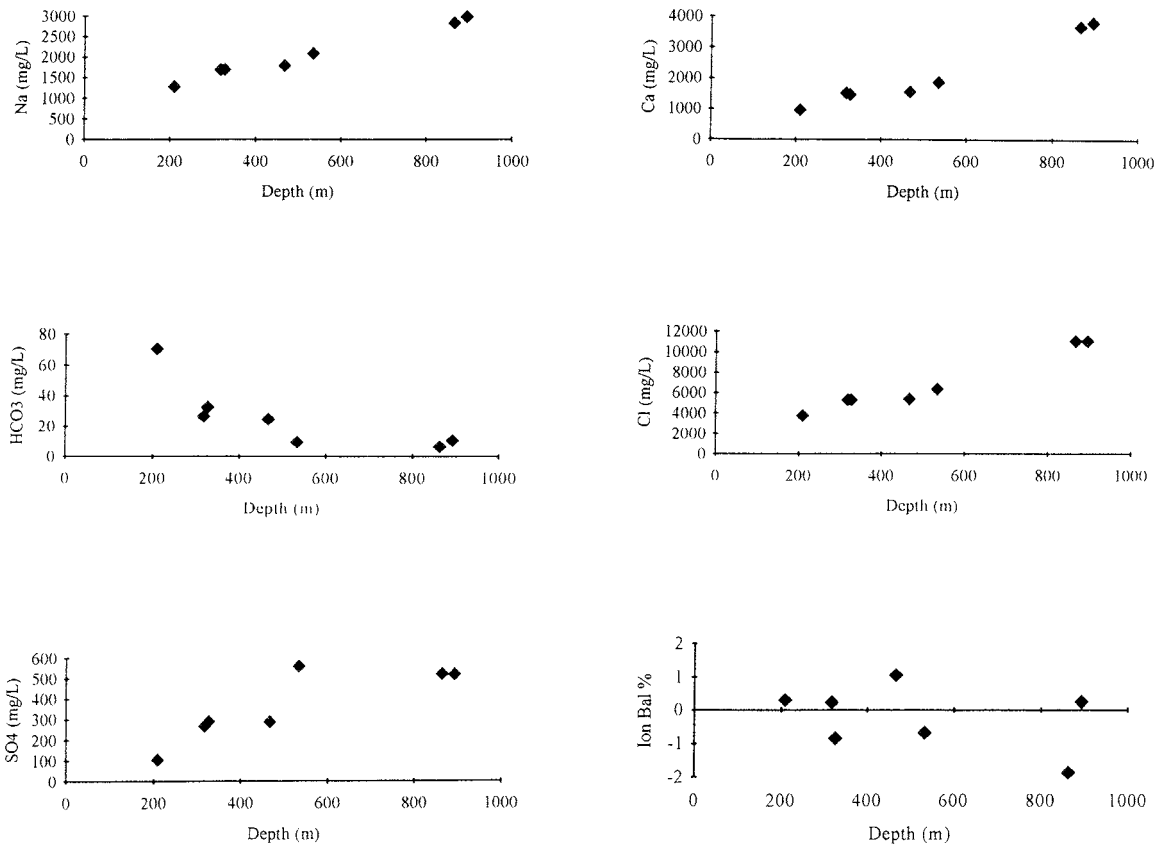
Figure 5.5. KAS02 groundwaters; major ion distributions and ionic charge balance.
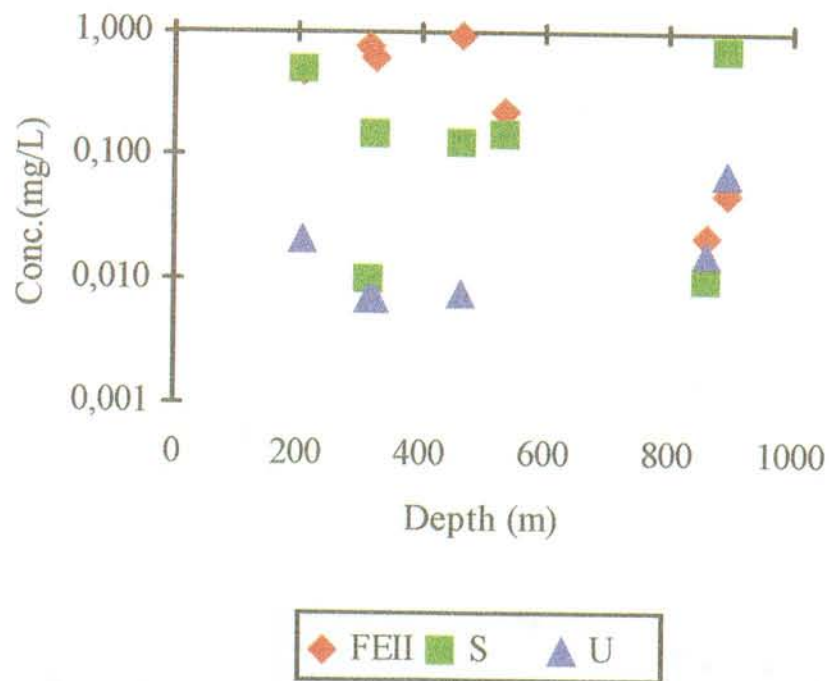
Figure 5.6. KAS02 groundwaters; distribution of selected redox-sensitive elements.
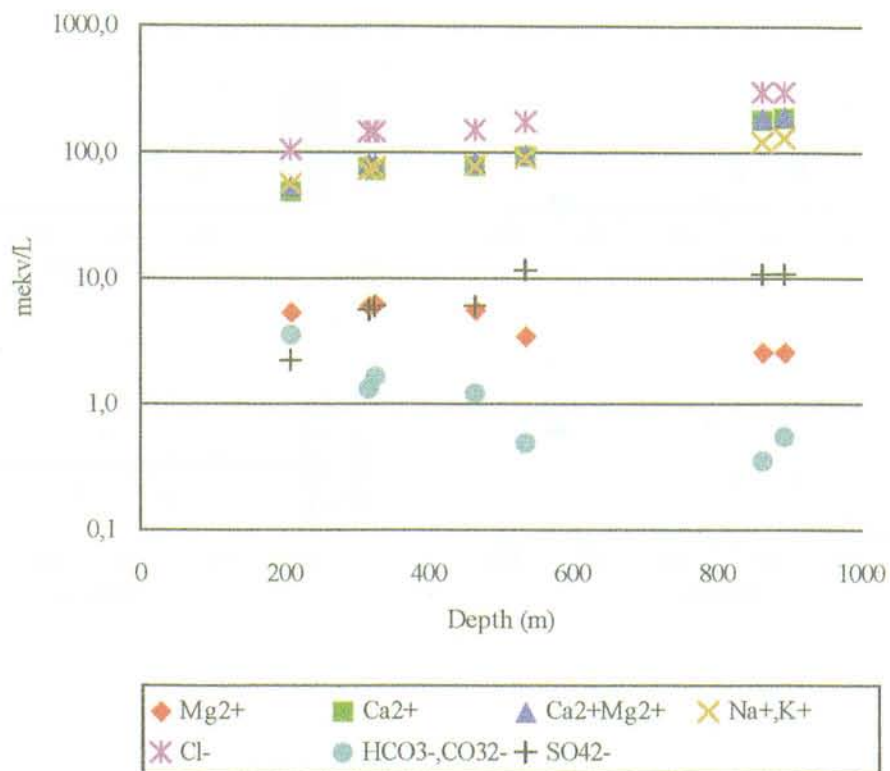
Figure 5.7. KAS02 groundwaters; Shoeller diagram showing the major ion distributions with depth.
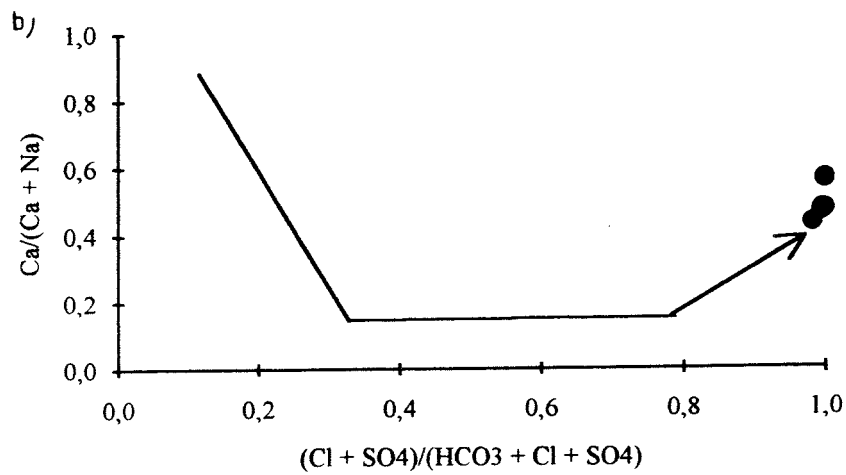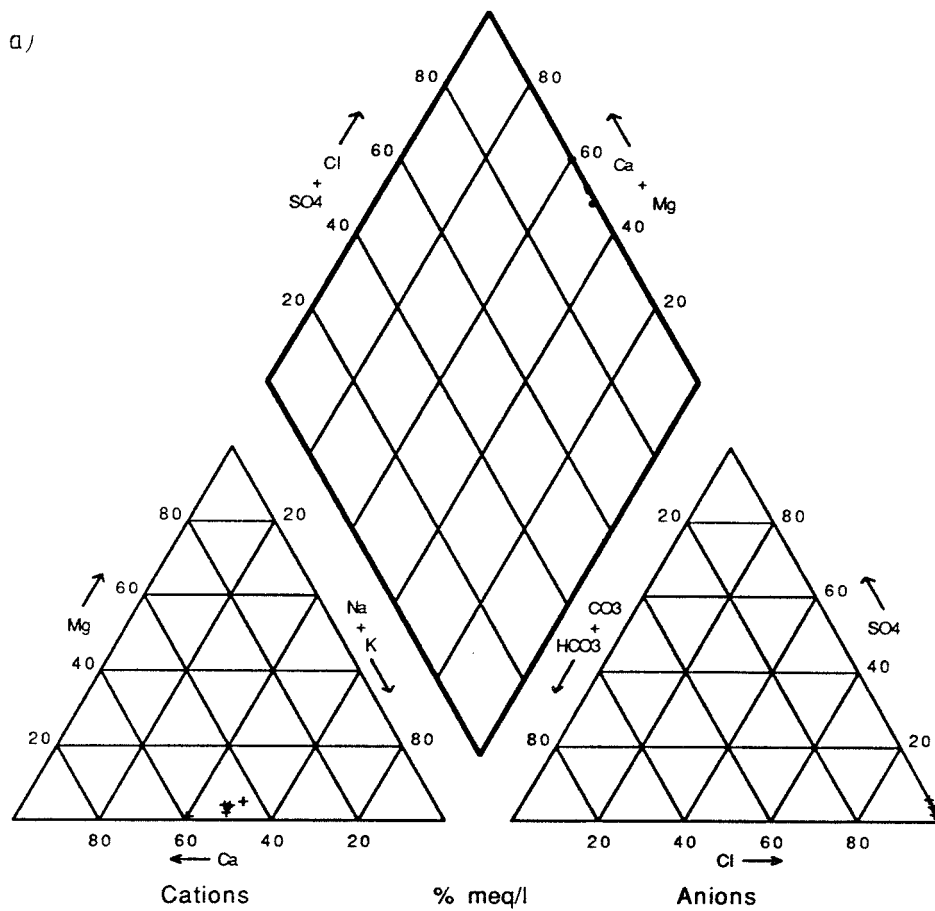
Figure 5.8. KAS02 groundwaters; a) Piper Plot of the major ion chemistry, and
b) modified Piper Plot showing the position of the KAS02 groundwaters
along an assumed chemical evolution path for average deep Swedish
groundwaters in crystalline rock.

borehole at 924 m where zone NE-1 is intersected. A zone of possible mixing occurs at the 314-319 m level.

The stable isotopic signatures of the KAS02 groundwaters plot near to the standard global meteoric water line and can be safely assumed to be meteoric in origin (Fig. 5.4). Apart from the uppermost level, all data cluster around a narrow range of both δD (-96.8 to -100.6‰) and $\delta^{18}O$ (-12.3 to -13.1‰). Such homogeneity suggests stagnation of very old groundwaters at depths greater than 300 m; this is supported by the very low percentage modern carbon present (17-21%, i.e. old apparent radiocarbon ages of ca. 13 000 BP at levels 314-319 m and 463-468 m). The anomalous isotopic signature in the upper 202-214.5 m level suggests mixing with near-surface recharge components as indicated by higher alkalinity and TOC content). This is supported by a greater content of percentage modern carbon (23%, i.e. an apparent radiocarbon age of ca. 10 500 BP).

Tritium values are consistently very low (<8 TU); where more precision was carried out at levels 202-214.5 m and 860-924 m, values were 0.3 and 0.2 TU respectively. In conclusion, no mixing of younger, near-surface derived water has been involved, at least within the range of tritium sensitivity, i.e. during the last 40 years or so.

Water/rock Interaction.

Water rock interaction and mixing is regarded to be an important factor contributing to the groundwater composition. In sections with a small or slow groundwater flow, and hence long contact residence times, water/rock interaction is especially important. In all boreholes detailed geological, mineralogical and geochemical data from specific sections are available (see Stanfors, 1988, Tullborg, 1989, Wikman et al., 1988, Stråle, 1988, 1989 and Sehlstedt and Stråle, 1989). One of the aims is to combine the geological information with groundwater chemistry by using major ion equilibrium calculations and hence to study the water/rock interaction. The calculations were carried out using PHREEQE (Parkhurst et al., 1980). This information may be used to indicate if the water composition reflects the local or regional hydrogeological situation. An indication of the water flow character (i.e. "stagnant" vs. flow) might also be revealed.

One drawback is that not all detailed fracture mineralogical data are necessarily from the same hydraulic fracture zone(s) sampled for groundwater characterisation. In some borehole sections there can be several fractures containing totally different rock and mineral types; these short-comings have been taken into consideration when possible.

Based on detailed examination of the core log descriptions, the percentage of the major rock types comprising borehole KAS02, the dominant host rock characterising each hydraulic zone(s) sampled for groundwater, and the identified macroscopic (and

when available the microscopic) fracture mineral phases (from two data sources) in
those hydraulic zone(s), are illustrated in Figures 5.9 and 5.10.
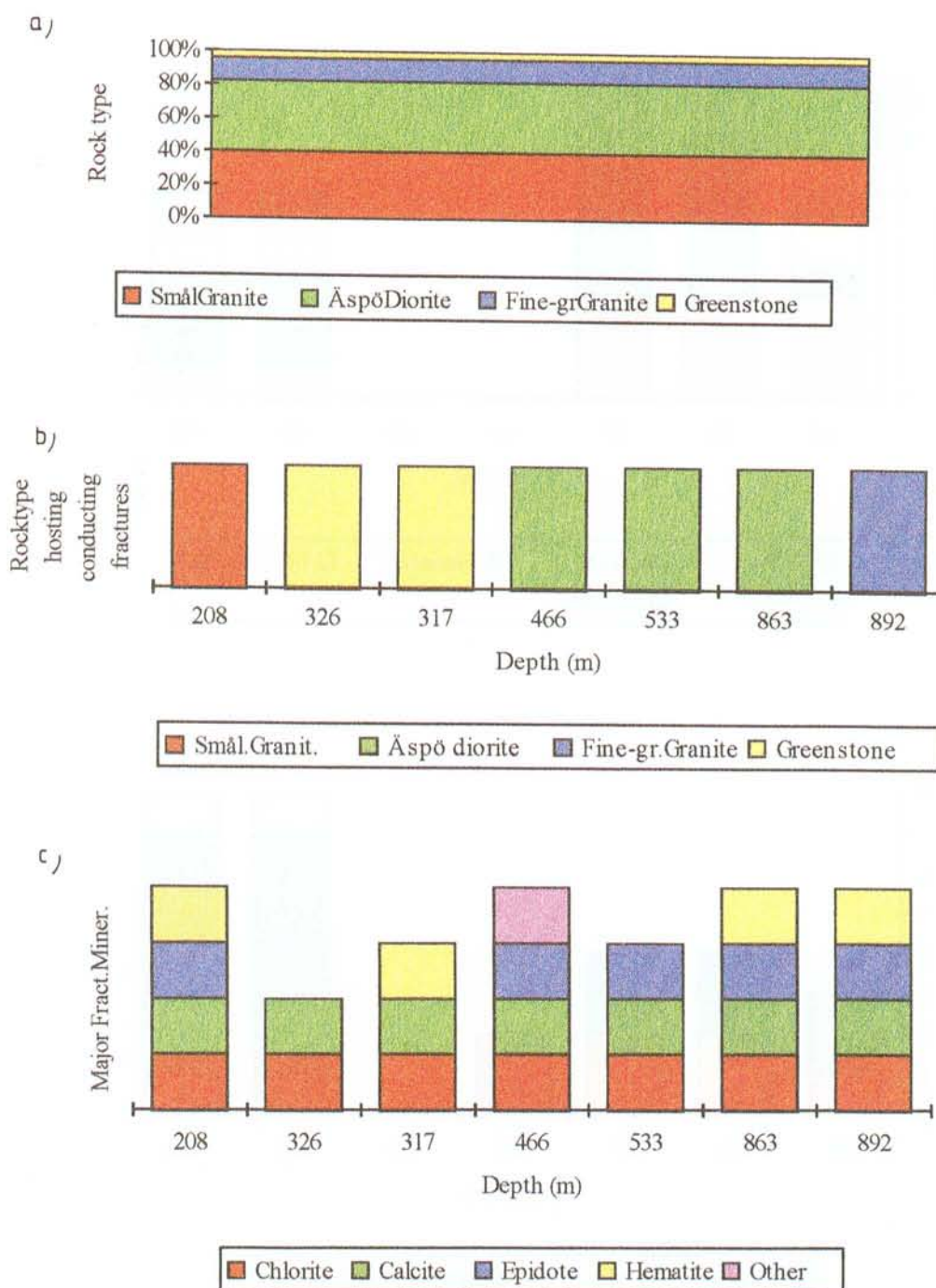
Figure. 5.9. Rock type and fracture mineralogy of KAS02: a) overview of the major
rock types (based on Stanfors, 1988), b) evaluation of probable rock
type hosting the fractures (based on Stanfors, 1988) and c) evaluation
of the major fracture minerals (based on Stråle, 1988, 1989 and Tullborg,
1989).
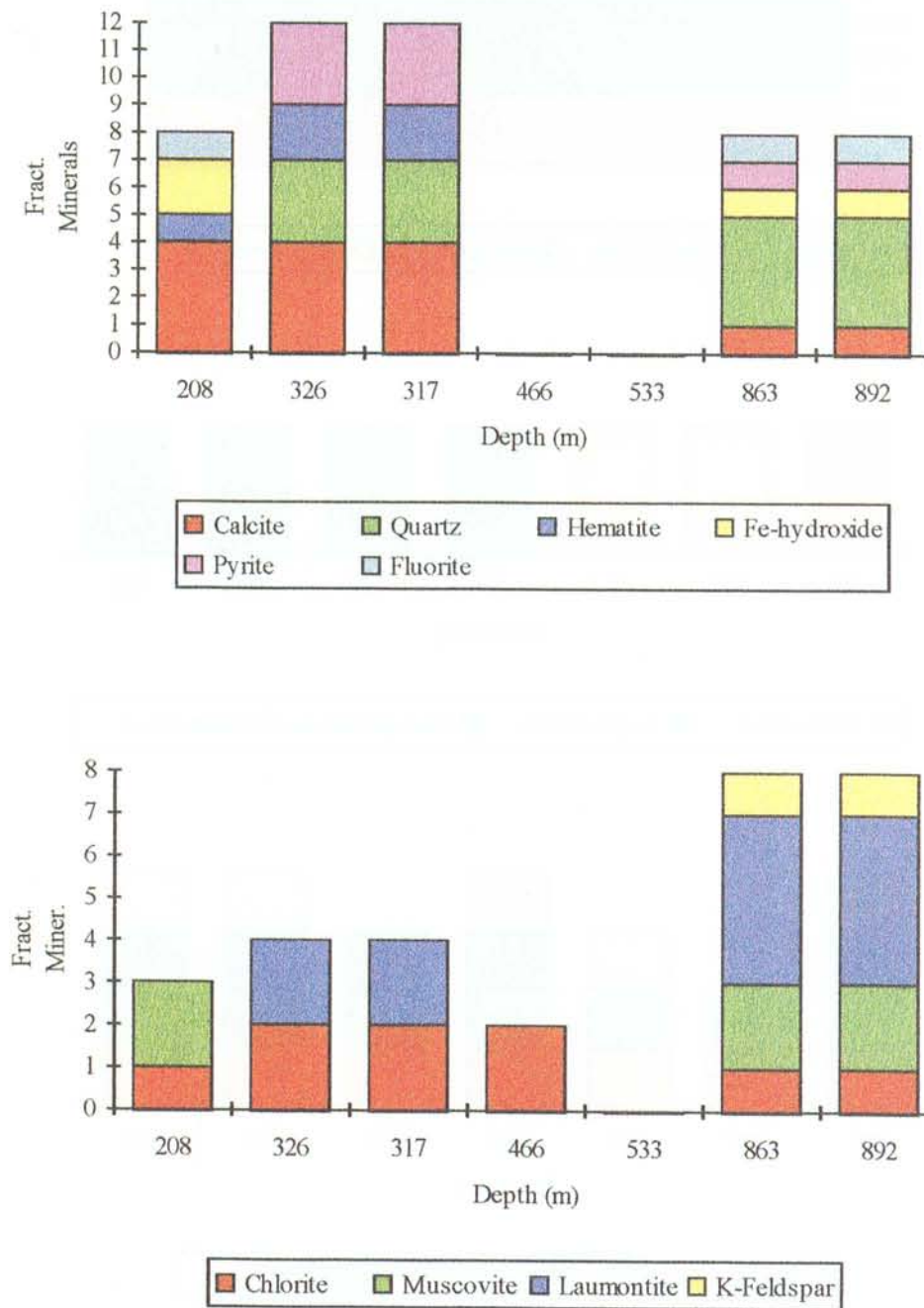
Figure 5.10. Fracture mineralogy of KAS02; evaluation of major (a) and minor (b) fracture minerals detected at, or in the vicinity, of the sampled hydraulic borehole sections (based on Wikman et al., 1988).

By relating the groundwater chemistry to the rock/fracture data an attempt was made to establish any obvious correlation trends. For example, groundwater in contact with greenstone is sometimes known to contain increased amounts of Mg, greenstones generally being richer in Mg than most other rock types. Consequently, some selected bedrock-sensitive elements are compared to host rock type. The water analyses (Fig. 5.11a; Table 5.1) indicate Mg to be higher in the upper part of the borehole where greenstones are reported (326-317 m), in contrast with less Mg in the lower sections which are dominated by Äspö diorite and the fine-grained granite/aplite. Furthermore, U, Th and Ra in the Äspö groundwaters are considered to be mainly derived from fine-grained granite/aplite, which constitutes distinct radioactive anomalies in the borehole gamma profile; no obvious correlation, however, is evident. The overall conclusion is that there is no convincing connection between the rock and groundwater chemistry in this case. This is perhaps not so surprising since the fracture mineral layers effectively isolate the groundwater from direct contact, and therefore reaction, with the host bedrock.

The relationship between groundwater and fracture mineralogy was therefore investigated using water/rock equilibrium saturation index calculations (Figs. 11b and c). Since some of the illustrated minerals resulting from the calculations are either absent at Äspö, or occur very sporadically, only those major phases present in reasonable amounts are discussed below. The positive mineral saturation indices indicate close saturation or a slight oversaturation with respect to calcite, fluorite, quartz and laumontite; these results essentially reflect the phases identified from the fractures. The saturation index for gypsum is negative throughout the borehole length which supports the small amounts detected in the fractures. Muscovite is strongly oversaturated at the 317 m level and deeper, but this is considered to reflect groundwater Al contamination originating from the sampling equipment (P. Wikberg , pers. comm. 1992). Hematite, iron hydroxide and pyrite are either strongly oversaturated (pyrite and Fe-oxyhydroxide less so) or undersaturated; no obvious depth variation is apparent.

The fluctuation in saturation indices for the iron mineral phases does not mirror their distribution in the fractures. This either suggests problems with the thermodynamic database or, more probably, reflects differences in the measured Eh values. For example, at levels 317 m and 466 m where hematite is present as a major fracture mineral, the measured groundwater composition is similar but with a 162 mV difference in the Eh readings (Cl= 5340 respective 5444 mg/L; $Fe_{(II)}$= 0.788 respective 0.941 mg/L; Eh= -382 mV (downhole electrode) respective -220 mV (on-line electrode at the surface). The calculation gives -4.6 respective +8.2 (log IAP/KT) as the saturation index for hematite; in one case the measured Eh value is too low (at 317 m) and the other is too high (at 466 m). The problems of measuring accurate Eh values are well known within the SKB programme. Despite long pumping times, small amounts of oxygen result in contamination of the surface installed electrodes making accurate readings impossible, especially if the $Fe_{(II)}$ content in the water is low (Wikberg, 1987; Grenthe et al., 1992).
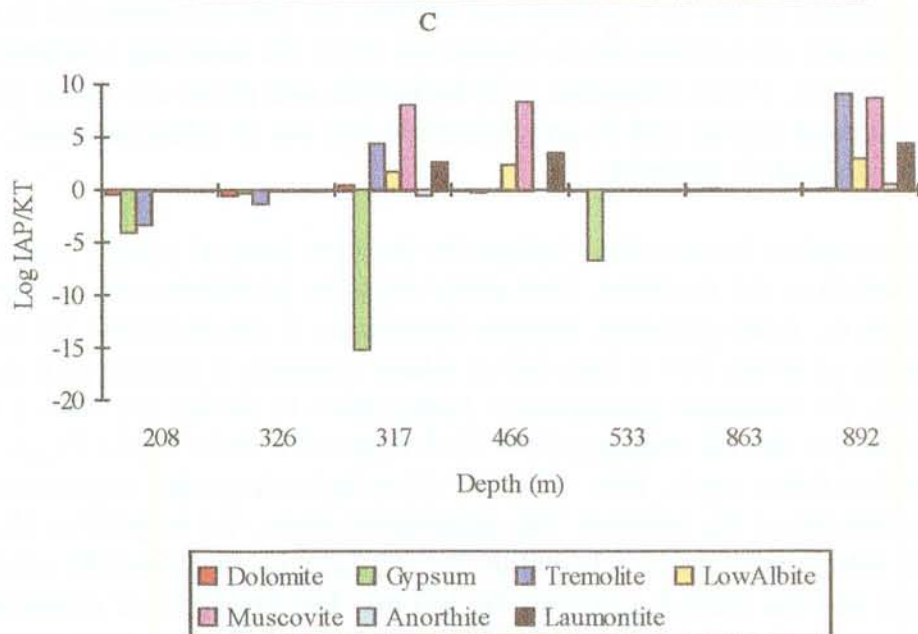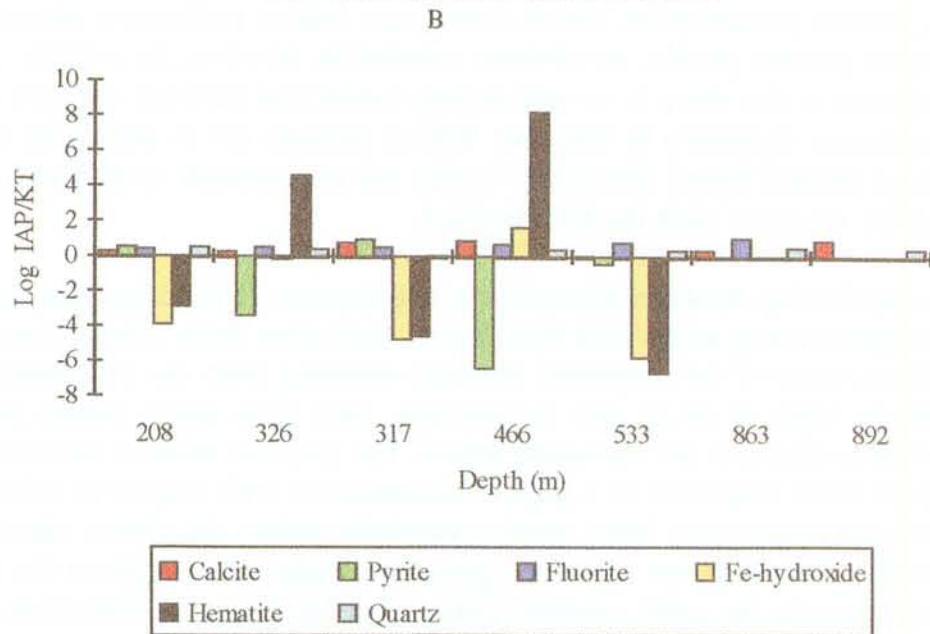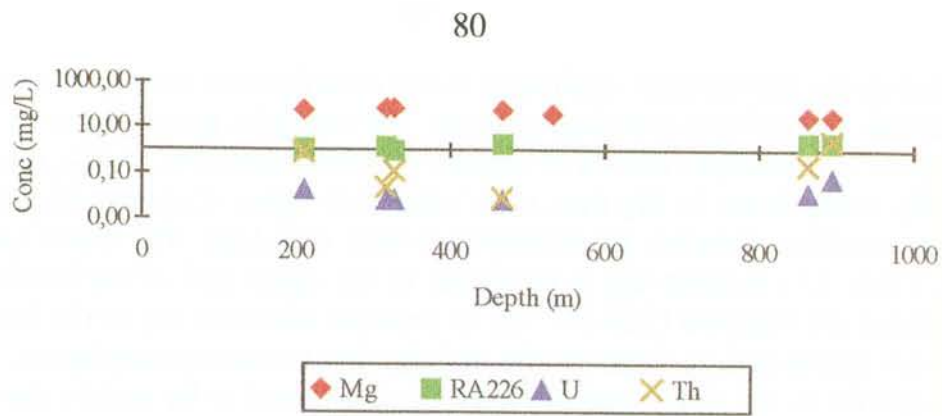
Figure 5.11. a) plotted concentrations of Mg, ^{226}Ra, U and Th measured in KAS02 groundwater, and b, c) results of equilibrium saturation index calculations using PHREEQE (Parkhurst et al. 1980).

In general, however, the saturation index calculations can be used to support the presence or absence of the major fracture minerals; calcite and gypsum are probably the only reliable mineral phases in that they rapidly approach saturation equilibrium with aqueous systems such as these described for Äspö. Broadly speaking, mineral calculations that show saturation or close to saturation may be used to indicate stable conditions, long bedrock residence/reaction times and slow to stagnant flow in the system.

Groundwater Mixing Ratios.

Evaluation of KAS02 (and the other boreholes; see below) has shown that mixing of groundwaters from different origins has occurred in some of the fracture zones sampled. In those cases, where the Cl (i.e. conservative) is present in high concentrations, mixing ratios may help us to understand the water evolution and bedrock hydraulics in the vicinity of the sampled borehole sections.

The flow paths, i.e. the mixing environment, tend to be complicated because of the geometric and geologic heterogeneity of the fracture zone(s). Furthermore, small changes in the groundwater level will locally effect mixing, but deeper derived, more regional changes in the hydrology, will be equally important, especially in an area of groundwater discharge.

Variation in Cl concentration has been earlier modelled to describe the mixing of surface and deep water at Äspö (Laaksoharju, 1990a); other constituents such as Br, Sr and Li, all being water conservative elements, can also be used in the mixing calculations. In this present case only the Cl-composition is employed as a tracer, and two end-member compositions were selected: KAS03:802-1002 m (deep concentrated member) and HAS05:50 m (shallow dilute member). Using a simple two component mixing model with a mixing ratio of (X-A)/(B-A), where X is the measured Cl-concentration in one of the KAS02 borehole sections, A is the Cl-concentration of the highly saline end-member (KAS03) and B is the Cl-concentration of shallow end-member (HAS05), the Cl contents from these two end-members were mixed in such proportions necessary to achieve the measured Cl content in the collected groundwater samples (see Section 2.11 for additional discussion). The calculated results for borehole KAS02 are shown in Figure 5.12a.

The calculations show a high input of shallow water (50-70%) down to a depth of 500 m; at this point there is a sharp decrease. This shallow input pattern is clearly supported by the TOC (total organic carbon) concentration (Fig. 5.12b) and less clearly by the calculated pCO_2 (Fig. 5.12c).

This two component mixing model obviously oversimplifies the real situation; a three component system including sea water input should be more realistic. For example, the calculated Br/Cl ratios for the KAS02 samples (Fig. 5.12d) show that the shallow
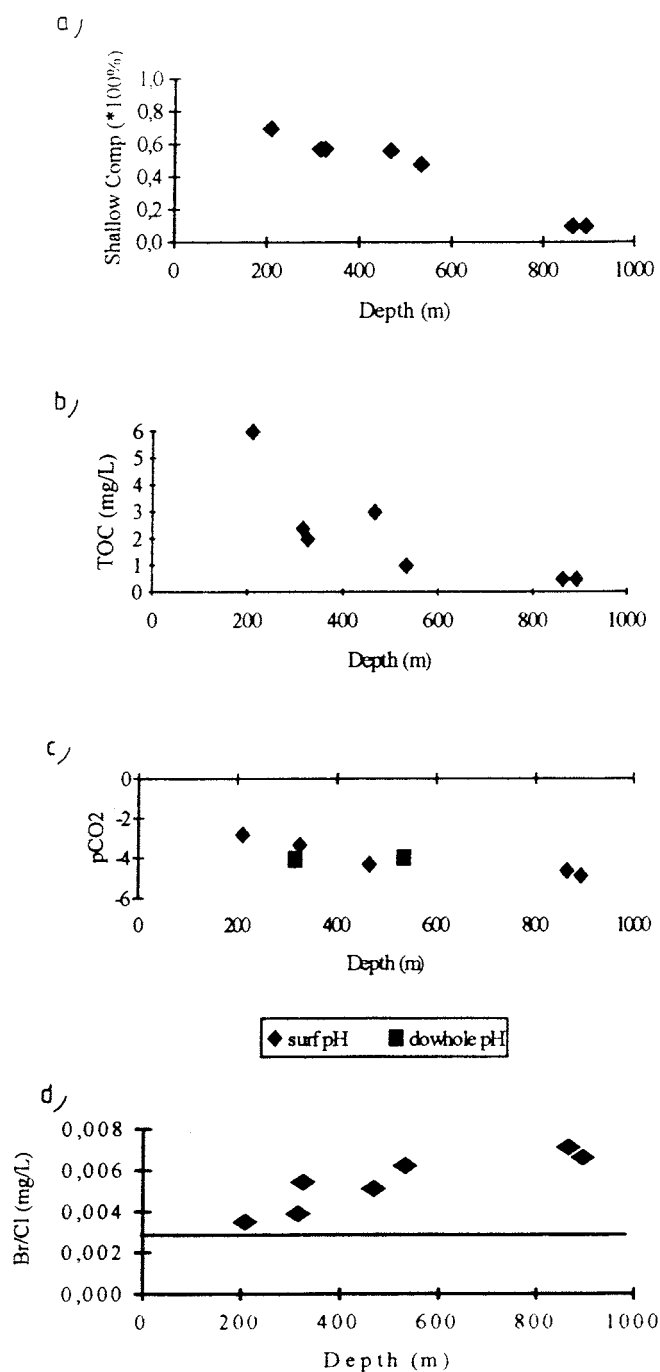
Figure 5.12. KAS02 groundwaters showing: a) calculation of the shallow water input
derived from a simple two component mixing model using Cl end members
from HAS05 and KAS03, b) TOC (total organic carbon) versus depth,
c) calculated pCO_2 pressures from dowhole and surface (on-line) pH
readings, and d) Br/Cl ratio versus depth; the horizontal line represents
the seawater Br/Cl ratio (0.0031) for reference.

samples lie closer to the sea water ratio than in the deeper parts of the borehole. Sea water input should not therefore be ruled out.

The simple two-component mixing model just discussed may also be used to describe the hydraulics of the borehole sections sampled. For example, in Figure 5.13a the KAS02 samples plot either on or near to the equilibrium mixing model line, and the deviation of the latter samples can be either explained by increased Cl dilution or concentration. Groundwaters that plot on the mixing line suggest derivation from a dynamic conductive fracture system where waters from various sources are adequately mixed and in the correct proportions according to the mixing model. In contrast, groundwaters plotting to either side of the mixing line suggest that the sampled fracture(s) is less conductive (i.e. isolated from the more dynamic hydraulic systems) and that groundwater mixing is incomplete. However, incomplete mixing (i.e. non-equilibrated) may also result from a very dynamic recharge/discharge situation within a highly conducting system. A final reason to be considered is that during the pumping/sampling procedures, groundwaters may be transported to the sealed off borehole section via fracture short-circuiting networks from higher (dilute) or from lower (concentrated) levels in the bedrock. This is especially true at high extraction pump flow-rates.

Figure 5.13a shows that down to approx. 500 m in KAS02 there is a Cl concentration excess, at 500 m mixing is complete, and near the borehole bottom there is Cl dilution. The Cl dilution is difficult to explain as this part of the borehole intercepts zone NE-1 which is considered to be discharging and water at that depth should therefore be highly saline (see Section 6.4). Some borehole activity contamination involving more surface-derived groundwaters cannot therefore be ruled out.

The mixing model described above can also be used to predict new mixing values for Na, Ca, HCO_3, SO_4, K and Mg (Fig. 5.13b and c) based similarly on end-member values. For better resolution each element is plotted as the relative percentage deviation in relation to the mixing model (Figs. 5.13b and c). Little or no deviation indicates that the element concentration can be explained by mixing; large deviations indicate sources (positive % value) or sinks (negative % value) for a particular element that are not accounted for by the mixing model.

The observed deviations in the figures can be due either to chemical reactions occurring in the fracture zone, to the presence of other groundwater types, or to an inappropriate mixing model. The compositional change at around 500 m is clearly shown by Mg and HCO_3 and to a lesser extent by Na and Ca; K may suggest a small increase below 500 m. At increasing depths losses of Na and Mg and gains of K, Ca, HCO_3 (after a marked loss to around 500 m) and possibly SO_4, are indicated, although at the greatest depth measured Na, Ca, SO_4 and HCO_3 all approach equilibrium mixing values. The loss of HCO_3 to around 500 m can best be explained by calcite precipitation, which is supported by the saturation index calculations. The small increase in SO_4 over the same depth is, however, contrary to what would be
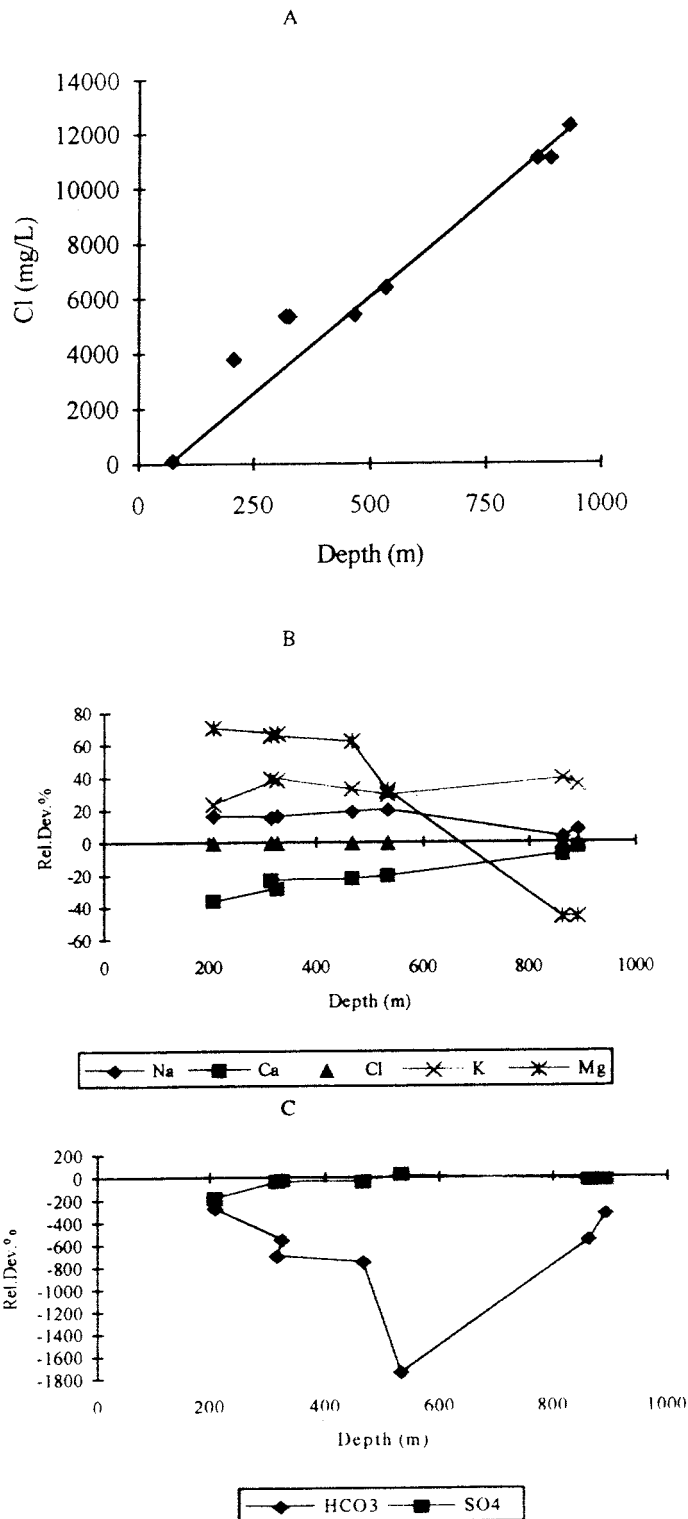
Figure 5.13. KAS02 groundwaters showing: a) plot of Cl vs depth related to the simple two component equilibrium mixing line, and b), c) depth trends of the major ions plotted as percentage relative deviation to the mixing model.

expected from pyrite dissolution but may be explained by gypsum instability and dissolution.

One reason for the general lack of correlation is probably the fact that two main groundwater processes are involved. There is the downward movement of agressive near-surface derived groundwaters which are undergoing some geochemical evolution by reacting with the bedrock. Somwhere between 200-300 m depth they are beginning to meet slowly upwelling saline groundwaters from great depth (>1000 m), forming a diffuse interface somewhere around the 400-600 m levels. As a result, normal groundwater chemical evolutionary trends are being masked by the saline groundwaters and therefore equilibrium geochemical models are not being entirely successful. A further complication may be the presence of chemical signatures from palaeogeochemical processes. This is discussed in detail in Section 6.

Uranium Geochemistry.

Figure 5.14 shows the solubility of different uranium oxide phases (thermodynamic data from Puigdomènech and Bruno, 1988) as a function of Eh (and pH). Plotted are the distribution of groundwater measurements from borehole KAS02 (together with KAS03 and KAS04; with pH values indicated) which show that the main solubility limiting phases are crystalline uraninite (UO_2) and the more amorphous U_4O_9 phase (P. Sellin, per. comm. 1992).

Uranium series data (Table 5.2) show high $^{234}U/^{238}U$ activity ratios (2.99-4.56) caused by a build-up of excess ^{234}U. This demonstrates that the groundwaters are moving sufficiently slowly through the bedrock so as to allow the excess ^{234}U to accumulate, and thereby supporting near stagnant conditions.
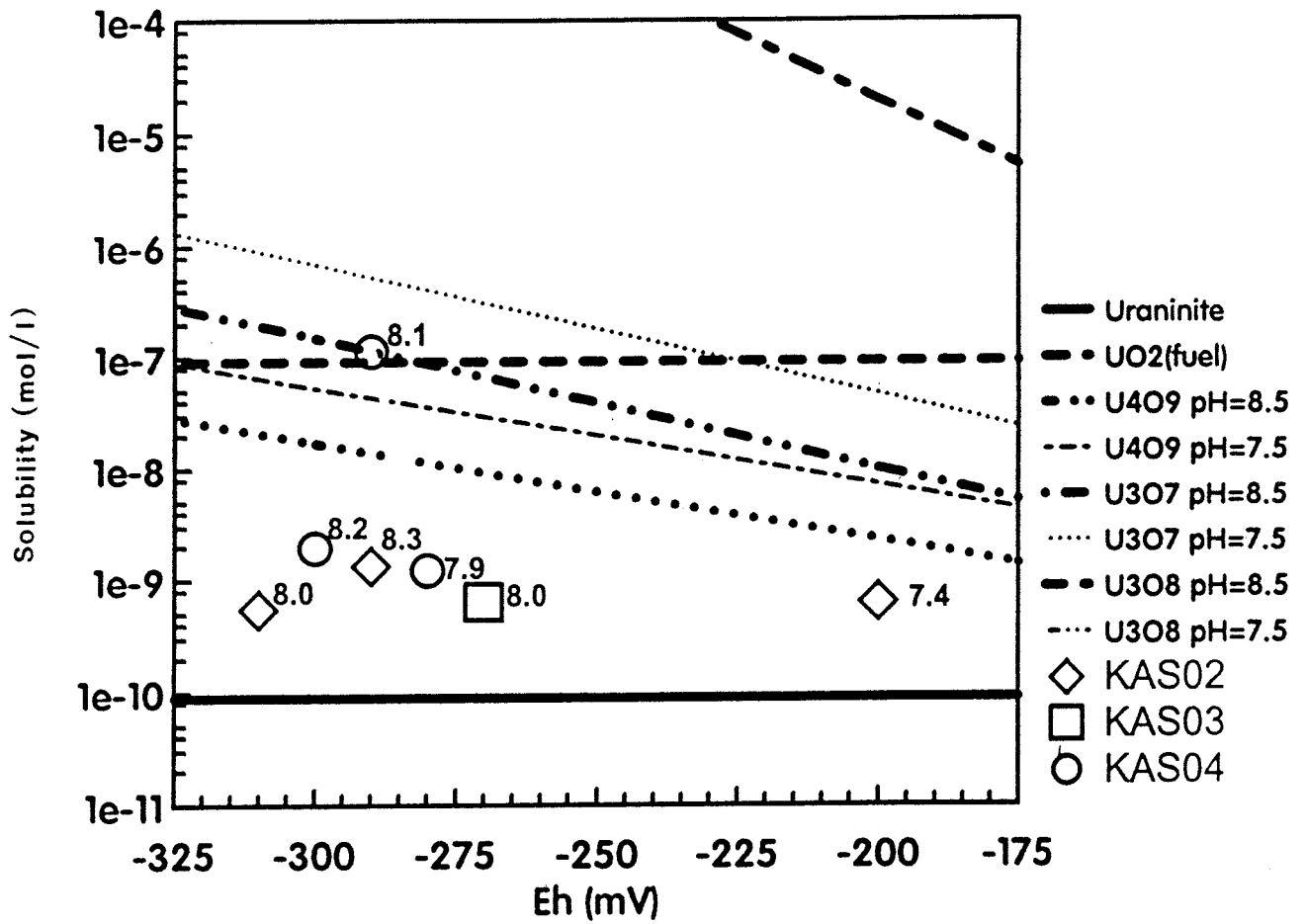
Figure 5.14. KAS02 groundwaters (with pH values indicated) related to the solubility of different uranium oxide phases plotted as a function of Eh (and pH). Thermodynamic data from Puigdomènech and Bruno, 1988).

Borehole	KAS02	KAS02	KAS02	KAS02	KAS02	KAS02	KAS02
Section m	202-214.5	308-344	314-319	463-468	530-535	802-924	860-924
Sampling method	CCC	SPT	CCC	CCC	CCC	SPT	CCC
Sample no.	1548	1474	1418	1428	1433	1470	1560
Date	890111	880927	880411	880424	880505	880920	890131
W.flow ml/m	61	5000	176	158	117	15200	135
Drillingwater %	0.80	0.70	0.6	0.40	0.30	0.20	0.22
Cond. mS/m	1060	1510	1580	1630	1890	2910	2970
Density g/ml	1.0006	1.0029	1.0034	1.0036	1.0046	1.0098	1.0103
pH	7.4	7.6	8.1	8.3	8.0	8.2	8.4
E_h (mV)	-260	-	-400	-290	-310	-	-
Alkalinity (mg/l BCO_3)	71.0	32.7	26.6	25.0	10.4	7.1	11.0
Charge balance mequiv./l	0.22	-3.49	0.25	0.53	-0.69	-14.14	-0.58
Rel. charge bal. error %	0.10	-1.11	0.08	0.17	-0.18	-2.22	-0.09

Element				mg/l			
Na	1300	1710	1700	1800	2200	2850	3000
K	6.6	8.8	9.00	8.1	8.1*	11.5	10.9
Ca	990	1480	1540	1580	1890	3690	3830
Mg	65	75	72	66	42*	39	31
Sr	-	27	26	30	35*	61	63
Mn	0.91	0.67	0.80	0.73	0.29*	0.19	0.23
Li	0.38	0.55	0.56	0.81	1.00*	1.80	1.9
Fe,tot	0.502	0.719	0.794*	0.964	0.244	0.027	0.051
Fe(+II)	0.483	0.624	0.788*	0.941	0.240	0.023	0.049
F	1.3	1.3	1.3	1.4	1.6	1.6	1.6
CL	3820	5360	5340	5440	6330	11000	11100
Br	13.4	29	21	28	42*	79	74
I	0.30	0.33	0.33	0.32	-	0.76	0.69
PO_4-P	<0.01	0.01	0.002	-	0.003	0.010	<0.02
SO_4	106	291	270	290	550	522	519
S_2^-	0.50	0.15	<0.01	0.13	0.18	0.01	0.72
NO_2-N	<0.001	0.001	-	-	-	0.001	<0.001
NO_3-N	<0.01	0.01	-	-	-	0.01	<0.01
NH_4-N	0.40	0.37	0.25	0.22	0.03	0.01	0.01
SiO_2-Si	6.0	4.4	2.0	3.3*	4.2	4.2	4.0
TOC	6.0	2.0	2.4	3.0	1.0*	0.5	<0.5

* No determination. The result from another sample in the same borehole section is presented.

Table 5.2: Uranium and isotopic analyses of groundwaters from borehole KAS02, Äspö.

Borehole	KAS02	KAS02	KAS02	KAS02	KAS02	KAS02	KAS02
Section m	202-214.5	308-344	314-319	463-468	530-535	802-924	860-924
Sampling method	CCC	SPT	CCC	CCC	CCC	SPT	CCC
Samle no.	1548	1474	1418	1428	1433	1470	1560
Date	890111	880927	880409	880425	880505	880920	890131
Percentage Modern Carbon (PMC)	23	-	21	17	-	-	-
^{14}C age BP	10435	-	12670	13910	-	-	-
age BP corr.		-	12960	13960	-	-	-
^{238}U (mBq/kg)	3.78	3.87	8.52	8.10	3.19	18.02	13.06
^{235}U (mBq/kg)	0.24	0.28	1.00	0.50	0.05	0.89	0.90
^{234}U (mBq/kg)	43.2	15.9	26.1	24.2	10.4	57.5	17.2
U_{tot} (ug/kg)	0.15	0.15	0.34	0.32	0.13	0.72	0.54
^{235}U/^{238}U	0.066	0.073	-	-	-	0.049	0.070
^{234}U/^{238}U	3.16	4.11	3.06	2.99	3.25	3.16	4.56
^{18}O (SMOW)	-13.9	-12.7	-12.3	-12.8	-12.3	-13.0	-13.1
^{2}H (SMOW)	-108.9	-99.8	-100.6	-99.9	-97.2	-96.8	-96.8
^{3}H (Bq/l) [1]	< 1	< 1	~ 1	~ 1	~ 1	~ 1	~ 1
^{3}H (TU) [2]	0.30	-	-	-	-	-	0.20

[1] Kjeller, Norway

[2] IAEA, Wienna

Borehole	KAS02	KAS02	KAS02	KAS02	KAS02	KAS02
Section (m)	309-345	309-345	309-345	309-345	309-345	309-345
Sample no	1636	1643	1647	1652	1677	1678
Sampling method	MONIT.	MONIT.	MONIT.	MONIT.	MONIT.	MONIT.
Date Collected	900503	900509	900514	900528	900606	900613
W.flow ml/m	300	310	310	330	330	320
Drilling water %	0.70	0.70	0.63	0.64	0.51	0.18
Cond. mS/m	-	-	-	-	1680	-
pH	6.9	7.2	7.0	6.8	7.0	7.0
Alkalinity (mg/l HCO_3)	47.9	47.2	47.0	49.8	48.7	47.7
Charge Balance %	-0.61	-2.78	-2.39	-1.92	-2.19	-1.72

Element				mg/l		
Na	1880	1790	1780	1790	1730	1750
K	(9.9)	-	9.6	-	9.8	9.9
Ca	1780	1670	1640	1640	1580	1580
Mg	72.0 (66.7)	71.0	71.0	72.0	73.0	73.2
Sr	29.1 (31.4)	28.7	28.2	28.1	26.7	27.0
Mn	0.76(0.68)	0.76	0.78	0.80	0.80	0.81
Li	0.95(1.20)	0.94	0.86	0.93	0.85	0.86
Fe(tot)	0.40(0.38)	0.37	0.42	-	0.47	0.63
Cl	6080	6010	5930	5860	5700	5680
F	1.6	1.7	1.7	1.6	1.8	1.6
S(ICP)	112.0 (152.3)	110.00	96.00	105.00	104.00	103.00
SO_4	336	330	288	315	312	309
SiO_2-Si	4.1 (3.6)	4.0	3.5	4.1	3.5	3.6

Borehole	KAS02	KAS02	KAS02	KAS02	KAS02	KAS02	KAS02
Section (m)	800-854	800-854	800-854	800-854	800-854	800-854	800-854
Sample no	1637	1644	1646	1653	1661	1676	1679
Sampling method	MONIT.	MONIT.	MONIT.	MONIT.	MONIT.	MONIT.	MONIT.
Date Collected	900503	900509	900514	900528	900530	900606	900613
W.flow ml/m	260	300	290	350	450	360	310
Drilling water %	1.60	1.79	1.70	1.60	-	1.20	0.42
Cond.mS/m	-	-	-	-	-	2680	2310
Density g/ml	-	-	-	-	-	-	-
pH	7.1	7.5	7.0	7.0	-	7.0	7.5
Alkalinity (mg/l HCO_3)	9.2	9.2	8.5	9.1	-	8.4	7.9
Charge Balance %	-2.10	-2.15	-2.23	-2.13	-	-1.96	-

Element				mg/l			
Na	2680	2620	2680	2720	2730	2690	-
K	-	11.5	10.9	-	-	10.6	-
Ca	3130	3150	3160	3180	3180	3230	-
Mg	33.8	32.3	31.7	31.7	31.2	31.3	-
Sr	52.0	53.5	54.1	55.5	55.2	53.6	-
Mn	0.21	0.21	0.20	0.21	0.21	0.19	-
Li	2.13	2.20	2.16	2.25	2.27	2.22	-
Fe(tot)	0.09	0.14	0.13	-	-	0.09	-
Cl	9830	9800	9930	9980	-	10000	9990
F	1.8	1.8	1.8	1.7	-	1.8	1.8
S(ICP)	177.00	172.00	172.00	181.00	-	180.00	-
SO_4^{2-} (calc)	531	516	516	543	-	540	-
SiO_2-Si	4.2	4.3	3.8	4.4	4.1	3.8	-

5.2. Borehole KAS03.

Borehole KAS03 (Fig. 5.15), located in the NW sector of Äspö, has an upper diameter of 155 mm down to 100 m and a lower diameter of 56 mm to the hole bottom at 1002 m. The borehole was drilled at an inclination of 85° to a vertical depth of approx. 1002 m to evaluate the bedrock geology, hydrology and hydrogeochemistry.

The most common rock encountered is the red-grey, fine- to medium-grained porphyritic granite-granodiorite of the Småland type; megacrysts are typically of microcline. This granite dominates to approx. 560 m whereupon the rock type changes to alternations of dark-grey, fine- to medium-grained diorites (occasionally containing red megacrysts of microcline and sometimes occurring as dykes and veins) and dark red to reddish-grey, fine-grained, fairly massive (aplitic) granites. These continue to dominate throughout the remaining length of the borehole. Occurring from about 220 m to the hole bottom are sporadic horizons (1-20 m thick) of greenstones (grey-black and fine-grained) which are mainly metavolcanic in origin. Along the total length of the drillcore the Småland granite accounts for 62% followed by the fine-grained aplitic granite (23%), diorite (12%) and finally greenstone (3%).

Borehole KAS03 intersects the northern margin of the hydraulically conductive, major EW-1 mylonite shear zone (Fig. 5.15b) which divides Äspö into two tectonic blocks. The zone (dipping 60°N) is topographically (50-100 m wide depression extending over several hundreds of metres) and geophysically (low magnetic and resistivity anomalies) distinct. Hydrothermal alteration (oxidation of magnetite) and the formation of other minerals phases) has served to the "seal" the zone. The most highly conductive parts therefore tend to be restricted to narrow highly fractured sections or single open fractures separated by slabs of Småland granite and up to one metre wide mylonite zones.

More minor tectonic influence is mainly observed as: a) <5 cm ductile shears which group at four levels spaced fairly regularly apart (about 200 m), and b) mylonitic zones, one of which intersects at 390-420 m depth and consists of two, approx. 1 m wide mylonites at 397 m and 403 m respectively. These are surrounded by brecciated rocks with intense foliation. Other, more minor examples occur at 456 m (in granite) and at 865 m and 920 m (coinciding with lithological boundaries). Further mylonite zones occur at 480-485 m, 626 m, 632-643 m and 661-687 m.

Investigations of the fracture systems (Fig. 5.16) from drillcore mapping and borehole geophysical methods such as single point resistance and sonic (Sehlstedt, 1988), reveal at least four distinct sections of high fracture frequency in the upper 500 m of the drillcore (217-222 m, 280-295 m, 370-385 m and 395-420 m). These zones are dominated by calcite, chlorite and hematite; an increased frequency in laumonite is found at approx. 220 m corresponding to the 217-220 m zone; Fe-oxyhydroxides are
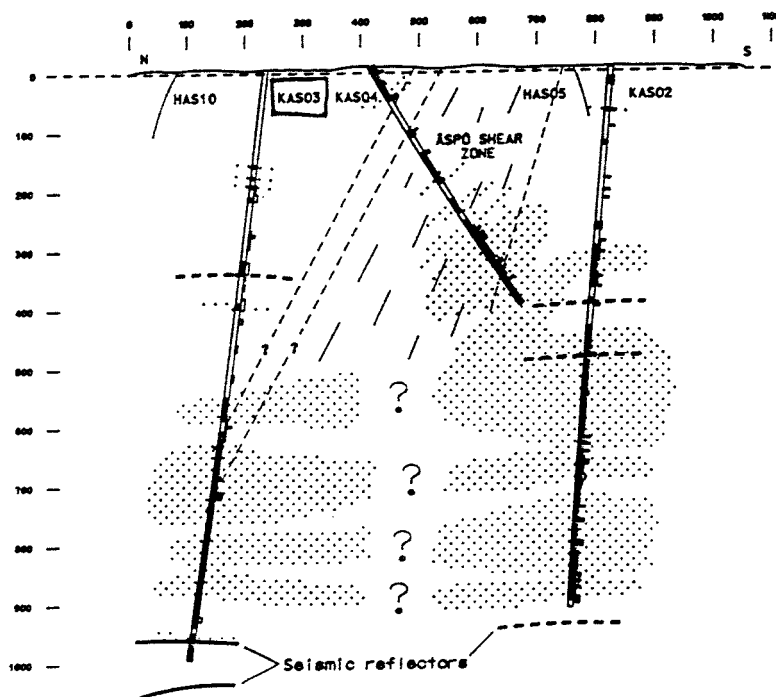
a)
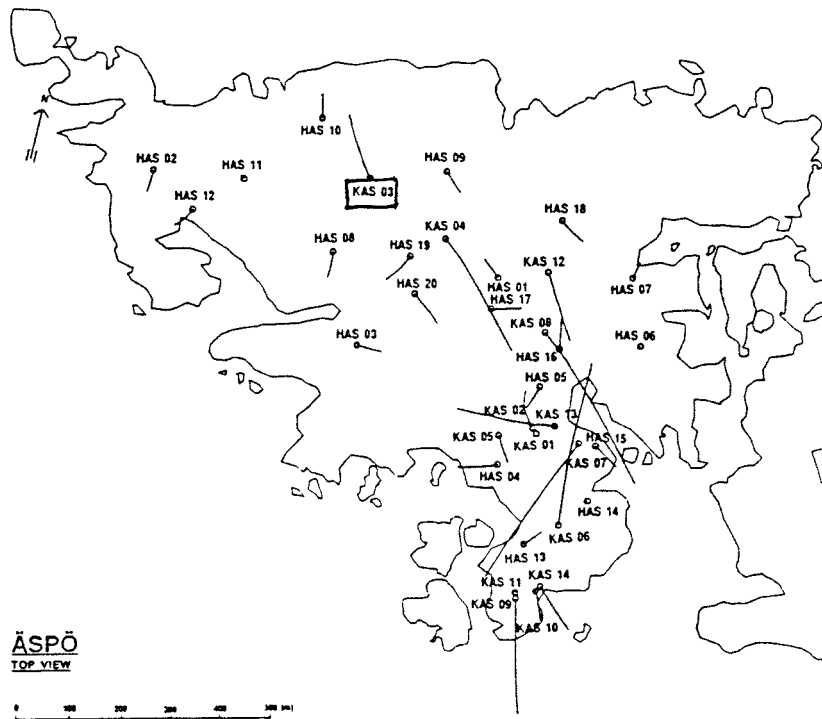
b)

Figure 5.15. Location of borehole KAS03 (a) and its relationship to the major Äspö EW-1 Shear Zone (b) (from Wikberg et al., 1991).

most frequent in the 380-410 m section. In the lower 500 m of the drillcore two distinct zones are apparent: at 610 m and 715 m which represent the interception of zone EW-1. These are characterised by calcite, hematite and epidote, with the latter zone showing steeply dipping fractures containing fluorite. An increase in epidote is observed between 775-800 m. Fracture mineral phase data plotted against depth show that surface related dissolution of calcite occurs down to approx. 30 m and that Fe-oxyhydroxides are present particularly in the upper 400 m with more sporadic occurrences at around 510-530 m, 610-650 m, 735 m and 870 m. Hematite is present throughout the drillcore length with the greatest occurrences coinciding with maximum Fe-oxyhydroxide formation.

Potentially conductive fracture zones have been identified by the geophysical logging supported by radar measurements. These zones, reflected by both the single point resistance and sonic profiles, correspond closely to the fracture zones described from the drillcore mapping above. Single hole radar reflection measurements have been carried out from 140-989 m and a total of 97 reflecting structures have been interpreted to intersect the borehole; the radar range is approx. 50 m in the rock adjacent to the hole. Areas of increased electrical conductivity appear between the depths of 195-230, 280-300, 390-415 and 580-635 m. From approx. 125-550 m (for hydraulic testing) and approx. 100-725 m (for spinner surveys) the areas of high hydraulic conductivity generally confirm the geophysical logging results.

The drilling log data show that no formational water was intercepted within the upper 100 m of the bedrock, i.e. presumably indicating very low conductivity. At increasing depth the measured hydraulic conductivity values taken every 3 m (103-547 m) and 30 m (103-703 m) intervals (see composite plot; Fig. 5.16) show an irregular distribution reflecting the heterogeneous occurrence of conducting fracture zones. Values average around 10^{-9} ms^{1} from 125-550 m with maximum conductivities around 10^{-6} ms^{-1}. These, together with the spinner measurements (taken every 1 m from 100-720 m), indicate conductive zones at depths of approx. 220, 250, 355, 370, 460, 530, 615 and 690 m. Based on this information sections were chosen for the various borehole activities, i.e. pump testing, hydraulic injection testing, tracer testing and groundwater chemical characterisation; these activities are listed in Table 3.2.

The transmissivity of the total borehole was determined at 1.6×10^{-5} m^{2}s^{-1}; selected borehole sections (Fig. 5.17b) show values ranging from 0.87×10^{-6} to 4.0×10^{-6} m^{2}s^{-1}; the highest values occurring within sections 610-622 m and 197-221 m (4.0×10^{-6} and 2.65×10^{-6} m^{2}s^{-1} respectively) and some of the lowest in the two deepest sections, i.e. 690-1002 m and 860-1002 m (1.6×10^{-6} m^{2}s^{-1}) and in section 453-480 m (1.1×10^{-6} m^{2}s^{-1}). The piezometric head values (M. Lidholm, per. comm., 1991) are all negative (Fig. 5.17c), the lowest value (-17.12 m) corresponding with the low transmissivity section at 453-480 m. The highest head value (-0.04 m) corresponds with the lowest transmissivity section at 129-134 m which supports the drill log observations that the upper 100 m is "tight".
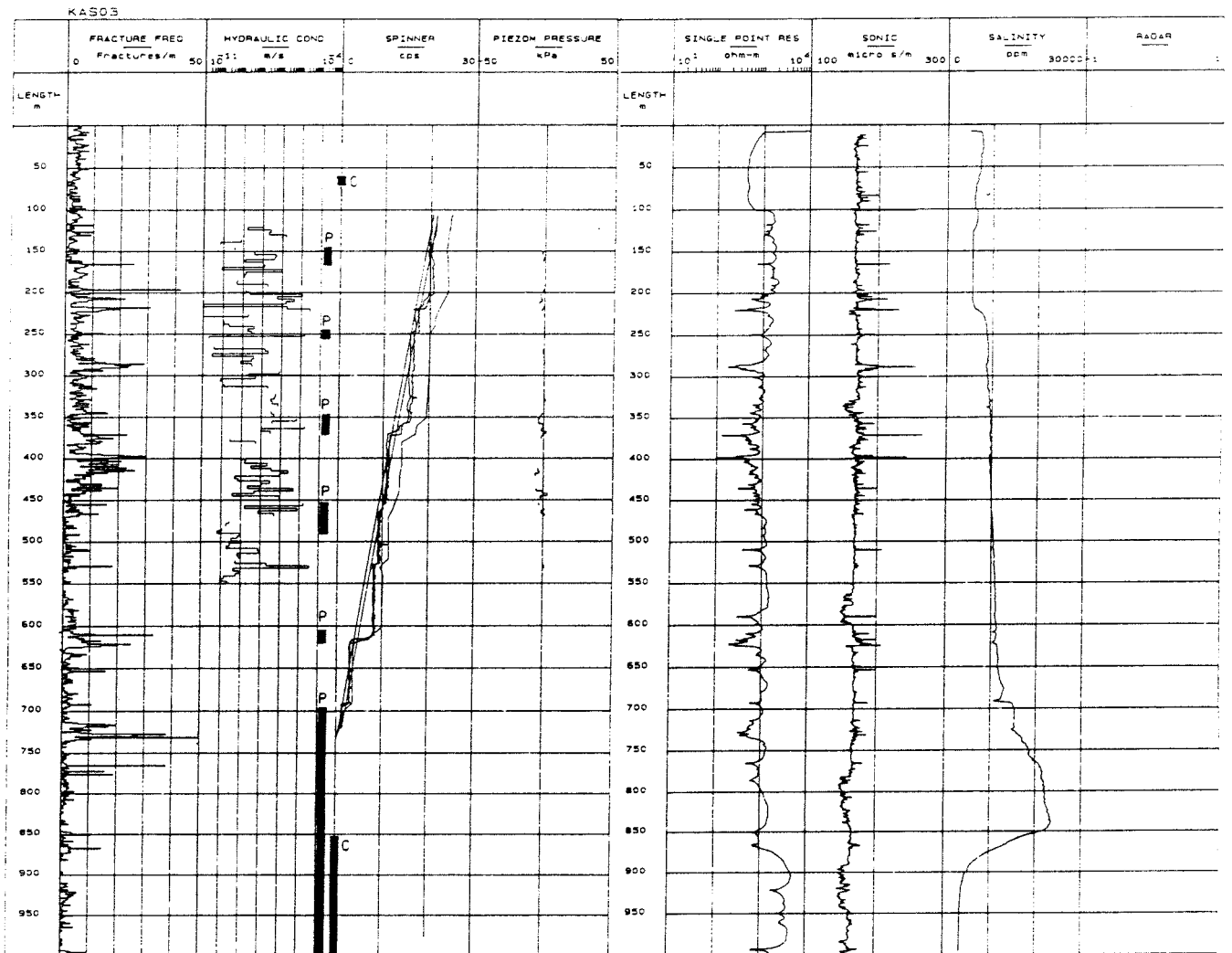
Figure 5.16. Composite log of borehole KAS03.
Bars placed between the hydraulic conductivity and spinner log columns
indicate the borehole sections sampled for groundwater chemistry;
(P= sampling during pump testing, C= normal sampling protocol).
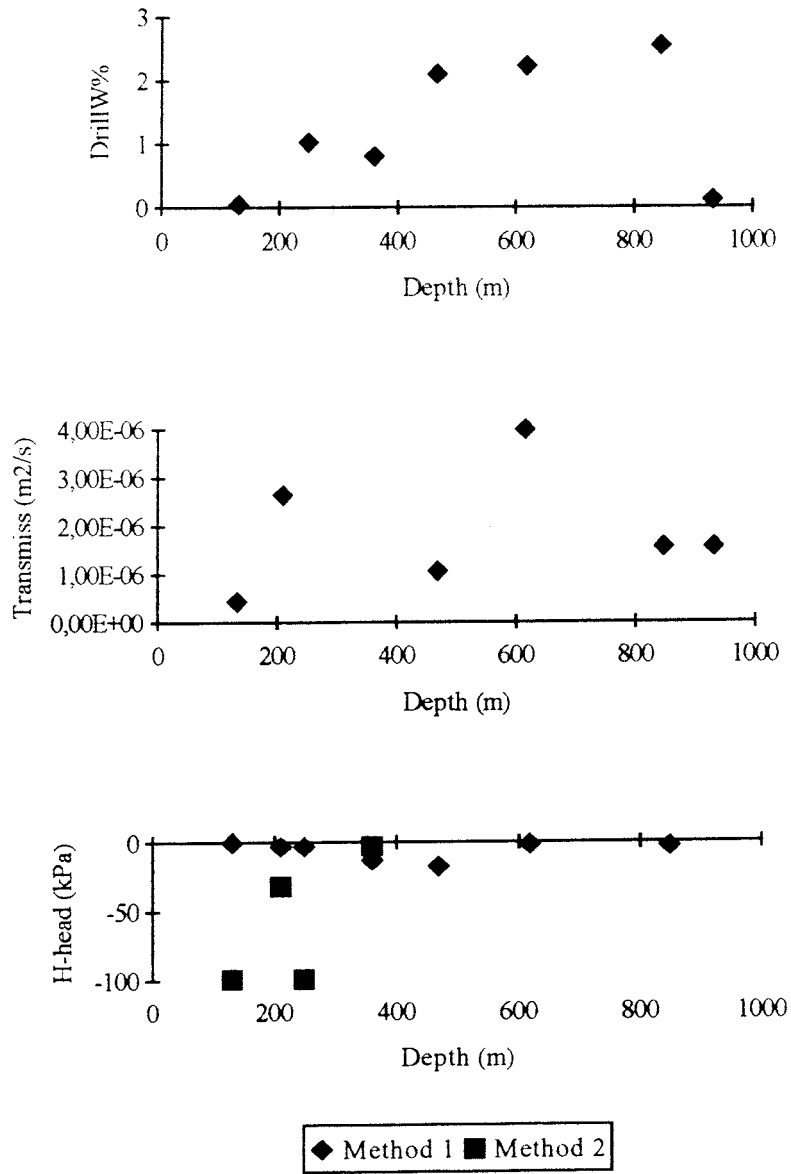
Figure 5.17. Summary of borehole measurements: a) uranine tagged activity water (from drilling and hydraulic injection tests), b) transmissivity, and c) piezometric head (Method 1 = VIAK; 2 = SGAB).

These data would suggest that in borehole KAS03 there is a distinct possibility that the central portion, i.e. from approx. 300-500 m and corresponding with an area of high fracture frequency, contains residual waters resulting from the various borehole activities, unless pumping has been adequate to remove all traces. However, because of the generally fairly high conductivities along the borehole section, excess pumping may also have resulted in unacceptable groundwater compositions from higher or lower levels being present.

5.2.1. Level 129-134 m.

The borehole length is characterised by the Småland granite sporadically containing red megacrysts of microcline. Generally the fracture frequency is low with an average of 5 fractures/metre, increasing to one narrow maximum of 10 fractures/metre at 130 m, where the main filling minerals, present in a sealed fracture, are chlorite, calcite and some epidote.

Hydrology.

The sampled section is located within a 30 m section (103-133 m) recording a hydraulic conductivity of 1.3×10^{-8} ms^{-1}. More precise data are obtained from the 3 m sections measured within and peripheral to the sampled level, i.e. sections 127-130 m, 130-133 m and 133-136 m, recording conductivities of 1.9×10^{-8}, 1.5×10^{-7} and 4.0×10^{-12} ms^{-1} respectively. The main conductive borehole length can therefore be restricted to the fracture zone contained in the 130-133 m section.

The sampled level is therefore characterised by a moderate hydraulic conductivity, restricted transmissivity and a piezometric pressure head about zero (-0.04 m). This would suggest that any groundwater contamination should be reasonably well restricted to within the immediate vicinity of the sampled level, and that the groundwater collected should be representative. This is supported by the negligible tagged activity water component in the analysed groundwaters (0.08-0.06%) and the background level of the tritium content (0.15 TU). Furthermore, monitoring during the presampling pumping showed very little chemical variation during a 24 hour period; for example pH, Eh and HCO_3 remained constant and of the major chemical parameters, only Cl varied from 1240-1220 mg/L, SO_4 from 33.3-31.1 mg/L and K from 2.2-2.4 mg/L. The tagged water component was also consistently low (0.08-0.06%).

Water Chemistry.

The sampled water (Table 5.5) has a mean pH value of 8.0 and a major ion range of values considerably more saline than a normal Swedish groundwater from crystalline rock (e.g. 4-15 mg/L Cl and 0.5-15 mg/L SO_4 etc). The water is of a Na-Ca(Mg) HCO_3-Cl type, corresponding to the Äspö Type A of Laaksoharju (1990a), and is characteristic of a near-surface groundwater environment, although the low TOC partly contradicts this assertion.

Redox-sensitive Parameters.

The iron and sulphide contents are fairly low and all of the iron is in the ferrous state; a reducing environment is further supported by a high negative Eh value (-260 mV).

Isotope Geochemistry.

Stable isotope values of $\delta^{18}O$ = -15.8 ‰ and δ^2H = -124.8 ‰ plot just below the meteoric water line (Fig. 5.18) suggesting either a depletion of δ^2H or enhancement of $\delta^{18}O$. The low tritium value (0.1 TU) indicates an absence of a young, surface water component, which is further supported by the low percentage modern carbon (2%; i.e. a very old apparent radiocarbon age of 31 365 BP; Table 5.6).

Uranium Geochemistry.

The total uranium value (Table 5.6) is low, 0.15 μg/L, suggesting a reducing environment and therefore supporting the other redox-sensitive parameters. The $^{238}U/^{234}U$ activity ratio is high (4.56) indicating widespread isotopic disequilibrium in the groundwaters and long bedrock residence/reaction times. This further supports the very old age of the water.

Summary.

The chemical and isotopic parameters show that this groundwater, although from a relatively near-surface environment, represents an old water with a long residence time. There has been little influence from younger, more surface-derived waters, probably due to the overall low conductivity of the bedrock at these shallow depths. This groundwater amy therefore be considered as representative for the section level sampled.
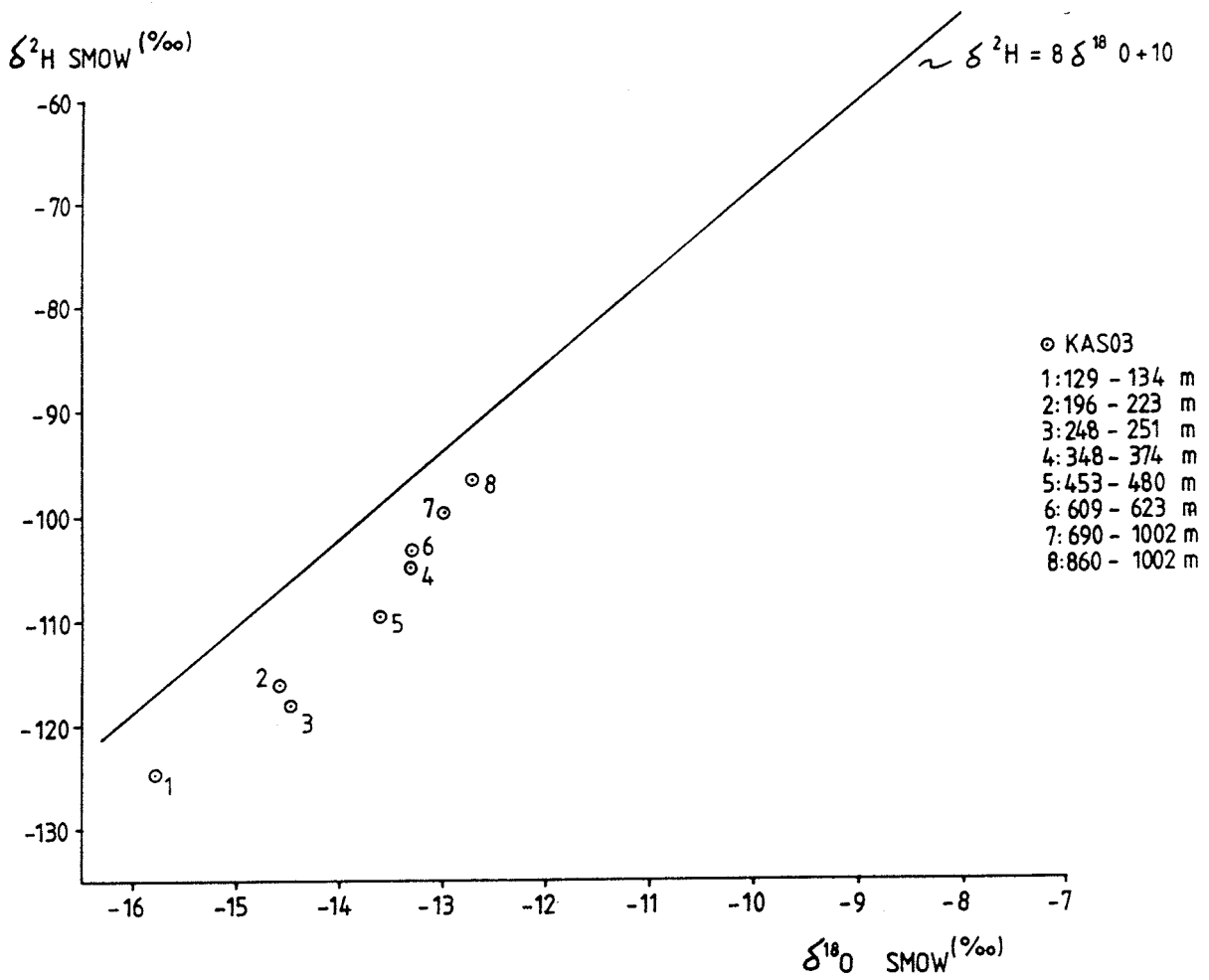
Figure 5.18. Stable isotope composition of borehole KAS03 groundwaters, Äspö.

5.2.2. Level 196-223 m.

The sampled section is composed of three rock types; the red, fine- to medium-grained granite/aplite (approx. 196-209 m), the Småland granitoid (approx. 209-217 m) and the metavolcanic greenstone (217-223 m). The core length contains an average of 6 fractures/metre with two more intensely fractured zones (up to 30-40 fractures/metre) occurring at approx. 195 m and 220 m, i.e. closely coinciding with both contacts of the fine-grained or aplitic granite. The mineral infilling phases are dominated by calcite, chlorite and hematite with minor Fe-oxyhydroxides.

Hydrology.

The sampled section lies within a 30 m section (193-223 m) recording a hydraulic conductivity of 2.3×10^{-7} ms^{-1}. From the measured 3 m sections the conductivity ranged from 2.8×10^{-6} ms^{-1} (near the bottom of the tested system at 220-223 m) to lower values of around 1.7×10^{-9} ms^{-1} (near the top of the tested section at 196-202 m). The highest value (1.1×10^{-6} ms^{-1}) occurs between 202-205 m. These data, together with a fairly strong response from the spinner survey at approx. 220 m, would suggest that the zone between 220-223 m is the main groundwater source. Transmissivity for the sampled section is fairly high (2.7×10^{-6} m^{2}s^{-1}), i.e. higher than the sampled level described above and the piezometric head is around zero (Figs. 5.16 and 5.17c).

Because of the relatively high hydraulic conductivity and moderate transmissivity, some contamination into the adjacent bedrock may have resulted. This is indicated by the decrease of the residual tagged activity water component in the groundwaters during presampling pumping (from 8.43 to 2.70% in about a 10 hour period). No values are available for the sampling period. Other chemical parameters which showed a response to the pumping included Cl (from 2640 to 2850 mg/L), SO$_4$ (from 65 to 31 mg/L); HCO$_3$, K, Ca and Mg were all stable.

Water Chemistry.

The sampled water (Table 5.5) has a pH of 7.7; the major ions Na, K, Ca, Mg and Cl are substantially higher than in the previous level, whilst HCO$_3$ and SO$_4$ are unaffected. The groundwater differs somewhat from level 129-134 m and can be expressed as a Na-Ca(Mg) Cl-HCO$_3$ type, similar to an Äspö Type B as classified by Laaksoharju (1990). The TOC is low (1.0 mg/L) suggesting the absence of a major younger water component.

Redox-sensitive Parameters.

No reliable Eh values or iron analyses are available; sulphide values are very low (0.05 mg/L).

Isotopic Geochemistry.

Similar to the previous level, the $\delta^{18}O$ and δ^2D values plot under the meteoric water line (Fig. 5.18). Very low tritium (<8 TU) together with a low percentage of modern carbon (7%; apparent radiocarbon age of 21 695 BP; Table 5.6) suggests that no major young, near-surface derived component is present. However, because a slightly higher percentage modern carbon content is present, when compared to the above sampled level, some dilution possibly due to a younger water component connot be neblected.

Uranium Geochemistry.

Uranium values (Table 5.6) remain low (0.19 µg/L) and are accompanied by a high $^{234}U/^{238}U$ activity ratio (3.54). Long residence times under reducing conditions are indicated by these data, similar to the 129-134 m level.

Summary.

The chemical parameters presented support a reducing, increasingly saline groundwater (when compared to the above level) with a long residence time and probably mixed with a younger, perhaps less saline water component (tagged activity water?), resulting from the borehole activities. In particular, the high extraction rate of water from this level (10 000 mL/min.), bearing in mind the relatively high hydraulic conductivity, may have facilitated the mixing of water from other levels and groundwater sources.

5.2.3. Level 248-251 m.

The sampled section is composed of a single rock type, the granite/aplite. The core length comprises an average of 4 fractures/metre with one marked fracture zone at 249-250 m containing up to 14 fractures/metre (Fig. 5.16). The main infilling minerals are calcite, chlorite and hematite; only minor Fe-oxyhydroxides are observed.

Hydrology.

The sampled section falls within the 30 m scale tested borehole length (223-253 m) which recorded an average hydraulic conductivity of 1.8×10^{-7} ms^{-1}. In greater detail the 3 m scale section (247-250 m) recorded a conductivity of 2.9×10^{-9} ms^{-1} with a low negative head pressure (-3.12 m) and an approximate transmissivity of 8.7×10^{-9} m^{2}s^{-1} (Fig. 5.17b and c). A small spinner response is observed at approx. 250 m. These data, characterised by a low to moderate conductivity and little pressure head difference, suggest that widespread bedrock contamination from borehole activities should not be a major problem. A low tagged water component is present (1.04%

during sampling), having decreased from 2.68% over a 24 hour period prior to sampling. Over this same period little change in the other chemical parameters was observed; only SO_4 decreased from 55 to 39 mg/L.

Water Chemistry.

The sampled waters (Table 5.5) have a pH of 7.7 and a major ion content which differs little from the preceding level described, i.e. Na-Ca(Mg) Cl-HCO$_3$ in type; TOC is very low.

Redox-sensitive Parameters.

No reliable Eh values are available but reducing conditions are indicated by the fact that most of the total iron is in the ferrous state; the sulphide content is low (0.17 mg/L).

Isotope Geochemistry.

In common with the preceding levels described, the $\delta^{18}O$ and δ^2H values (-14.5 ‰ and -118.1 ‰) plot below the meteoric water line (Fig. 5.18) and a similar percentage modern carbon content (8%; apparent radiocarbon age of 20 090 BP; Table 5.6). Tritium is very low (<8 TU).

Uranium Geochemistry.

The total dissolved uranium (Table 5.6) remains low (0.49 μgL) but higher than the preceding levels; the $^{238}U/^{234}U$ activity ratio is still high (4.23) indicating widespread isotopic disequilibrium of the groundwaters and long bedrock residence/reaction times.

Summary.

For all purposes this groundwater is identical to the preceding level described. Some residual tagged activity water is present and the duration of pumping has been inadequate to remove it all, even though a fairly high pump extraction rate was used (4 000 mL/min).

5.2.4. Level 347-374 m.

The sampled section, which consists only of the Småland granitoid, extends from the contact with metavolcanic greenstones at 347 m from the top end of the sampled section, down to 374 m where large microcline megacrysts become more common. The section has a background fracture density of around 7 fractures/metre with more pronounced fracture zones (up to 20 fractures/metre) occurring at approx. 357 m and

372 m (Fig. 5.16). The infilling minerals are still dominated by chlorite and hematite with lesser calcite and some Fe-oxyhydroxides.

Hydrology.

Along the 30 m scale tested section from 373-403 m, the average hydraulic conductivity can be considered moderate to low with a value of 6.8×10^{-9} ms^{-1}. Along the 3 m scale section lengths, conductivities range from low (10^{-12} ms^{-1}; 349-352 m and 358-361 m) to moderate (10^{-8} ms^{-1}; 346-349 m and 355-358 m). The most conductive sections indicated by the spinner survey (1.7×10^{-6} and 6.4×10^{-7} ms^{-1}; 361-364 m and 352-355 m respectively) do not correspond to any marked fracture zone(s). A strong spinner effect occurs, however, from packer tests installed at approx. 371 m. The sampled section (Fig. 5.17a-d) is characterised by a marked negative piezometeric head (-12.92 m); the transmissivity is approximately 1.9×10^{-6} m^{2}s^{-1}. These data, i.e. the combination of moderate conductivity with negative head, indicate the possibility of bedrock contamination in the near-vicinity of the borehole at this level. This has undoubtedly happened, but the presampling pumping/monitoring period (duration of 24 hours) shows that almost all tagged activity water has been effectively removed (decrease from 7.89 to 0.83%), although the high extraction pump rate (18 000 mL/min) may also have served to draw in water from other levels and sources. The available tritium data are not precise enough (<8 TU) to pursue this further.

Water Chemistry.

The water sampled (Table 5.5) has a pH of 7.8; the major ions show an increasingly more saline groundwater with depth, with marked increases in Ca, Cl and SO$_4$ (and to a lesser extent Na) and a corresponding decrease in HCO$_3$. Potassium and Mg remain unchanged. The water can be considered Na-Ca(Mg) Cl-SO$_4$ in type, equivalent to Äspö Type C after Laaksoharju, (1990a).

Redox-sensitive Parameters.

In the absence of any reliable Eh data, reducing conditions are indicated by the high content of ferrous iron which, in common with the other described levels, is assumed to constitute the total dissolved iron (no value available) in the groundwater. The sulphide content is very low (0.05 mg/L).

Isotope Geochemistry.

The stable isotope values ($\delta^{18}O = -13.3$ ‰; $\delta^2H = -104.9$ ‰) show the same trend as for the preceding plots, i.e. plotting below the groundwater meteoric line (Fig. 5.18). Tritium is very low (<8 TU) and no radiocarbon data are available (Table 5.6).

Uranium Geochemistry.

Dissolved uranium contents (Table 5.6) are still low (0.08 μg/L); the $^{234}U/^{238}U$ activity ratios are lower than in the shallower levels (decrease to 3.0) but still relatively high. Once again, these data suggest adequate residence times to allow the excess build-up of ^{234}U, probably by recoil effects.

Summary.

This sampled section marks the transition to an even more saline groundwater environment where the water is still strongly reducing and the residence time is adequate to produce the high uranium isotope activity ratios. Residual tagged borehole activity waters were contained within the more conductive fracture zones, but these appear to have been largely removed during the presampling and sampling stages. The high pump extraction rate of 18 000 mL/min. may have led to some groundwater mixing from other levels and sources as indicated by a change in the Ca, Cl and SO_4 concentrations with pumping.

5.2.5. Level 453-480 m.

The sampled section forms part of the Småland granitoids, characterised by xenoliths or schlieren of metavolcanic greenstone and small dykes and veins of the fine-grained granite/aplite. The fracture frequency decreases markedly to an average of 2-3 fractures/metre along the complete borehole from approx. 450 m to the hole bottom; the level sampled has an average of 1-2 fractures/metre. Three important fracture zones have been observed; at 455, 462 and 467 m (also indicated by the geophysical logs; Fig. 5.16) and are characterised by mineral infillings of chlorite and hematite with subsidiary calcite. The zone at 455 m is considered sealed.

Hydrology.

The 30 m scale section which contains the sampled level has an average hydraulic conductivity of 10^{-8} to 10^{-7} ms^{-1}. The location of the two major fractures in the 3 m scale sections correspond to moderate to high average hydraulic conductivities (1.6×10^{-6} ms^{-1} at 454-457 m and 4.8×10^{-8} ms^{-1} at 466-469 m) and a fairly high transmissivity value (1.1×10^{-6} m^{2}s^{-1}). A weak spinner response occurs at approx. 455 m and, furthermore, the section is characterised by a highly negative piezometric head value (-17.12 m). Taken together, these hydraulic data would suggest the potential for contamination from the tagged activity waters. This is supported by a content of 2.13% uranine tagged water present in the groundwaters sampled for chemical characterisation. The monitoring data prior to sampling showed a decrease from 3.62% over a period of 24 hours; however this pumping period has been inadequate to remove all the contaminating influences. The other chemical parameters show marked changes during this pumping period, specifically Ca, Cl and to a lesser

extent SO_4 and Na, all of which show increases from 1260 to 1400 mg/L (Ca), 4810 to 5180 mg/L (Cl), 320 to 370 mg/L (SO_4) and 1740 to 1770 mg/L (Na) respectively; K and HCO_3 remain fairly constant. Pump extraction rates were high (16 000 mL/min) which would suggest that water might have been drawn in from other levels and sources; available tritium data are not precise enough (<8 TU) to pursue thay further.

Water Chemistry.

The pH value (Table 5.5) is 7.8 in common with the two preceding levels sampled; of the major ions, Na and K show little change from the preceding level, but Ca, Cl and SO_4 (slight decreases) and HCO_3 (increase) indicate that a significant compositional change has occurred. Although still regarded as Na-Ca(Mg) Cl-SO_4 in type, the compositional variations show clearly that some groundwater from a higher level has been sampled (particularly suggested by the higher HCO_3 content), at least from level 248-251 m and upwards. The presence of residual tagged water (>2%) in the sampled groundwater, together with the fact that it is derived from the upper approx. 100 m of the bedrock characterised by Na-Ca(Mg) Cl-HCO_3 waters of lower Cl and SO_4 contents, could indicate that it may be the main source of contamination.

Redox-sensitive Parameters.

No reliable Eh data are available but, in common with the other levels described, reducing conditions are indicated by the fact that almost all dissolved iron is in the ferrous state. The sulphide content is 0.11 mg/L.

Isotope Geochemistry.

In common with the preceding level, the stable isotope data show a slight trend towards heavier isotopic values as compared with the uppermost 3 levels; the values, however, still remain below the meteoric water line in common with all the other levels (Fig. 5.18). Tritium is low (<8 TU); no radiocarbon data are available (Table 5.6).

Uranium Geochemistry.

The total dissolved uranium contents (Table 5.6) are higher (0.36 μg/L) than most of the upper levels sampled (with the exception of level 248-251 m) and the $^{234}U/^{238}U$ activity ratios are lower (2.90). Based on the above discussion of the other parameters for this level, it is suspected that these changes may be due to the incursion and mixing of waters from other sources.

Summary.

The hydrological character of this section points to the possibility of groundwater contamination, i.e. a combination of high hydraulic conductivity and transmissivity coupled to a fairly high negative piezometric head. This is confirmed by the presence, even after pumping prior to and during the groundwater sampling period, of residual tagged actvity water (>2%), and the general groundwater compositional changes from the preceding levels. The indications are that water from a higher, more HCO_3-rich, and Cl- and SO_4-poor source, have been introduced either through the tagged water source (i.e. HAS05) or by drawing shallower water into the sampled section by excessive pump extraction rates (16 000 mL/min).

5.2.6. Level 609-623 m.

The sampled section incorporates two rock types; a red/grey to dark red fine-grained granite extending from approx. 607-612 m (i.e. straddling the packer at the upper end of the section), and a red, fine- to medium-grained granite variety which continues to approx. 623m at the contact with a narrow greenstone horizon; the upper extent of the packer coincides with this contact. The general section contains <5 fractures/metre; of interest are two marked fracture zones (up to 30 fractures/metre and also indicated by a strong signal from the geophysical logs; Fig. 5.16) occurring at 610 m and 618 m respectively. The major mineral infilling phases comprise chlorite, hematite and Fe-oxyhydroxides with minor calcite.

Hydrology.

From the 30 m scale tested sections, the 609-623 m level straddles two measured sections: 583-615 m and 613-643 m. The former records an average hydraulic conductivity of 3.0×10^{-11} ms^{-1} and the latter an average conductivity of 1.1×10^{-6} ms^{-1}; no further data are available for the 3 m scale sections greater than 550 m depth. The spinner survey showed a strong response at 618 m which coincides with the area of greatest fracture frequency. A transmissivity value of 4.0×10^{-6} $m^2 s^{-1}$ and negative head value of -5.5 m were calculated for the section (Fig. 5.17b,c). The indications are that the section is characterised by a fairly highly conductive zone of moderate transmissivity and negative head; contamination into the bedrock immediate to the section is therefore a possibility. This is supported by the content of residual tagged activity water which decreased from 3.92-2.23% uranine over a 24 hour period at an extraction rate of 18 800 mL/min. Of the major chemical components, Ca, Cl and SO_4 (and to a lesser extent Na) all showed systematic decreases; K and HCO_3 remained constant. No tritium data are available. Indications are that residual tagged activity water still remains in the bedrock vicinity of the section and has not been adequately removed by pumping.

Borehole section 533-636 m was monitored for one month (Table 5.7) some fourteen months after the main groundwater sampling phase (i.e. Table 5.5). The groundwater chemistry, although sampled from a longer borehole section and therefore not directly comparable, showed only a small dilution when compared to the 609-623 m section. However, more importantly, there were no significant changes in the major chemistry during monitoring.

Water Chemistry.

The sampled groundwater (Table 5.5) shows a marked increase in salinity from the previous level; a small increase to pH= 8 also occurs. Salinity is reflected by increases in Na, Ca, Cl and SO_4; K and HCO_3 remain at stable levels (6.3 and 11.2 mg/L respectively). TOC is very low (0.5 mg/L) The water can be characterised as Na-Ca (Mg) Cl-SO_4 in type, equivalent to the 500-1000 m Äspö Type D (Ca-Na-Cl) of Laaksoharju (1990a).

Redox-sensitive Parameters.

No reliable Eh measurements are available; general reducing conditions are indicated by most of the dissolved iron being in the ferrous state (i.e. $Fe_{(II)}$ = 0.065 vs. Fe_{tot} = 0.072 mg/L). Iron values at this level are lower than any of the previously described levels; the sulphide content is also low (0.1 mg/L).

Isotope Geochemistry.

The $\delta^{18}O$ and δ^2H isotopic values continue to shift towards heavier signatures with increasing depth whilst still plotting below the meteoric water line (Fig. 5.18). Tritium is low ($\leq$8 TU); no radiocarbon data are available (Table 5.6).

Uranium Geochemistry.

The dissolved uranium content is low (0.15 µg/L); the $^{234}U/^{238}U$ activity ratio is 3.34 (same range as the uppermost three sampled levels) indicating long groundwater bedrock residence/reaction times.

Summary.

The groundwaters sampled show a continuing increase of salinity with depth. Borehole hydraulics point to potential contamination occurring in the bedrock in the near-vicinity of the sampled section. This is supported by the residual tagged activity water contents and shows that pumping has not removed all effects of the earlier borehole activities. The excessive pump extraction rates (18 800 mL/min) may also have had some influence shore-circuiting waters from other, possibly deeper levels (seen by increasing salinity) in the bedrock via interconnecting fracture systems and/or from around the packer contacts.

5.2.7. Level 690-1002 m.

This sampled section incorporates a series of rock types representing all the units characteristic for these Småland granite/granitoid complexes. In general, from approx. 690-790 m and 848-888 m the granite/aplite dominates, from approx. 780-846 m and 965-1000 m the diorites (sometimes foliated and containing microcline megacrysts) occur, and from 888-958 m, the Småland granitoids are present as dykes and veins. Background fracture frequency is generally low, around 2-3 fractures/metre; one area of more intense fracturing (30-50 fractures/metre) occurs at approx. 730-735 m, another less intense area (around 20 fractures/metre) at approx. 765-775 m, and a more minor area (15 fractures/metre) at approx. 865-870 m. All three areas are reflected in the geophysical logs as distinct responses (Fig. 5.16). The fracture fillings are characterised mostly by hematite and chlorite with subsidiary Fe-oxyhydroxides. High fracturing of the rocks in this section indicates the interception of EW-1 shear zone by KAS03.

Hydrology.

Few hydraulic data are available; the last 30 m scale section tested extended from 673-703 m and recorded an average hydraulic conductivity of 2.9×10^{-7} ms^{-1}. Transmissivity (from the pump testing) has been calculated to 1.6×10^{-6} m^{2}s^{-1} and a negative piezometric pressure head of -1.8 m has been estimated (Fig. 5.17b,c). With respect to potential groundwater quality, the residual tagged activity water records a value of 2.57% uranine in the sampled groundwater; presampling pumping of the section for a period of approx. 16 hours only resulted in a reduction of 0.35% from a starting value of 2.92%. The other chemical parameters show, within the same time period, small decreases in salinity (i.e. 2960-2670 mg/L for Ca; 8900-8080 mg/L for Cl and 71-51 mg/L for Br). With pump extraction rates of 13 000 mL/min., this may suggest less saline groundwater being leaked round the packers from higher levels in the borehole, or may also represent the removal of highly saline groundwater which has entered the sampled section when the borehole has been left open between activities.

Water Chemistry.

The sampled groundwater (Table 5.5) is characterised by a pH of 8 and a highly saline composition of Ca-Na(Mg) Cl-SO$_4$ type, where Ca begins to dominate over Na.

Redox-sensitive Parameters.

No reliable Eh data are available; in common with the previously described levels the dissolved iron is mostly ferrous suggesting a reducing environment. The sulphide content is low 0.10 mg/L.

Isotopic Geochemistry.

The stable isotopic trends reflected by the other levels continue with depth, i.e. increase towards heavier isotopic values for both $\delta^{18}O$ and δ^2H (Fig. 5.18). Tritium is low (≤ 8 TU); no radiocarbon data are available (Table 5.6).

Uranium Geochemistry.

A slightly higher dissolved uranium content (Table 5.6) is present (0.58 µg/L) compared to the previous levels. The high $^{234}U/^{238}U$ activity ratio (4.83) reflects widespread isotopic disequilibrium in the groundwaters and long residence times.

Summary.

Groundwater compositions show increasing salinity with depth and a continuation of the chemical and isotopic trends observed for the higher levels described. The source of the sampled groundwaters are assumed to come from one or more of the three main fracture zones identified from the drillcore and the geophysical logs which relate to the EW-1 shear zone. The moderate transmissivity and the small negative head value suggest that some groundwater contamination may have resulted from the borehole activities. This is confirmed by the >2.5% content of the tagged activity water which was unsuccessfully removed prior to or during pumping, even at the high extraction rate used (13 000 mL/min.). Some contamination by more highly saline waters from greater depth, which resulted from open hole effects, is indicated by the initial removal of a more highly saline water from the conductive borehole sources by pumping prior to sampling. This would suggest that the main groundwater source was located at a higher level in the packed-off section, still not as saline as indicated at greater depths. An obvious source would be the major fracture zone at 730-735 m.

5.2.8. Level 860-1002 m.

The geology of the sampled section is similar to that described for the previous level; apart from a weak fracture zone at approx. 865-870 m; there is no other indication of a potential conducting source for groundwater.

Hydrology.

Little data are available; no hydraulic conductivity measurements have been carried out and only a calculated transmissivity value of 1.6×10^{-6} m^{2}s^{-1} is available, which may not relate to this present section length. The pump extraction rates used were very low (120 mL/min.) and this may account for some of the tagged activity water still remaining in the sampled groundwater samples. Presampling pumping showed a decrease from 3.92-2.23%.

Groundwater Chemistry.

A pH of 8 is similar to the previously described level; the groundwater is much more saline (12 300 mg/L Cl) although still Ca-Na(Mg) Cl-SO$_4$ in type. TOC is very low (0.5 mg/L; see Table 5.5).

Redox-sensitive Parameters.

An Eh value of -240 mV, together with all the dissolved iron present in the ferrous state, and a relatively high sulphide content of 1.1 mg/L (compared to the upper levels), show the strong reducing nature of this deep groundwater.

Isotope Geochemistry.

Similar stable isotope trends to the previous levels are recorded. Tritium is very low (0.40 TU); no radiocarbon data are available (Table 5.6).

Uranium Geochemistry.

Low dissolved uranium (0.5 µg/L) and the highest $^{234}U/^{238}U$ activity ratios recorded in this borehole (6.3) show the widespread isotopic disequilibrium of the groundwaters and further support the very long residence times.

Summary.

This sampled section represents the deepest and most saline groundwater environment of the borehole. The assumed low hydraulic conductivity was compensated by using a very low pump extraction rate which minimised any potential drawdown around the packers. The resulting water, although still containing significant tagged activity water, is probably reasonably representative for these depths.

5.2.9. Borehole summary and discussion.

Geological Setting.

From geological, geophysical and hydrogeological considerations, eight suitably conducting horizons were selected from borehole KAS03 (Fig. 5.15) for hydrogeochemical characterisation of the groundwaters. Ductile structures, sometimes intensified and sheared, occur, together with zones which are even more intensively sheared and mylonitised, represent the interception of KAS03 with the major Äspö shear zone, EW-1. Fracture zones are numerous throughout KAS03 with the greatest concentration occurring from approx. 160-470 m; here there is a background of 5-10 fractures/metre with intensified zones of up to 30 fractures/metre. From 470 to the hole bottom at 1002 m, the general background is around 1-3 fractures/metre with a

few intensely fractured zones. The uppermost approx. 200 m is more uniformly fractured (2-5 fractures/metre) with only very rare intense fracturing.

When considered together with the geophysical logs (Fig. 5.16), the most potential conductive fractures are found to correspond with those areas of greatest fracture intensity. When compared further with the spinner survey, these potential conducting fracture zones can be narrowed down to specific conducting zones of interest. These spinner data support the hydraulic testing carried out along 30 m and 3 m sections, between 103-703 m for the former and between 103-547 m for the latter.

Hydraulic Character and Water Quality.

From a hydrogeochemical point of view, the fewer borehole activities carried out prior to groundwater sampling the better. As can be seen from Table 3.2, there was considerable activity in the borehole before sampling was carried out. Uranine tagged water, used for flushing during drilling and for water injection during hydraulic testing, is still present in the bedrock surrounding the borehole; only the uppermost sampled level (129-134 m) shows that no major tagged water volume has entered the bedrock formation. This is both reflected by the bedrock hydraulics at this level, and the fact that this groundwater is extremely old (2 pmc; apparent age of 31 365 BP), that it contains negligible tritium (0.10 TU) and that the $^{234}U/^{238}U$ activity ratio is high (4.56). All these factors point to a relatively undisturbed groundwater environment with long residence times and where rock/water equilibrium interaction might be expected.

The other sampled levels all show evidence of perturbance, the extent of which is very much dependent on the borehole hydraulics and the excessive extraction of large volumes of water. The drilling logs record a loss of 22 m^3 water during drilling (472 m^3 introduced and 450 m^3 successfully removed) and an unknown amount during the hydraulic testing. It is obvious that for the majority of the sampled sections this has not been fully removed, even though pump testing has been carried out on at least 7 occasions (Table 3.2) at various levels and at various times. A drawdown pump test was carried out for a 54 hour period, removing 93.6 L/min and showing a rapid hydraulic connection with HAS08, HAS11 and HAS12 (Fig. 5.15). Interference testing showed a clear connection with the upper section of KAS04 (0-185 m), HAS01 (0-100 m), HAS08 (66-125 m) and HAS11 (0-30 m and 31-125 m). Furthermore, from all the sections pump tested in KAS03, there was a hydraulic connection around the packers to the borehole water above and below the tested section (Gentzschein and Andersson, 1988b).

Apart from the percentage of tagged activity water observed in the sampled groundwaters, only one section showed a clear change in the major chemistry which can be probably linked to groundwater mixing from other sources. Level 453-480 m is characterised by a relatively high conductivity and transmissivity coupled with a fairly high negative piezometric head. Furthermore, a high pump extraction rate was

employed for groundwater sampling (16 000 mL/min.). Two observations: a) even after pumping prior to and during groundwater sampling, appreciable tagged activity water (>2%) remained, and b) the general chemistry indicated that waters from higher, more HCO_3-rich and Cl- and SO_4-poor origin, have been introduced either by the tagged water source (e.g. HAS05) or by drawing shallower-derived water into the sampled section by excessive pump extraction rates. Such waters can be obtained through an interconnecting fracture system in the bedrock up to shallower levels, or, by a short-circuit through the bedrock to the borehole water above the section. Levels 196-223 m and 248-251 m, although not as influenced as level 196-223 m, have also been affected to some extent. These effects are most readily indicated by the radiocarbon data, i.e. an increase to 7-8 pmc (i.e. markedly younger by some 10 000 BP than the uppermost level), which suggests that some dilution of the groundwaters has occurred. If dilution had been caused by the removal of modern ^{14}C in association with the precipitation of calcite, then the calculated apparent ages should give an older age rather than a younger estimate. It is therefore suggested that dilution by more surface-derived waters is the most plausible explanation.

The rapid hydraulic connection with other boreholes during the interference testing was considered worrying. In particular, the connection between KAS03 level 196-223 m with HAS06 (66-125 m level) and HAS11 (0-30 m and 31-125 m levels) and KAS03 level 347-374 m with KAS04 (0-185 m level) and HAS01 (0-100 m level). The high pump extraction rates, 10 000 and 18 000 mL/min. respectively, may have contributed to some unwanted groundwater mixing from other levels and sources.

In terms of the groundwaters being representative for the depths sampled, the levels, in order of decreasing reliability are considered to be:

a) levels 129-134 m, 860-1200 m
b) levels 248-251 m, 609-623 m
c) levels 196-223 m, 347-374 m
d) level 690-1002 m
e) level 453-480 m

Chemical and Isotopic Features.

The groundwaters (summarised in Figs. 5.19 to 5.22) are shown to be reducing (available Eh data record values of -240 to -260 mV; nearly all the total iron is in the ferrous state; total dissolved uranium is very low ranging from 0.08-0.58 µg/L), moderately alkaline (pH from 7.7-8.0), and changing from a Na-Ca(Mg) HCO_3-Cl type at the near-surface (0-150m), through a Na-Ca(Mg) Cl-HCO_3 type at depths of 150-300 m, to a Na-Ca(Mg) Cl-SO_4 type at depths of 300-800 m, and finally the deepest, most saline waters are of Ca-Na(Mg) Cl-SO_4 type occurring from approx. 800 m to the hole bottom and beyond. These correspond approximately to the general classification of Laaksoharju (1990a).
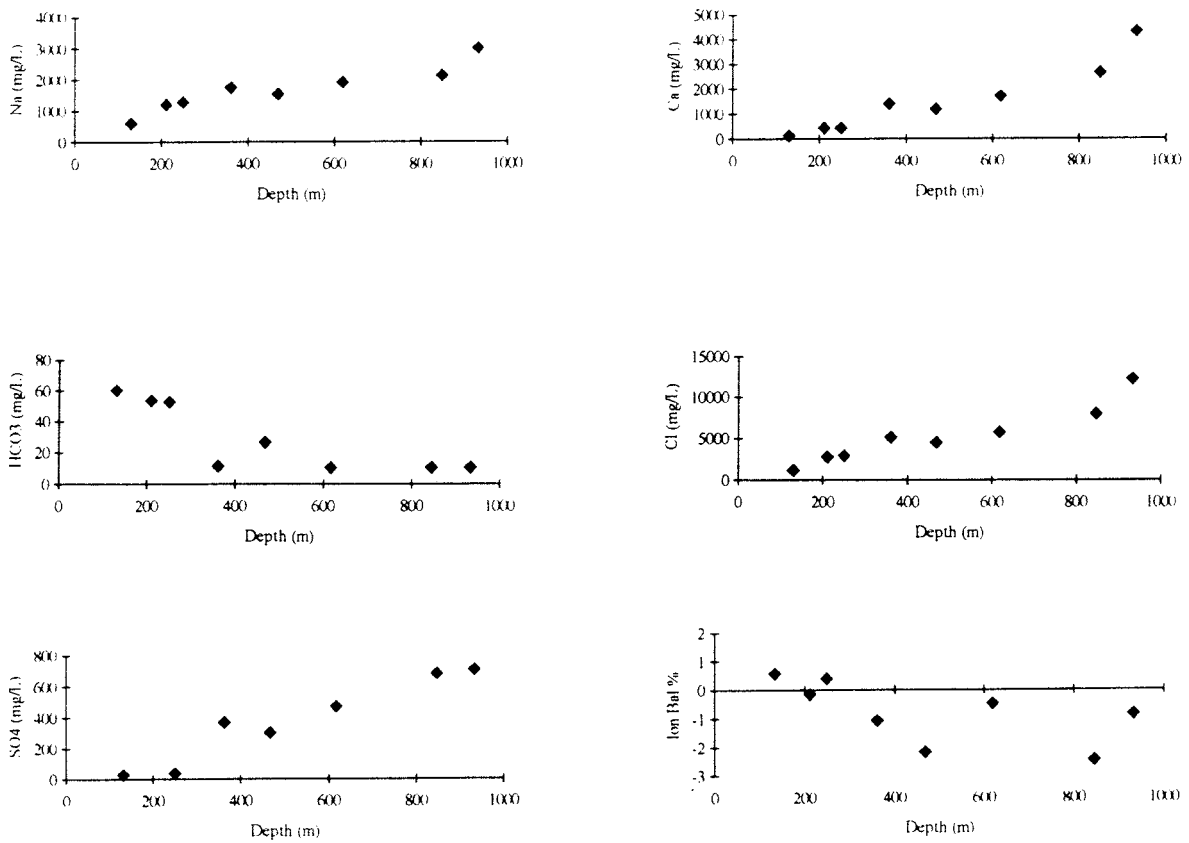
Figure 5.19. KAS03 groundwaters: major ion distributions and ionic charge balance.
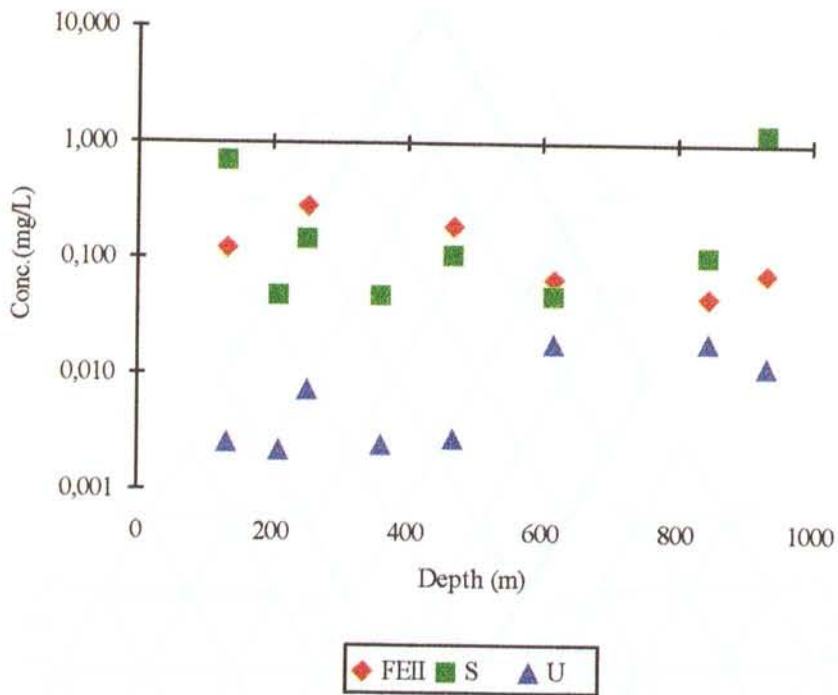
Figure 5.20. KAS03 groundwaters: distribution of selected redox-sensitive elements.
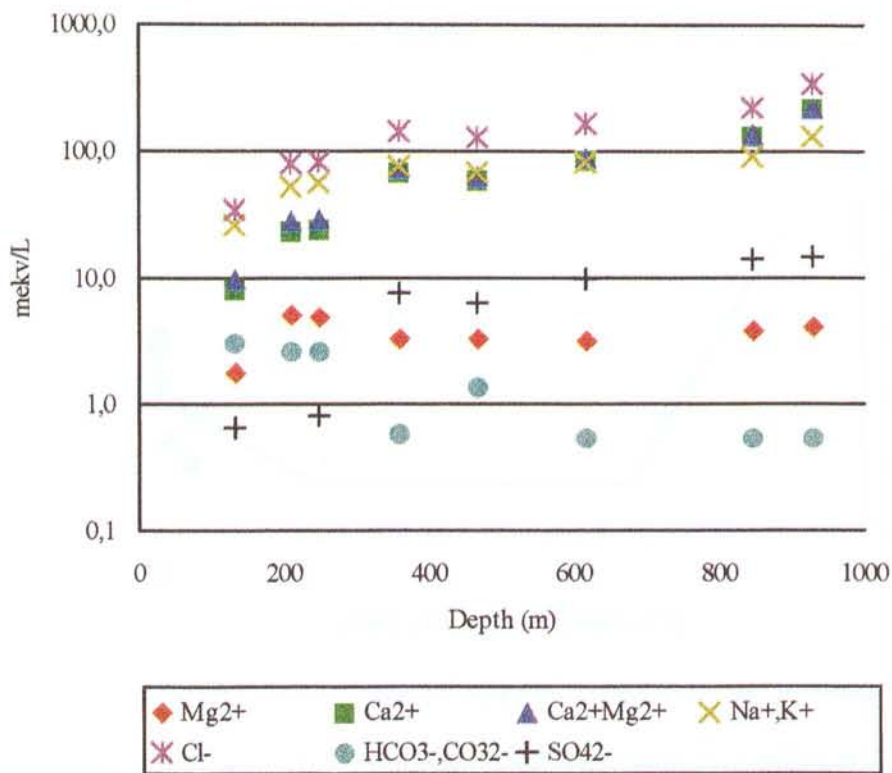
Figure 5.21. KAS03 groundwaters: Shoeller diagram showing the major ion distributions with depth.
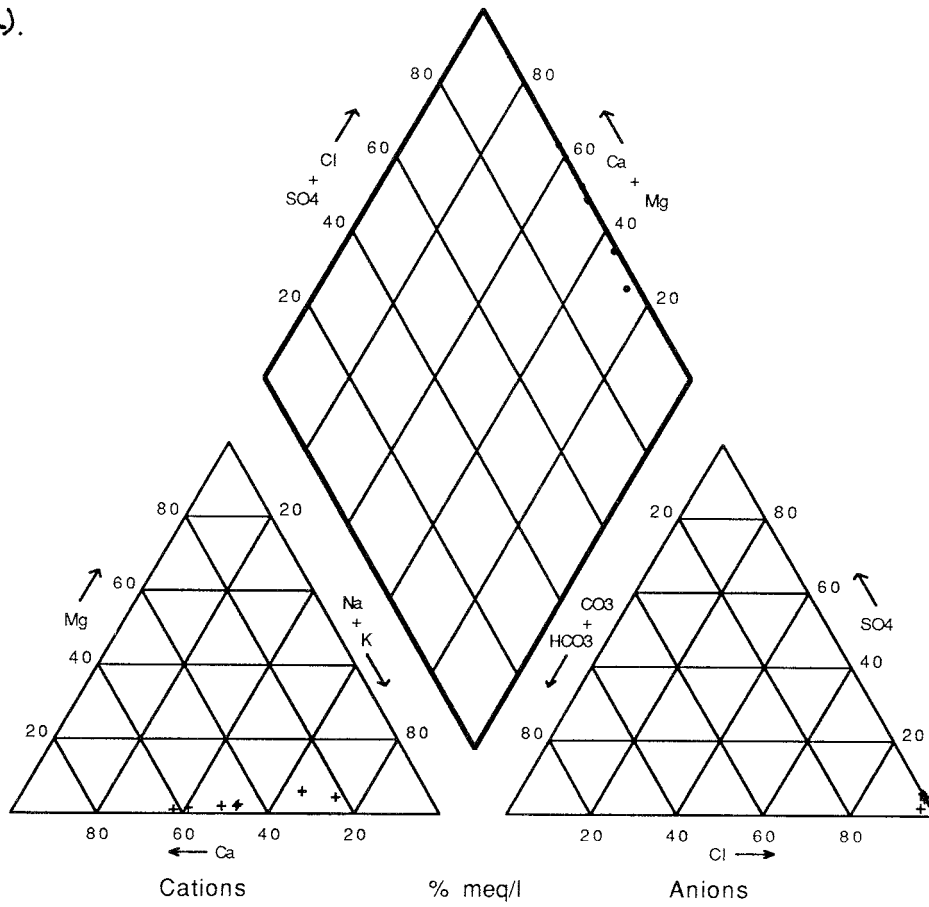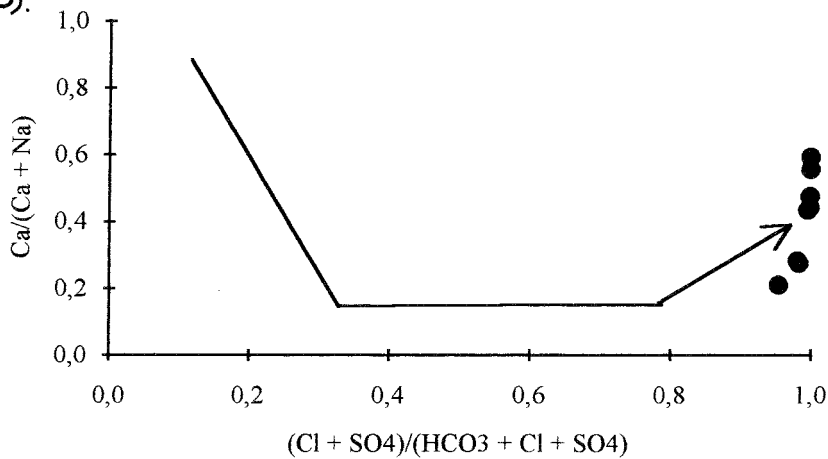
Figure 5.22. KAS03 groundwaters: a) Piper Plot of the major ion chemistry, and b) modified Piper Plot showing the position of the KAS03 groundwaters along an assumed chemical evolution trend for average deep Swedish groundwaters in crystalline rock.

The variation in chemistry with depth partly follows the normal evolutionary trend in Swedish crystalline rocks, i.e. an uppermost horizon with a paucity of calcite (due to the dissolution effect of downward percolating, moderately acid rainwater), a lower horizon characterised by precipitation of calcite (when the downward percolating groundwaters become carbonate supersaturated), and finally the lowermost horizon where calcite is by and large absent (precipitation complete). Tullborg (1988) has mapped the distribution of calcite coated fractures from KAS03 and found that the above described horizons correspond to depths of approx. 0-40 m, 40-250m and finally 250 m-downwards.

The increase in salinity with depth is clearly shown by the chemistry and by the salinity log (Fig. 5.16). The salinity log, measured in the open borehole, shows fairly uniform values to approx. 225 m whereupon the salinity increases gradually to approx. 690 m. At this point there is a marked change and the salinity increases more rapidly to 850 m when the logging was stopped; the increase in salinity coincides with the intersection of zone EW-1 by KAS03. Although caution has to be employed when interpreting these logs, as the distribution of the saline groundwaters is usually a reflection of open hole hydraulics, the borehole pattern shown in Figure 5.16 conforms closely with the chemical characterisation of the groundwaters sampled from isolated borehole sections.

The stable isotope data are interesting; plots for all the sampled levels fall below the global meteoric water line (Fig. 5.18). Not only that, but there is a distinct increase in $\delta^{18}O$ and δ^2H with depth, apart from level 453-480 m which, in common with the chemical data, indicates a contribution of shallower water.

The variation in isotopic signatures, together with the chemical and other isotopic data, reflects the location of KAS03 within and adjacent to the recharging EW-1 zone. Recharge is partly supported by the calcite dissolution front which extends to approx. 40 m at KAS03 compared to only 10 m at KAS02. The shallow levels outside the influence of zone EW-1 show anomalously light isotopic signatures (suggesting cold climate recharge), whilst deeper levels closer to and within zone EW-1 indicate increasing mixing with the deep Ca-rich waters characterised by heavier isotopic signatures. This is discussed further in Section 6.

Water/rock Interaction.

In common with KAS02, the percentage of the major rock types comprising borehole KAS03, the dominant host rock characterising each hydraulic zone(s) sampled for groundwater, and the identified macroscopic (and when available the microscopic) fracture mineral phases (from two data sources) in those hydraulic zone(s), are illustrated in Figures 5.23 and 5.24.
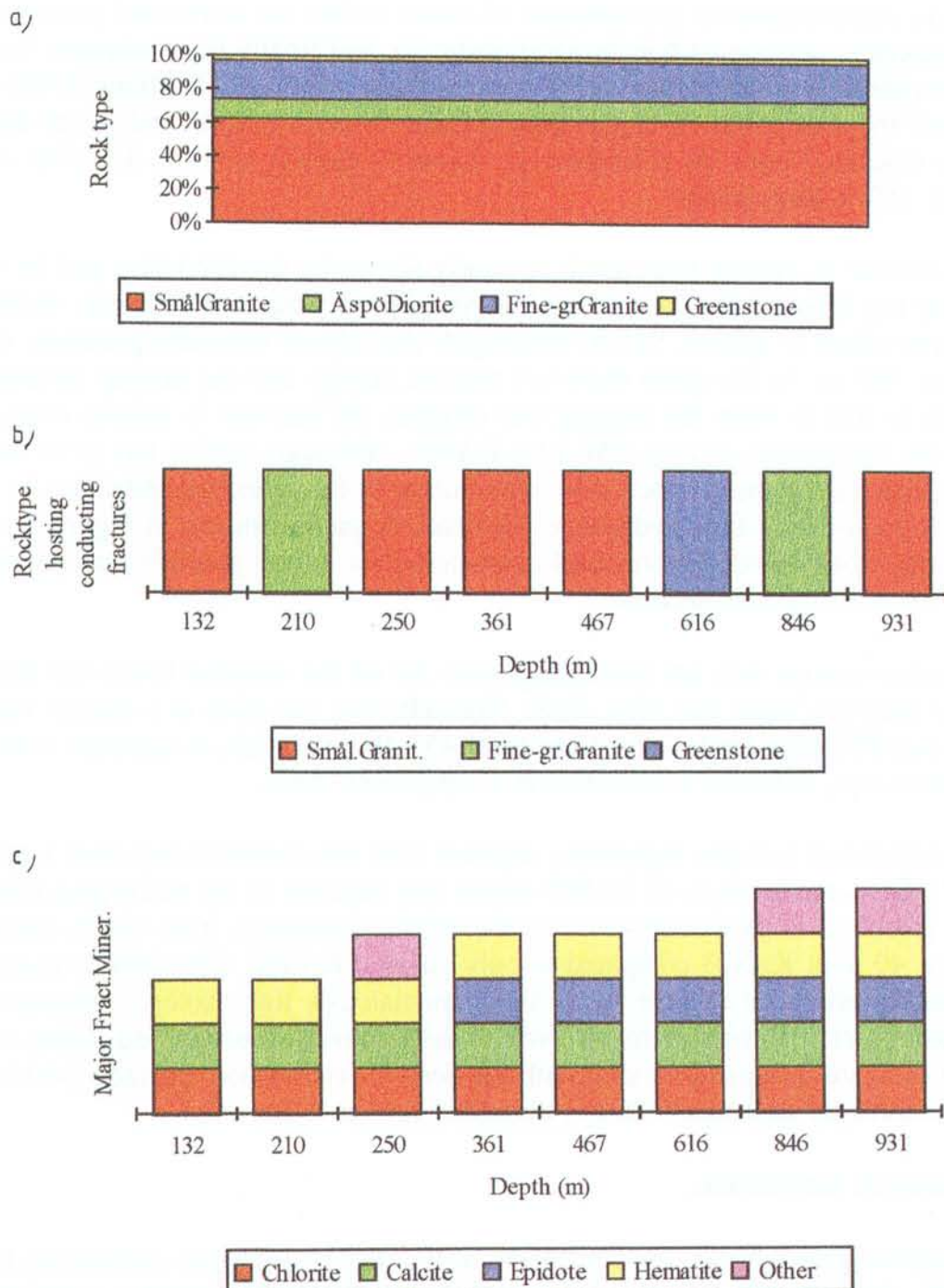
Figure 5.23. Rock type and fracture mineralogy of KAS03: a) overview of the major
rock types (based on Stanfors, 1988), b) evaluation of probable rock
type hosting the fractures (based on Stanfors, 1988), and c) evaluation
of the major fractures minerals (based on Stråle, 1988 and Tullborg, 1989).
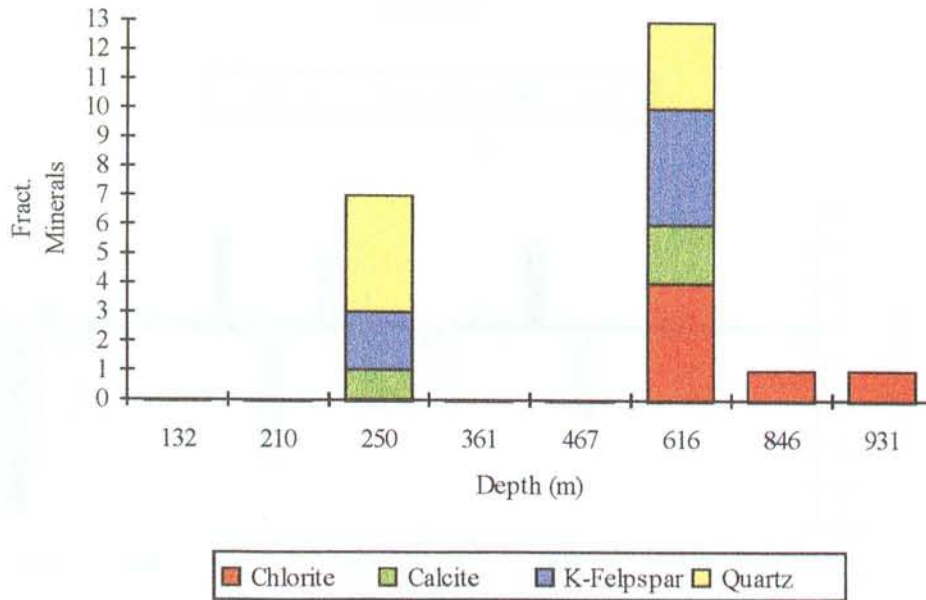
Figure 5.24. Fracture mineralogy of KAS03: evaluation of major fracture minerals detected at, or in the vicinity of, the sampled hydraulic borehole sections (based on Wikman et al., 1988).

Comparing groundwater analyses of some of the more bedrock sensitive elements (Fig. 5.25a) with different bedrock compositional types (Figs. 5.23 and 5.24) shows no clear correlation for Mg, U, Ra and Th. The relationships between the groundwater and the fracture mineral phases using equilibrium calculations of the saturation indices are presented in Figures 25b and c. The positive indices indicate close to saturation or slight oversaturation for calcite, fluorite, quartz and laumontite; both calcite and quartz are reported as fracture minerals. The saturation index for gypsum, in common with KAS02, is negative for the whole borehole reflecting the small amounts observed as a fracture mineral. The oversaturation of muscovite at the 846 m section is once again attributed to Al contamination from the sampling equipment. As discussed with KAS02, the interpretation of hematite, iron hydroxide and pyrite is uncertain because of potential problems with the thermodynamic database and/or field Eh measurements.
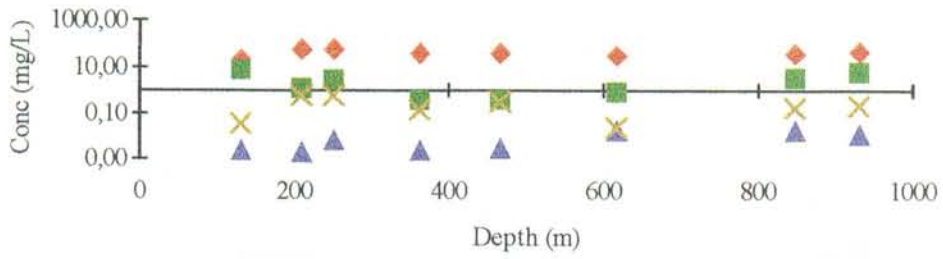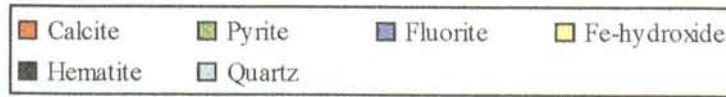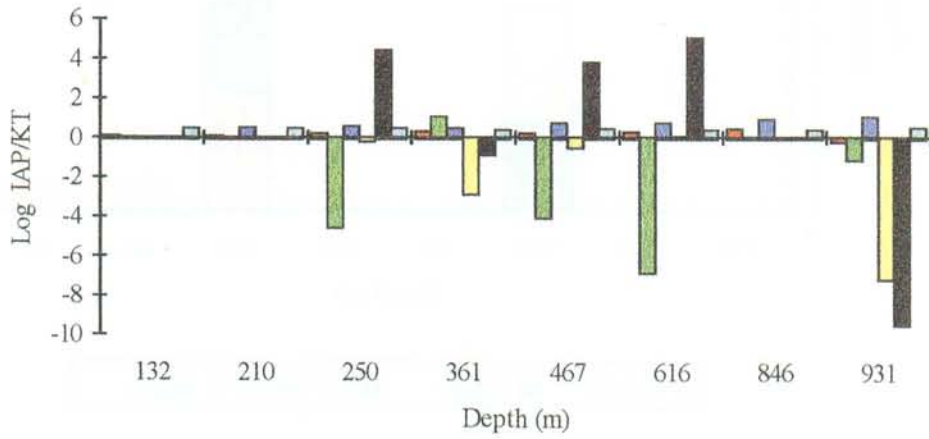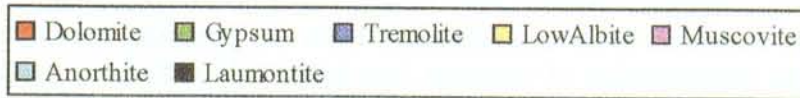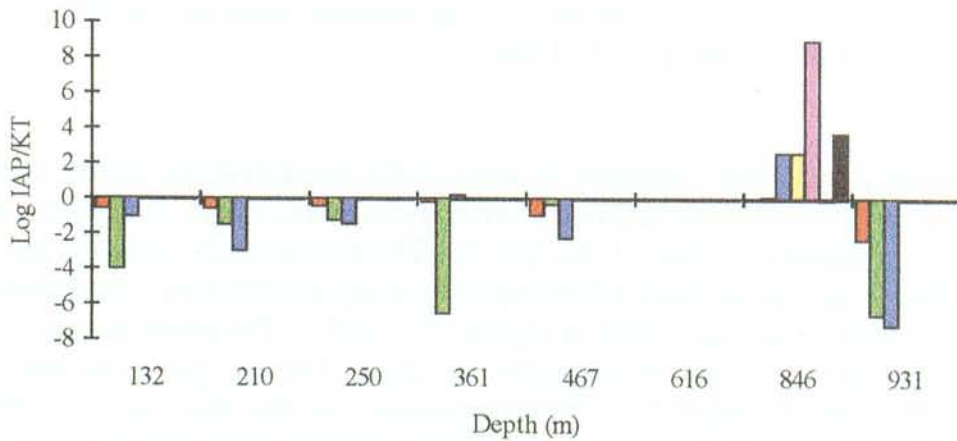
Figure 5.25. a) plotted concentrations of Mg, ^{226}Ra, U and Th measured in KAS03 groundwater, and b, c) results of equilibrium saturation index calculations using PHREEQE (Parkhurst et al., 1980).

Groundwater Mixing Ratios.

Using the simple two component mixing model described and discussed for KAS02 (see Section 5.1.8), the calculations show a high input of shallow water (50% plus) down to 600 m; at this point there is a gradual decrease to zero corresponding to the deepest samples collected (Fig. 26a). The shallow input can also be observed in the TOC (total organic carbon) for the most shallow samples (to around 250 m) and for the sample at the 616 m level (Fig. 5.26b). The TOC increase at around 600 m is reflected by a sympathetic decrease in the calculated pCO_2 (Fig. 26c), which otherwise shows higher values than atmospheric pressure (i.e. -3.5) in the shallow samples.

The calculated Br/Cl ratios (Fig. 5.26d) are lower for the shallow samples (to around 500 m), i.e. closer to the sea water ratio, than in the deeper parts of the borehole. An increase is once again evident at the 616 m level. Sea water input cannot therefore be ruled out.

Considering the Cl mixing model (Fig. 27a) the calculations show that equilibrium mixing is closely approached at 250 m depth. At around 350 there is a small Cl concentration increase and, from 500 to 850 m depth there is a marked Cl dilution.

For Na, Ca, SO_4, Cl, K and Mg (Figs. 5.27b and c) there is a marked deviation from equilibrium mixing from the surface down to around 350 m; from this depth to the borehole bottom equilibrium mixing is closely approached. The only exception to this is HCO_3 which shows an increasing deviation with depth.

The general patterns shown by the mixing model, i.e. significant changes at around 300-350 m and 500-600 m, may be explained by the structures intercepted by KAS03. For example, the former correspond to sections of high fracture frequency and increased hydrauliuc conductivity extending from 200-400 m, and the latter corresponds to the intersection of KAS03 with the major EW-1 shear zone at around 600 m. Two main chemical regimes are indicated: a shallow (0-350 m) zone where there is a large near-surface component (e,g, TOC, pCO_2 and seawater) and a deeper zone where deep-derived saline waters are more dominant.

Mixing of Cl in the shallow zone is close to equilibrium suggesting a hydraulic system which is sufficiently open to facilitate mixing. Non-equilibrium mixing at depth within the EW-1 shear zone suggests either: 1) hydraulic conductivities are too low, and/or 2) there is an influx of other groundwaters of different origin. On the other hand equilibrium mixing of the other major ion components is incomplete in the shallow zone yet nearing equilibrium mixing in the deeper zone. This may partly be explained by the smaller concentrations of these ions in comparison with Cl, which renders them more sensitive to groundwater chemical fluctuations, particularly in the shallow zone (e.g. seawater input, precipitation recharge, rock/water interactions etc.). At greater depths within the EW-1 zone, where there is a decreasing influence of the shallow input coupled with decreasing hydraulic conductivity, the significant near-surface deviation from equilibrium mixing conditions gradually becomes less significant.
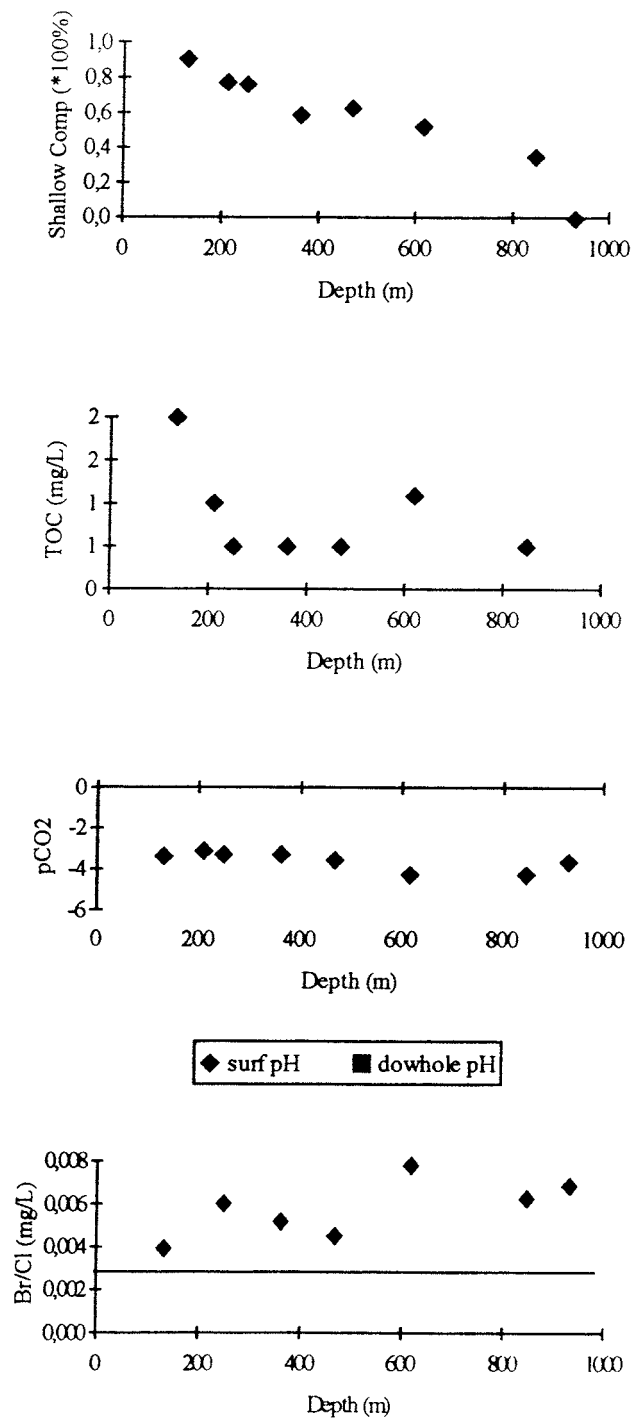
Figure 5.26. KAS03 groundwaters showing: a) calculation of the shallow water input derived from a simple two component mixing model using Cl end members from HAS05 and KAS03, b) TOC (total organic carbon) versus depth, c) calculated pCO_3 pressures from downhole and surface (on-line) pH readings, and d) Br/Cl ratio versus depth; the horizontal line represents the seawater Br/Cl ratio (0.0031) for reference.
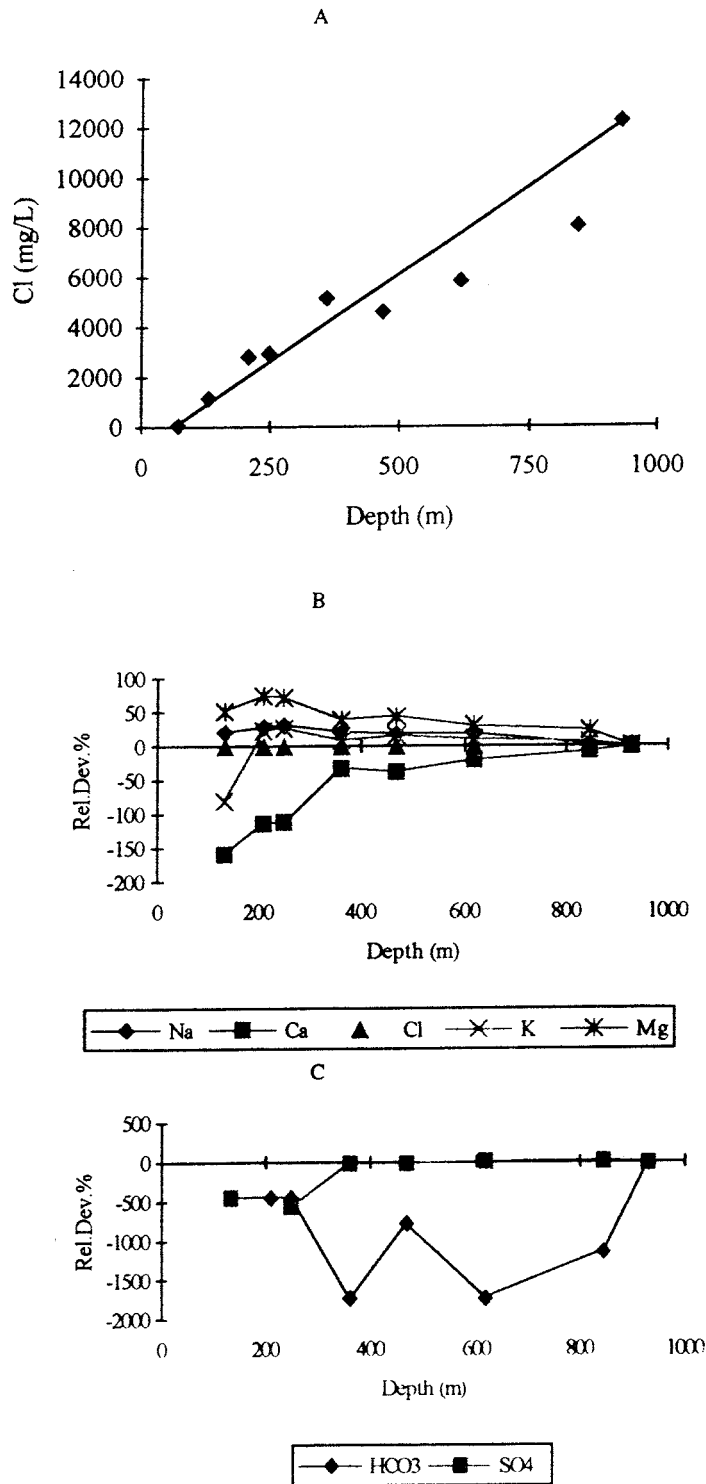
Figure 5.27. KAS03 groundwaters showing: a) plot of Cl vs depth related to the simple two component mixing line, and b), c) depth trends of the major ions plotted as percentage relative deviation to the mixing model.

Uranium Geochemistry.

Figure 5.28 shows the solubility of different uranium oxide phases (thermodynamic data from Puigdomènech and Bruno, 1988) as a function of Eh (and pH). Plotted are the distribution of groundwater measurements from borehole KAS03 (together with KAS02 and KAS04; with pH values indicated) which show that the main solubility limiting phases are crystalline uraninite (UO_2) and the more amorphous U_4O_9 phase (P. Sellin, per. comm. 1992).

Uranium series data (Table 5.6) show high $^{234}U/^{238}U$ activity ratios (2.9-6.3) caused by a build-up of excess ^{234}U. This demonstrates that the groundwaters are moving sufficiently slowly through the bedrock so as to allow the excess ^{234}U to accumulate, and thereby supporting near stagnant conditions.
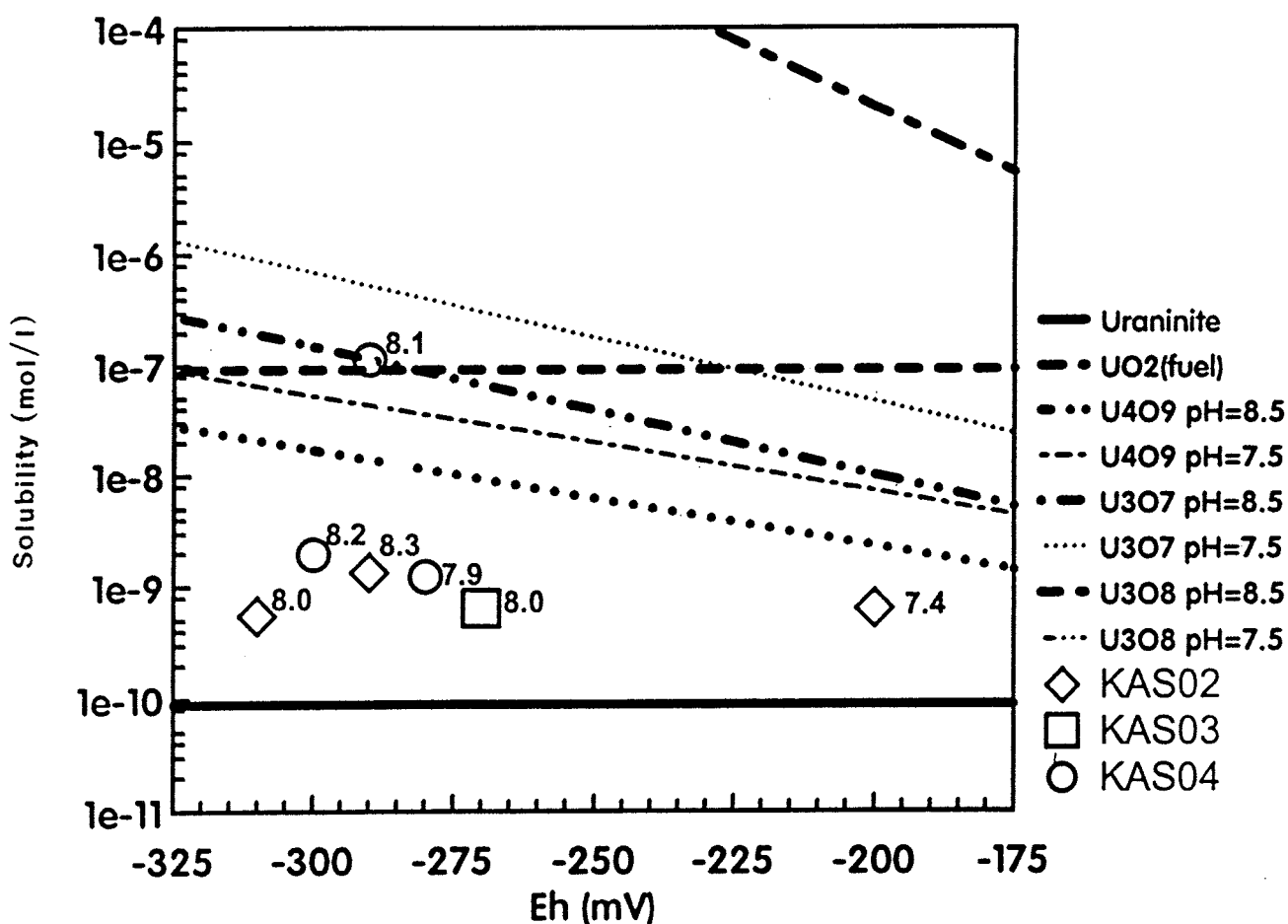
Figure 5.28. KAS03 groundwaters (with pH values indicated) related to the solubility of different uranium oxide phases plotted as a function of Eh (and pH). Thermodynamic data from Puigdomènech and Bruno, 1988).

Table 5.5: Chemical analyses of groundwater samples from borehole KAS03, Äspö.

Borehole	KAS03	KAS03	KAS03	KAS03	KAS03	KAS03	KAS03	KAS03
Section m	129-134	196-223	248-251	347-374	453-480	609-623	690-1002	860-1002
Sampling method	CCC	SPT	SPT	SPT	SPT	SPT	SPT	CCC
Sample no.	1569	1437	1448	1441	1445	1452	1456	1582
Date	890221	880810	880828	880816	880822	880903	880908	890315
W.flow ml/m	122	10000*	4000	18000	16000	18800	13000	118
Drillingwater %	0.06	2.7	1.0	0.8	2.1	2.2	2.6	0.1
Cond.mS/m	450	910	930	1370	1400	1700	2260	3390
Density g/ml	0.9979	0.9998	0.9998	1.0028	1.0021	1.0036	1.0066	1.0118
pH	8.0	7.7	7.8	–	7.8	8.0	8.0	8.0
E_h mV	-270	–	–	–	–	–	–	-270
Alkalinity (mg/l HCO_3)	61.3	54.0	53.0	12.0	27.0	11.2	11.0	10.6
Charge balance mequiv./l	0.42	-0.34	0.39	-4.06	-6.45	-2.78	-11.17	-8.77
Rel. charge bal. error %	0.58	-0.21	0.23	-1.33	-2.42	-0.79	-2.35	-1.22

Element					mg/l			
Na	613	1200	1290	1770	1550	1920	2130	3020
K	2.4	6.3	6.5	5.9	6.2	6.2	6.6	7.3
Ca	162	472	490	1400	1190	1740	2670	4380
Mg	21	61	58	40	40	38	45	50
Sr	3.3	10	10	26	21	28	44	78
Mn	0.10	0.39	0.35	0.27	0.27	0.24	0.23	0.20
Li	0.13	0.28	0.30	0.63	0.61	0.73	0.83	1.65
Fe,tot	0.125	–	0.290*	0.200	0.196*	0.072*	0.053	0.078
Fe(+II)	0.123	–	0.288*	–	0.194*	0.068*	0.047	0.077
F	2.1	1.8	1.8	1.5	1.6	1.5	1.5	1.6
CL	1220	2850	2950	5180	4600	5880	8080	12300
Br	4.8	27*	18	27	21	46	51	85
I	0.10	0.41	0.36	0.43	0.42	0.05	0.65	0.70*
PO_4-P	0.001	0.003	0.003	0.001	0.005*	0.006*	0.002	0.002
SO_4	31.1	31*	39	370	300	470	680	709
S_2	0.71	0.05	0.15	0.05	0.11	0.05	0.11	1.28
NO_2-N	0.001	–	–	–	–	–	–	0.001
NO_3-N	0.01	–	–	–	–	–	–	0.01*
NH_4-N	0.04	–	0.09*	–	0.07*	0.05*	0.05*	0.01
SiO_2-Si	4.9	4.7	4.4	4.2	4.1	3.9	3.9	4.2
TOC	2.0	1.0	0.5	0.5	0.5	1.1	0.5	0.5*

* No determination. The result from another sample in the same borehole section is presented.

Borehole	KAS03	KAS03	KAS03	KAS03	KAS03	KAS03	KAS03	KAS03
Section m	129-134	196-223	248-251	347-374	453-480	609-623	690-1002	860-1002
Sampling method	CCC	SPT	SPT	SPT	SPT	SPT	SPT	CCC
Sample no.	1569	1437	1448	1441	1445	1452	1456	1582
Date	890221	880810	880828	880816	880822	880903	880908	890315
Percentage Modern Carbon (PMC)	2	7	8	-	-	-	-	-
^{14}C age BP	31365	21695	20090	-	-	-	-	-
age BP corr.	-	21880	20245	-	-	-	-	-
^{238}U (mBq/kg)	3.76	4.89	12.4	2.05	9.06	3.84	14.80	3.27
^{235}U (mBq/kg)	0.26	1.50	1.79	0.30	0.40	0.29	2.03	0.82
^{234}U (mBq/kg)	17.2	17.3	52.6	6.2	26.3	12.8	71.2	20.7
U_{tot} (ug/kg)	0.15	0.19	0.49	0.08	0.36	0.15	0.58	0.13
$^{235}U/^{238}U$	0.070	-	0.144	-	0.045	0.076	0.137	0.250
$^{234}U/^{238}U$	4.56	3.54	4.23	3.00	2.9	3.34	4.83	6.3
^{18}O (SMOW)	-15.8	-14.6	-14.5	-13.3	-13.6	-13.3	-13.0	-12.7
^{2}H (SMOW)	-124.8	-115.3	-118.1	-104.9	-109.6	-103.4	-99.7	-96.4
^{3}H (Bq/l) [1]	< 1	~ 1	~ 1	< 1	< 1	~ 1	~ 1	< 1
^{3}H (TU) [2]	0.10	-	-	-	-	-	-	0.40

[1] Kjeller, Norway
[2] IAEA, Wienna

Table 5.7: Monitoring analyses from the 533-636 m level, borehole KAS03, Äspö.

Borehole	KAS03	KAS03	KAS03	KAS03	KAS03
Section (m)	533-636	533-636	533-636	533-636	533-636
Sample no	1645	1651	1657	1669	1681
Sampling method	MONIT.	MONIT.	MONIT.	MONIT.	MONIT.
Date Collected	900509	900514	900528	900606	‾900613
W.flow ml/m	250	270	270	270	290
Drilling water %	1.90	1.30	1.20	0.73	0.33
Cond.mS/m	-	-	-	1500	1510
Density g/ml	-	-	-	-	-
pH	7.4	7.5	7.7	7.5	7.5
Alkalinity (mg/l HCO_3)	31.5	25.3	27.1	22.6	18.3
Charge Balance %	-3.29	-2.59	-2.59	-2.55	-2.29

Element	mg/l				
Na	1680	1700	1700 (1700)	1720	1730
K	-	7.5	(7.80)	-	6.9
Ca	1340	1350	1340 (1330)	1330	1330
Mg	41.0	42.0	42.0 (40.1)	42.0	41.0
Sr	23.6	23.7	23.6 (24.2)	23.5	23.1
Mn	0.28	0.29	0.32 (0.28)	0.31	0.29
Li	0.73	0.74	0.72 (0.82)	0.75	0.76
Fe(tot)	0.05	0.05	0.08 (0.06)	0.13	0.17
Cl	5170	5160	5130	5140	5130
F	1.8	1.8	1.8	1.8	1.8
S(ICP)	115.00	115.00	116.00 (116.30)	117.00	119.00
SO_4^{2-}(calc)	345	345	348 (349)	351	357
SiO_2-Si	3.1	2.9	3.4 (2.9)	3.7	3.3

5.3. Borehole KAS04.

Borehole KAS04 (Fig. 5.29), with an upper diameter of 155 mm (down to 100 m) and a lower diameter of 56 mm (to the full length of the hole at 481 m), was drilled at an inclination of 60°SE to investigate the bedrock geology, hydrogeology and hydrogeochemistry across the major ENE striking EW-1 Äspö mylonitic shear zone which effectively divides Äspö into a northern and southern block. Because of the inclined drilling angle, references to metres in the following section relate to borehole length and not to bedrock depth, unless otherwise stated.

Five main rock groups are intercepted by KAS04 consisting of Småland granitoids with red megacrysts of microcline (37.5%), diorites (+/- red megacrysts of microcline) (20%), fine-grained granites or aplites (32%), greenstones (0.5%) and mylonite (10%). The granitoids dominate at approx. 70-170 m, 230-265 m and 290-310 m, the diorites at approx. 265-290m, 290-310 m and 455-481 m, the aplites at approx. 35-70 m and 330-455 m, the mylonite at approx. 170-220 m and the greenstones at approx. 2-17 m together with four narrow horizons (3-10 m) occurring mostly within the granitoids at 110-175 m. Aplitic horizons (<1-10 m) are common throughout the drilled sequence.

Generally the bedrock has undergone a strong mechanical deformation although in some cases the drillcore is surprisingly competent. Tectonically the bedrock section is dominated by the major mylonitic zone at 170-217 m which comprises two fine-grained epidote-rich mylonites at 176-182 m and 214-217 m respectively. These coincide with zones of higher fracture frequency separated by several minor horizons of mylonite material.

Singlehole radar reflection measurements were carried out between 110 and 469 m depth. Intersection angles with the borehole axis were mostly from 0-50°; no horizontal or subhorizontal fracture zones were indicated. Strong indications occurred at 250-340 m coinciding with the intersection of the southern boundary of the major EW-1 shear zone (see below).

In KAS04, three fracture zones appear to demarcate the major extent of the EW-1 shear zone (Fig. 5.25); zones 75°NW (northern margin), 88°NW (central area) and 78°SE (southern margin). As stated for KAS03, the shear should be regarded as a complex zone composed of highly fractured (crushed), mineralogically altered metre wide sections, separated by slabs of Småland granite (less fractured but hydrothermally altered) and metre wide mylonites (more or less fractured). Alteration includes the hydrothermal oxidation of magnetite to hematite and new minerals such as epidote; probably low temperature alteration (e.g. hematite to Fe-oxyhydroxides) has also occurred.

Relating the borehole geophysical measurements to the drillcore logging (Fig. 5.30) shows considerable fracturing from close to the bedrock surface to 450 m. The general background fracture frequency for the borehole is around 5 fractures/metre with several highly fractured zones (to a maximum of 40 fractures/metre) occurring at approx. 65 m (25 fractures/metre), 115 m (20 fratcures/metre), 175 m (20 fractures/metre), 230 m (30 fratcures/metre), 335-345 m (20-30 fractures/metre), 355 m (25 fractures/metre), 380-400 m (25-40 fractures/metre), 415 m (25 fractures/metre) and 430 m (23 fractures/metre). Of
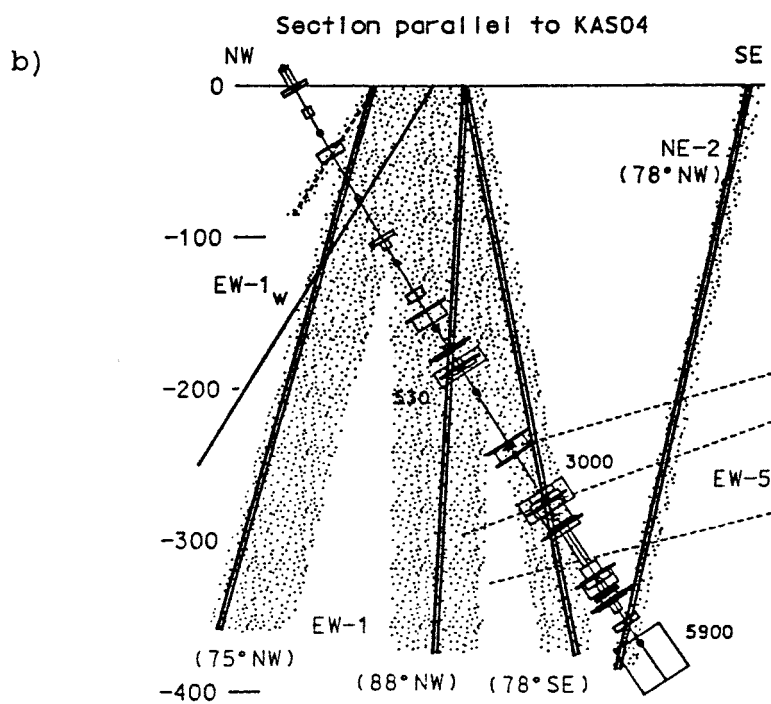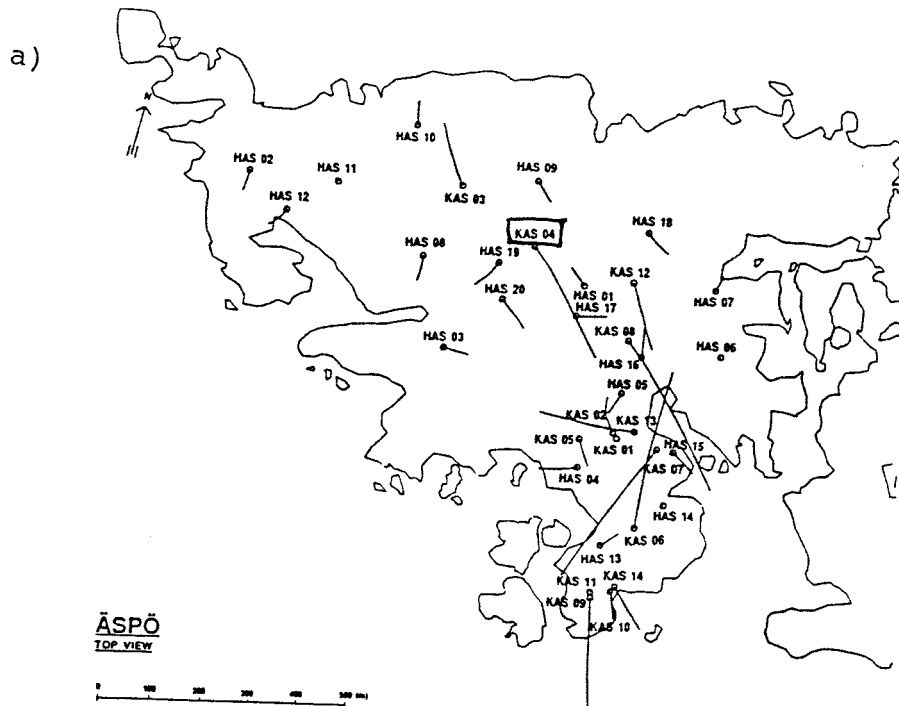
Figure 5.29. a) Location of borehole KAS04, and b) its relationship to the major EW-1 and NE-2 shear zones (from Wikberg et al., 1991).

these, the high fracture frequency at: a) 65 m corresponds (Fig. 5.29) to the borehole intersection with the northern margin of the Äspö shear zone (EW-1;75°NW), b) 230 m approximates to the intersection with the central EW-1;88°NW fracture zone, c) 335-345 m corresponds to the intersection with the southern margin (EW-1; 78°SE), and d) 415-430 m corresponds to the intersection with zone NE-2; 78°NW.

Another major fracture zone, EW-5, striking more or less EW and dipping approx. 30-35°N, outcrops just at the southern part of Äspö and terminates at the EW-1 shear zone at around 280-370 m vertical depth (Fig. 5.29). Its expression in KAS04 is unclear but it may account for the increase in fracture frequency observed at 380-400 m.

The gamma log shows the normal increase in radioactivity associated with the aplitic rock types. In addition, the fracture zone at 335-345 m (near the aplite/diorite contact at 330 m) shows a decrease in activity, compared to the background, which may be an indication that uranium has or is being removed at this fracture by circulating groundwaters. At this same point there is a very marked increase in hydraulic conductivity and an increase of salinity in the groundwater.

In general terms the borehole salinity from 0-100 m is around 3 500 mg/L equivalent NaCl and decreases to 2 000 mg/L (roughly at the intersection with the northern margin of the EW-1 shear zone). This level is maintained to 337 m whereupon it increases to a maximum of around 8 000 mg/L (i.e. the southern margin of the EW-1 shear zone) before decreasing to around 4 000 mg/L at 415 m (i.e. the intersection with the major N-2 zone).

These geophysical logs show quite clearly that the EW-1 shear zone is conducting fresher, less saline water to depth, and that the groundwater more representative of the bedrock, i.e. bounded by EW-1 to the north and N-2 to the south, is very saline at the maximum depth of the hole and substantially saline even to very shallow depths (<50 m).

Throughout the drillcore length the average total distribution of natural vs. sealed fractures present are 6.00 and 1.64 fractures/metre respectively. The fractures in the uppermost zone at 60-70 m are dominated by infilling phases such as chlorite, epidote, hematite and Fe-oxyhydroxides; calcite is depleted. An increasing frequency of hematite and laumontite is observed from 175-190 m; from 320-400 there is a marked increase of fracture coatings comprising mainly hematite, Fe-oxyhydroxides, calcite and epidote (339-340 m) and also fluorite (395-402 m). Along the drillcore there is a dominant association between the distribution of hematite and Fe-oxyhydroxides; the main exceptions occur from 10-60 m, around 250-300 m and from 420-480 m. This may indicate the extent of recent groundwater rock interactions in the system. Distribution plots of fracture calcite coatings show that surface-related calcite dissolution is confined to a maximum depth of around 10 m, similar to that observed for KAS02.

The general hydraulic character of the borehole KAS04 is illustrated in Figures 5.30 and 5.31. From the hydraulic injection tests (3 m intervals from 133-454 m; no 30 m interval testing was carried out) and the spinner survey (1 m intervals from 100-417 m) the areas of high hydraulic conductivity
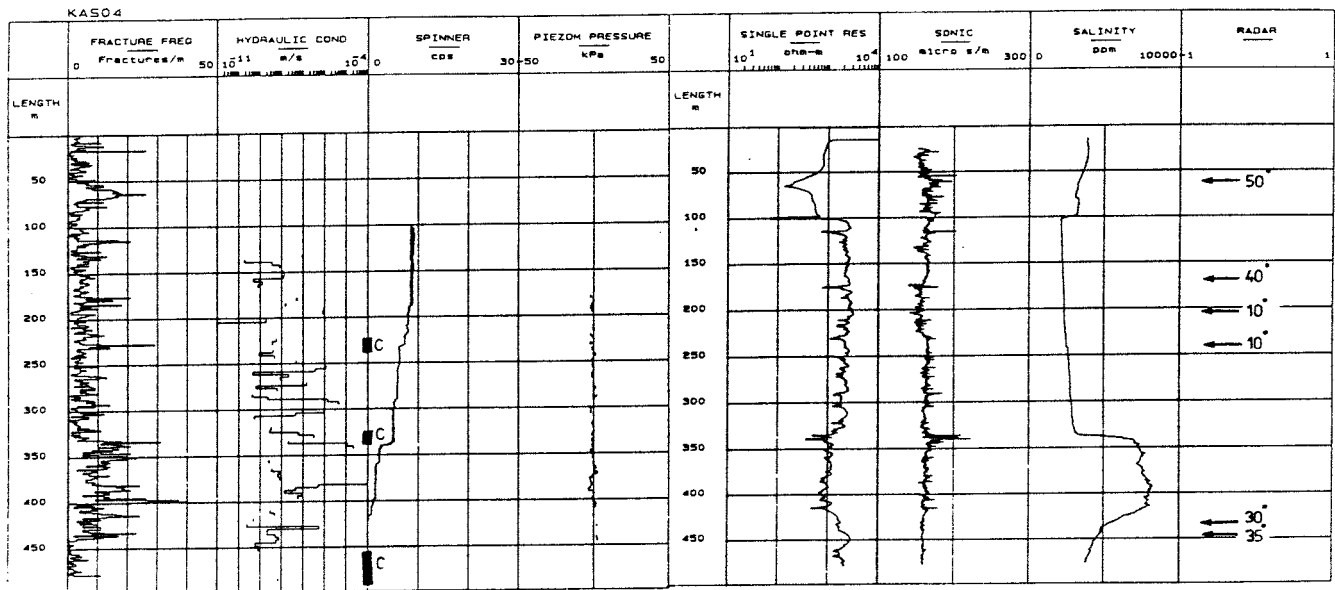
Figure 5.30. Composite log of borehole KAS04.

Borehole sections sampled for hydrogeochemistry are indicated by the
vertical bars at the right-hand margin of the hydraulic conductivity
column.

(P= sampling during pump testing, C= normal sampling protocol)
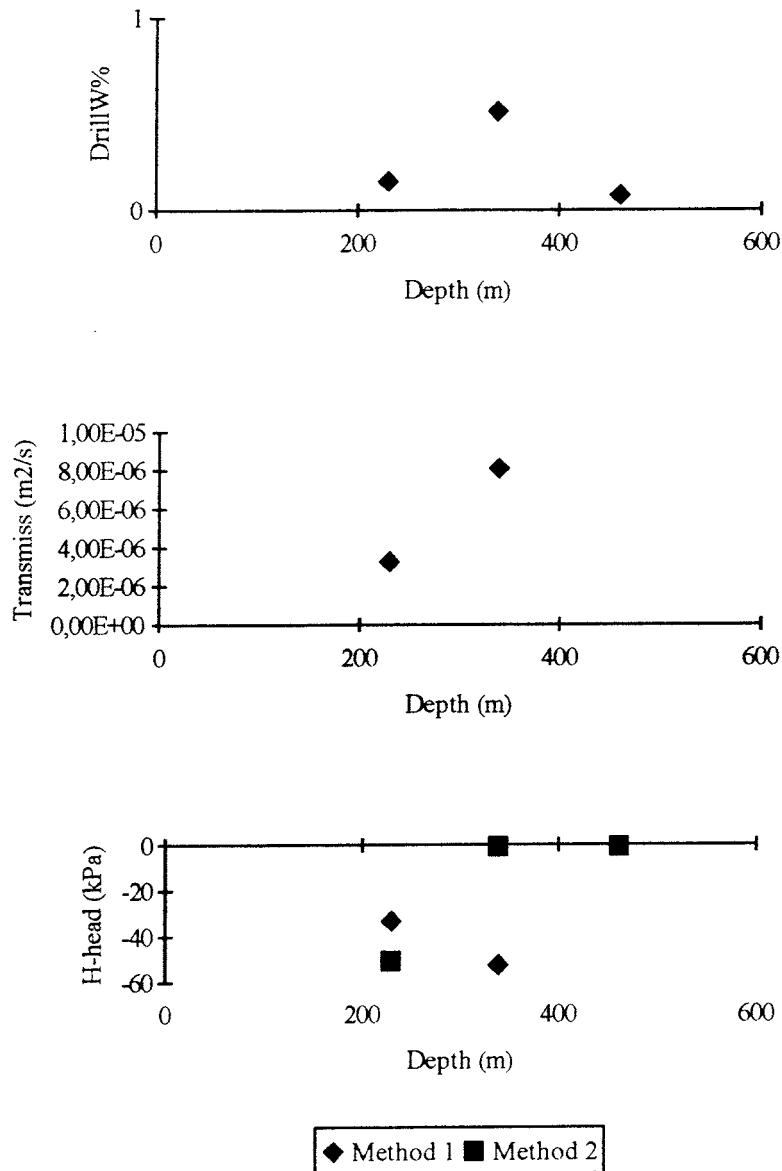
Figure 5.31. Summary of borehole measurements: a) uranine tagged activity water
(from drilling and hydraulic injection tests), b) transmissivity, and c) piezometric
head (Method 1 = VIAK; 2 = SGAB).

largely conform to the geophysical logging results. General conductivities along the borehole are irregular, varying from 10^{-8} to 10^{-5} ms^{-1}, and show a response to both marked and more discrete fracture zones. Maximum conductivity ranges correspond to sections 250-260, 290-310, 335-350, 380-400 and 430 m. The spinner survey recorded an irregular profile with a trend to decreasing hydraulic conductivity with depth; marked responses occur at 187-197, 217-220, 230-234, 290-301, 335-345, 356-362, 396-408 and 415-418 m. The majority of transmissivity values range from 1.9 to 2.5×10^{-6} m^{2}s^{-1} with two maxima occurring at 335-345 m (8.1×10^{-6} m^{2}s^{-1}) and at 230-234 m (3.5×10^{-6} m^{2}s^{-1}).

Pump tests carried out in KAS04 for a 44 hour period showed good hydraulic contact with boreholes KAS01, KAS02, HAS01, HAS04, HAS08 and HAS11 (see Fig. 5.29), indicating two major water-bearing zone directions, one E-W (from KAS04 to HAS08) and one NW-SE (from KAS04 to KAS01), resulting in calculated transmissivities of 5.7×10^{-5} m^{2}s^{-1} and 6.5×10^{-5} m^{2}s^{-1} respectively.

In summary, these data indicate high hydraulic conductivities and transmissivities along most of the KAS04 borehole with more dynamic groundwater flow conditions possibly occurring within the extent of the EW-1 shear zone. This is reflected in changes of salinity and the hydraulic connection with other boreholes within this borehole section; large recorded irregularities in temperature also support the apparent variability and heterogeneity of groundwater flow within EW-1. Contamination from borehole activities might be expected in such an environment but, as discussed in Section 3.2.4, tagged borehole activity water consistently lies under 1% uranine. Interestingly, from 226-235 m the tagged activity water is low (0.19-0.15%) but the tritium content is relatively high (up to 4.3 TU at 226-235 m), thus supporting the downward mixing of younger formational waters via short-circuiting from the borehole itself or from conductive fractures within EW-1.

5.3.1. Level 226-235 m.

The selected borehole section straddles the contact between greenstone and the Småland granite; at the contact, and corresponding to the fracture zone at 230-232 m, is an aplitic to aplite/granite transition. The background fracture frequency in the vicinity of the fracture zone is low (mean 5 fractures/metre) with an increase to 30 fractures/metre at the fracture zone itself. The main fracture filling phases are calcite, hematite, Fe-oxyhydroxide, chlorite, muscovite and possibly some illite.

Hydrology.

The sampled borehole length includes three, 3 m tested sections which record very low conductivities across the fracture zone (7.3×10^{-13} ms^{-1}) compared to only slightly higher values at either side ($3.7\text{-}3.9 \times 10^{-9}$ ms^{-1}). The spinner measurement at 230-234 m recorded a transmissivity of 3.3×10^{-6} m^{2}s^{-1}. Taking into consideration the absence of tagged activity water and the presence of tritium in this sample, there is a clear indication that the water may be have been collected via short-circuiting through the bedrock or around the packers. The monitoring log shows that after the initial 3-4 days of extraction, whereupon the groundwaters became less saline and more reducing, the system stabilised and

compositions became uniform. At the same time the presence of borehole activity water remained constantly very low (<0.2%).

Water Chemistry.

The collected groundwater (Table 5.8) has a pH of 8.2, is of high alkalinity (215 mg/L HCO$_3$) and relatively low salinity (530 mg/L Cl). Combined with a general low ionic content (as compared to overall Äspö groundwaters) and high TOC (6.9 mg/L) this sample has all the characteristics of a near-surface derived groundwater of Na-Ca Cl-HCO$_3$(SO$_4$) type (i.e. Type A of Laaksoharju, 1990a).

Redox-sensitive Parameters.

The groundwater is very reducing, indicated by a negative redox potential (-300 mV) and high sulphide content (1.10 mg/L);iron is present in very small quantities and is in the ferrous state (both Fe$_{(tot)}$ and Fe$_{(II)}$ = 0.04 mg/L).

Isotopic Geochemistry.

The stable isotope data plots just below the global meteoric line (Fig. 5.32); tritium is high (4.3 TU) and the percentage modern carbon is relatively high (40%; an apparent radiocarbon age of 7 795 BP: Table 5.9).

Uranium Geochemistry.

The uranium content (Table 5.9) is low (0.46 µg/L) and the ^{234}U/^{238}U activity ratio is high (5.10). This supports a reducing groundwater environment with widespread isotopic disequilibrium resulting from long bedrock residence/reaction times.

Summary.

The groundwater chemistry supports the hydrogeological data in that this sample does not appear to be totally representative for this depth. The low hydraulic conductivities suggest that a younger groundwater component from above the installed packer system, accumulated from shallower levels (perhaps via conductive fractures such as that indicated by the borehole radar at 226 m), has been short-circuited to the sampled section. This is supported by the presence of tritium and the general near-surface chemistry of the water; there is no influence of contamination from the tagged activity water.

5.3.2. Level 334-343 m.

The sampled section comprises mainly aplite with some granitic horizons <1 m wide and is highly fractured; the fractures are considered to be open. Borehole radar measurements show these fractures to be steep and intersect the borehole axis at 15°; i.e. the southern margin of the major EW-1 shear zone. Fracture filling mineral phases are dominated by chlorite, hematite and Fe-oxyhydroxide (± calcite).
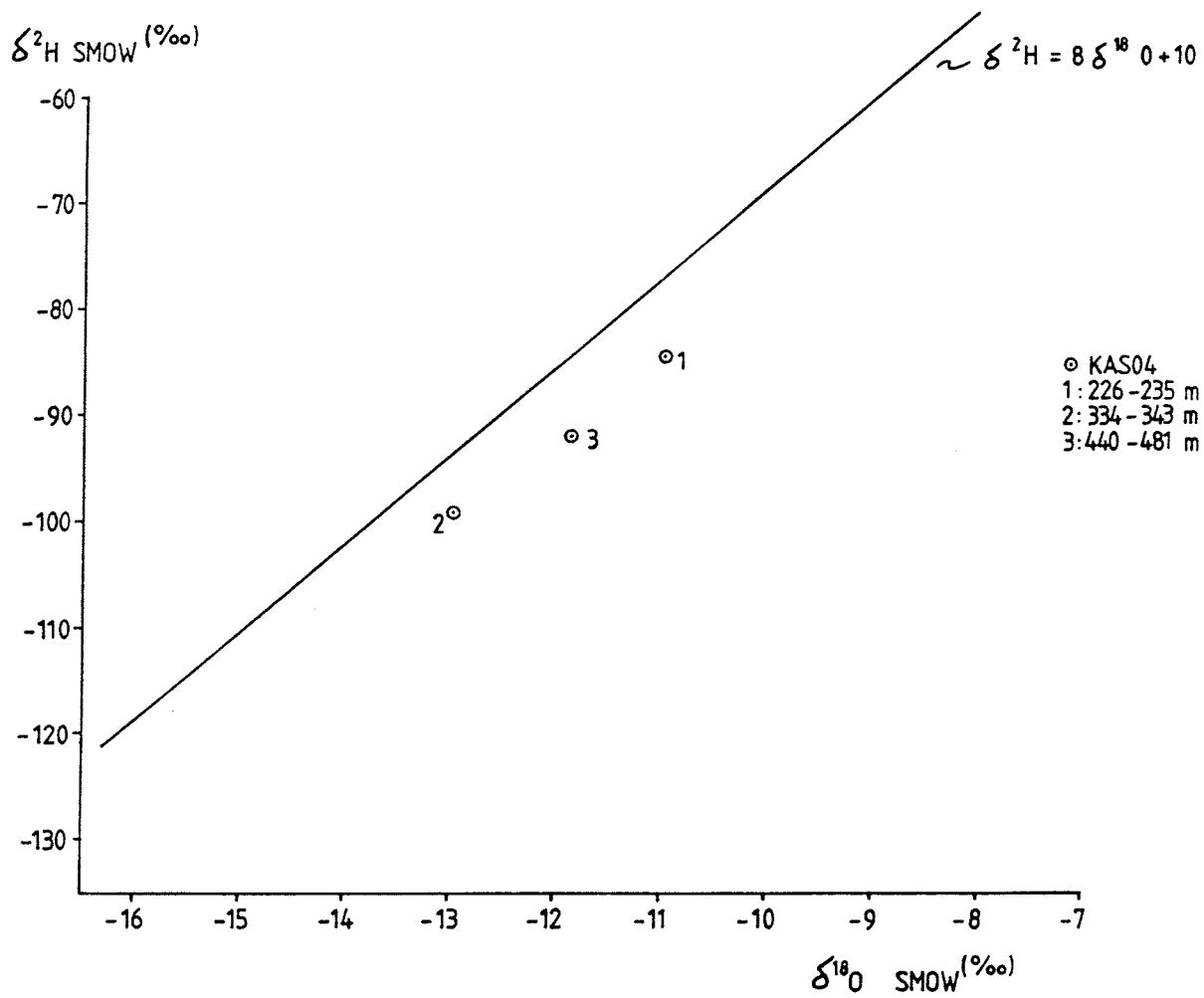
Figure 5.32. Stable isotope composition of borehole KAS04 groundwaters, Äspö.

Hydrology.

Three, 3 m intervals were measured within the sampled section. The 337-343 m interval recorded hydraulic conductivities ranging from $1.1\text{-}2.2\text{x}10^{-5}$ ms^{-1}, corresponding to the most fractured part of the borehole section, The remaining length, 334-337 m, recorded a slightly lower conductivity ($2.0\text{x}10^{-8}$ ms^{-1}). The spinner survey recorded a high transmissivity of $8.1\text{x}10^{-6}$ m^{2}s^{-1} at the 335-345 m interval with maximum flow at 339 m; head values are extremely negative (Fig. 5.31c). This highly conductivity zone may therefore be expected to be a source of contamination from the various borehole activities unless quickly flushed out of the system prior to sampling. Pumping during the eight days of sampling showed very uniform and stable conditions apart from the first day when the chemistry was more diluted.

Water Chemistry.

Compared to the preceding level (Table 5.8) this groundwater sample has a slightly lower pH (7.9 vs. 8.2) and an overall higher saline character. There is a general increase in the ionic composition with the exceptions of alkalinity (215 to 70 mg/L HCO_3), fluorine (4.0 to 2.6 mg/L) and TOC (6.9 to 5.3 mg/L). The groundwater is more Na-Ca(Mg) Cl-$SO_4(HCO_3)$ in type.

Redox-sensitive Parameters.

A reducing character is indicated by a high negative Eh (-280 mV), all dissolved iron is present in the ferrous state (0.315 mg/L) and sulphide is present, albeit in small quantities (0.40 mg/L).

Isotopic Geochemistry.

The stable isotopic data plot just below the meteoric water line in commmon with most Äspö data (Fig. 5.32). Tritium content is low (0.50 TU); no radiocarbon data are available (Table 5.9).

Uranium Geochemistry.

In common with the preceding level (Table 5.9) the uranium content is low (0.29 µg/L) and the $^{234}U/^{238}U$ activity ratio is high (4.6). Reducing groundwater conditions are indicated with widespread isotopic disequilibrium resulting from long residence/reaction times in the bedrock.

Summary.

This sampled section represents a well defined highly conductive zone coupled to a high negative head. For this reason some residual borehole activity water may have been expected to show up during the sampling period. To the contrary, the groundwater chemistry was quite stable and uniform after the initial days pumping, and the general absence of tagged borehole activity water (<1%) and tritium (0.50 TU) during this period

further indicate that the groundwater is representative for this conductive fracture EW-1 (78°SE) zone.

5.3.3. Level 440-481 m.

This long borehole section from 440 m to the hole bottom includes the transition from the aplite and aplite/granite to the diorite which also contains thin horizons (<1 m) of granite. The general fracture frequency is low (2-3 fractures/metre) and only one sealed fracture has been mapped at 461-462 m. Hematite is the dominant fracture filling phase.

Hydrology.

Hydraulic conductivities, recorded from the 3 m interval testing (439-454 m), are generally low ranging from 5.6-7.4×10^{-9} ms^{-1} at 439-445 m to 5.7×10^{-10} to 7.3×10^{-13} ms^{-1} at 445-454 m. No spinner measurements are available. The monitoring log shows uniform chemistry and redox conditions during the extraction period of 12 days; tagged borehole activity water is absent (<0.1%).

Water Chemistry.

Increased salinity, together with further decreases in alkalinity, fluorine and TOC, show this groundwater to be Na-Ca(Mg) Cl-SO_4 in type (equivalent ot Type C after Laaksoharju, 1990a) and of deeper origin than the previous two upper levels (Table 5.8).

Redox-sensitive Parameters.

Groundwaters are still strongly reducing; redox potential of -290 mV, all dissolved iron is in the ferrous state (0.260 mg/L) and sulphide is present (0.60 mg/L).

Isotope Geochemistry.

Stable isotope data plot, in common with the preceding levels, just below the meteoric water line (Fig. 5.32). Tritium content is very low (0.03 TU); no radiocarbom data are available (Table 5.9).

Uranium Geochemistry.

The uranium content (27.0 µg/L) and isotope activity ratio (7.2) are extremely, and anomalously, high, considering the very reducing character of the groundwater. Furthermore, there is no indication from the gamma log that a particularly radioactive rich zone is present in the sampled bedrock section.

Summary.

The borehole section is characterised by low hydraulic conductivity and the most saline groundwater collected from KAS04. The almost total absence of fractures mapped from the drillcore section, together with very low hydraulic properties, would suggest that water is

being short-circuited from above the installed packer system. The salinity log (Fig. 5.30) shows a fall-off of salinity from around 420 m which continues with depth. If the log measurements are reliable, then the obvious source of the saline groundwater collected is from the higher fractured level, corresponding with the major EW-1 fracture zone which extends its influence from 333-400 m.

5.3.4. Borehole summary and discussion.

Geological Setting.

Borehole KAS04 was drilled to establish the geological and hydrogeological interrelationships of the major Äspö shear zone (EW-1) which effectively divides the island into two blocks, a northern and a southern block. Three horizons were chosen to characterise the hydrogeochemistry within and around this complex zone; one within the EW-1 shear zone at 226-235 m, one at the southern boundary at 334-345 m, and one outside the shear zone further to the south at 440-481 m. Apart from the deepest level sampled, the other two levels clearly represent highly fractured, hydraulically conductive sections, as demarcated by drillcore mapping, geophysical logging and hydraulic measurements.

Hydraulic Character and Water Quality.

Based on all available hydraulic data, borehole KAS04 shows that groundwater containing a young, fresh water component, is actively recharging down through the EW-1 shear zone. Some of the constituent fractures in the shear zone are more conductive than others, so that mixing is taking place between the very old saline water normally existing near the bedrock surface (see salinity log), and a limited fresh component. This young component appears to persist to the EW-178°SE southern boundary fracture zone at 334-343 m whereupon there is a strong influx of highly saline groundwater from the surrounding bedrock, possibly facilitated by the shallow dipping EW-5 fracture zone which intercepts the EW-1 zone at 280-370 m.

Contamination from tagged borehole activity water was minimal at all three sampling locations; the high tritium content (and relatively young apparent radiocarbon age) at 226-235 m is due to a young, near-surface derived component.

Chemical and Isotopic Features.

Groundwaters of different compositions are present (see Figs. 5.33 to 5.36), varying from containing a high near-surface component of $Na-Ca:Cl-HCO_3(SO_4)$ type (Type A of Laaksoharju, 1990a) at 226-235 m, through a more saline groundwater of $Na-Ca(Mg):Cl-SO_4(HCO_3)$ type (Type B of Laaksoharju, 1990a) at 334-343 m, to finally a highly saline groundwater of $Na-Ca(Mg):Cl-SO_4$ type (Type C of Laaksoharju, 1990a) at 440-481 m. Without exception the groundwaters are very reducing and long residence/reaction times are indicated.

The stable isotope signatures plot over a large compositional range just under the standard global meteoric water line, in common with the other borehole data.
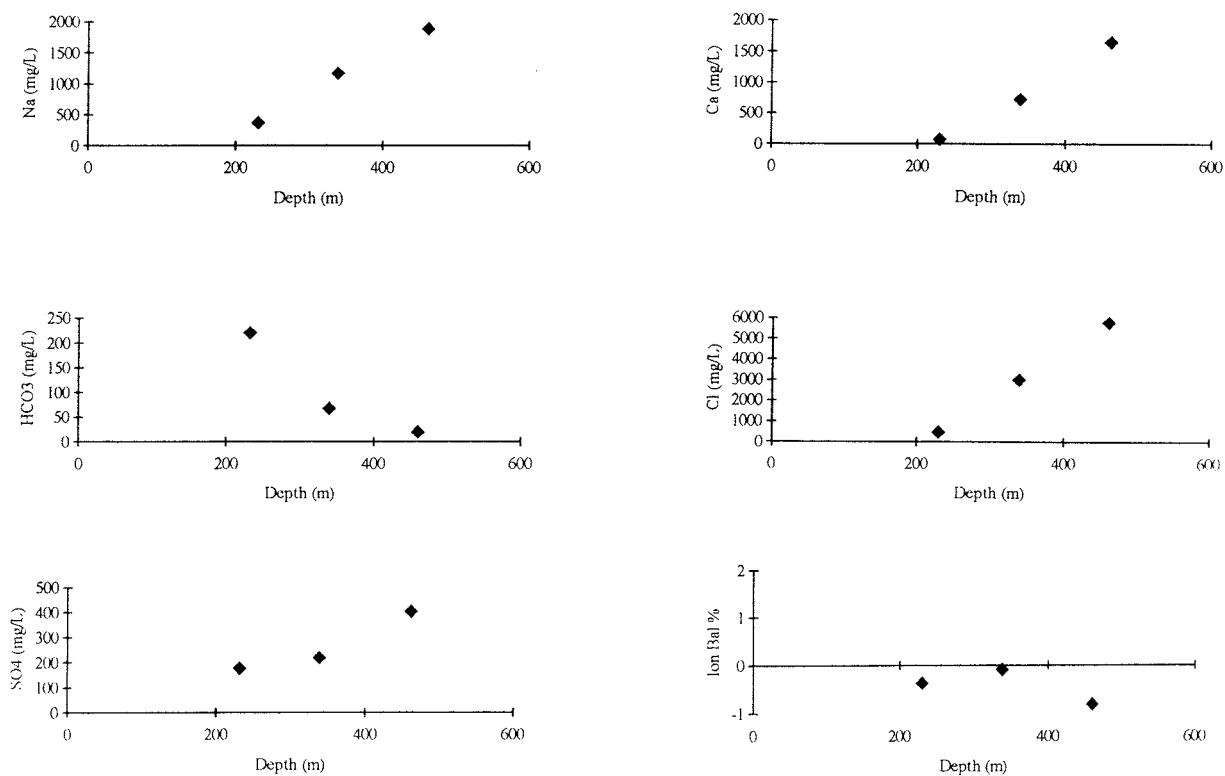
Figure 5.33. KAS04 groundwaters; major ion distributions and ionic charge balance.
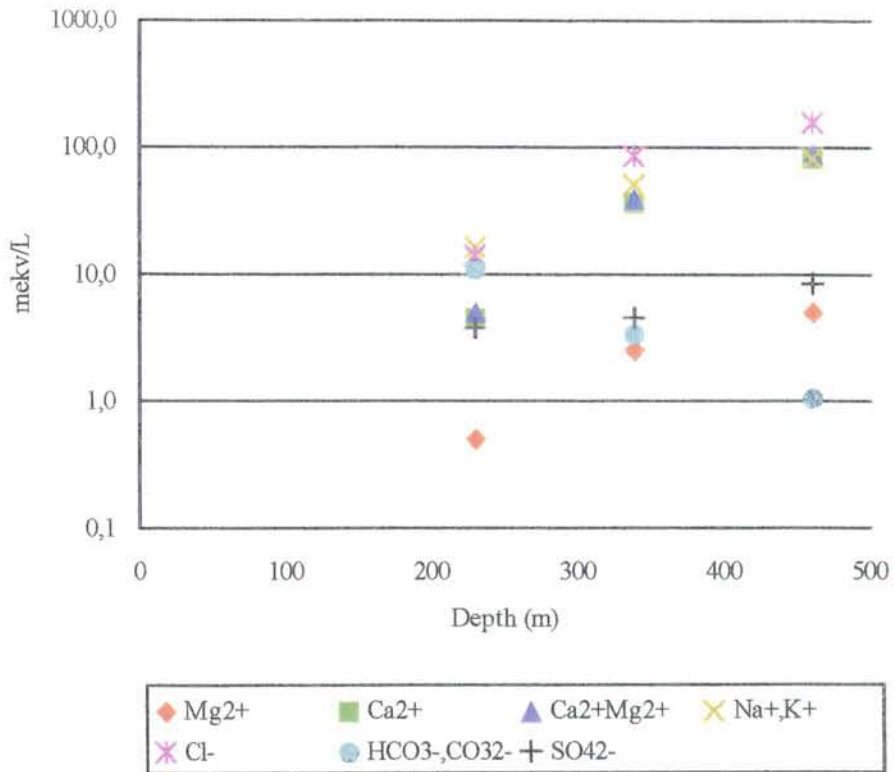
Figure 5.34. KAS04 groundwaters; distribution of selected redox-sensitive elements.
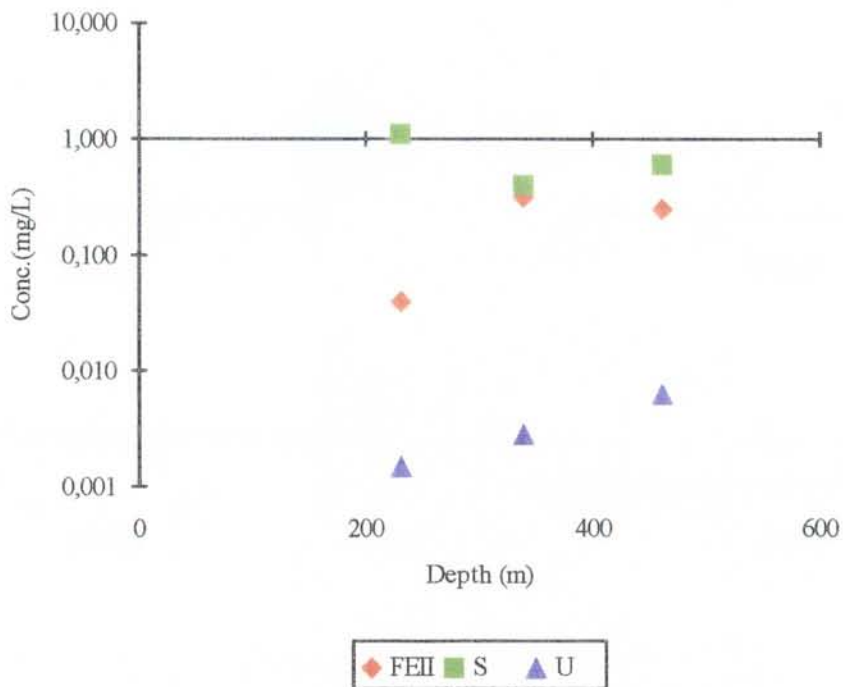
Figure 5.35. KAS04 groundwaters; Shoeller diagram showing the major ion distributions with depth.
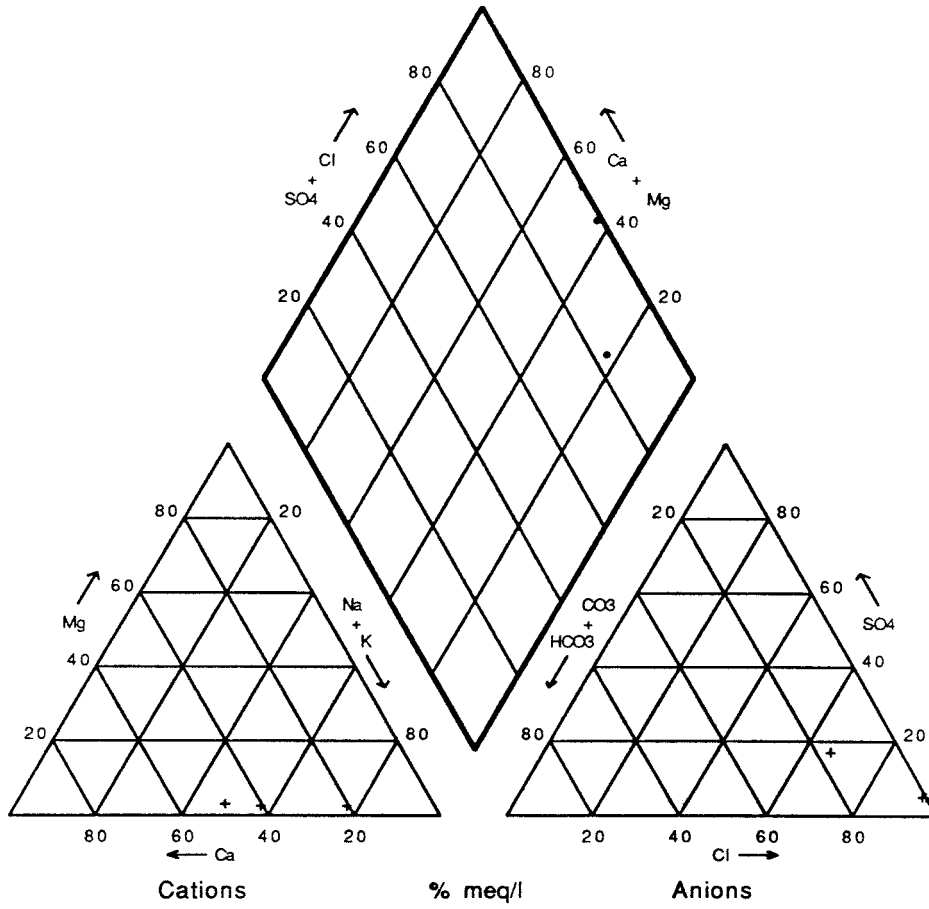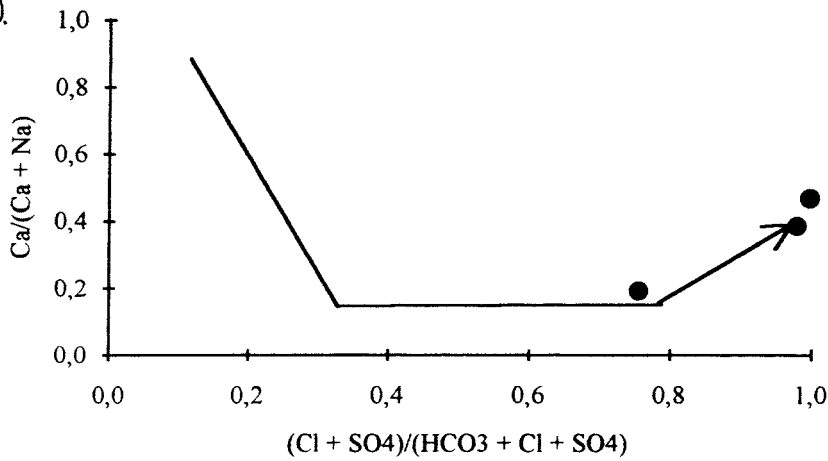
Figure 5.36. KAS04 groundwaters; a) Piper Plot of the major ion chemistry, and
b) modified Piper Plot showing the position of the KAS04 groundwaters on an assumed chemical evolution trend for average deep Swedish groundwaters in crystalline rock.

Water/rock Interaction.

The percentage of the major rock types comprising borehole KAS04, the dominant host rock characterising each hydraulic zone(s) sampled for groundwater, and the identified macroscopic (and when available the microscopic) fracture mineral phases (from two data sources) in those hydraulic zone(s), are illustrated in Figures 5.37 and 5.38.

Comparison of rock type with rock-sensitive elements such as Mg, U, ^{226}Ra and Th in groundwater shows small systematic increases with depth; this may reflect the fact that that it is the same fine-grained granite type which hosts all three sampled hydraulic zones (compare Figs. 5.37a and b and 5.39a).

The relationship between groundwater and the fracture infilling phases using equilibrium calculations of the saturation indices is presented in Figures 5.39b and c. The results indicate close to saturation or slight oversaturation for calcite, fluorite and quartz; calcite and quartz are also observed as fracture mineral phases. The saturation index for gypsum and dolomite is negative for the complete borehole, reflecting the reported rarity or absence of these minerals in the fractures. Pyrite, which is oversaturated, is not reported as a fracture mineral. Hematite and iron hydroxide are strongly undersaturated in the lower part of the borehole. Apart from calcite and gypsum, which are known to rapidly approach saturation equilibrium in aqueous systems, the remaining data must be considered doubtful.

Groundwater Mixing Ratios.

Using the simple two component mixing model described and discussed for KAS02 (see Section 5.1.8), the calculations show a very high shallow water component at the 226-235 m level, decreasing steadily with depth to the 440-481 m level, although up to a 50% component is still indicated. This trend is supported by the TOC and pCO_2 distributions, and Br/Cl shows a more gradual decrease in seawater input if the upper and lower level sampled horizons are compared. These distributions support the recharge character of this major EW-1 zone.

Considering the Cl mixing model (Fig. 5.41a) the calculations show a steady approach to equilibrium mixing with depth; this may simply reflect the more active recharging environment near the surface (i.e. too dynamic for equilibrated mixing). Increasing depth coupled with decreasing hydraulic conductivity (Fig. 5.30) would help to stabilise the the hydraulic mixing of the recharging groundwaters. The strongly recharging environment is supported by the Cl dilution to around 400-450 m.

For K, Mg and Ca there is a sharp change from a negative to a positive relative deviation at around 300 m suggesting that either all three ions are being removed in the upper 300 m and then being available at greater depth, or, waters coming from depth (i.e. higher Ca and K; Mg is more variable) are being diluted when coming in contact with recharging groundwaters. Na and SO_4 show little change and HCO_3 shows a marked decrease possibly in conjunction with calcite precipitation, although this is not reflected by the Ca.

It is quite clear that the observed trends in groundwater chemistry are not readily explained by rock/water interaction or this simple two component mixing model. This complexity is discussed further in Section 6.4.
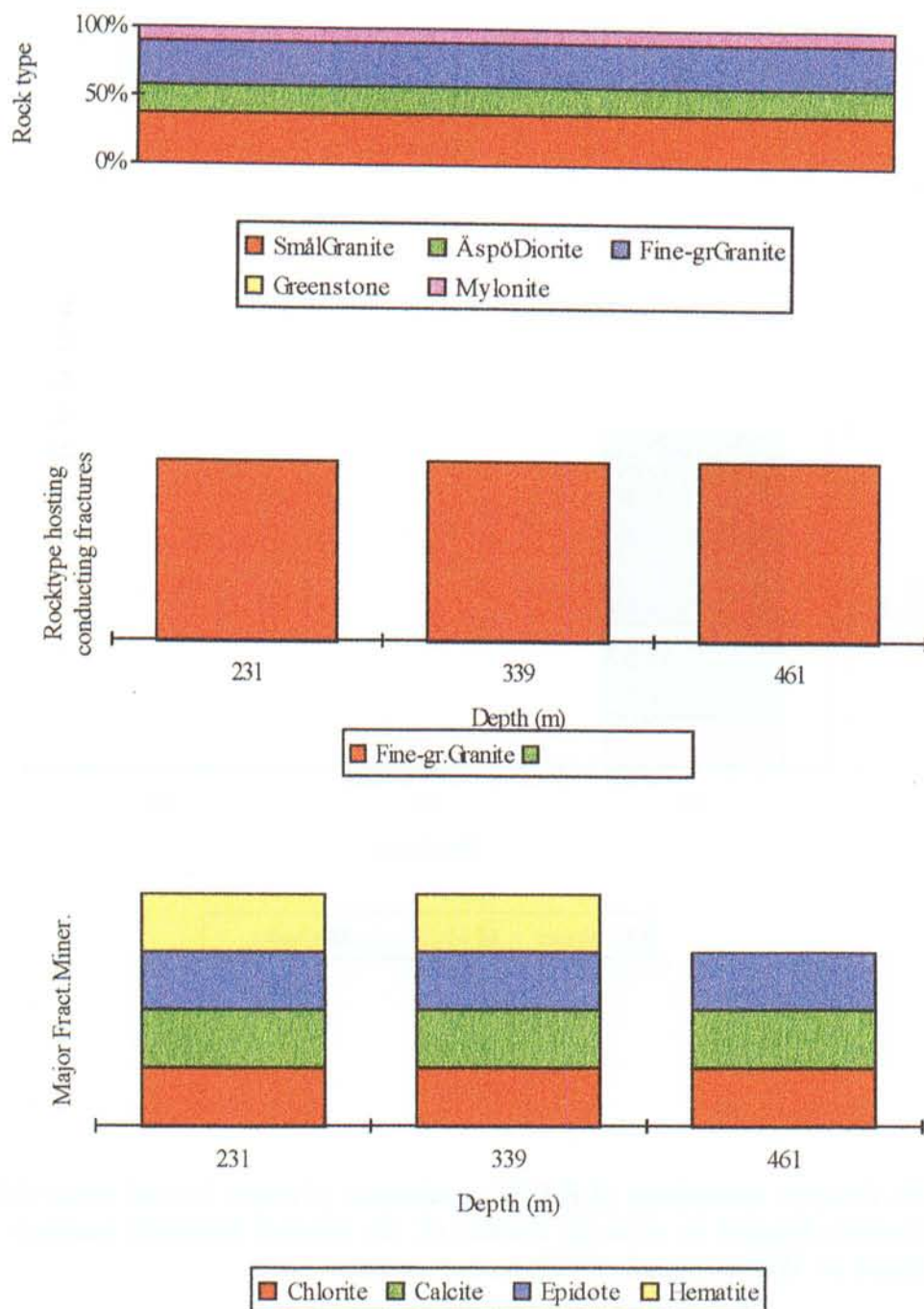
Figure. 3.37. Rock type and fracture mineralogy of KAS04: a) overview of the major rock
types (based on Stanfors, 1988), b) evaluation of probable rock type hosting
the fractures (based on Stanfors, 1988), and c) evaluation of the major
fracture minerals (based on Stråle, 1988 and Tullborg, 1989).
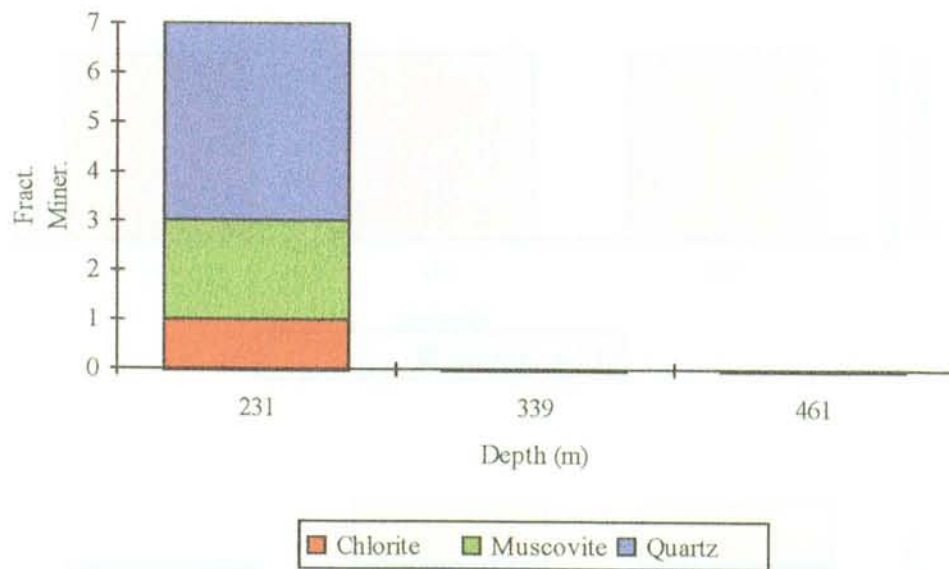
Figure 3.38. Fracture mineralogy of KAS04: evaluation of major (a) and minor (b) fracture minerals detected at, or in the vicinity of, the sampled hydraulic borehole sections (based on Wikman et al., 1988).
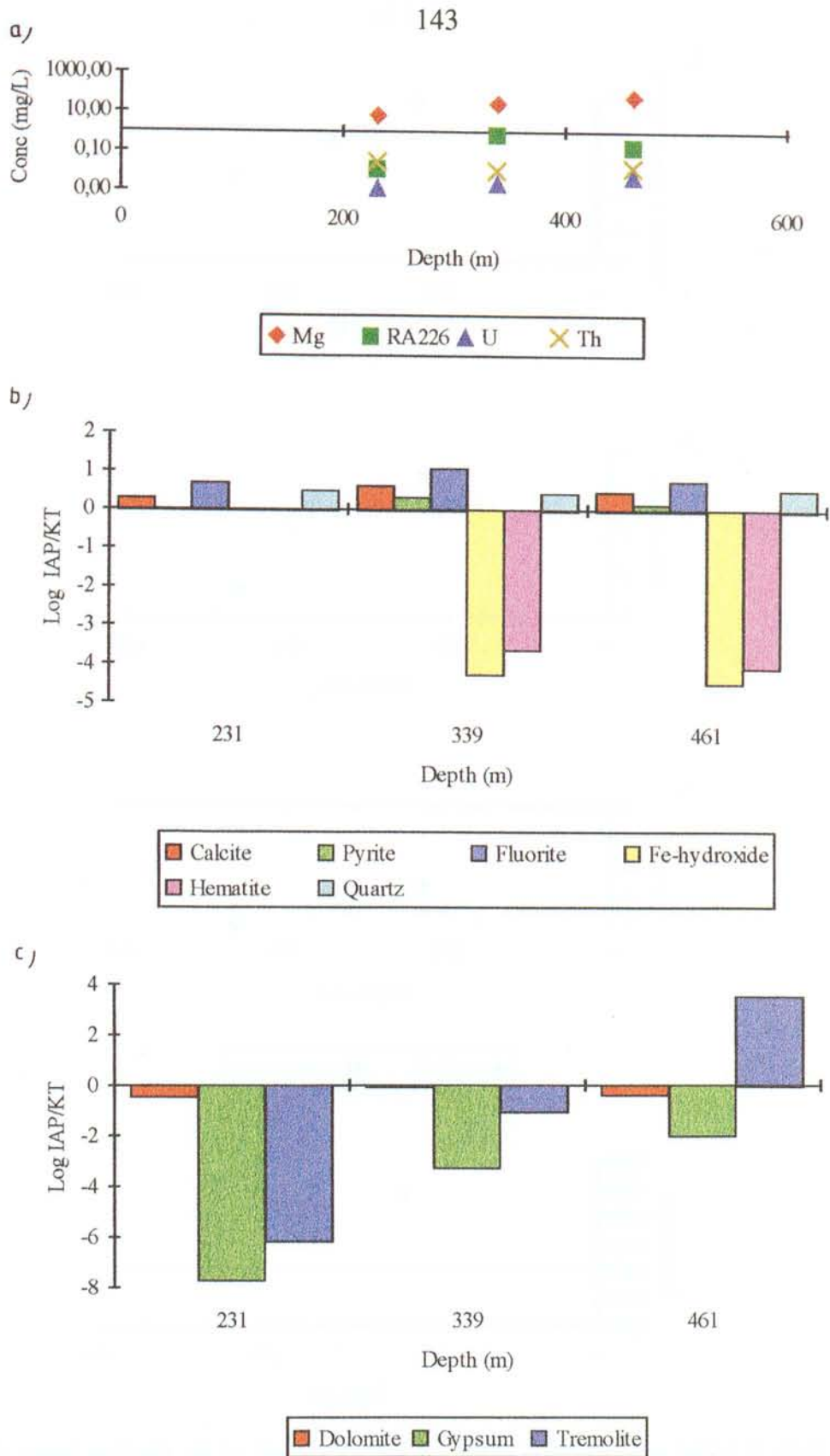
Figure 5.39. a) plotted concentrations of Mg, [226]Ra, U and Th measured in groundwater, and b, c) results of equilibrium saturation index calculations using PHREEQE (Parkhurst et al. 1980).
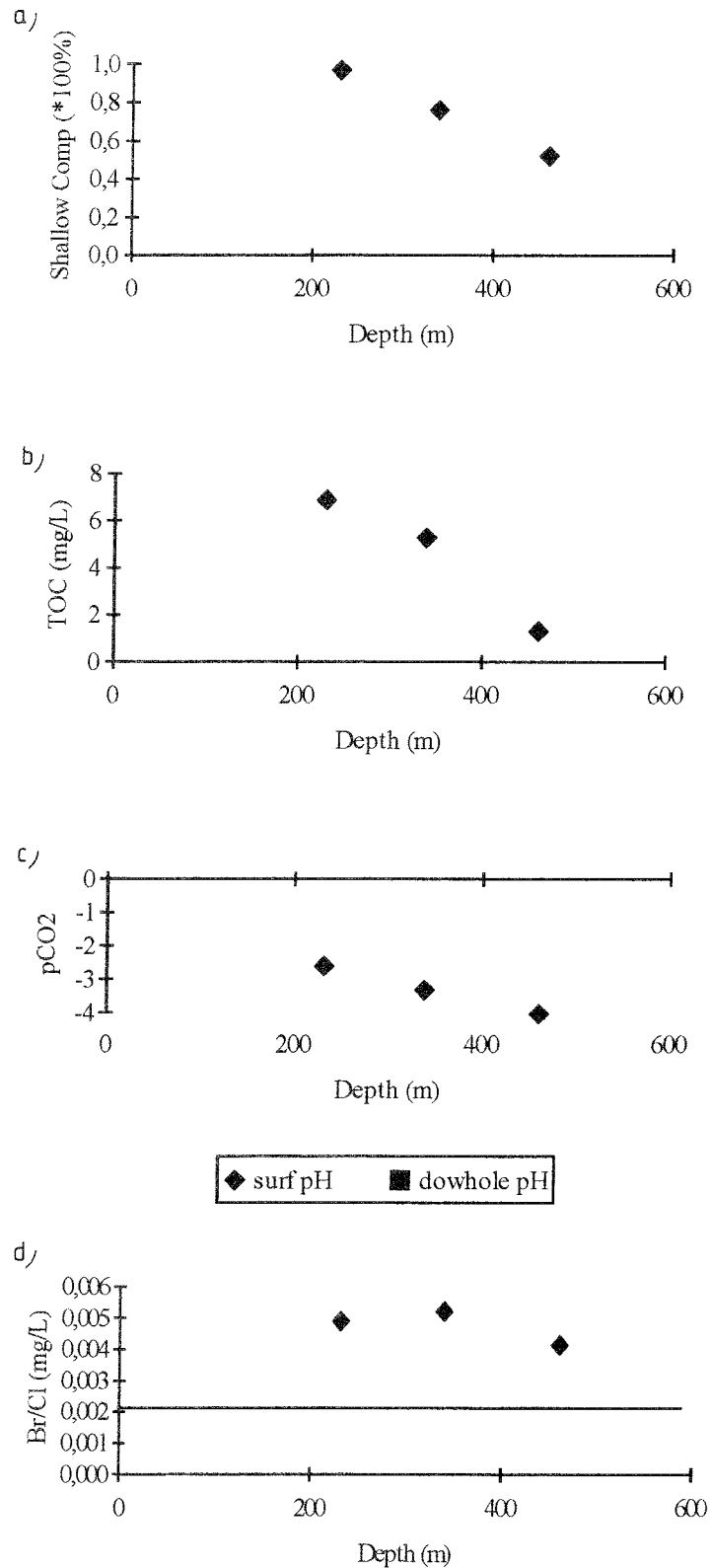
Figure 5.40. KAS04 groundwaters showing: a) calculation of the shallow input derived from a mixing model using Cl end members from HAS05 and KAS03, b) TOC (total organic carbon) versus depth, c) calculated pCO_2 pressures from downhole and surface (on-line) pH readings, and d) Br/Cl ratio versus depth; the horizontal line represents the seawater Br/Cl ratio (0.0031) for reference.
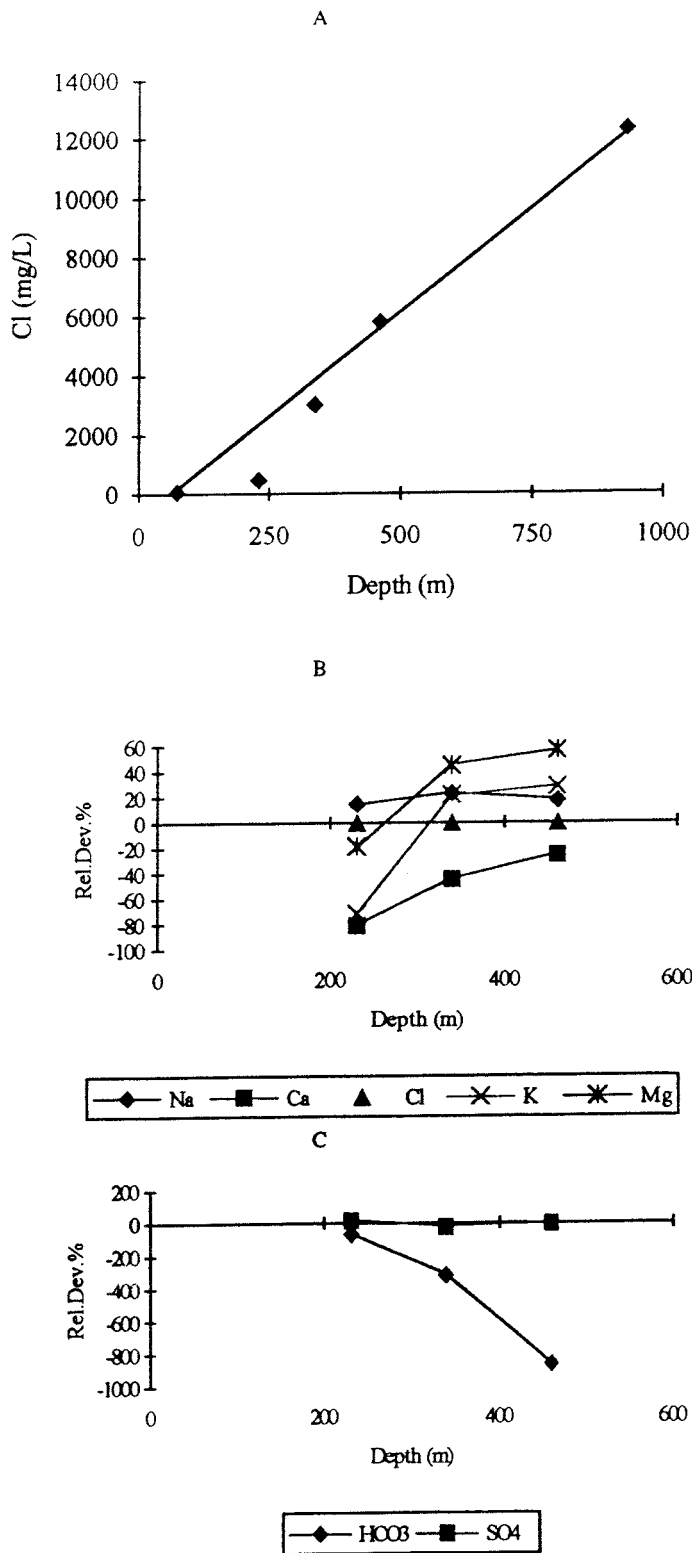
Figure 5.41. KAS04 groundwaters showing: a) plot of Cl vs depth related to the
simple two component mixing line, and b), c) depth trends of
the major ions plotted as percentage relative deviation to the mixing model.

Uranium Geochemistry.

Figure 5.42 shows the solubility of different uranium oxide phases (thermodynamic data from Puigdomènech and Bruno, 1988) as a function of Eh (and pH). Plotted are the distribution of groundwater measurements from borehole KAS04 (together with KAS02 and KAS03; with pH values indicated) which show that the main solubility limiting phases are crystalline uraninite (UO_2) and the more amorphous U_4O_9 phase (P. Sellin, per. comm. 1992).

Uranium series data (Table 5.9) show high $^{234}U/^{238}U$ activity ratios (4.6-7.2) caused by a build-up of excess ^{234}U. This demonstrates that the groundwaters are moving sufficiently slowly through the bedrock so as to allow the excess ^{234}U to accumulate, and thereby supporting near stagnant conditions.
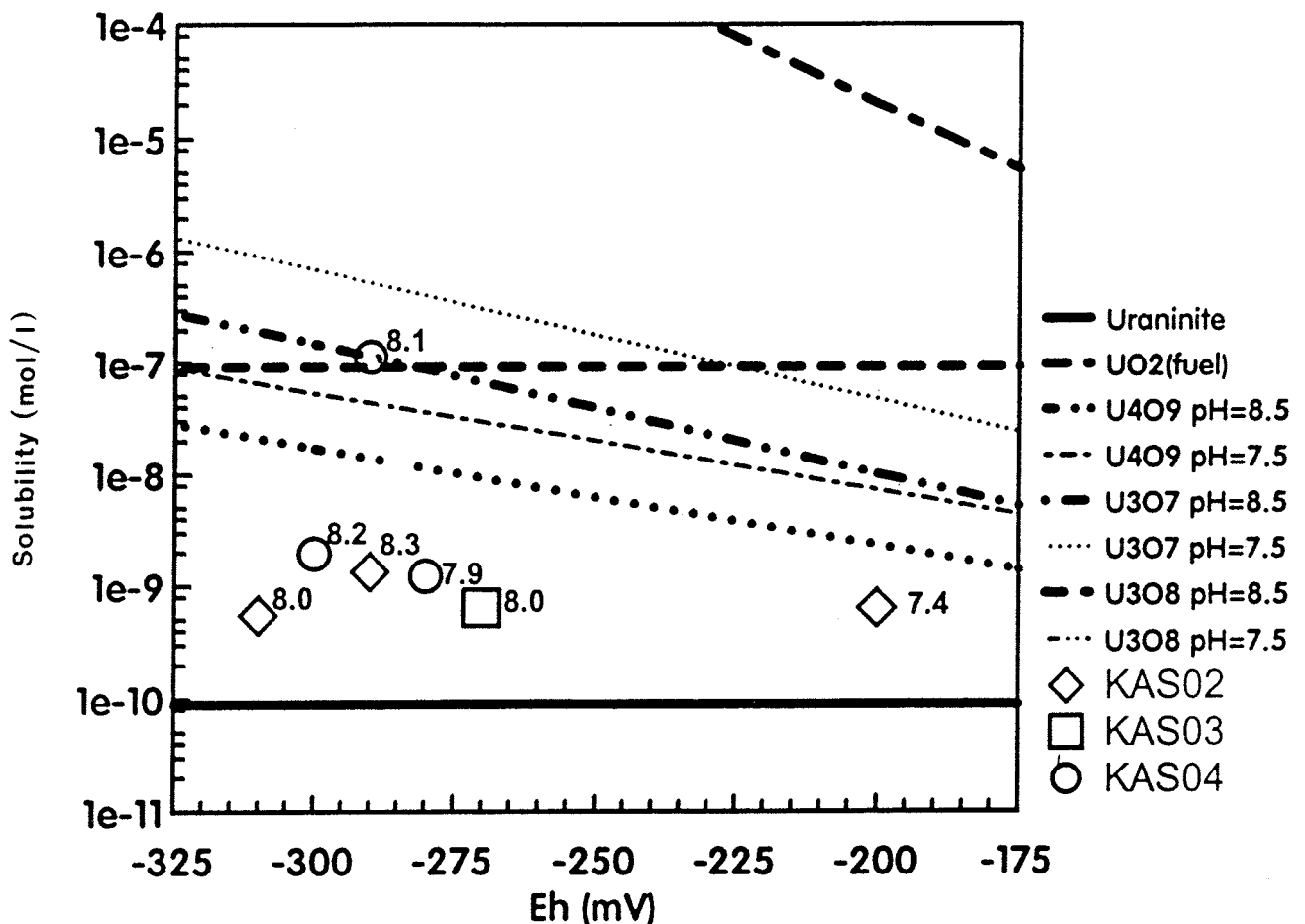
Figure 5.42. KAS04 groundwaters (with pH values indicated) related to the solubility of different uranium oxide phases plotted as a function of Eh (and pH). (Thermodynamic data from Puigdomènech and Bruno, 1988)

Table 5.8: Chemical analyses of groundwater samples from borehole KAS04, Äspö.

Borehole	KAS04	KAS04	KAS04
Section (m)	226-235	334-343	440-481
Sampling method	ccc	ccc	ccc
Sample no.	1596	1603	1588
Date	890417	890427	890403
W.flow ml/m	100	108	93
Drillingwater %	0.16	0.52	0.08
Cond. mS/m	255	1030	1830
Density g/ml	0.9967	0.9999	1.0036
pH	8.2	7.9	8.1
E_h mV	-300	-280	-290
Alkalinity (mg/l HCO_3)	222	69	21
Carge balance mequiv./l	-0.02	-0.48	-3.57
Rel. charge bal. error %	-0.04	-0.26	-1.04

Element

Na	382	1180	1890
K	2.4	6.1	7.8
Ca	91	740	1660
Mg	6.2	30	61
Sr	1.8	12.6	28.9
Mn	0.06*	0.31	0.44
Li	0.09*	0.38	0.94
Fe,tot	0.041	0.327	0.259
Fe(+II)	0.040	0.324	0.256
F	4.0	2.6	1.5
CL	508	3030	5840
Br	2.5	15.9	24.4
I	0.07	0.16	0.44
PO_4-P	0.008	0.003	0.001
SO_4	180	220	407
S_2	1.10	0.41	0.60
NO_2-N	<0.001	0.001	<0.001
NO_3-N	<0.01	0.01	<0.01
NH_4-N	0.01	0.09	0.05
SiO_2-Si	4.8	4.1	5.0
TOC	6.9	5.3	1.3

* No determination. The result from another sample in the borehole section is presented.

Table 5.9: Uranium and isotopic analyses of groundwaters from borehole KAS04, Äspö.

Borehole	KAS04	KAS04	KAS04
Section (m)	226-235	334-343	440-481
Sampling method	CCC	CCC	CCC
Sample no.	1596	1603	1588
Date	890417	890427	890403
Percentage Modern Carbon (PMC)	40	-	-
^{14}C age BP	7795	-	-
age BP corr.	-	-	-
^{238}U (mBq/kg)	11.70	7.30	685
^{235}U (mBq/kg)	1.60	0.98	180
^{234}U (mBq/kg)	60.0	33.9	4950
U_{tot} (ug/kg)	0.46	0.29	27
$^{235}U/^{238}U$	0.140	0.130	0.260
$^{234}U/^{238}U$	5.10	4.60	7.20
^{18}O (SMOW)	-11.0	-13.0	-11.9
^{2}H (SMOW)	-84.8	-99.6	-92.3
^{3}H (Bq/l) [1]	< 1	< 1	< 1
^{3}H (TU) [2]	4.30	0.50	0.03

[1] Kjeller, Norway
[2] IAEA, Wienna

5.4. Borehole KAS06.

Borehole KAS06 (Fig. 5.43), with an upper diameter of 155 mm (down to 100 m) and a lower diameter of 56 mm (to the full length of the borehole at 602 m), was drilled at an inclination of 60° to investigate the bedrock geology, hydrogeology and hydrogeochemistry at and in the vicinity of the shallow dipping EW-5 tectonic zone. This zone, trending E-W across Äspö, is topographically evident as a 10 m wide depression bounded by scarps and geophysically distinct as a low magnetic and resistivity anomaly.

Four major rock types were encountered during drilling, the most common being the diorites (56%) which extend over the full length of the drillcore, followed by the red, fine-grained granites or aplites (24%) which occur mainly at 460-535 m with more minor horizons (<1 m) at 280-290 m and 360-370 m, then the Småland granites (10%) mainly at 60-120 m with a minor horizon at 435-460 m, and finally greenstones (10%) at 230-275 m with several minor horizons (<1 m) between 60-230 m.

Fracturing is not marked along the drillcore apart from two sections; from 60-75 m which coincides with the major EW-3:82°SE fracture zone, and to a lesser extent from 440-475 m. Borehole radar reflections confirm the existence and orientation of the EW-3 zone at 60-75 m, and a further zone at 78 m which intersects the borehole axis at 40° and interpreted to be zone NE-1. No horizontal or subhorizontal fracture zones are indicated; this is contrary to what would be expected considering the presence of the EW-5/EW-X gently dipping zone (Fig. 5.43).

The borehole geophysical logs (Fig. 5.44) support the general lack of fracturing in the bedrock (background mean of 2-5 fractures/metre). In addition to the two higher fracture frequencies described above at 60-75 m (maximum of 30 fractures/metre) and at 440-475 m (range of 15-40 fractures/metre), weaker fracturing (supported by the single point resistence and sonic logs) occurs at 90-95 m, 230-240 m, 305-315 m and 500-510 m, all showing a maximum range of around 5-25 fractures/metre. Statistically, the distribution of open fractures is 3.58 fractures/metre compared to 1.42 fractures/metre for the sealed variety. The dominant open fracture filling phases are chlorite and calcite with subordinate hematite, Fe-oxyhydroxide, pyrite and epidote; in the sealed fractures epidote, chlorite and calcite dominate. Some quartz and zeolite (laumonite) have also been identified. The frequency of hematite and Fe-oxyhydroxide coated fractures with depth indicates an increase for both varieties near the bedrock surface (0-80 m), but mainly hematite in more sporadic distributions at 450-560 m. Rare occurrences of gypsum have been reported.

The gamma log (not shown) shows increases in activity mainly in association with the more granitic/aplitic horizons which are often fractured (e.g. 70-120 m, 260-290 m and 440-540 m), and less commonly coincident with only fractured/crushed sections (e.g. 350 m).

Hydraulic conductivities (measured in 3 m intervals from 105-591 m) range from 10^{-9} to 10^{-5} ms^{-1} and the spinner survey (measured in 1 m intervals from 100-597 m) shows a steady decrease of conductivity with depth; piezometric head values generally cluster about zero apart from around 200-250 m where negative heads coincide with the open fracture zones (Figs. 5.44 and 5.45c). The spinner survey identified conductive zones located at

a)

ÄSPÖ
TOP VIEW
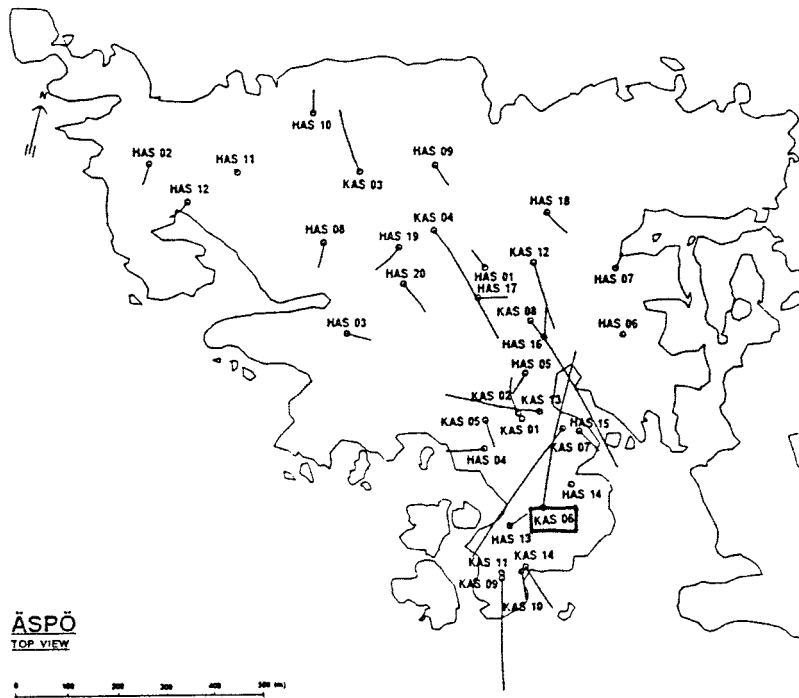
b)
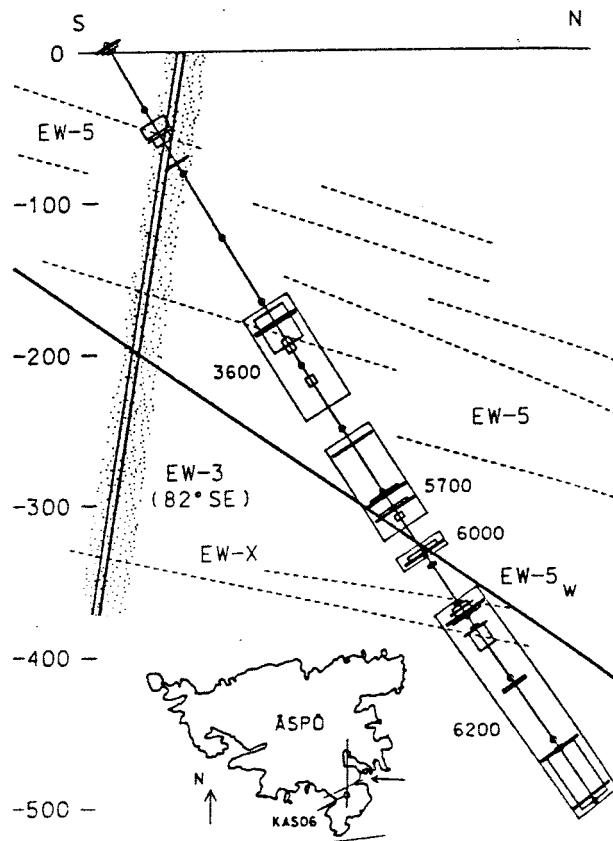
Figure 5.43. Location of borehole KAS06 (a) and its relationship to the major EW-5 shear zone (b) (from Wikberg et al., 1991).
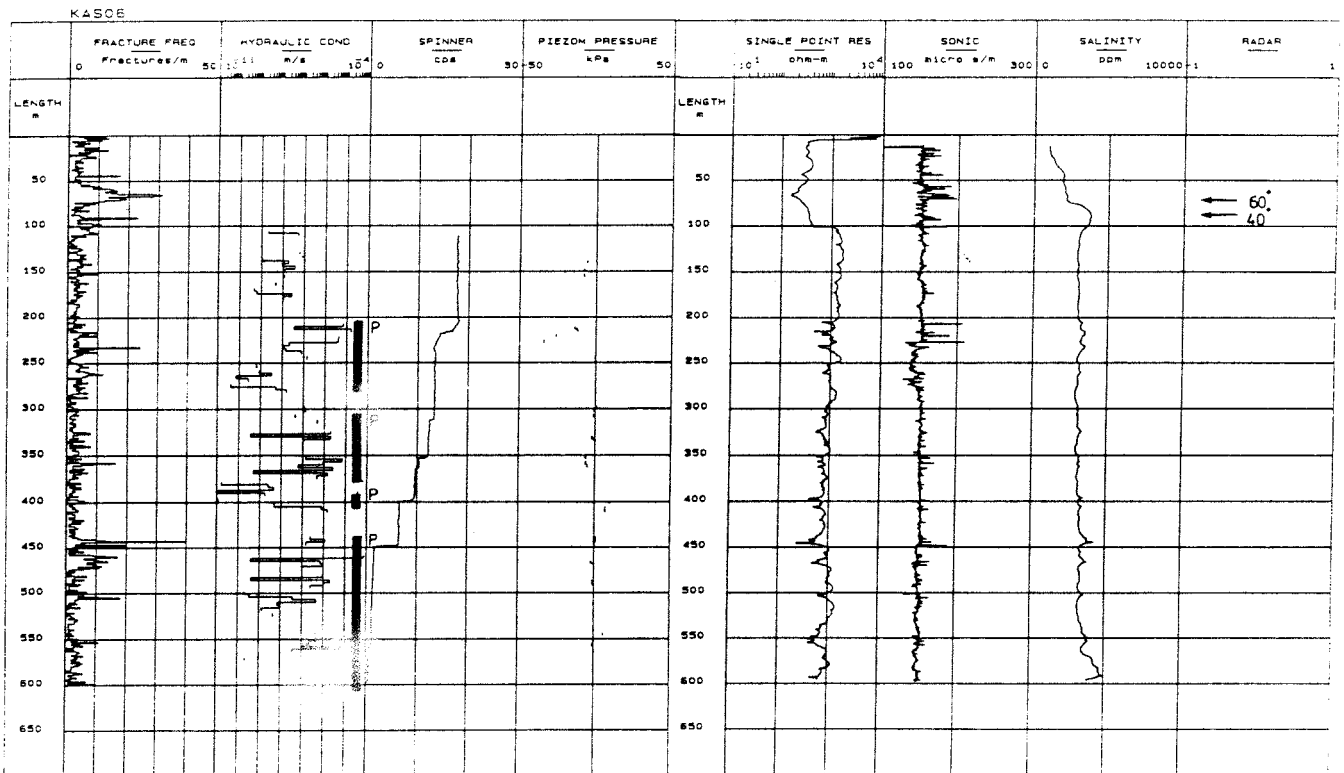
Figure 5.44. Composite log of borehole KAS06.

Borehole sections sampled for hydrogeochemistry are indicated by the vertical bars
at the right-hand margin of the hydraulic conductivity column.

(P= sampling during pump testing, C= normal sampling protocol)
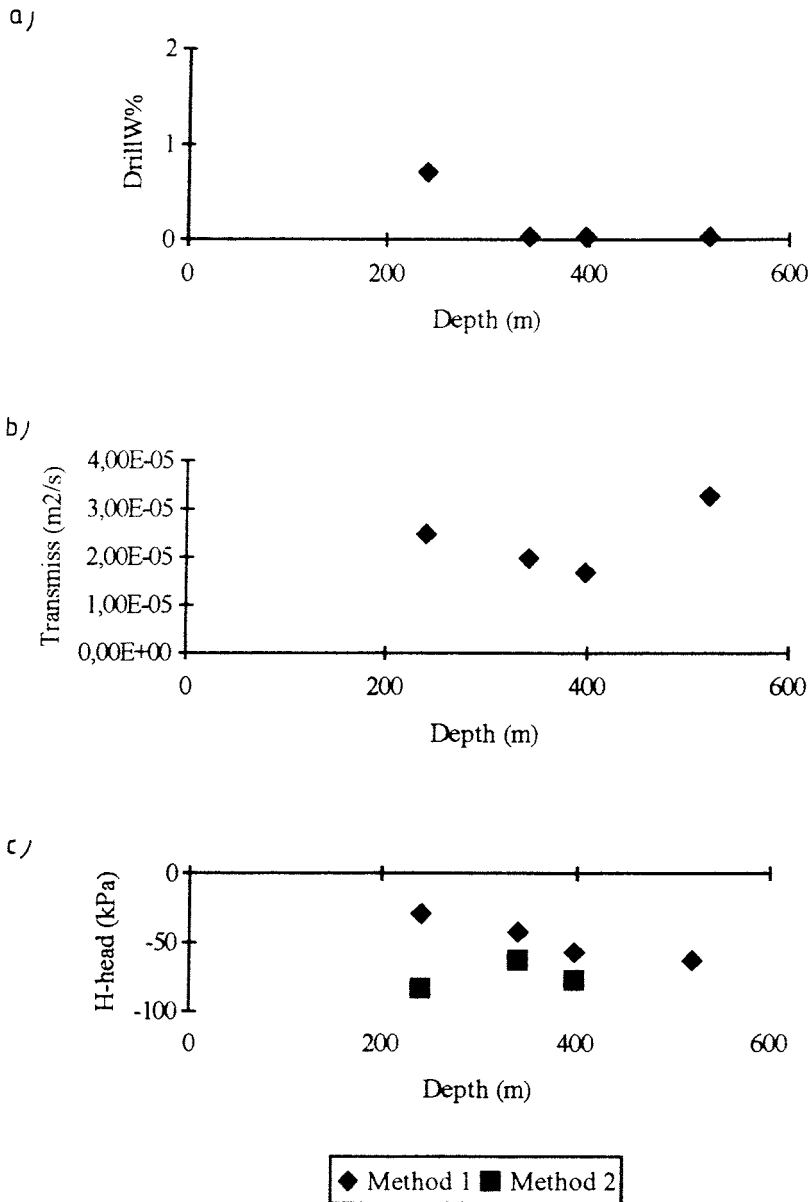
Figure 5.45. Summary of borehole measurements: a) uranine tagged activity water
(from drilling and hydraulic injection tests), b) transmissivity, and c) piezometric
head (Method 1 = VIAK; 2 = SGAB).

208-234, 312-313, 351-354, 362-365, 396-400, 447-450 and >557 m, many of which correspond to water-filled fractures derived from downhole geophysical methods. Long-term pump tests (period of 66 hours) showed a hydraulic connection with several boreholes in the vicinity of KAS06. These include (see Fig. 5.43 for locations) KAS02, HAS06, HAS07 and HAS13; calculated transmissivities were high (10^{-4} m^2s^{-1}) and suggested hydraulic contact via a major water-bearing zone in a NNE-SSW direction.

The salinity log (Fig. 5.44), after an initial increase from approx. 1 000 mg/L equivalent NaCl at 15 m to a maximum of approx. 3 700 mg/L at 85 m, is very regular with increasing depth, showing only a small variation from 3 500 mg/L at 100 m to 5 000 mg/L at almost 600 m. The temperature log within the upper 100 m and at 210-225 m is irregular, both corresponding to hydraulically conducting fracture zones; otherwise the temperature shows a normal increase with depth from the surface of 9-14°C.

The general hydraulic features and the contamination risk factor for sampling in KAS06 are illustrated in Figures 5.44 and 5.45. In summary, the high hydraulic conductivity and transmissivity reflected by the borehole measurements, coupled to a general high negative piezometric head at 200-250 m, might be expected to result in some residual borehole activity water. The discussion in Section 3.2.4 showed that three of the four levels sampled lacked any tagged activity water (<1%), contrasting with the 204-277 m level (as inferred above) which contained 1.19% uranine prior to sampling, although this was quickly removed during the pump test. However, two of the levels, at 204-277 m and 439-602 m, contained appreciable amounts of tritium (3.5 and 3.8 TU respectively) which show that groundwaters at these depths contain a young, near-surface derived component. Some downward (recharge?) movement of groundwater is suggested from plots of the percentage of calcite coated fractures against depth which show that the calcite dissolution front lies around 10-20 m; furthermore, magnetite oxidation has extended to a depth of 70 m.

The stability/representativity of the groundwater systems sampled can be obtained by comparing the above groundwater chemistry (Fig. 5.10) with monitoring analyses (Fig. 5.12) carried out from levels 191-249 m and 431-500 m one year later. The packed off borehole sections monitored were not exactly coincident with the earlier sampling campaign, and the groundwater extraction rates were much lower. The shallower level was more saline than earlier; the deeper level showed little difference. The high extraction rates may therefore explain why there is a significant younger groundwater component present in the 204-277 m section (see below).

5.4.1. Level 204-277 m.

The selected borehole section is mainly composed of grey-black, fine-grained greenstone (228-277 m) with subsidiary diorite (204-228 m); thin horizons (<1 m) of aplite occur at 260-277 m. Fracturing is very low (mean background of 2-3 fractures/metre) with only two restricted fractures (of around 40 fractures/metre) occurring at 215 m and 233 m respectively. Fracture filling phases along the section include hematite, Fe-oxyhydroxides, chlorite, calcite and epidote.

Hydrology.

The sampled section includes 24, 3 m long measured sections giving a range of hydraulic conductivity from 10^{-5} to 10^{-12} ms^{-1}. The two potential conducting zones, at 215 and 233 m, give conductivities of 1.6×10^{-5} ms^{-1} (213-216 m) and 9.7×10^{-9} ms^{-1} (231-233 m) respectively. Other zones include 6.7×10^{-6} ms^{-1} (207-210 m) and 4.0×10^{-6} ms^{-1} (222-225 m). The spinner survey identified maximum water inflow zones at 216 m and 218 m, and a calculated transmissivity of 2.5×10^{-5} m^{2}s^{-1} at 208-234 m.

Pumping prior to and during sampling (15 000 mL/min extraction rate) showed a steady decrease in salinity (4 800 to 3 310 mg/L Cl) and borehole activity water content (1.19 to 0.72%) over a period of 3 days. Other chemical parameters showed similar responses. This reflects the hydraulic properties of this section, i.e. high condctivity coupled with negative head, which appears to have been conducive to contamination from both saline (from higher levels?; see salinity log, Fig. 5.44) and borehole activity water. The three days pumping was adequate to remove all the tagged activity water but more pumping time was required to achieve stability of the other physico-chemical parameters.

Water Chemistry.

The groundwater (Table 5.10) has a pH of 7.6, is moderately saline (3 630 mg/L Cl) and alkaline (90 mg/L), has a significant TOC content (4.7 mg/L) and is Na-Ca(Mg):Cl-SO$_4$(HCO$_3$) in type. The alkalinity and TOC suggest a near-surface groundwater component.

Redox-sensitive Parameters.

That almost all the dissolved iron is in the ferrous state (Fe$_{(tot)}$ = 0.442; Fe$_{(II)}$ = 0.440 mg/L) and sulphide is present (0.17 mg/L) indicates reducing groundwater conditions; no redox potential measurements are available.

Isotope Geochemistry.

The stable isotope data plot well under the meteoric water line (Fig. 5.46). The radiocarbon data (41% pmc; i.e. an apparent age of 7 435 BP) and the tritium content are both significantly high (3.80 TU).

Uranium Geochemistry.

The low uranium content (0.39 µg/L) and the associated moderately high ^{234}U/^{238}U activity ratio (Table 5.10) point to reducing groundwater conditions and widespread isotopic disequilibrium from long residence times.

Summary.

The hydraulic and chemical parameters point to a groundwater which has resulted from the mixing of an older saline water with a significant amount of a young, near-surface derived component. This younger component is indicated particularly by the tritium content and the

groundwater chemistry, and by a higher percentage modern carbon content when compared to other Äspö groundwaters from a similar depth. The source of the younger component may be through a hydraulic connection between the EW-3 trending fracture zone and its intersection (at approx. 70 m) with the subvertical EW-5 zone (Fig. 5.36). The hydraulic connection has probably been increased (or may be caused) by the large extraction rate of the water at this level (15 000 mL/min). This is supported by the monitoring analyses (Fig. 5.12) carried out at 300-310 mL/min which recorded greater salinity than at the higher extraction rates.
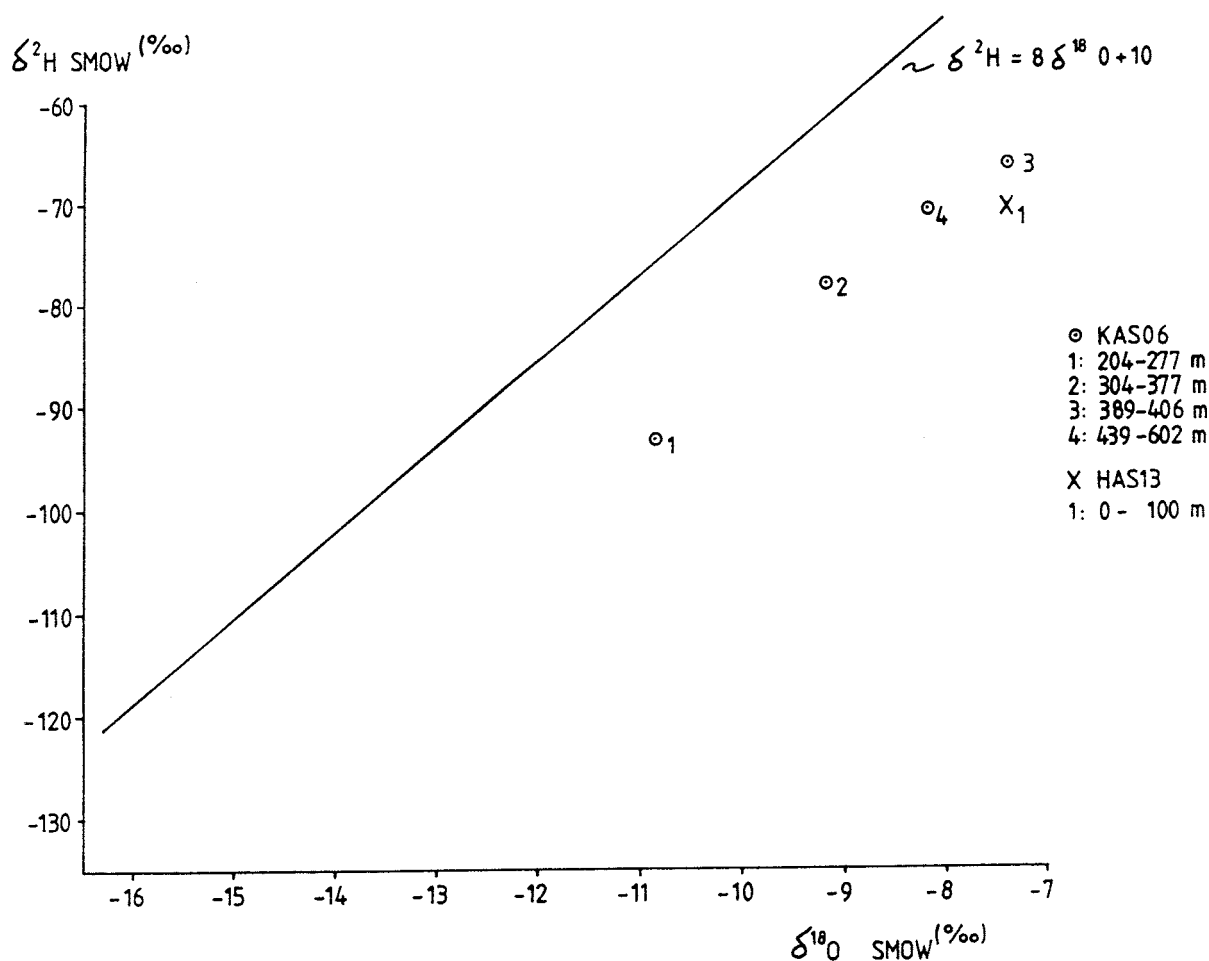
Figure 5.46. Stable isotope composition of borehole KAS06 groundwaters, Äspö.

5.4.2. Level 304-377 m.

This section lies completely within the diorites; three thin horizons of aplite (1-5 m) occur at 360-375 m and several greenstone bands (<1 m) occur throughout the section. The general background fracture frequency is around 2-3 fractures/metre with one marked zone (35 fractures/metre) which coincides with the contact between the diroite and the larger aplitic horizon at 360 m. Small bands of oxidised rock, some associated with sealed fractures (e.g. 327 m and 340 m), are also present. Fracture filling mineral phases are calcite, chlorite, hematite and minor Fe-oxyhydroxide.

Hydrology.

A total of 25, 3 m interval hydraulic tests, have been conducted within the selected borehole section giving a range of hydraulic conductivity from 10^{-6} to 10^{-12} ms^{-1}. In the near vicinity of 360 m, the location of the open fracture, the conductivity ranged from 8.5×10^{-7} to 6.8×10^{-6} ms^{-1} (354-360 m). Other similarly conductive sections occur at 324-327 m (1.9×10^{-6} ms^{-1}) and 363-366 m (2.5×10^{-6} ms^{-1}). Piezometric head values (Figs. 5.44 and 5.45c) are mostly around zero with small negative heads indicated at the 360 m fracture.

These data, comprising moderately high hydraulic conductivity coupled to a small negative piezometric head at the 360 m level, may have resulted in some contamination during borehole activities. However, with the exception of the first day, all monitored and measured parameters were stable for the duration of the pump test and sampling campaign, even bearing in mind the very large groundwater extraction rates (16 300 mL/min). Both the tritium and tagged activity water contents were low (0.30 TU and <0.05% uranine).

Water Chemistry.

Compared to the previous level, this groundwater (Table 5.10) has a similar pH (7.5), is less alkaline (49 mg/L HCO_3) and generally more saline (5680 mg/L Cl and 283 mg/L SO_4); TOC is now almost absent (0.1 mg/L). The water is Na-Ca(Mg) Cl-SO_4(HCO_3) in type and shows no large-scale mixing with any younger, near-surface component, as indicated in the previous level.

Redox-sensitive Parameters.

Iron is mostly present in the ferrous state; the sulphide content is very low (0.02 mg/L). In the absence of any redox potential measurements, only the iron can be relied upon to indicate that groundwater conditions are probably reducing.

Isotope Geochemistry.

The stable isotope data, in common with the previous level, plot well below the meteoric water line (Fig. 5.46). Radiocarbon data (19% pmc; apparent age of 13 280 BP) indicate a lack of any significant radiocarbon dilution from younger groundwater mixing. This is further supported by the very low tritium content (0.30 TU).

Uranium Geochemistry.

Uranium content (Table 5.11) is very low (0.22 µg/L) and the $^{234}U/^{238}U$ isotopic activity ratio is very high (6.0). This indicates very reducing conditions and long groundwater residence/reaction times in the bedrock.

Summary.

The hydraulics of the selected borehole section show small areas of moderately high conductivity with a near zero to small negative head character. There is no evidence of tagged activity water contamination nor of any mixing with a younger, near-surface derived component. This groundwater should therefore be regarded as representative for the level sampled.

5.4.3. Level 389-406 m.

This short section is completed contained within the diorites; there is little evidence of major fracturing or signs of alteration. The general fracture frequency is low (2-3 fractures/metre) and are both sealed (main filling minerals of chlorite and epidote) and open (chlorite and calcite with rare Fe-oxyhydroxide) types occur.

Hydrology.

Reflecting the competent nature of the drillcore, hydraulic testing along seven, 3 m sections (387-408 m), recorded generally low hydraulic conductivities (10^{-9} to 10^{-12} ms^{-1}); the one section with the highest conductivity (7.7x10^{-7} ms^{-1}) is located at the bottom margin of the packed-off section at 405-408 m. The spinner survey (Fig. 5.44) identified only one maximum water inflow point at 399 m; the 396-400 m section recorded a transmissivity of 1.7x10^{-5} m^{2}s^{-1}.

Bearing in mind the overall low hydraulic conductivity and short sampling length of the section, the high extraction rates used (15 000 mL/min) might conceivably result in groundwater short-circuiting around the packed-off section from the open borehole above, or from higher or lower bedrock sections. The very uniform chemistry of the groundwater, the absence of significant tagged activity water (<0.1%) after the first of the four day pump test, and the very low tritium content (0.60 TU), all point to either a representative groundwater from the level sampled, or, the mixing of water from this section with the previous level caused by an excess groundwater extraction rate.

Water Chemistry.

The groundwater chemistry (Table 5.10), as predicted from above, is very similar to the previous level apart from a small increase in salinity and perhaps a small but significant increase in alkalinity. It is suggested that this groundwater represents a mixture of slightly more deeper saline water (perhaps from the packed-off section itself), a slightly younger water (from the uppermost level at 204-277 m?), and the major component from the previous conducting level sampled at 304-377 m. Mixing has resulted from the short-

circuiting around the packed-off section from the open borehole above the packer where groundwaters from different sources have accumulated.

Redox-sensitive Parameters.

Because of the absence of redox potential measurements, no ferrous iron analyses and a very low sulphide content (0.01 mg/L), there is no direct evidence of the redoc character of the groundwater. It is assumed to be similarly reducing to the previous two sampled levels.

Isotopic Geochemistry.

The stable isotopes plot below the meteoric water line but are isotopically much heavier than all previous Äspö plots (Fig. 5.46). No radiocarbon data are available and the tritium content is low (0.60 TU).

Uranium Geochemistry.

The dissolved uranium content (Table 5.11) continues to be low (0.05 µg/L) and the $^{234}U/^{238}U$ activity ratio high (4.40).

Summary.

Considering the lack of fracturing coupled to the low hydraulic conductivity of the borehole section sampled, it is not too surprising that at the high groundwater extraction rates employed, mixing of groundwaters from differing bedrock levels has occurred by short-circuiting the packer system during the pump test. The main groundwater source appears to be from the previous conducting level at 304-377 m with minor near-surface amounts from higher levels (perhaps at 204-277 m) and a more saline component either from the 389-406 m section itself, or from hydraulic connections deeper in the bedrock via fracture zone EW-5$_w$ or from the open borehole under the lower packer.

5.4.4. Level 439-602 m.

Three rock types comprise this section; Småland granite (439-460 m), fine-grained granite/aplite (460-536 m) and greenstone (to 602 m). The portion from 439-475 m is highly tectonised (partly oxidised) with a background frequency of 2-11 fractures/metre and two concentrated zones at 440-450 m (up to 40 fractures/metre) and 460 m (also 40 fractures/metre). The remainder of the drillcore, apart from 500-510 m where another thin zone of 40 fractures/metre occurs, appears to be more competent with a fairly uniform background of 2-3 fractures/metre. A further small tectonised zone occurs at 550-560 m which is reflected in an increase to 10 fractures/metre.

Both sealed and open infilled fractures characterise the section; in the tectonised zones the sealed fractures are associated with mostly calcite, chlorite and more minor epidote, whilst the open fractures more commonly contain calcite, chlorite and Fe-oxyhydroxide (+/- hematite). In the non-tectonised remainder of the core the sealed fractures increasingly

contain more epidote at the expense of chlorite; a similar trend is observed in the open fractures.

Hydrology.

Hydraulic conductivities measured range from 10^{-5} to 10^{-12} ms^{-1} along the section. The highest conductivity (7.8×10^{-5} ms^{-1}) occurs at 459-462 m (corresponding to the fracture zone at 460 m) with other high areas at 438-447 m (1.4×10^{-7} to 1.2×10^{-6} ms^{-1}), corresponding to the zone at 440-450 m, and at 486-492 m (1.0-1.9×10^{-6} ms^{-1}) and 558-561 m (6.4×10^{-6} ms^{-1}), the latter corresponding to the zone at 550-560 m. The spinner survey identified a maximum water inflow zone at 448, 558 and 596 m, with measured transmissivities of 2.8×10^{-5} m^{2}s^{-1} and 5.1×10^{-6} m^{2}s^{-1} within sections 447-450 mand >557 m respectively. Piezometric head values all centre around zero.

The hydraulic properties of the borehole suggest that provided adequate air-lift flushing and presampling pumping is carried out, then no significant near-surface groundwater component or tagged activity water should remain. Furthermore, the length of the section and the moderate to high hydraulic conductivities should ensure that an adequate water resevoir is available even at the high extraction rates used (25 000 mL/min). This is supported by the monitoring analyses (Fig. 5.12) carried out one year later and at a much reduced extraction rate (280-310 mL/min); little difference in groundwater chemistry is observed (compare 5.10). Airlift tests carried out in KAS06 identified section 396-505 m as the most permeable part of the borehole.

The absence of tagged activity water during the 4 days of pumping support the above assumptions, but a significant tritium content (3.50 TU) indicates nevertheless that a young, near-surface component is still present even at these depths.

Water Chemistry.

The groundwater (Table 5.10) is only marginally more saline than the previous level; otherwise the chemistry is similar to the preceding two levels, i.e. Na-Ca(Mg) Cl-SO$_4$(HCO$_3$) in type.

Redox-sensitive Parameters.

No redox potential measurements are available and the sulphide content is very low (0.02 mg/L). However the dissolved iron shows that nearly all is in the ferrous state (Fe$_{(TOT)}$ = 0.631 mg/L and Fe$_{(II)}$ = 0.627 mg/L) which supports a reducing groundwater environment.

Isotopic Geochemistry.

The stable isotopic data show similar trends to the previous levels (Fig. 5.46). No radiocarbon data are available and tritium is present in significant quantities (3.50 TU).

Uranium Geochemistry.

In common with the other levels, uranium dissolution is low (0.07 µg/L) and the isotopic activity ratio is high (4.90), supporting a reducing groundwater environment and long bedrock residence/reaction times.

Summary.

Hydraulically this sampled profile overlaps with the most permeable section in the borehole at 396-505 m. Thus, even at the high groundwater extraction rate of 25 000 mL/min, there should be an adequate groundwater source from within the packed-off section to prevent any short-circuiting from the open borehole. However, the presence of tritium indicates that mixing is occurring with a younger water component, and the only access to such water is either from the open borehole above the upper packer (where younger water may have accumulated from higher levels) or there is a short-circuiting through the bedrock to higher levels. Unless a leaky packer has been used, the former explanation can be dismissed, particularly with regard to the previous level whereupon a hydraulic connection with the open borehole was postulated. In this case, and with the higher 304-377 m level, the tritium values were extremely low. This leaves the possibility of a bedrock connection. From Figure 5.43 the most conductive part of the 439-602 m section is associated with the subhorizontal EW-X zone (part of the overall major EW-5 fracture zone) which is in direct connection with zone EW-3:82°SE which continues to the bedrock surface. Hydraulic contact with the NNW-trending fracture zones is also possible.

5.4.5. Borehole summary and discussion.

Geological Setting.

Borehole KAS06 was drilled to investigate the bedrock geology, hydrogeology and hydrogeochemistry at and in the near vicinity of the subvertical EW-3:82°SE tectonic zone. The shallow-dipping EW-5 tectonic zone, less constrained and outcropping along the southern margin of Äspö, intersects EW-3 at approx. 50-350 m. The intersection of EW-3 with KAS06 is observed by increased fracture frequencies and crush zones at 60-75 m; intersection with EW-5 may account for weaker fracture frequency increases at 440-475 m, and possibly also at 220 m. Comprising part of EW-5 is the EW-5, hydraulically conductive zone, also demarcated by a high fracture frequency, which intersects KAS06 at approx. 390 m.

Hydraulic Character and Water Quality.

Against a general borehole background of low hydraulic conductivity (10^{-12} ms^{-1}), these fractured/crushed zones record conductivities of 10^{-7} to 10^{-5} ms^{-1}. The spinner survey identified conductive, maximum water flow zones which also corresponded to many of the above-mentioned fracture zones; hydraulic conductivity is shown to steadily decrease with depth. Calculated transmissivities at various levels in the boreholes are high (10^{-6} to 10^{-5} m^{2}s^{-1}) and the transmissivity for the whole borehole was determined to be 1.0×10^{-4} m^{2}s^{-1}.

Piezometric heads are normally around zero, the exception being a zone of fracturing at 200-250 m where marked negative heads were recorded.

Airlift testing of the borehole resulted in a similar order of transmissivity to those of pump tests (9.2×10^{-5} m^{2}s^{-1}); zone 396-505 m is considered to be the most permeable section of KAS06. Long-term pump tests showed a hydraulic connection between KAS06 with KAS02, HAS06, HAS07 and HAS13; this indicated that KAS06 has been drilled near to a major water-bearing zone extending in a probable NNE-SSW direction.

The salinity log (Fig. 5.44) shows an initial increase in salinity generally corresponding to the borehole intersection with zone EW-3 at 75-80 m; from here to the hole bottom there is only a slight increase in salinity.

The sampled groundwaters have in some cases a distinct younger component (<45 a) as shown by the tritium content in sections 204-277 m and 439-602 m which, incidently, are the most conductive in KAS06. Of the other two sections, level 304-377 m appears to illustrate the most representative groundwater with no younger component as indicated by a low percentage modern carbon content (19% pmc; an apparent radiocarbon age of 13 280 BP). This groundwater can be interpreted as being truly representive of the bedrock level at this depth, and therefore infers that there is no hydraulic connection with fractures that could access a young groundwater component. Level 389-406 m, because of its restricted length and low hydraulic conductivity, essentially represents the same water as that collected from level 304-377 m.

Chemical and Isotopic Features.

The groundwaters are generally Na-Ca(Mg) Cl-SO$_4$(HCO$_3$) in type throughout the borehole length sampled. Even so, some variation occurs with depth within this broad classification, and these are illustrated in Figures 5.47 to 5.50. In general, however, only the shallow sample differs significantly from the three deeper zones, with the exception of SO$_4$ which shows a systematic increase with depth.

In order to explain this relatively uniform chemistry, at least from around 300 m to a depth of 600 m, three hypotheses can be forwarded: a) that this is an active recharge area and the mixing of saline and non-saline groundwater is uniform to at least 600 m, b) that groundwater mixing is occurring within the EW-5 zone, which is tapping groundwaters from different origins over a large aerial extent of Äspö, so by the time EW-5 is intercepted by KAS06, the groundwater compositions are relatively homogeneous, and c) that during pump testing and sampling the extraction rates are so high that water is drawn into the borehole section from the nearby EW-3:82°SE zone via intersecting hydraulically conducting fractures from the EW-5 zone.

Of the three hypotheses presented above, the available data point to (c) as the best explanation to account for the younger groundwater component present in the collected samples. The groundwaters normally contained within the extent of the EW-5 zone (at this location from 50-400 m depth) appear to be meteoric, very old, moderately saline, and of long bedrock residence/reaction time. Against this background the drilling of KAS06 has subsequently intercepted discrete hydraulic fracture zones (particulary at levels 204-277 m
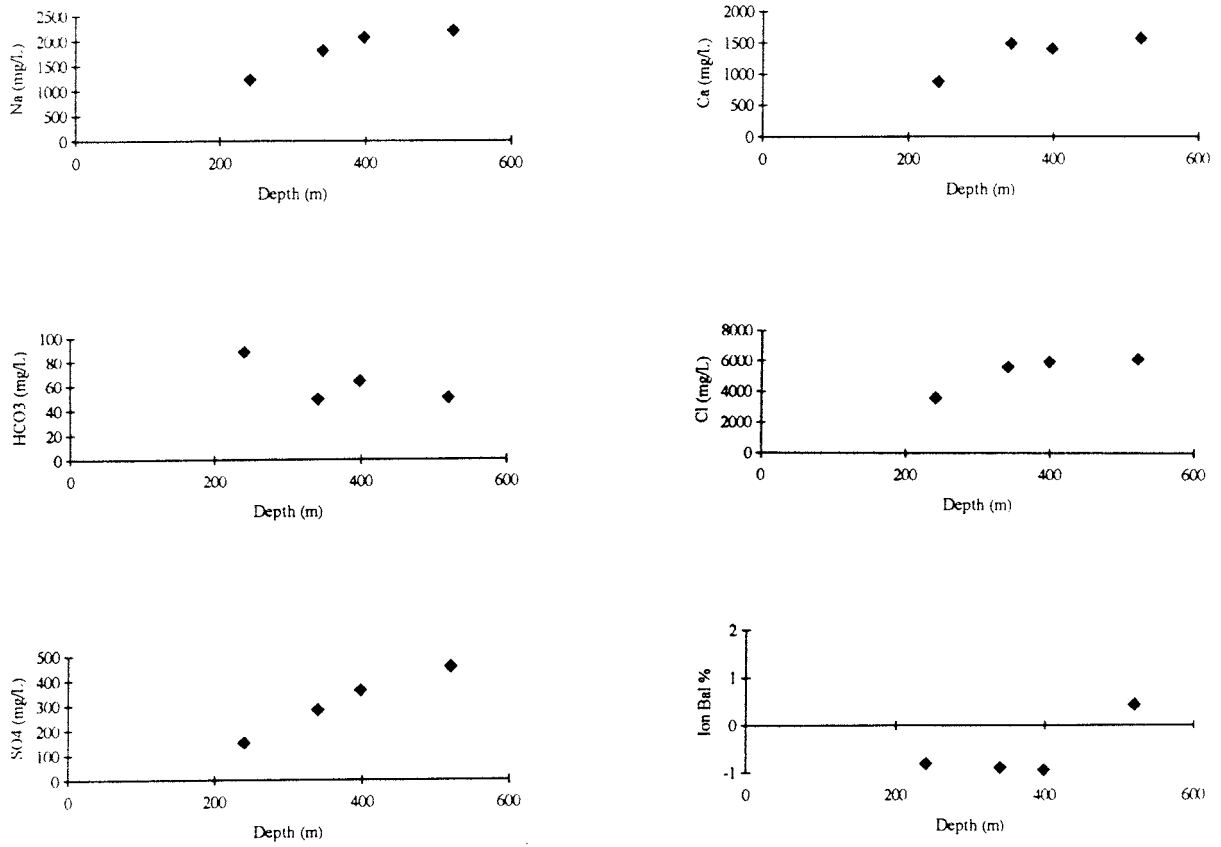
Figure 5.47. KAS06 groundwaters; major ion distributions and ionic charge balance.
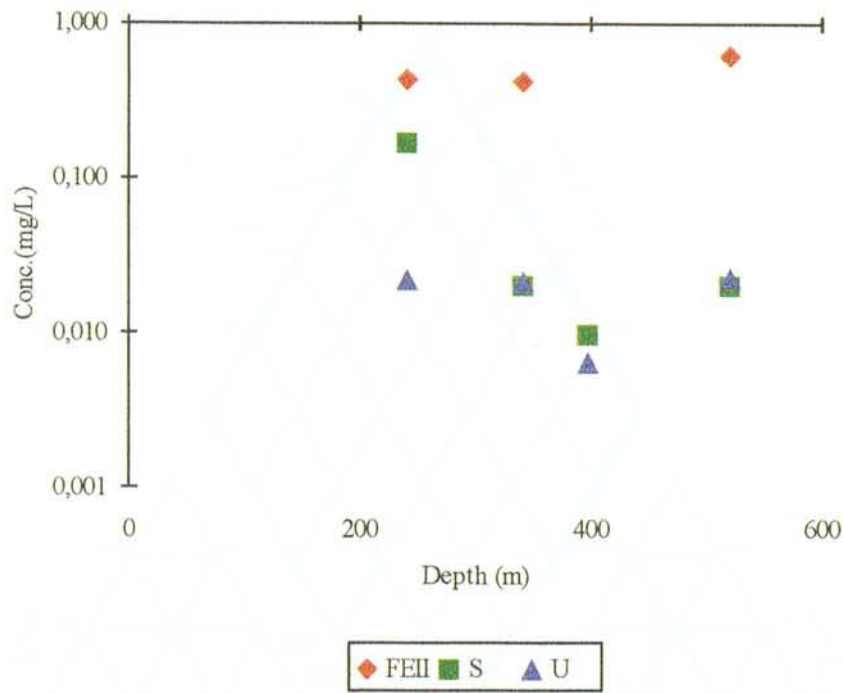
Figure 5.48. KAS06 groundwaters; distribution of selected redox-sensitive elements.
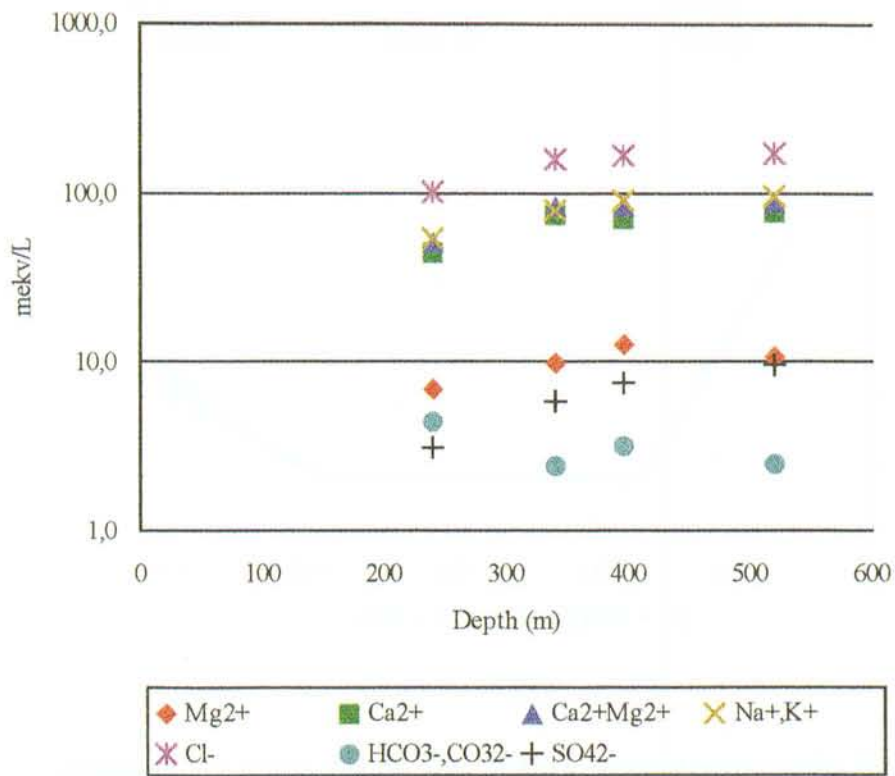
Figure 5.49. KAS06 groundwaters; Shoeller diagram showing the major ion distributions with depth.
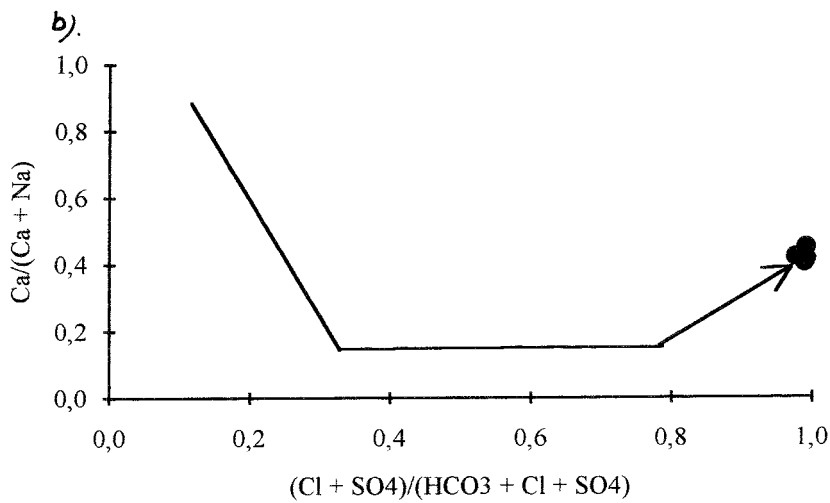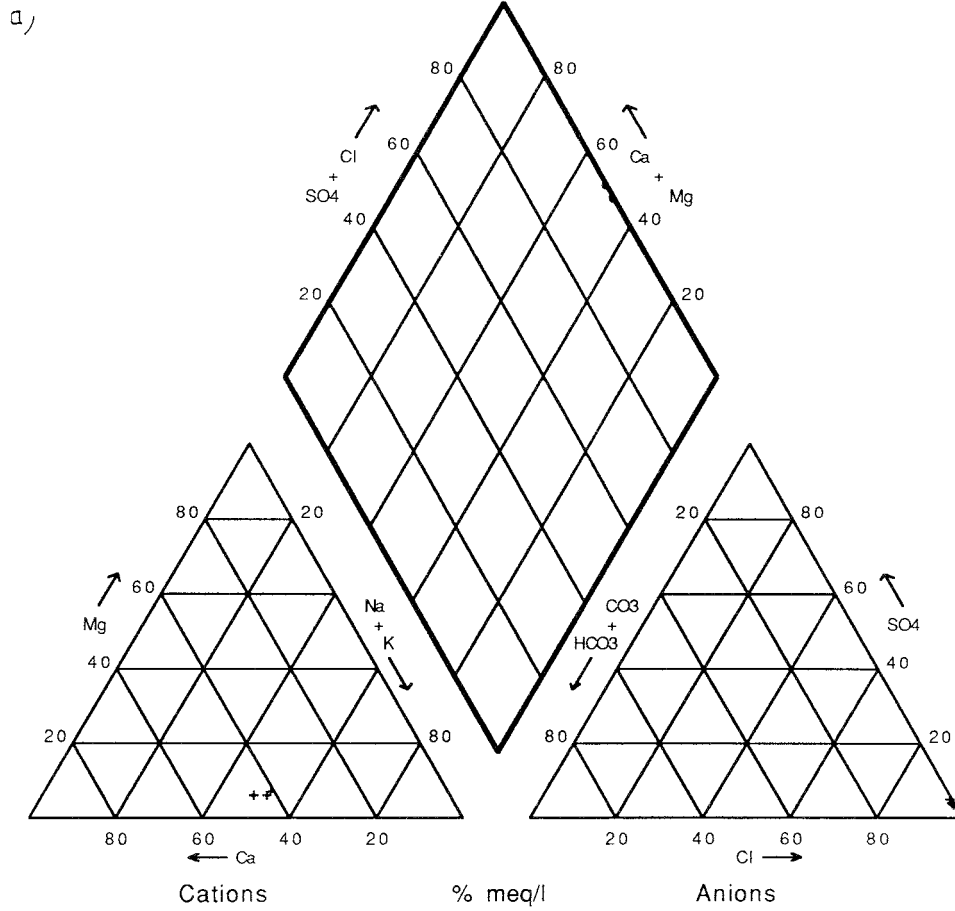
Figure 5.50. KAS06 groundwaters; a) Piper Plot of the major ion chemistry, and b) modified Piper Plot showing the position of the KAS06 groundwaters along an assumed chemical evolution path for average deep Swedish groundwaters in crystalline rock.

and 439-602 m) which characterise the EW-5 zone. During pump testing at high extraction rates these fractures, which also intersect the subvertical EW-3 zone to the north, have facilitated the short-circuiting of small amounts of younger, near-surface derived water from EW-3 to two of the packed-off borehole sections in KAS06. Mixing has taken place resulting in some dilution of the in situ saline groundwaters.

All the groundwaters are meteoric in origin, as determined from the stable isotope data, but are characterised by a much heavier isotopic composition than the other boreholes described above (with the exception of the upper level of KAS04). Shallow groundwaters (normally containing tritium) tend to be enriched in ^2H and ^{18}O relative to samples of older (tritium-free) water from greater depths. In general, these isotopic trends in KAS06 support the overall chemistry in suggesting that a major proportion of the groundwater is of a shallow meteoric origin with, in two cases, a significant young near-surface derived component.

Water/rock Interaction.

The percentage of the major rock types comprising borehole KAS06, the dominant host rock characterising each hydraulic zone(s) sampled for groundwater, and the identified macroscopic (and when available the microscopic) fracture mineral phases (from two data sources) in those hydraulic zone(s), are illustrated in Figure 5.51.

Comparing groundwater analyses of some of the more bedrock sensitive elements (Fig. 5.52a) with different bedrock compositional types (Figs. 5.51) shows no clear correlation for Mg, U, Ra and Th. The relationships between the groundwater and the fracture mineral phases using equilibrium calculations of the saturation indices are presented in Figures 5.53b and c. The positive indices indicate close to saturation or slight oversaturation for calcite, fluorite and quartz; calcite is reported as fracture mineral. The saturation index for gypsum is negative for the complete borehole reflecting the reported rarity of this mineral in the bedrock. Pyrite, which is oversaturated, is not reported as an important fracture mineral. Hematite and iron hydroxide are strongly undersaturated throughout the complete borehole. The hematite undersaturation does not reflect the amount of hematite observed in the borehole section (341, 521 m); on the other hand no hematite is reported in sections 341 and 398 m, which agrees with the calculated negative value. These Fe-mineral data should be treated with caution as already discussed for KAS02 in Section 5.1.8.

Groundwater Mixing Ratios.

Using the simple two component mixing model, the calculations show a high shallow water component input from around 70% in the uppermost zone to around 50% for the remaining sampled zones. This is supported by a seawater input as suggested from the calculated Br/Cl ratios (Fig. 5.53c), but not by the TOC which drops dramatically to near zero for the three deeper sampled sections (Fig. 5.53b), although this may be a dilution effect resulting from the long-term groundwater extraction rates. The unclear pCO_2 relationship (i.e. below 300 m higher values than atmospheric pressure) is probably due to the surface pH measurements.
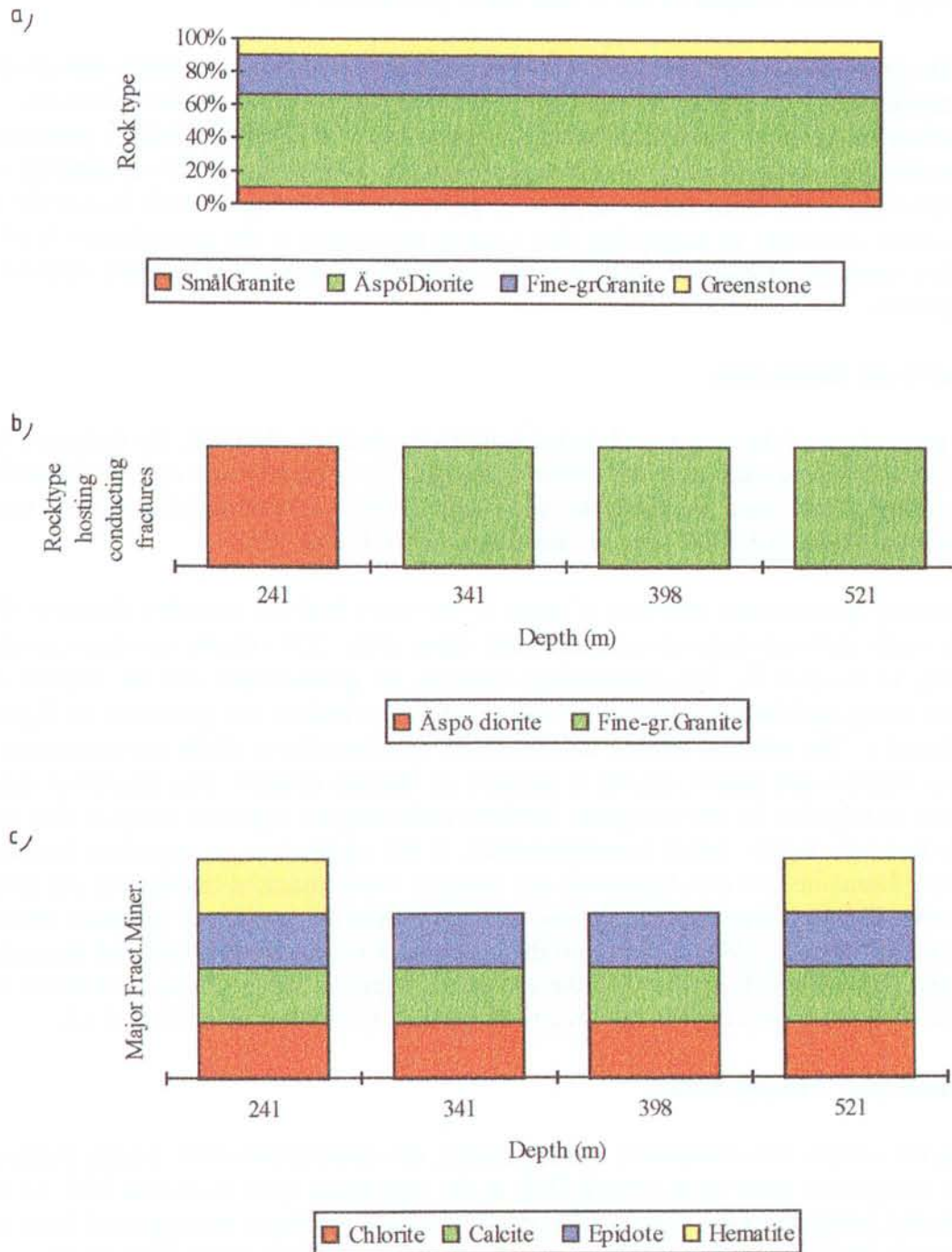
Figure. 5.51. Rock type and fracture mineralogy of KAS06: a) overview of the major
rock types (based on Stanfors, 1988), b) evaluation of probable rock type hosting
the fractures (based on Stanfors, 1988) and c) evaluation of the major fracture
minerals (based on Stråle, 1988 and Tullborg, 1989).
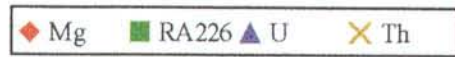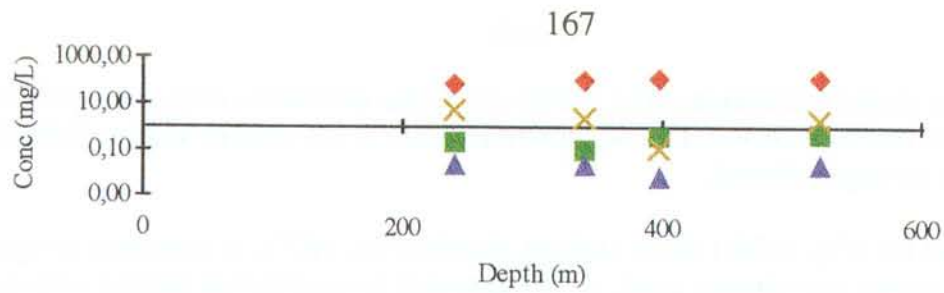
B
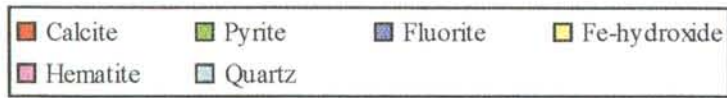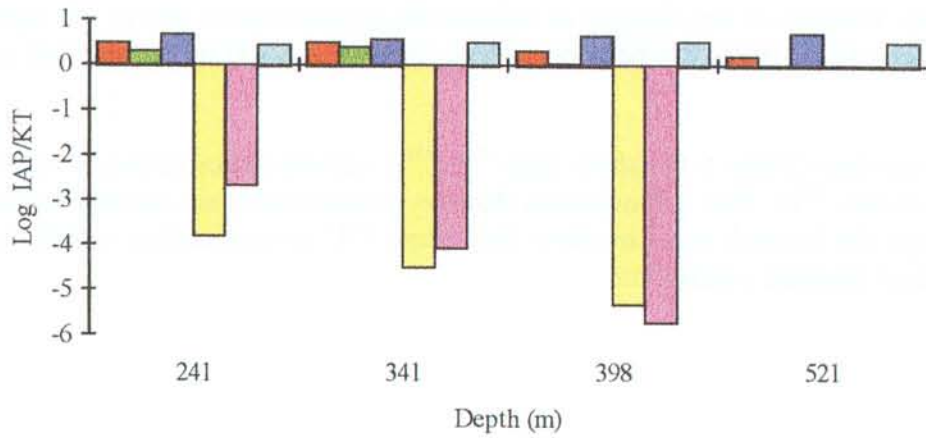
C
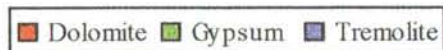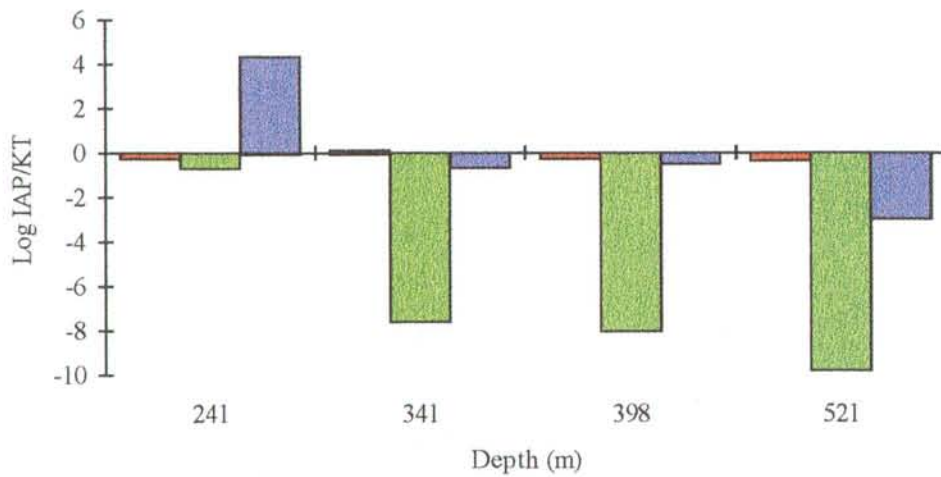
Figure 5.52. a) plotted concentrations of Mg, ^{226}Ra, U and Th measured in
groundwater, and b, c) results of equilibrium saturation index
calculations using PHREEQE (Parkhurst et al., 1980).

The Cl mixing model calculations (Fig. 5.54a) show that deviations from the equilibrium mixing line are due to increased Cl concentrations; only at the bottom section (439-602 m) is equilibrium mixing indicated.

K, Na, Mg and Ca (Fig. 5.54b) show uniform distributions, HCO_3 is somewhat irregular and only SO_4 shows any distinct trend, i.e. an approach to equilibrium mixing with depth (Fig. 54c).

Uranium Geochemistry.

Unfortunately, because of the absence of reliable Eh measurements due to the high extraction pump rates, it has not been possible to include KAS06 in the uranium solubility calculations.

Uranium series data (Table 5.11) show high $^{234}U/^{238}U$ activity ratios (2.6-6.0) caused by a build-up of excess ^{234}U. This demonstrates that the groundwaters are moving sufficiently slowly through the bedrock so as to allow the excess ^{234}U to accumulate, and thereby supporting near stagnant conditions.
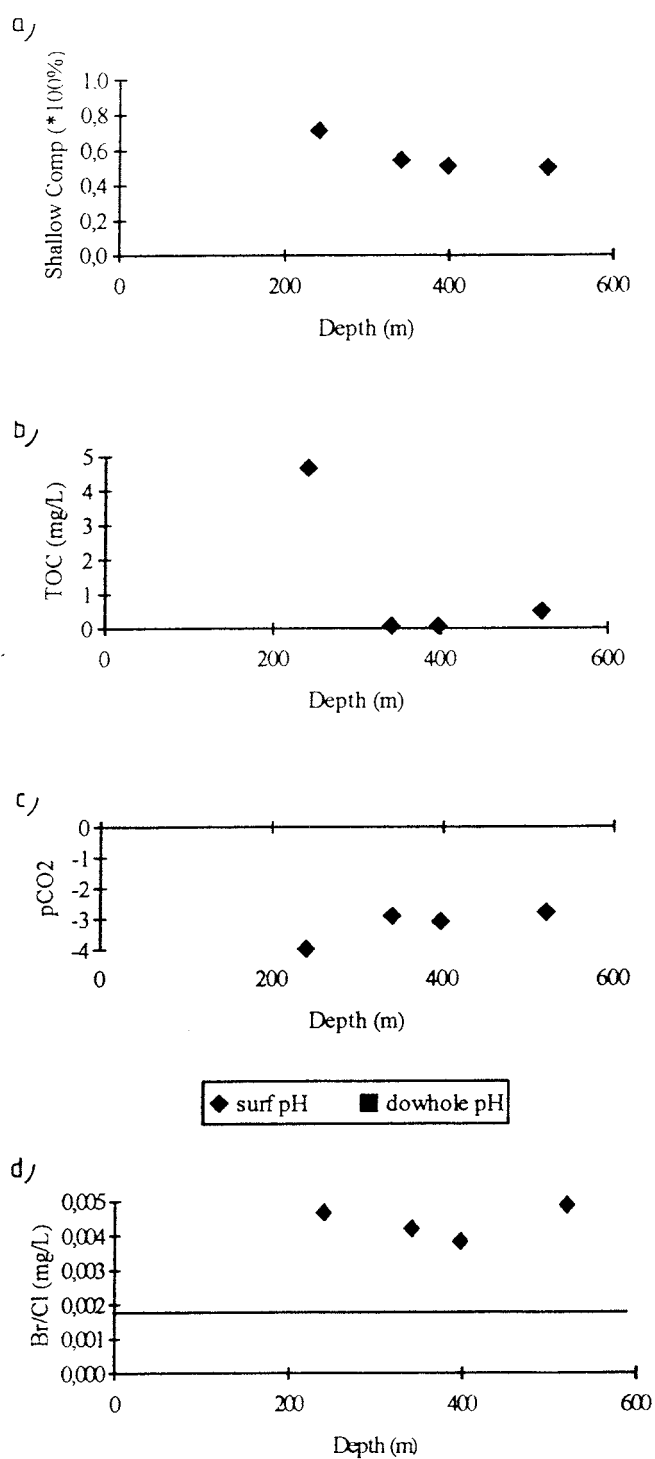
Figure 5.53. KAS06 groundwaters showing: a) calculation of the shallow water input
derived from a simple two component mixing model using Cl end members from
HAS05 and KAS03, b) TOC (total organic carbon) vs depth, c) calculated
pCO_3 pressures from downhole and surface (on-line) pH readings, and d) Br/Cl
ratio versus depth; the horizontal line represents the seawater Br/Cl ratio
(0.0031) for reference.
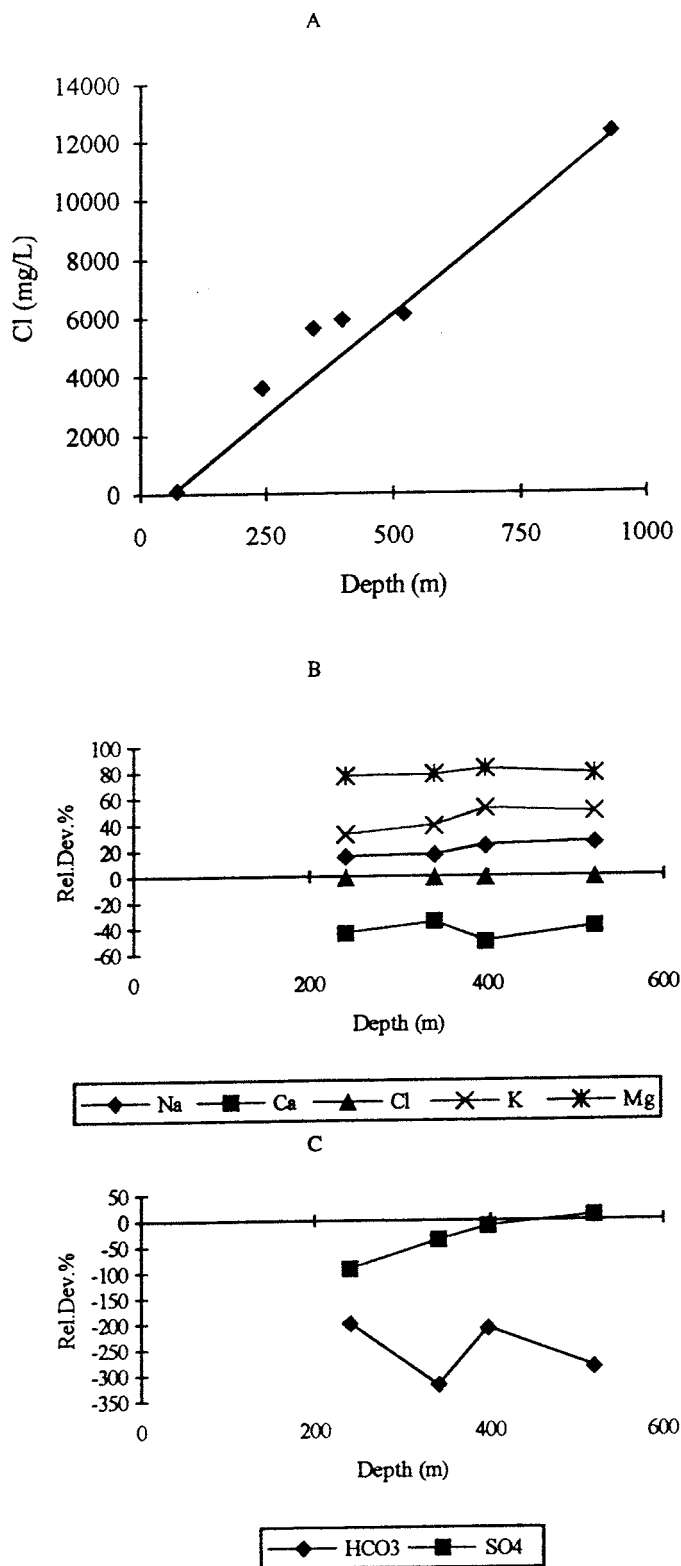
Figure 5.54. KAS06 groundwaters: a) plot of Cl vs depth related to the simple two component equilibrium mixing line, and b), c) depth trends of the major ions plotted as percentage relative deviation to the mixing model.

Table 5.10: Chemical analyses of groundwater samples from borehole KAS06, Äspö.

Borehole KAS06	KAS06	KAS06	KAS06	KAS06
Section m	204-277	304-377	389-406	439-602
Sampling method	SPT	SPT	SPT	SPT
Sample no.	1606	1610	1614	1618
Date Collected	890531	890607	890613	890621
W.flow ml/m	15000	16300	15000	25000
Drillingwater %	0.72	0.03	0.03	0.05
Cond.mS/m	1080	1680	1750	1810
Density g/ml	1.0001	1.0031	1.0034	1.0039
pH	7.6	7.5	7.3	7.3
Alkalinity (mg/l HCO_3)	89	49	64	50
Charge balance mequiv./l	-2.15	-3.63	-3.94	0.83
Rel. charge bal. error %	-1.01	-1.10	-1.12	0.22

Element		mg/l		
Na	1230	1820	2070	2200
K	7.4	9.1	11.7	11.1
Ca	893	1490	1410	1570
Mg	82	119	153	130
Sr	16.7	24.9	22.4	25.8
Mn	0.68	0.83	1.11	0.88
Li	0.39	0.66	0.55	0.74
Fe,tot	0.442	0.431	0.848	0.631
Fe(+II)	0.440	0.425	-	0.627
F	1.7	1.9	1.8	1.7
CL	3630	5680	5970	6150
Br	17	24	23	30
I	0.21	0.46	0.36	0.46
PO_4-P	0.003	0.005	0.005	0.004
SO_4	150	283	362	459
S_2	0.17	0.02	0.01	0.02
NO_3-N	0.01	0.01	0.01	0.01
NH_4-N	0.27	0.44	0.42	0.41
SiO_2-Si	5.8	6.1	5.8	5.8
TOC	4.7	0.1	0.1	0.5

Table 5.11: Uranium and isotopic analyses of groundwaters from borehole KAS06, Äspö.

Borehole	KAS06	KAS06	KAS06	KAS06
Section m	204-277	304-377	389-406	439-602
Sampling method	SPT	SPT	SPT	SPT
Sample no.	1606	1610	1614	1618
Date Collected	890531	890607	890614	890621
Percentage Modern Carbon (PMC)	41	19	-	-
^{14}C age BP	7435	13280	-	-
age BP corr.	-	-	-	-
^{238}U (mBq/kg)	9.90	5.70	6.80	5.8
^{235}U (mBq/kg)	0.32	0.28	0.35	0.41
^{234}U (mBq/kg)	26.1	34.6	29.6	28.5
U_{tot} (ug/kg)	0.39	0.22	0.27	0.23
$^{235}U/^{238}U$	0.030	0.050	0.050	0.070
$^{234}U/^{238}U$	2.60	6.00	4.40	4.90
^{18}O (SMOW)	-10.9	-9.2	-7.4	-8.2
^{2}H (SMOW)	-94.3	-77.8	-69.2	-70.8
^{3}H (Bq/l) [1]	< = 1	< 1	< 1	< 1
^{3}H (TU) [2]	3.80	0.30	0.60	3.5

[1] Kjeller, Norway
[2] IAEA, Wienna

Table 5.12: Monitoring analyses from levels 191-249 m and 431-500 m in borehole KAS06, Äspö.

Borehole	KAS06	KAS06	KAS06	KAS06	KAS06	KAS06
Section (m)	191-249	191-249	431-500	431-500	431-500	431-500
Sample no	1667	1688	1640	1656	1666	1687
Sampling method	MONIT.	MONIT.	MONIT.	MONIT.	MONIT.	MONIT.
Date Collected	900606	900613	900509	900528	900606	900613
W.flow ml/m	300	340	280	310	300	310
Drilling water %	0.33	0.26	0.12	0.24	0.14	0.07
Cond. mS/m	1430	-	-	-	1760	1690
pH	7.4	7.2	7.4	7.5	7.3	7.2
Alkalinity (mg/l HCO_3)	52.3	51.0	67.0	57.6	62.1	63.1
Charge Balance %	-2.31	-2.24	-2.21	-2.89	-2.16	-3.53

Element	mg/l		mg/l			
Na	1480	1470	2060	2060	2070	2020
K	-	11.0	-	-	-	12.6
Ca	1250	1240	1344	1380	1370	1320
Mg	111	109	152	140	144	145
Sr	22.1	22.2	21.9	22.9	22.5	21.8
Mn	0.97	0.97	1.06	0.97	0.99	0.97
Li	0.48	0.49	0.54	0.58	0.55	0.53
Fe(tot)	0.85	0.94	0.82	0.85	0.96	0.90
Cl	4890	4850	5970	6080	6000	6010
F	1.5	1.5	1.8	1.8	1.8	1.7
S(ICP)	63.5	65.00	124.00	130.00	127.00	128.00
SO_4^{2-}(calc)	191	195	372	390	381	384
SiO_2-Si	4.4	4.1	5.7	5.9	6.0	5.0

5.5. Borehole HAS13.

Little geological information exists for percussion borehole HAS13. It is located close to KAS06 (Fig. 5.56) and has been percussion drilled to a vertical depth of 100 m. At 50 m depth a major conductive water-bearing zone was breached. Airlift tests and a single hole pump test show that HAS13 has amongst the highest values of specific gravity measured at Äspö (0-50 m of 1.8×10^{-6} and 0-100 m of 2.1×10^{-5} Q/s/(m^{2}s^{-1})); the transmissivity was calculated to be 2.0×10^{-4} m^{2}s^{-1}.

Hydrology.

See above.

Water Chemistry.

The groundwater (Table 5.13) is saline (5070 mg/L Cl) with a pH of 7.3 and a moderately high alkalinity (132 mg/L HCO$_3$); TOC content is significant (1.7 mg/L). It is essentially Na-Ca:Cl-(SO$_4$-HCO$_3$) in type with a sizeable near-surface derived component.

Redox-sensitive Parameters.

Dissolved iron is high and all in the ferrous state (Fe$^{(tot)}$ = 2.730 mg/L; Fe$^{(II)}$ = 2.690 mg/L) and there is a virtual absence of sulphide. No redox potential measurements are available.

Isotope Geochemistry.

The stable isotope data show enrichment and plot below the meteoric water line (Fig. 5.46). Tritium is present in small amounts (1.20 TU); no radiocarbon data are available (Table 5.14).

Uranium Geochemistry.

The uranium content (Table 5.14) is very low (0.05 µg/L) and the ^{234}U/^{238}U activity ratio is high 3.5) which suggests a reducing groundwater environment and widespread isotopic disequilibriun caused by long groundwater bedrock residence/reaction times.

Summary.

Borehole section 0-100 m shows a groundwater which is strongly saline but has a significant younger, near-surface derived component (i.e. alkalinity and the presence of tritium). The water is largely reducing and long bedrock residence/reaction times are indicated by the very low uranium concentration and the high isotope activity ratio. The fact that there is only small amounts of tritium present, indicates that either the upper 50 m of bedrock is very "tight" (low conductivity). The water originates from the conducting 50 m level where there may also be some hydraulic contact with deeper conductive bedrock levels.

HAS 10

HAS 02
HAS 11
HAS 12

HAS 09

HAS 18

KAS 03

KAS 04
KAS 12

HAS 08
HAS 19

HAS 07

HAS 20
HAS 01
HAS 17

KAS 08

HAS 06

HAS 03
HAS 16

HAS 05

KAS 02 KAS 13

KAS 05 KAS 01
HAS 15

HAS 04
KAS 07

HAS 14

KAS 06

ÄSPÖ
HAS 13
KAS 14

TOP VIEW
KAS 11
KAS 09
KAS 10

0   100   200   300   400   500 (m)
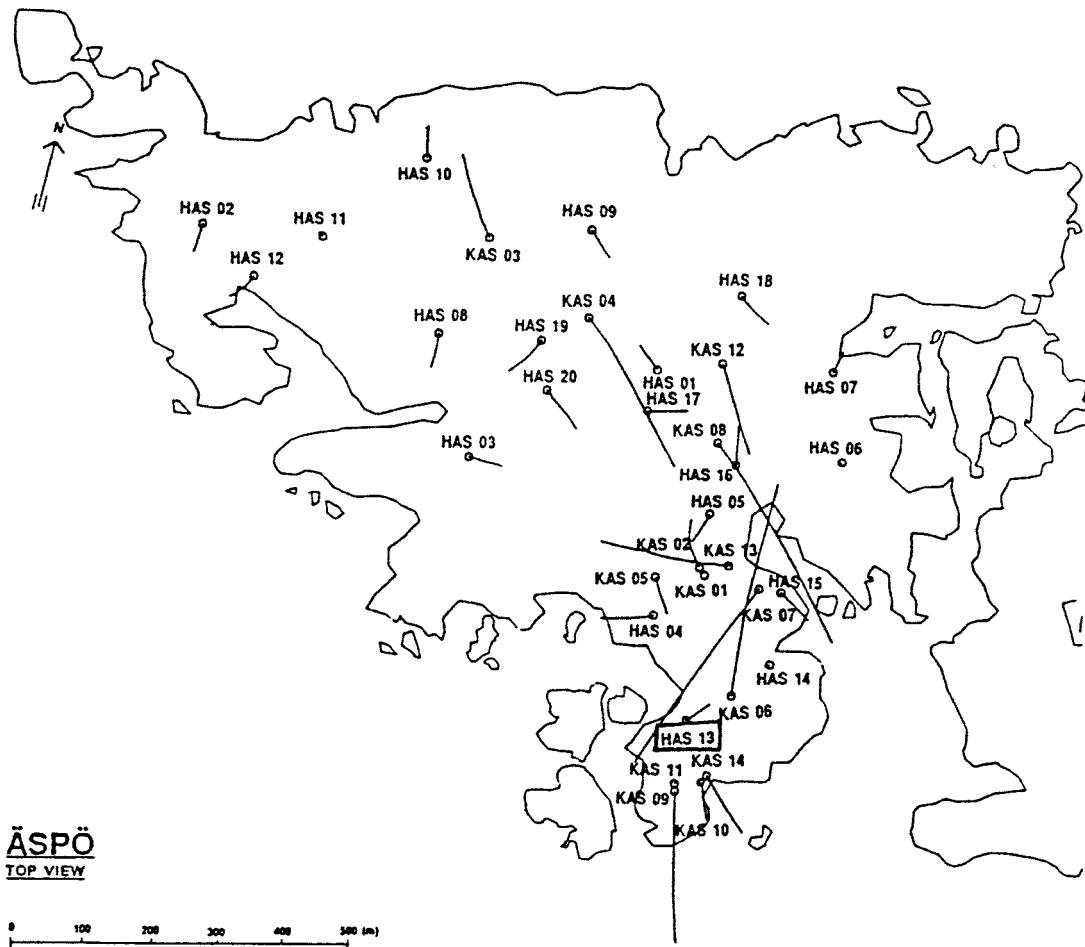
Figure 5.56. Location of borehole HAS13 (from Wikberg et al., 1991).

Table 5.13: Chemical analyses of groundwater samples from borehole HAS13, Äspö.

Borehole	HAS13
Section m	0-100
Sampling method	SPT
Sample no.	1622
Date Collected	890703
W.flow ml/m	115000
Drillingwater %	-
Cond.mS/m	1530
Density g/ml	1.0019
pH	7.3
Alkalinity (mg/l HCO_3)	132
Charge balance mequiv./l	4.23
Rel. charge bal. error %	1.41

Element	mg/l
Na	1880
K	32.8
Ca	1040
Mg	219
Sr	11.9
Mn	2.57
Li	0.26
Fe,tot	2.73
Fe(+II)	2.69
F	2.0
CL	5070
Br	37
I	4.3
PO_4-P	0.004
SO_4	136
S_2	<0.01
NO_2-N	-
NO_3-N	<0.01
NH_4-N	1.10
SiO_2-Si	5.0
TOC	1.7

Table 5.14: Uranium and isotopic analyses of groundwaters from borehole HAS13, Äspö.

Borehole	HAS13
Section m	0-100
Sampling method	SPT
Sample no.	1622
Date Collected	890703

Percentage Modern Carbon (PMC)	-
^{14}C age BP	-
age BP corr.	-
^{238}U (mBq/kg)	155
^{235}U (mBq/kg)	7.90
^{234}U (mBq/kg)	539
U_{tot} (ug/kg)	6.1
$^{235}U/^{238}U$	0.050
$^{234}U/^{238}U$	3.50
^{18}O (SMOW)	-7.2
^{2}H (SMOW)	-69.3
^{3}H (Bq/l) [1]	< 1
^{3}H (TU) [2]	1.20

[1] Kjeller, Norway
[2] IAEA, Wienna

5.6. Drilling and monitoring analyses.

During drilling, groundwater samples were taken for selected chemical analyses (L. Nilsson, 1989). Drilling was interrupted every 100 m, a single packer installed and water from a 100 m section was brought to the surface by air-lift pumping. Two or three samples were taken from each section; the first was collected after at least one section volume of water had been removed, the second when about 1.2 m^3 of water had been pumped out. The water was not filtered prior to analysis. The analyses are tabulated in Appendix 2.

When available, monitoring analyses from selected boreholes and section lengths have been incorporated into the various borehole descriptions presented above. The additional data from other boreholes have been used to help construct the groundwater flow conceptual model described in Section 6.5. Monitoring, in general, has been carried out after the pump tests, usually 12 to 18 months following hydrogeochemical characterisation. Since then the installed packer systems have remained in position, in all boreholes tested, until monitoring started, apart from being removed for minor repairs lasting for short periods of 1-2 days. In all cases low pump extraction rates were used (230-410 mL/min), which are in strong contrast to the pump-test extraction rates employed (4 000-25 000 mL/min; 115 000 mL/min for HAS13) for some of the hydrogeochemical characterisation described in this report. These monitoring data are tabulated in Appendix 3.

6. Evaluation, Summary and Discussion of the Results.

The results obtained from this hydrogeochemical study can be used for different purposes depending on the scale or degree of interpretation required. If the overall purpose is to describe the large-scale distribution of the major chemical constituents (i.e. the global approach), often very useful for general modelling requirements or as a back-up for hydrogeological interpretation, then the quality of data (i.e. analytical precision) need not be more than qualitative. If, however, the purpose of the exercise is to describe the natural undisturbed hydrogeochemical system, then carefully sampled representative groundwaters are a necessary prerequisite to obtain precise values for master variables such pH, Eh and the minor element concentrations, which form, for example the basis for radionuclide solubility and speciation modelling in assessing repository performance. The various levels of ambition can often be accomodated if proper planning of the borehole activities are carried out well in advance, so that unnecessary contamination and perturbance of the groundwater environment, prior and during sampling, can be avoided.

6.1 Quality of the groundwaters.

A large section of this report has been devoted to the detailed investigation of each individual zone hydraulically selected, tested and sampled for hydrogeochemical characterisation. The main objective was to establish the reliability or representativeness of each groundwater collected, in relation to the bedrock level sampled. Only by achieving a set of representative groundwater samples and hence a reliable set of chemical analyses, can some of the detailed hydrogeochemical studies be carried out. For example, the presented saline/non-saline mixing models are very much depth dependent, whilst the water rock interaction and chemical equilibrium modelling depend on precise pH and Eh input data, two variables which are very sensitive to borehole activities. Furthermore, for water rock interaction studies it is essential to know the rock type, fracture type and the fracture mineral infilling phases from the conductive fracture contributing most, if not all, the groundwater sampled. This is a very tedious and often impossible task (e.g. when a long borehole section is sampled) and underlines the need for strong interdisciplinary cooperation so that the correct positions of the borehole are sampled for rock, fracture mineral filling phases and groundwater.

The potential quality of the Äspö groundwaters has been discussed in Section 3.2, where the borehole activities for each of the boreholes KAS02, KAS03, KAS04 and KAS06 were examined in detail. Activities considered included drilling (i.e. the flushing fluids used), gas or air lift pumping, geophysical logging, hydraulic injection testing, spinner hydraulic surveys, interference pumping tests and groundwater extraction for hydrochemical characterisation and, more recently, tracer groundwater flow studies. The most serious contaminant is the introduction of large volumes of groundwater of differing chemistry and physico-chemical properties from sources other than the bedrock locality and depth being drilled. In practice these sources include shallow formational waters used for flushing during drilling and as the fluid injection medium for hydraulic testing. In both cases the waters are tagged using uranine so that any contamination can subsequently be readily detected during the hydrogeochemical studies. Other sources are groundwaters derived from shallower or deeper levels which have been transported to the depth of sampling by

short-circuiting through the bedrock fracture systems. Depending on the bedrock hydraulics, this can occur at low pump extraction rates, but is probably a greater problem at excessive extraction rates. Such waters can be traced if their chemistries differ substantially from the level being sampled, and sometimes by their isotopic signatures (e.g. tritium characterising a near-surface component).

The new modified core-drilling technique introduced at Äspö was expected to reduce the amount of drilling water usually lost to the highly conductive upper bedrock horizons. The objective of the system is to create a pressure draw-down in the borehole during drilling so that the formation water and drilling flushing fluids accumulating in the hole can be pumped readily to the surface carrying the various rock debris. Rapid removal of these components should prevent their penetration into the bedrock via conductive fracture zones. Furthermore, as the first 100 m of the hole is by air-flush percussion, the required air pressure is reasonably low and should not therefore unduly affect the bedrock chemistry. At 100 m depth the hole is temporarily cased and drilling by narrow (56 mm) rotary diamond core methods using water flushing then continues to the depth desired. This essentially was one of the recommendations that materialised from earlier evaluations of site-specific studies carried out during the last 10 years or so as part of the SKB radioactive waste programme (Smellie et al., 1985, 1987; Smellie and Wikberg, 1991).

In practice, however, at Äspö the first 100 m were drilled by rotary diamond core methods mainly to secure a drillcore profile, and this may have resulted in groundwater contamination in the upper part of the bedrock. However, the present drilling campaign (both percussion and rotary core methods and subsequent hydraulic tests) have shown that the upper approx. 100 m of bedrock in the northern part of Äspö appears to be "dry", i.e. not particularly conductive, and little flushing water should have therefore been lost to the bedrock. This is supported by the drilling logs which record little water loss. In the southern part of the island, however, the bedrock seems to be more conductive at these higher levels and groundwater contamination cannot therefore be totally ruled out.

Generally, the following sequence of borehole activities have been carried out at the Äspö sites subsequent to chemical sampling:

* borehole clearance using gas-lift pumping coupled with spinner surveys along the entire borehole

* pumping tests of the entire borehole

* geophysical logging of the entire borehole

* hydraulic injection tests along selected 3 and 30 m sections

* based on the above test results, specific conductive borehole sections were selected for transient interference tests, and dilution tests were performed on some boreholes sections

* groundwater sampling from isolated sections of approx. 3-10 m length

The sequence of activities from drilling to groundwater sampling are not always systematic; groundwater sampling (sometimes only limited to uranine monitoring of the flushing water contents) has been carried out at various occasions in association with drilling, borehole clearance and pump tests etc. (see Tables 3.1 and 3.2).

As referred to above, and discussed in detail by Smellie et al. (1985), borehole activities, when carried out prior to groundwater sampling, can have a detrimental effect on the water quality. Raising and lowering of geophysical probes results in groundwater perturbation, and injection testing, carried out by introducing clean formational water (i.e. from HAS05 in the northern part of Äspö; partly from HAS13 and KAS11 in the southern part) between two packers positioned 3 and 30 m apart respectively, can result in direct contamination. Contamination need not relate to major compositional changes of the groundwaters, but may mean introducing waters which have undergone pH and Eh changes through degassing and oxidation etc. This, however, relates mostly to the upper 100 m of bedrock where the introduced waters are derived from the same bedrock depth. At greater depths, where the groundwaters are highly saline, drilling and hydraulic testing effectively introduces a fresh, non-saline component into the most conductive zones intercepted by the boreholes.

Open hole effects may also contribute to a general mixing of groundwater types in the borehole; at Äspö the degree of mixing between non-saline and saline groundwaters has posed a major problem in interpretation. The degree of mixing will depend on the hydraulic properties of the borehole and on groundwater density variations.

Table 6.1 presents a classification of the Äspö groundwaters used in this present study. The groundwaters are classified as "representative" or "not representative" based on the presence or absence of tagged borehole activity water and tritium, and on the groundwater extraction pump rates used. In some borehole sections the extraction pump rate, chosen to conduct downhole hydraulic interference tests, was based on hydraulic rather than hydrogeochemical criteria. Consequently, and depending on the hydraulic properties of the interconnected conductive zones, groundwaters are being removed which are a mixture of waters from varying levels and origins in the bedrock. In addition, at high flow rates it is not possible to accurately measure important parameters such as the redox potential. For hydrogeochemical purposes, therefore, the lower the extraction rate the less perturbation of the system and therefore the closer one can approach the natural groundwater flow conditions.

A cursory glance at Table 6.1 reveals that most of the representative samples were, as expected, collected at low extraction rates (A), and the three not regarded as suitable (C) were mainly due to short-circuiting of borehole water from higher bedrock levels (e.g. at level 226-235 m in KAS04 this was corroborated by the presence of tritium and the general major ion chemistry). Short-circuiting has resulted from the choice of a borehole section of very low hydraulic conductivity, such that, even at the low extraction rates used (<200 mL/min), there was inadequate groundwater available from the packed off section.

Table 6.1: Classification of sampled groundwaters from Äspö.

Borehole /section (m)	Representative		Not Representative			
	A	B	C	D	E	F
KAS02						
202-214.5	x					
308-344	x					
314-319		x				
463-468			x			
530-535	x					
802-924		x				
860-924		x				
KAS03						
129-134	x					
196-223				x	x	
248-251		x				
347-374		x				
453-480				x	x	
609-623					x	
690-1002				x	x	
860-1002	x				x	
KAS04						
226-235			x			x
334-343	x					
440-481			x			
KAS06						
204-277				x		x
304-377	x					
389-406				x		
439-602				x		x
HAS13						
0-100				x		x

A= Representative groundwater for the sampled isolated level (Assumed limited sampling radius because of the low extraction pump rates: <200 mL/min).

B= Representative groundwater for the sampled isolated level (Assumed large sampling radius because of the high extraction pump rates: 1500 to 18800 mL/min).

C= Non-representative groundwater at low extraction pump rates.

D= Non-representative groundwater at high extraction pump rates.

E= Containing borehole activity water (>1% uranine).

F= Containing a young (<45 a) groundwater component (>2 TU).

Most of the non representative samples are a product of high extraction rates (D) coupled to either excess tagged activity water (E) or excess tritium (F). In reality, the presence of borehole activity water should also mean some anomalous tritium content. However, the chemistry of the Äspö shallow groundwaters, i.e. the source of the drilling water (e.g. HAS13), often records a very low tritium content (1.2 TU in HAS13), such that even small dilution effects will tend to mask any young water tritium component. Nevertheless, several representative groundwater samples resulting from high extraction rates have been reported (B). This shows that there are large conductive groundwater aquifers in the near vicinity of selected borehole sections which are sufficiently adequate (in terms of water volume), chemically homogeneous and also representative for a particular stratigraphic level or large-scale fracture zone, which are not directly hydraulically interconnected with excessively shallow or deep groundwater sources.

The correlation between high extraction rates and a non representative groundwater sample is of no great surprise at Äspö. From the hydraulic investigations several large-scale water conducting fractures control the groundwater flow through the island. Interference tests have shown the interconnection between these zones, some recharging (e.g. EW-1 and the NNW-trending vertical to subvertical fracture zones), some discharging (e.g. subvertical zone NE-2). High extraction rates, in some cases, will obviously force in groundwaters from shallow and/or deeper bedrock levels, depending on borehole location and which fracture zones are intercepted and the hydraulic properties of those zones.

Treated individually, the data presented in Table 6.1 may not appear too promising. However, from the detailed studies reported in Section 5, it is possible to know with reasonable certainty the origin of the groundwaters, at low extraction rates, that have been short circuited (e.g. type "C"). This has played an important role in establishing the levels of groundwater mixing and also in explaining some of the discrepancies (i.e. pH and Eh) in the water rock and chemical equilibrium modelling. At high extraction rates this detective work is more difficult, but nevertheless the major ion fluctuations have been extremely useful in helping to construct the conceptual groundwater flow model described and presented in Section 6.5.

Still, it is important to remember the difficulty in having to judge the quality of a sample. An anomalous value can indicate contamination, but depending on the initial concentration and the hydrogeochemical environment, the disturbance may have been nullified by natural chemical reactions in the bedrock prior to sampling. Of the many variables measured, elements at low concentration and particularly the redox sensitive values, tend to be the most sensitive to perturbations, whilst other variables show little change. A degree of uncertainty always hangs over samples collected for analysis; the only way to increase the level of reliability and confidence is to minimise any disturbance as much as possible to the natural groundwater system.

Table 6.1, therefore, should be regarded as an interpretative guide to any study which involves a groundwater medium, where different levels of accuracy are required. For example, colloidal, organic and microbial studies require a high degree of finesse with regard to origin, groundwater chemistry and transport pathways. In these cases, well defined sampling sections at low extraction rates are of paramount importance. For other studies, such as major ion geochemistry to support large-scale groundwater flow path

directions, all chemical information at both low and high extraction rates are important. Based on the above table, future programmes of study can be facilitated with regard to which sections are the most suitable for a specific set of requirements.

Groundwater quality: a semi-objective modelling approach.

As just described, Table 6.1 represents a simplified synthesis of water quality based on establishing and understanding the interplay between the many variables which can influence the quality of a sampled groundwater. This has been achieved, as this report shows, by being familiar with the analytical data and systematically approaching each borehole and borehole section in order to address the variables which can contribute to (and also identify) all the potential sources of groundwater contamination. A certain amount of subjectivity is sometimes necessary to judge how important certain variables are, and to predict their consequences. Experience in groundwater systems is an obvious prerequisite.

In order to try and base some of these evaluations mathematically, and thereby objectively, preliminary attempts are being made to apply a multivariant analytical approach to the problem (see Section 2.10). This forms part of a joint venture to try and integrate and classify hydrogeochemical systems in Sweden and Finland presently being investigated by SKB and TVO. No publishable results are yet available, but a working approach has been established; this is outlined in Table 6.2.

Table 6.2: Selected parameters to evaluate groundwater quality.

Quantitative Parameters	Semi-quantitative Parameters	Descriptive Parameters
Major/minor ions: HCO_3, Cl, Br, SO_4, PO_4, NH_4, Na, K, Ca, Mg etc.	**Pump rate.**	**Open hole effect.**
	Water budget: Drilling water, hydrotesting,	**Adjacent hole(s).**
Field measurements: pH, Eh, cond., temp., diss. O_2	open-hole effects	**On-going, nearby, site investigations.**
	Sampling methods:	
Redox-sensitive: $Fe_{(tot)}$, $Fe_{(II)}$, S, Mn, U.	1) downhole (in-situ Eh & pH) 2) surface (Eh, pH)	**Regional pump-tests.**
	3) during hydrotesting	**Drilling activities.**
Isotopes: ^2H, ^3H, ^{18}O, U-series.	4) open-hole tube tube sampler	**Groundwater**
	5) simplified, portable	**sampling**
Analytics: Ionic balance	sampler	
Drilling water: Uranine and iodide		

(after Laaksoharju, Lampén and Smellie).

In Table 6.2 three subdivisions have been recognised: quantitative, semi-quantitative and descriptive parameters. The quantitative and descriptive parameters are fairly straight forward, the former including those variables which are directly measureable, and the latter including those variables which are too complex to mathematically constrain. The semi-quantitative parameters, on the other hand, are those which may be addressed mathematically, for example, the sampling method can be allocated a number and, if the drilling and hydrotesting protocols are known and hydrogeology is well characterised, the water budget can be calculated for each borehole and each borehole section sampled. By combining the pump extraction rates with the hydrogeological data (if available), the local widespread effects of pumping may be semi-quantifiable on a local scale.

As an initial approach to groundwater quality evaluation, it would appear that the application of multivariant analyses to those measureable quantitative parameters (and any available semi-quantitative parameters), could potentially be very useful in differentiating between areas of analytical uncertainty, areas of gross chemical contamination and areas of promise, especially when confronted by considerable volumes of analytical data. Some scoping studies have already been attempted on data from Äspö and Olkiluoto in Finland. Ultimately, however, the final decision will have to be based on experience and being able to integrate all parameters (objective and subjective) to adequately describe the systems under investigation.

6.2. General hydrochemical characteristics and evolution of the groundwaters.

6.2.1 Hydrochemical Character.

Major trends.

The chemistry of the Äspö groundwaters (summarised in Tables 6.3 and 6.4 and Figs. 6.1 and 6.2) are shown to be mainly reducing (available Eh data record values of -240 to -300 mV; nearly all the total iron is in the ferrous state; sulphide is mostly present in small quantities from 0.02 to 1.10 mg/L; total dissolved uranium is very low ranging from 0.08-0.58 ug/L), moderately alkaline (pH from 7.3-8.3 units), and changing from a Na-Ca(Mg) HCO_3-Cl type at the near-surface (0-150m), through a Na-Ca(Mg) Cl-HCO_3 type at depths of 150-300 m, to a Na-Ca(Mg) Cl-SO_4 type at depths of 300-800 m, and finally the deepest, most saline waters are of Ca-Na(Mg) Cl-SO_4 type occurring from below approx. 800 m. This corresponds to the general classification of Laaksoharju (1990a) who identified four major classes based on the chloride composition: Class A from 0-100 m (Na-HCO_3) with 0-300 mg/L Cl, Class B from 100-150 m (Na-HCO_3-Cl) with 300-1000 mg/L, Class C from 100-500 m (Na-Ca-Cl) with 1000-6500 mg/L and Class D from 500-1000 m (Ca-Na-Cl) with 6500-13000 mg/L.

Laaksoharju (1990a) has also subdivided the major groundwater chemistry into three groups based on the influence of pH and Eh on the major ion behaviour. Increasing with depth are Cl, Br, Na, Ca, SO_4, Sr and Li, i.e. constituents which can be derived from water/rock interaction during long residence times in the bedrock (e.g. contributions from slowly dissolving minerals such as feldspar and increased exposure to ion-exchange processes). Decreasing are HCO_3, Mn, Mg, $Fe_{(tot)}$, $Fe_{(II)}$ and TOC, i.e. constituents influenced by reactions occurring in the soil cover and in the upper part of the bedrock where conditions are oxidising and the pH is low. Decreasing $Fe_{(tot)}$ and $Fe_{(II)}$ with depth can be caused by a pH increase resulting in oversaturation and precipitation of iron minerals in combination with changes in the overall redox system. Finally, those constituents which are considered more or less constant, include SiO_2, Al, K, F, PO_4, I, NO_2 and NO_3.

It is important, however, to bear in mind that the above depth-dependent subdivisions are only approximate; in reality highly saline groundwaters can be found within 50 m from the bedrock surface, whilst in other cases waters with a recognisable near-surface component can be detected at least down to 300 m. As presented in Section 6.5, the distribution of groundwater chemistry is very heterogeneous when Äspö is considered as a whole. If only the conducting fracture zones are considered, i.e. where the majority of water samples have been sampled, then the groundwaters tend to have more uniform compositions because they obtain their character through mixing along fairly rapid conductive flow paths, i.e. mainly determined by the hydraulic gradient, rather than by chemical rock/water interaction. Thus, in the knowledge that most of the samples have been taken from water conducting fractures, the above general subdivisions are broadly true.

The changes of groundwater chemistry with depth are further illustrated in the trilinear Piper Plot (Fig. 6.1) which shows some kind of "evolutionary" path from fresh/brackish
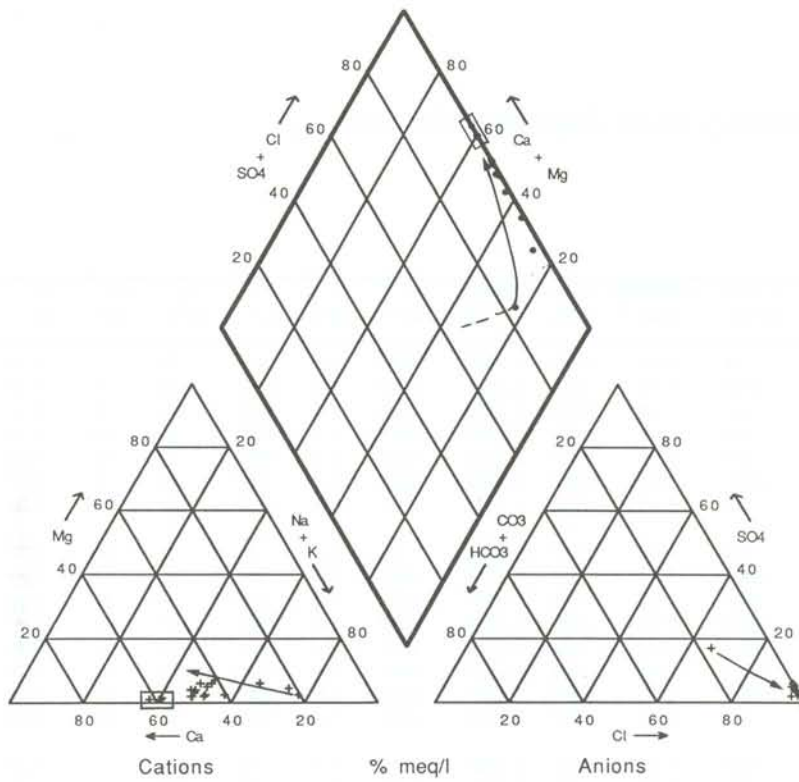
Figure 6.1. Piper plot showing the main groundwater compositions from Äspö.
(Arrow represents evolutionary paths; deep saline waters are boxed).
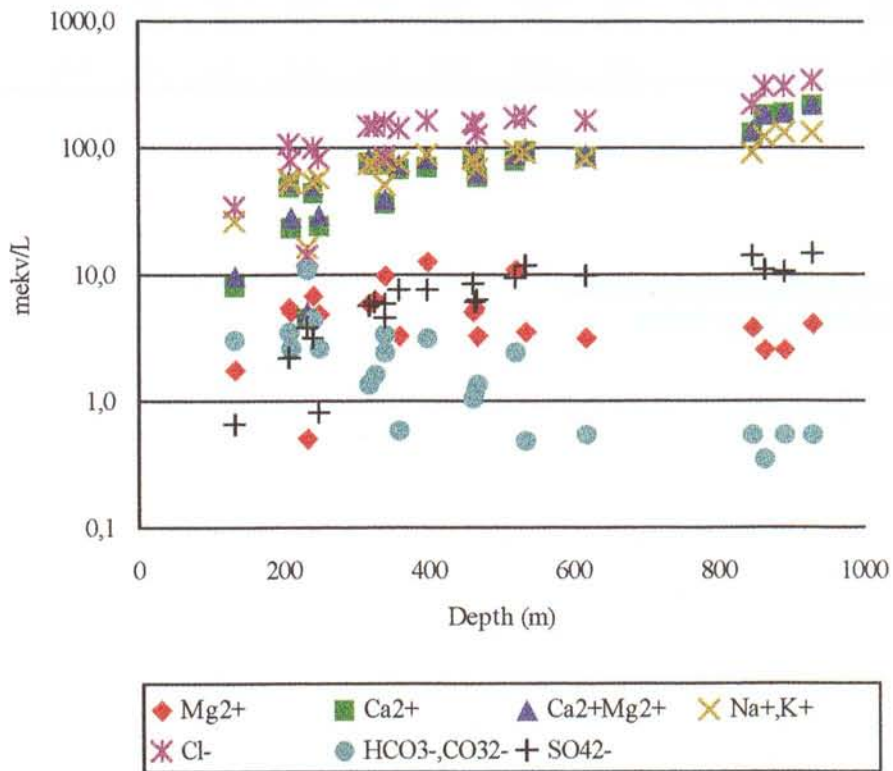
Figure 6.2. Modified Shoeller plot showing major ion trends with depth.

Table 6.3: Chemistry of the Äspö groundwaters.

Borehole /section (m)	Sampling method	W.flow ml/min	Drilling-water %	Cond. mS/m	Density g/ml	Na mg/l	K mg/l	Ca mg/l	Mg mg/l	Sr mg/l	Mn mg/l	Li mg/l	Fe,tot mg/l	Fe(+II) mg/l
KAS02 /202-214.5	CCC	61	0.80	1060	1.0006	1300	6.6	980	68		0.91	0.38	0.502	0.483
KAS02 /308-344	SPT	5000	0.70	1510	1.0029	1720	8.8	1480	75	27	0.94	0.55	0.715	0.622
KAS02 /314-319	CCC	180	0.60	1580	1.0034	1700	9.0	1540	75	26	0.80	0.56	0.794	0.788
KAS02 /463-468	CCC	160	0.40	1630	1.0036	1800	8.2	1570	66	30	0.70	0.80	0.507	0.505
KAS02 /530-535	CCC	117	0.30	1890	1.0046	2100	8.1	1890	42	35	0.29	1.00	0.228	0.226
KAS02 /802-924	SPT	15200	0.20	2910	1.0098	2800	11.7	3690	39	61	0.28	1.80	0.027	0.023
KAS02 /860-924	CCC	130	0.22	2970	1.0103	3000	10.9	3830	30		0.23	1.80	0.051	0.049
KAS03 /129-134	CCC	120	0.07	450	0.9979	600	2.4	162	20	3.3	0.10	0.13	0.120	0.120
KAS03 /196-223	SPT	10000	2.70	910	0.9998	1200	6.3	480	60	10	0.39	0.28	-	-
KAS03 /248-251	SPT	4000	1.00	930	0.9998	1300	6.6	500	54	10	0.35	0.30	0.290	0.288
KAS03 /347-374	SPT	18000	0.80	1370	1.0028	1730	6.3	1400	45	26	0.27	0.63	0.200	-
KAS03 /453-480	SPT	16000	2.10	1400	1.0021	1710	6.2	1200	40	21	0.27	0.61	0.196	0.194
KAS03 /609-623	SPT	18800	2.20	1700	1.0036	2000	6.3	1740	39	28	0.24	0.73	0.072	0.068
KAS03/690-1002	SPT	13000	2.60	2260	1.0066	2130	6.6	2660	63	44	0.23	0.83	0.065	0.059
KAS03/860-1002	CCC	120	0.15	3380	1.0118	3050	7.3	4400	50	75	0.20	1.65	0.075	0.075
KAS04 /226-235	CCC	100	0.16	260	0.9967	400	2.4	95	6.8		0.06	0.09	0.040	0.040
KAS04 /334-343	CCC	100	0.55	1030	0.9999	1180	6.1	750	30	13	0.30	0.40	0.315	0.315
KAS04 /440-481	CCC	95	0.06	1830	1.0036	2000	7.8	1700	60	29	0.44	0.95	0.260	0.260
KAS06 /204-277	SPT	15000	0.72	1080	1.0001	1130	6.9	809	72	15	0.60	0.37	0.442	0.440
KAS06 /304-377	SPT	16300	0.03	1680	1.0031	1850	9.0	1490	119	25	0.85	0.66	0.430	0.425
KAS06 /389-406	SPT	15000	0.03	1750	1.0034	2060	11.8	1410	153	22	1.10	0.55	0.850	
KAS06 /439-602	SPT	25000	0.05	1810	1.0039	2200	11.1	1560	130	26	0.87	0.74	0.631	0.627
HAS13 / 0-100	SPT	115000	-	1530	1.0019	1880	32.8	1040	219	12	2.55	0.26	2.73	2.69

CCC = Complete Chemical Characterisation
SPT = Sampled during Pump Testing

Table 6.3 (contd.): Chemistry of the Äspö groundwaters.

Borehole /section (m)	HCO$_3$ mg/l	F mg/l	Cl mg/l	Br mg/l	I mg/l	PO$_4$-P mg/l	SO$_4$ mg/l	S^{2-} mg/l	NO$_2$-N mg/l	NO$_3$-N mg/l	NH$_4$-N mg/l	SiO$_2$-Si mg/l	pH	E$_h$ mV	TOC mg/l
KAS02 /202-214.5	71.0	1.3	3840	14	0.30	<0.01	108	0.50	<0.001	<0.01	0.40	6.0	7.4	-260	6.0
KAS02 /308-344	32.7	1.3	5300	29	0.33	0.007	290	0.16	0.001	0.01	0.37	4.3	7.6		2.0
KAS02 /314-319	26.6	1.3	5340	23	0.33	0.002	270	<0.01			0.26	2.0	8.2		2.4
KAS02 /463-468	25.6	1.4	5450	28	0.32	0.004	290	0.13			0.22	3.3	8.3	-300	3.0
KAS02 /530-535	10.4	1.6	6370	42	-	0.003	550	0.18			0.03	4.1	8.3	-300	1.0
KAS02 /802-924	7.1	1.6	11000	78	0.76	<0.002	522	0.01	0.001	0.01	0.01	4.3	8.2		0.5
KAS02 /860-924	11.0	1.7	11100	74	0.69	<0.02	520	0.72	<0.001	<0.01	0.01	4.0	8.5	-320	<0.5
KAS03 /129-134	61.3	2.1	1230	5	0.10	0.002	32	0.70	0.001	0.01	0.04	4.8	8.0	-270	2.0
KAS03 /196-223	60.0	1.8	2900	27	0.41	0.003	31	0.05			-	4.6	7.7		1.0
KAS03 /248-251	53.0	1.8	3000	18	0.36	0.003	40	0.17			0.09	4.4	7.8		0.5
KAS03 /347-374	12.0	1.6	5180	30	0.43	<0.002	340	0.05			-	4.2	7.8		0.5
KAS03 /453-480	27.0	1.5	4600	28	0.42	0.005	300	0.11			0.07	4.1	7.8		0.5
KAS03 /609-623	11.2	1.5	5880	46	0.05	0.006	470	0.10			0.05	3.9	8.0		1.1
KAS03/690-1002	11.0	1.6	8100	51	0.65	0.004	680	0.10			0.05	3.9	8.0		0.5
KAS03/860-1002	10.6	1.6	12300	85	0.70	0.002	720	1.10	0.001	0.01	0.01	4.2	8.0	-250	0.5
KAS04 /226-235	215.0	4.0	530	3	0.07	0.004	180	1.10	<0.001	<0.01	0.01	4.9	8.2	-300	6.9
KAS04 /334-343	70.0	2.6	3030	15	0.16	0.005	210	0.40	0.001	0.01	0.10	4.1	7.9	-270	5.3
KAS04 /440-481	20.6	1.5	5900	26	0.44	<0.002	410	0.60	<0.001	<0.01	0.05	5.0	8.0	-280	1.3
KAS06 /204-277	90.0	1.7	3630	17	0.21	0.003	150	0.17		0.01	0.30	5.8	7.6		4.7
KAS06 /304-377	49.0	1.6	5680	24	0.46	0.005	283	0.02		0.01	0.40	6.1	7.5		0.1
KAS06 /389-406	64.0	1.8	5970	23	0.36	0.005	362	0.01		0.01	0.40	5.8	7.3		0.1
KAS06 /439-602	50.0	1.8	6150	30	0.46	0.004	459	0.02		0.01	0.40	5.8	7.3		0.5
HAS13 / 0-100	132.0	2.0	5070	37	4.30	0.004	136	<0.01		<0.01	1.10	5.0	7.3		1.7

Table 6.4: Uranium and isotopic analyses of the Äspö groundwaters.

Borehole /section (m)	^{14}C age BP	^{14}C age BP corr	^{238}U mBq/kg	^{235}U mBq/kg	^{234}U mBq/kg	U_{Tot} ug/l	$^{235}U/^{238}U$	$^{234}U/^{238}U$	^{18}O SMOW	^{2}H SMOW	^{3}H (Bq/l) Kjeller	^{3}H (TU) IAEA Wienna	Average temp. °C borehole sond
KAS02 /202-214.5	10435		3.78	0.24	43.2	0.15	0.07	3.86	-13.9	-108.9	< 1	0.30	
KAS02 /308-344			3.87	0.28	15.9	0.15	0.07	4.11	-12.7	-99.8	< 1		
KAS02 /314-319	12670	12960	8.52	1.0	26.1	0.34	-	3.06	-12.3	-100.6	~ 1		12.4
KAS02 /463-468	13910	13960	8.10	0.50	24.2	0.32	-	2.99	-12.8	-99.9	~ 1		15.5
KAS02 /530-535			3.19	0.50	10.4	0.13	-	3.25	-12.3	-97.2	~ 1		15.2
KAS02 /802-924			18.2	0.89	57.5	0.64	0.05	3.16	-13.0	-96.8	~ 1		
KAS02 /860-924			13.6	0.90	17.2	0.54	0.07	3.16	-13.1	-96.8	~ 1	0.20	
KAS03 /129-134	31365		3.76	0.26	17.2	0.15	0.07	4.56	-15.8	-124.8	< 1	0.10	10.2
KAS03 /196-223	21695	21880	4.89	1.50	17.3	0.19	-	3.54	-14.6	-115.3	~ 1		
KAS03 /248-251	20090	20245	12.4	1.79	52.6	0.49	0.14	4.23	-14.5	-118.1	~ 1		
KAS03 /347-374			2.05	0.30	6.2	0.08	-	3.00	-13.3	-104.9	< 1		
KAS03 /453-480			9.06	0.40	26.3	0.36	0.05	2.90	-13.6	-109.6	< 1		
KAS03 /609-623			3.84	0.29	12.8	0.15	0.08	3.34	-13.3	-103.4	~ 1		
KAS03/690-1002			14.8	2.03	71.2	0.58	0.14	4.83	-13.0	-99.7	~ 1		
KAS03/860-1002			3.27	0.82	20.7	0.13	0.25	6.30	-12.7	-96.4	< 1	0.40	
KAS04 /226-235	7795		11.7	1.6	60.0	0.46	0.14	5.10	-11.0	-84.8	< 1	4.3	10.8
KAS04 /334-343			7.3	0.98	33.9	0.29	0.13	4.60	-13.0	-99.6	< 1	0.50	12.1
KAS04 /440-481			685	180	4950	27.0	0.26	7.20	-11.9	-92.3	< 1	0.03	13.3
KAS06 /204-277	7435		9.9	0.32	26.1	0.39	0.03	2.60	-10.9	-94.3	<= 1	3.8	
KAS06 /304-377	13280		5.7	0.28	34.6	0.22	0.05	6.00	-9.2	-77.8	< 1	0.30	
KAS06 /389-406			6.8	0.35	29.6	0.27	0.05	4.40	-7.4	-69.2	< 1	0.60	
KAS06 /439-602			5.8	0.41	28.5	0.23	0.07	4.90	-8.2	-70.8	< 1	3.5	
BAS13 / 0-100			155	7.90	539	6.11	0.05	3.50	-7.2	-69.3	< 1	1.2	

water to more marine mixed types; the highly saline waters plot in a separate group. These trends are also reflected in Figure 6.2, where once again the highly saline types show a clear distinction from the shallow and mixed varieties. The predominance of highly evolved or mixed groundwater types at Äspö, related to an assumed evolutionary path for average Swedish groundwaters from crystalline bedrock, is illustrated in Figure 6.3. Similarities to these general groundwater patterns from Äspö have been described from two localities in Finland; from Hästholmen (Nordstrom, 1986) and more recently from Olkiluoto (Pitkänen et al., 1992).
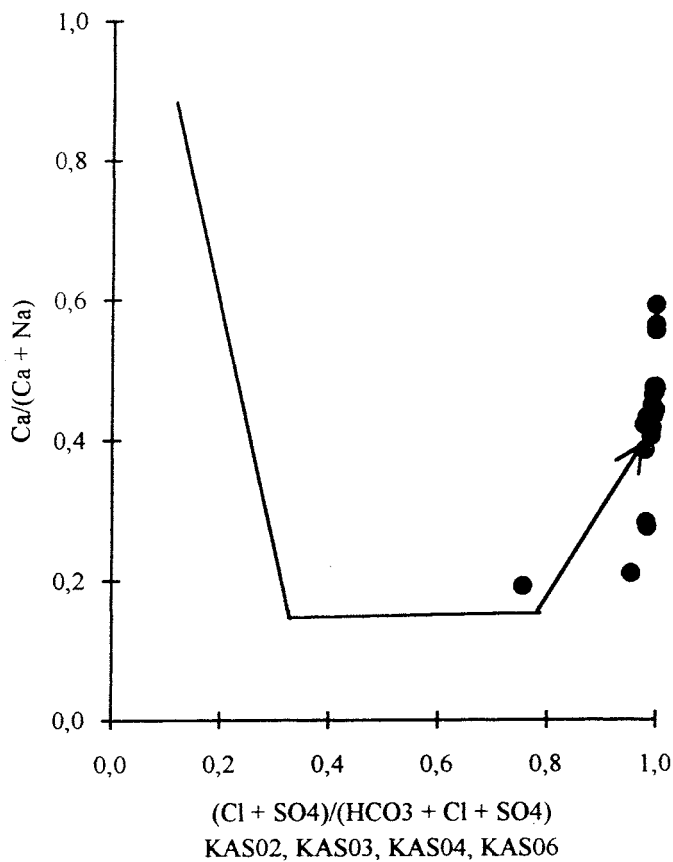
Figure 6.3. Distribution of Äspö groundwaters along an assumed evolution line for Swedish groundwaters in crystalline rock.

General redox conditions and the geochemical behaviour of uranium.

The redox character of the Äspö groundwaters is discussed in detail in Section 6.3 which centres around the recharging EW-1 shear zone. The near-surface (0-100 m) redox system is presently being investigated as part of the "redox zone project" (Barnwart et al., 1992). Presented here is the distribution of the in situ measured Eh and pH values for the Äspö groundwaters as a whole (Figs. 6.4 and 6.5); in both cases downhole and surface
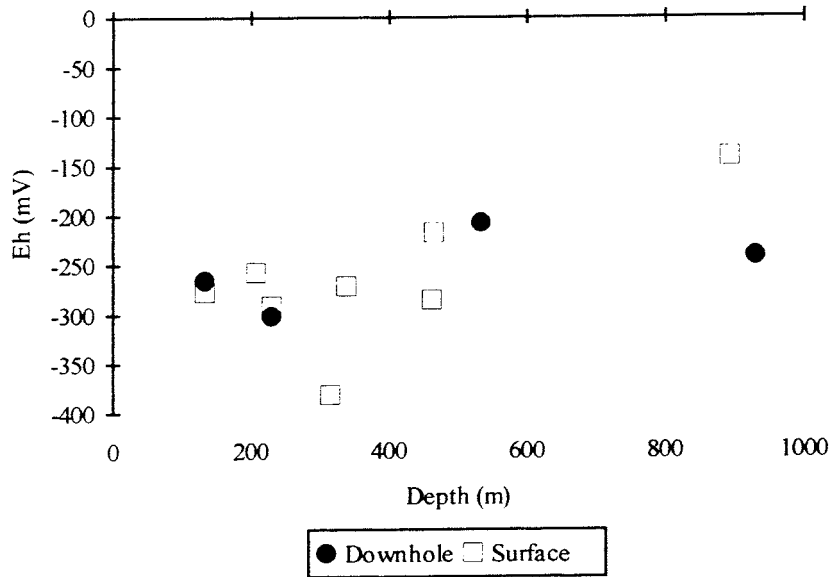
Figure 6.4. In situ redox potential (Eh) measurements of the Äspö groundwaters.
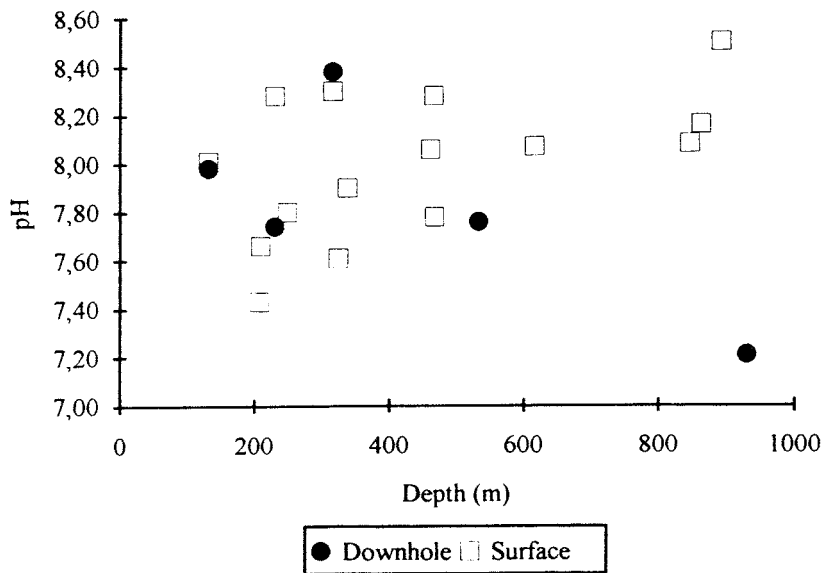
Figure 6.5. In situ pH measurements of the Äspö groundwaters.

measurements are compared. The groundwaters are generally reducing with maximum values ranging from -250 to -320 mV and pH ranges from 7.3 to 8.3 units; the reducing conditions are supported, as mentioned earlier, by almost all the iron being in the ferrous state and often small amounts of detectable sulphide. As shown by Banwart et al. (1992) the major active redox couple is that of $Fe_{(tot)}/Fe_{(II)}$. It would appear that even at very shallow depths (~50 m) efficient buffering reactions are occurring within the conducting fracture zones ensuring a rapid drop in the redox potential during groundwater recharge.

The geochemical behaviour of uranium is very much redox dependent, in addition to the total concentrations of ligands which form complexes of relative strength with uranium in its different oxidation states, i.e. carbonate, biophosphate etc. (see Section 2.6). Further to the Eh redox trends described above, there are also consistently low uranium contents (apart from two samples) in the groundwaters, where values range from 0.08-0.72 µg/L (Table 6.4). These low contents also indicate reducing conditions. Low dissolved uranium usually relates to high $^{234}U/^{238}U$ activity ratios, the latter often reflecting near stagnant conditions required to allow the build-up of excess ^{234}U from recoil effects. At Äspö the $^{234}U/^{238}U$ activity ratios are high to very high, ranging from 2.6-7.2 (Table 6.4).
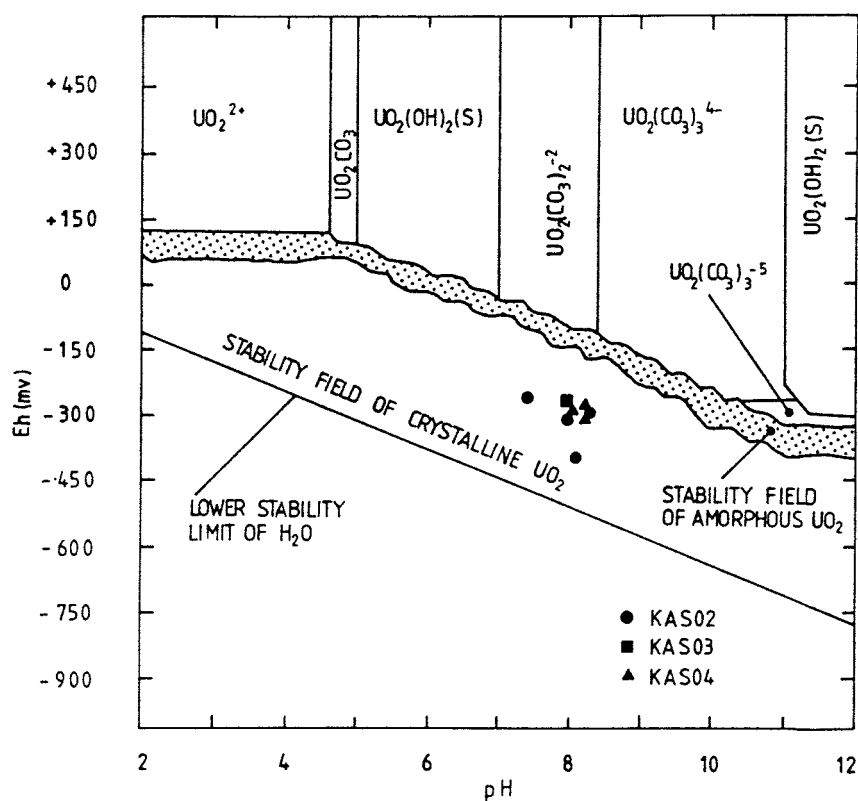
Figure 6.6. Eh-pH diagram showing the stability fields of the more important U (VI), U(V) and U (IV) complexes considered relevant to groundwater compositions derived from crystalline bedrock environments in Sweden. The choice of thermodynamic parameters is summarised and discussed by Bruno et al. (1984). Uranium boundaries are shown for equilibria with crystalline UO_2 (lower boundary) and with amorphous UO_2 (upper boundary).

Table 6.5: Redox-sensitive parameters and pH for reducing groundwaters from Äspö.
(Eh$_h$ = measured; Eh$_t$ = calculated).

| Borehole	Level	pH	U	Eh$_m$ (mV)	Eh$_t$ (mV)
KAS02	202-214.5	7.4	0.15	-260	-258
KAS02	463-468	8.3	0.32	-300	-417
KAS02	530-535	8.3	0.13	-300	-295
KAS02	860-924	8.5	0.54	-320	-382
KAS03	129-134	8.0	0.15	-270	-317
KAS03	860-1002	8.0	0.13	-250	-176
KAS04	226-235	8.2	0.46	-300	-249
KAS04	334-343	7.9	0.29	-270	-327
KAS04	440-481	8.0	27	-280	-348

As the Eh is a critical parameter in the geochemical behaviour of uranium, Table 6.5 presents measured and calculated Eh values for the Äspö groundwaters, in addition to the pH and uranium contents. The relationship between the measured Eh and the uranium content has already been presented for each borehole section where measurements are available (see Section 5). These calculations show that for all groundwaters (with the exception of KAS04:440-481 m which recorded 27 μg/L U) the main solubility limiting phases are crystalline uraninite (UO_2) and the more amorphous U_4O_9 phase. Figure 6.6 illustrates the position of these reducing groundwater compositions, together with the uranium (IV) and uranium (VI) stability field systems, based on Eh-pH criteria. It can be clearly seen that all the groundwaters plot within the stability field of uranium (IV), which again supports the reducing nature of the Äspö groundwater environment.

The solubility limiting uranium oxide phases predicted from the calculations are very difficult to identify mineralogically from the fracture zones; they exist probably as very small discrete crystals (uraninite) and as surface coatings (the more amorphous types) in close association with the micaceous (chlorite) and hematite/Fe-oxyhydroxide phases. As suggested by Andrews and Kay (1983): "crystalline UO_2 boundaries are appropriate for groundwater equilibration with rock matrices containing well-crystallised UO_2, as for example in some granitic (i.e. crystalline bedrock) environments".

6.2.2. Groundwater Evolution.

Fracture mineral studies within the upper 0-350 m of Äspö partly support the premise that hydrogeochemical changes within this interval appear to follow the normal evolutionary trend in fractured conductive Swedish crystalline rocks, i.e. an uppermost horizon with a paucity of calcite (due to the dissolution effect of downward percolating, moderately acid rainwater), a lower horizon characterised by a precipitation of calcite (when the downward

percolating groundwaters become carbonate supersaturated), and finally the lowermost horizon where calcite is by and large absent. Tullborg (1988) has mapped the distribution of calcite coated fractures from KAS02, KAS03, KAS04 and KAS06 and found that the above described horizons correspond to depths of approx. 0-40 m, 40-250 m and finally 250 m downwards. This depth penetration of near-surface derived groundwater is clearly supported by comparing other surface-sensitive parameters such as pCO_2, TOC, HCO_3 and tritium.

At greater depths, however, the normal evolutionary chemical trends from one end-member to the other become less clear. This is mostly coupled to increasing salinity which is clearly illustrated by the chemistry and supported by the salinity logs for the various boreholes; Cl contents commonly exceed 10 000 mg/L at and below 800 m. As suggested from the chemistry and discussed in more detail in Section 6.4.2, these saline waters should be considered as a separate, deep, possibly regional groundwater system, which is almost stagnant except when intercepted by deeply penetrating conducting fracture zones that locally encourage partial mixing with upper, near-surface derived more dynamic groundwater systems. Groundwater mixing, and the associated hydrogeochemical repercussions, is therefore a major process to be addressed in order to interpret the chemical evolution of the groundwaters.

Mixing of the groundwaters is relatively simple to model with regards to the chloride content, the most conservative ion present and the most concentrated, as demonstrated by applying a simple two-component Cl mixing model for each borehole (see Section 5). For the other major ions present in smaller amounts, such as Na, Ca, HCO_3 and SO_4, the model indicates some marked deviations from ideal mixing, which suggests that other processes must be contributing to the chemistry within this mixing interval to account for the elemental deviations registered. Figure 6.7 shows the combined mixing calculation data for the Äspö groundwaters. These ionic distributions show, once again, the three main general hydrogeochemical categories: shallow mixed (0-250 m), intermediate mixed (250-600 m) and deep (>800 m).

According to the mixing model, the interface between shallow and intermediate is characterised, in particular, by an increased relative deviation in Ca, K and SO_4 and a decreased relative deviation of HCO_3; Na usually shows an antipathetic relationship to Ca. The interface between intermediate and deep shows a continued increase in the relative deviation of Ca, but no change in SO_4 or K. In contrast with previous interface, however, HCO_3 shows a marked increase, and decreases in Na and Mg occur. To explain these ionic deviations, two main water/rock mechanisms are generally invoked, mineral precipitation/dissolution and ion exchange. For example, the dissolution of calcite or plagioclase, and/or Na-Ca ion exchange, may be a source for Ca, the formation of a Mg-rich chlorite, and/or Ca-Mg ion exchange, may account for the depletion of Mg, and Ca-K ion exchange might explain the initial increase in K (to around 500 m); the formation of potassium clay phases may help to explain the K decrease at greater depths. Finally, the increase in SO_4 distribution may be dependent on the stability of gypsum or due to other processes such as bacterial action.

To address the precipitation/dissolution hypothesis, mineral equilibrium calculations (using PHREEQE) were carried out using a realistic mineral database based on actual
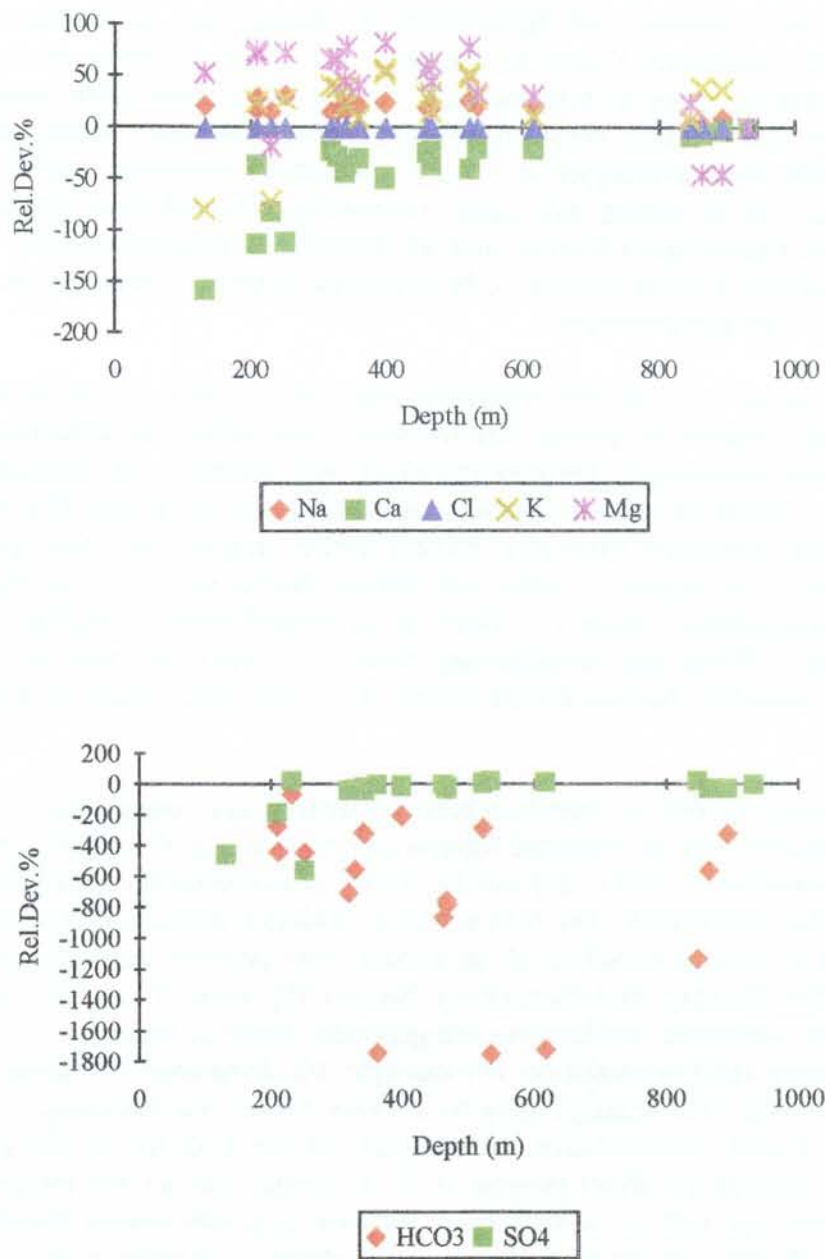
Figure 6.7. Depth trends of the major ions plotted as percentage relative deviation to the simple two component Cl ideal mixing model.

mineralogical observations. These calculations show that positive mineral saturation indices indicate close saturation or a slight oversaturation with respect to quartz, fluorite, laumonite and calcite; this essentially reflects the phases identified from the fractures. In contrast gypsum is always undersaturated, which supports the small amounts recorded from the fractures, and that pyrite (only sporadically present) is generally (but not always) oversaturated. Evaluation of the hematite and Fe-oxyhydroxide phases (locally highly represented), which can be either strongly over- or under-saturated, is complicated by their sensitivity to the Eh input (i.e. reliability of the field measurements) and/or inadequacies in the thermodynamic database.

In conclusion, the data do not clearly correlate with a sytematic evolutionary sequence of mineral dissolution/precipitation necessary to explain the observed chemical trends to 1 000 m. Calcite instability can explain some of the Ca trends in the uppermost 300 m or so, but the steady increase of Ca and sympathetic decrease of Na with depth needs an alternative mechanism. The breakdown of plagioclase followed by albite recrystallisation is a mechanism favoured to explain the present day increase in Ca and depletion of Na with increasing depth at Olkiluoto (Pitkänen et al., 1992). Mineral chemistry (microprobe) and textural relationships at Äspö support this reaction, where plagioclase of oligoclase composition has been progressively altered to albite with subsidiary muscovite/sericite (T. Eliasson, per. comm., 1992).

To address the ion exchange hypothesis, the relevant exchange ions (Na, Ca, K and Mg) have been compared to chloride (e.g. see Section 6.3, Fig. 6.12) to try and obtain a clear picture of trends in the water chemistry related to seawater dilution, and to limit the number of possible options open for interpretation. Sodium, the most dominant ion after Cl, shows close similarities with the seawater dilution line in the upper 200-250 m but is markedly depleted relative to seawater at greater depths. Calcium shows a strong enrichment relative to seawater and Mg and K show depletion. These trends thus infer the possibility that when seawater enters a freshwater aquifer, ion exchange processes remove Na, K and Mg from the seawater in exchange for Ca.

Sulphate, when compared to Cl, initially shows a congruent trend with seawater at shallower depths and depletion relative to seawater dilution at greater depth. This depletion would suggest that bacterial sulphate reduction might be occurring in the saline groundwaters. Sulphur isotope studies (and the detectable odour of H_2S) conducted in groundwater samples from Laxemar, located adjacent to Äspö, would appear to support this process (Wallin, 1990). The odour of H_2S has recently been detected in the excavation tunnel at Äspö in the near-vicinity of the large discharging NE-1 zone (per. comm. I. Rhen, 1992). Since the saturation index for gypsum is undersaturated in all samples, gypsum precipitation does not play a role in affecting the sulphate concentrations.

In summary, whilst the application of both mineral dissolution/precipitation and ion exchange processes to explain the observed hydrochemical trends at Äspö have been partly successful, some important areas of uncertainty still remain. As discussed by Nordstrom (1986) for the Hästholmen groundwaters, model calculations indicate that cation exchange is insufficient to account for the change in water chemistry, assuming that there is an intrusion of seawater into freshwater aquifers. In addition, the general lack of widespread clay mineral occurrences (usually only represented locally) in the bedrock at Äspö

(Tullborg, 1988 in Wikman et al., 1988) would serve to reduce the overall ion exchange capacity of the system. In contrast, there is some evidence that mineral stabilities may possibly explain the increasing Ca/Na ratio with depth. These reactions, however, which incorporated meteoric-derived waters, occurred deep in the bedrock under hydrothermal conditions during much younger periods in the geological history of the granite. Subsequent mixing with additional meteoric groundwaters (and fluids derived from other sources) has resulted in present day compositions and Ca/Na signatures.

However, it is important to bear in mind that there are at least three groundwater sources which are entering and mixing within the upper 500 m of the Äspö site; there is no single, evolutionary flowpath from surface to great depth convenient for interpretation and modelling. The trends in the upper 250-300 m are dominated by the downward movement of potentially aggressive surface-derived waters (e.g. as indicated by the pCO_2 trends), where mineral dissolution/precipitation and ion exchange processes have to some extent contributed to the groundwater chemistry. However, this water also contains a significant component of both modern and ancient Baltic seawater. At greater depths highly saline groundwaters also mix to limited degrees. A mixing interface between these deep saline and the more surface-derived varieties extends approximately from 300-500 m depth.

This working hypothesis was tested using the NETPATH program (Plummer et al., 1991) which combines both the modelling of geochemical reactions (i.e. equilibrium mineral stabilities and ion exchange processes) occurring along a flow path, with mixing of waters from different sources (see Section 2.9). Preliminary results show close agreement with the simple two componet mixing model employed, which supports the hypothesis that the major hydrogeochemical characteristics of the Äspö groundwaters can be explained by the mixing of waters from two major sources (shallow "fresh" vs. deep saline), with more subordinate effects resulting from rock/water interactions, and components of modern Baltic seawater and relict ancient marine waters.

6.3. Modelling of the EW-1 shear zone.

The EW-1 shear zone is a major influence on the groundwater chemistry at Äspö. It has been referred to on many occasions as a dominant recharge zone, and its influence on the groundflow directions is illustrated and discussed in Section 6.5. Because of its recharge character, coupled with the fact that it has been intersected by three boreholes, it presents a unique opportunity to study groundwater evolution, in a fairly well constrained environment, in terms of hydrogeology, water/rock chemistry and redox chemistry.

Zone EW-1 (ENE/ 80°NW) is 50-100 m wide extending to at least 600-700 m depth (Wikberg et al., 1991). The surface expression of the zone has been identified by topography and ground geophysical methods (magnetic, seismic and electric). The geology has been investigated by drilling KAS03, KAS04 (55-70, 115, 175-190 m), KAS12 (10-70 m) and HAS01, 05, 18, 19, 20 (0-100 m). Geohydrological information is available from KAS04 (0-185 m) with interference test data from KAS03 (349-373. 455-475, 610-622, 691-694 m) and from downhole spinner surveys. Groundwater sampling within the zone or in the near-vicinity has been performed in HAS05 (45 m), KAS 03 (347-374, 453-480, 609-623, 690-1002, 860-1002 m) and KAS04 (226-235, 334-343 m). Refer to Section 5 for further details.

6.3.1. Geological Features.

The rock types found close to EW-1 consist of Småland granite, Äspö diorite, fine-grained granite (aplite) and greenstone. EW-1 is regarded as a complex zone composed of some highly fractured (crushed), more or less mineralogically altered, metre wide sections, separated by slabs of Småland granite (less fractured but hydrothermally altered) and up to metre wide fractured mylonites. Shear zones with epidote alteration are common; hydrothermal alteration (oxidation of magnetite to hematite and red-straining of fractures) also occurs. The fracture filling mineralogy, listed in descending order of frequency and importance (E-L. Tullborg pers. comm. 1992), comprises:

A) Chlorite, calcite,
B) Hematite, iron oxyhydroxide, epidote, fluorite,
C) Pyrite, magnetite, laumontite/prehnite, gypsum and smectite

6.3.2. Geohydrological Features.

Hydraulically, the formation of different fracture minerals is believed to have an important sealing effect within the main part of the zone. The most conductive part of the zone consists of a series of narrow, highly fractured sections or single open fractures which probably are not continuously connected along the entire length of the zone. Pumping tests to identify hydraulic connections were carried out at 349-373, 455-473, 610-622 and 691-694 m in KAS02 indicating an ENE striking structure intersecting KAS04 at 0-185 m and HAS01 at 0-100 m. There may well be several ENE structures causing this response, but for modelling purposes it is assumed that the response is best explained by a single structure parallel to EW-1 with a dip of 60°N. The pumping test in HAS20 also indicated a good hydraulic contact with the northern part of Äspö, probably because of the EW-1w
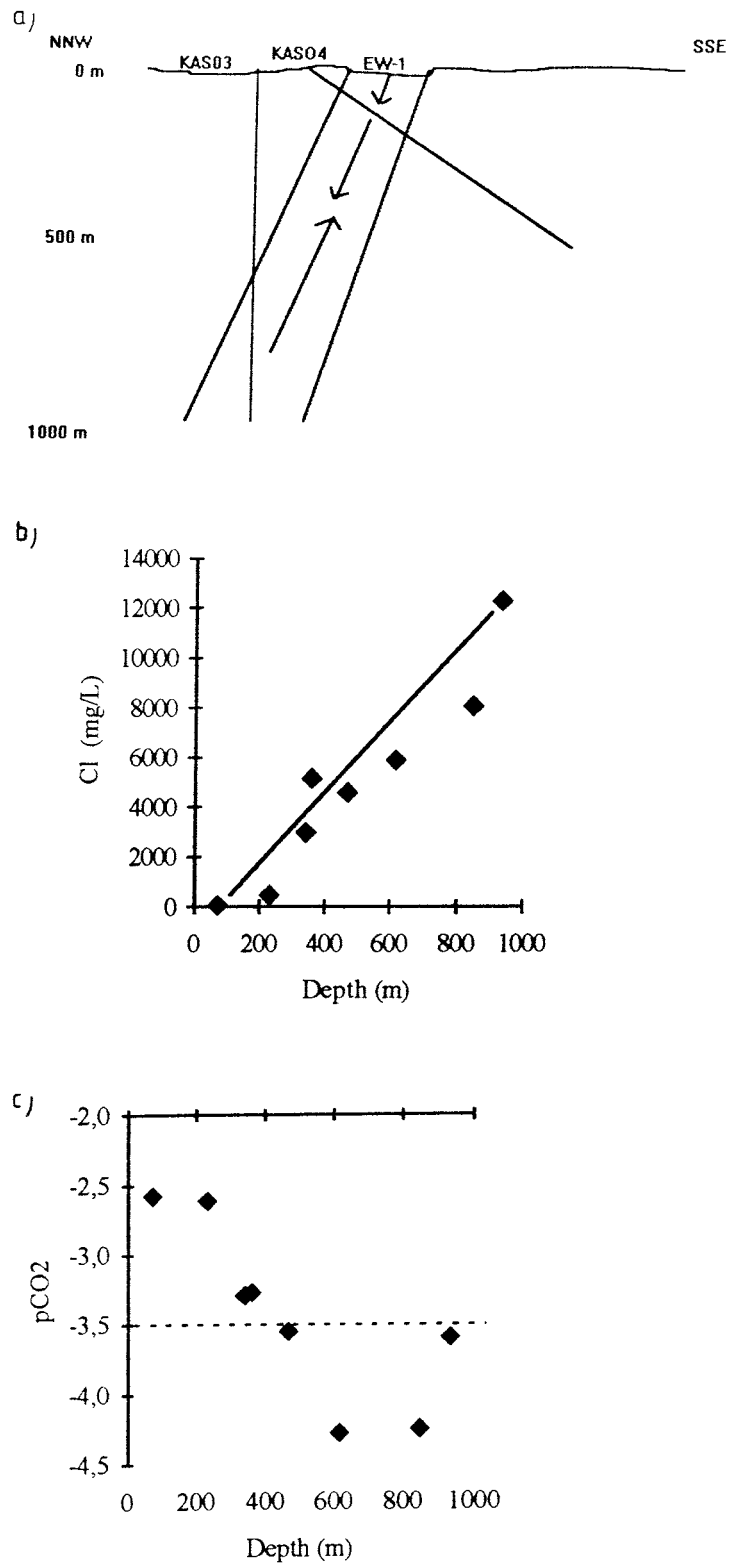
Figure 6.8. a) Schematic diagram of EW-1 indicating major flow path directions,
b) Cl vs. depth in EW-1 indicating the two component mixing line between
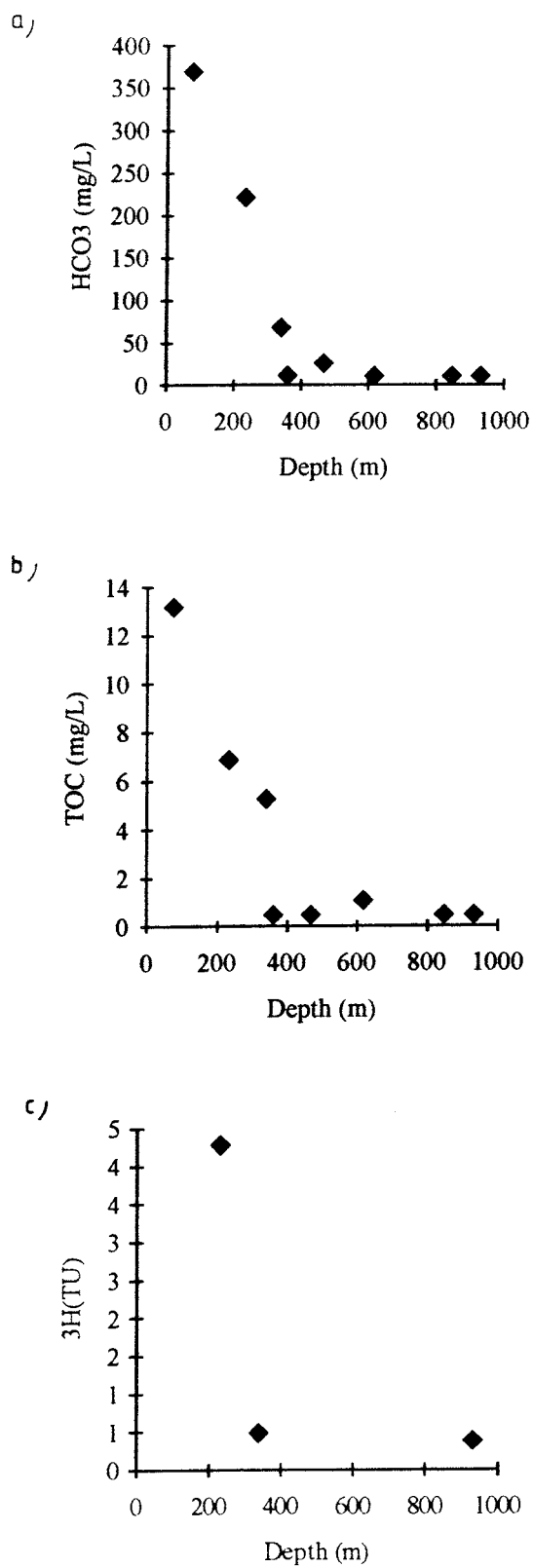HAS05 and KAS03:860-1002 m, and c) pCO_2 vs. depth.

Figure 6.9. Zone EW-1: a) HCO_3 vs. depth, b) TOC vs. depth, and c) ^3H vs. depth.

zone. The overall estimated transmissivity is $T=2.0 \times 10^{-5} m^2/s$; in the eastern part of the zone the transmissivity is assumed to be 1×10^{-6} m^2/s (Rhén, 1989; L. Nilsson, 1989).

6.3.3. Hydrogeochemical Features.

The groundwaters are changing from a Na-Ca(Mg):Cl-HCO$_3$ type in the shallow part (45-250m) to a Na-Ca(Mg):Cl-SO$_4$ type at the intermediate level (250-650m) and the deepest level (650-1000m) is characterised by a more Ca-rich water of Ca-Na(Mg):Cl-SO$_4$ type. The pH is ranges from neutral to moderate alkaline (7.3-8.5 units). Reducing conditions are indicated by Eh measurements (-250 to -320 mV), low uranium (0.01-0.31 ppb) content and nearly all total iron is in the ferrous state (see section 6.2.1 and below for redox discussion).

6.3.4. Groundwater Mixing.

For Äspö as a whole, and zone EW-1 in particular, there are two main groundwater flow directions; downward flow of shallow fresh/brackish water (with a subsidiary marine component) and potentially the very slow upwelling of deep saline groundwaters (Figs. 6.8a and 6.21). The mixing interface is estimated to be at a depth of 400 m. For a more comprehensive discussion of the flow system see section 6.5.

The salinity within EW-1 is generally more diluted when compared with samples from other boreholes at corresponding depths. This dilution, which resembles the inflow of fresh water into the system, can be observed as a negative deviation of Cl from the mixing line calculated from the shallow (HAS05) and the deep (KAS03:860-1002) end-members (Fig. 6.8b). The weak upward flow may be indicated by an increase in Cl concentration or a positive deviation from the mixing line at the KAS03:467m.

The effect from shallow input is best described by increased values of HCO$_3$, TOC and ^{3}H (Fig. 6.9) and the calculated pCO$_2$ pressures. The pCO$_2$ appears to be one of the most sensitive parameters indicating open conditions (>-3.5 units) down to 400 m and a closed system (<-3.5 units) at greater depths (Fig. 6.8c). The seawater dilution line is compared to the mixing line, once again described by the shallow water (HAS05) and the deep (KAS03:860-1002) end-members (Fig. 6.10a); the shallow-deep water mixing model seems to describe the system better. However, this does not mean that seawater influx is less important, as shown by Br in Figure. 6.10b.

The mixing model (for model description see Section 5.1.8 for KAS02) can also be used to calculate the percentage portions of shallow water input into zone EW-1 (Fig. 6.11). The interface between these two end-members is clearly seen at around 400 m depth.
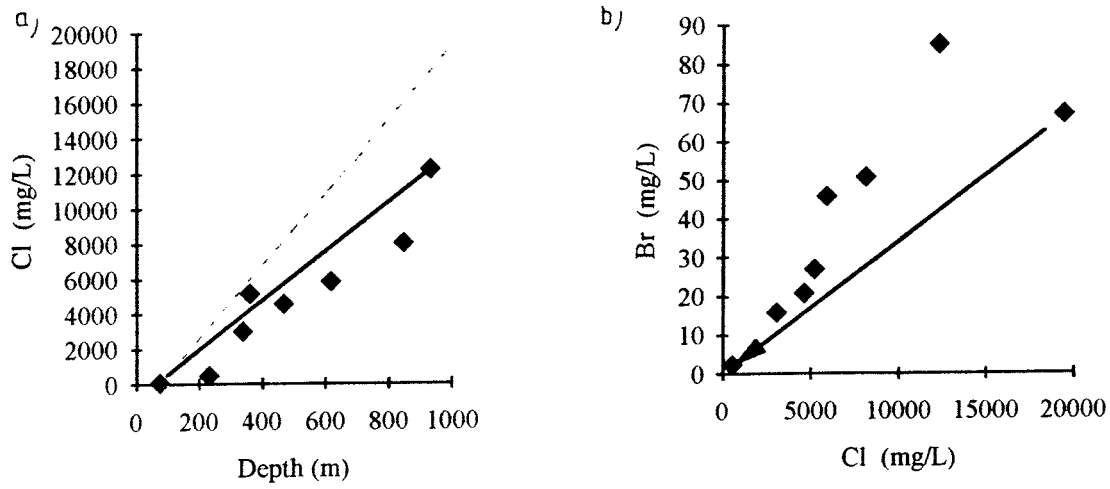
Figure 6.10. Zone EW-1: a) Cl vs. depth; the lower line represents the mixing line between
HAS05 and KAS03:806-1002 m and the upper line the seawater dilution line;
b) Br vs. Cl concentration; arrow represents the seawater dilution line.
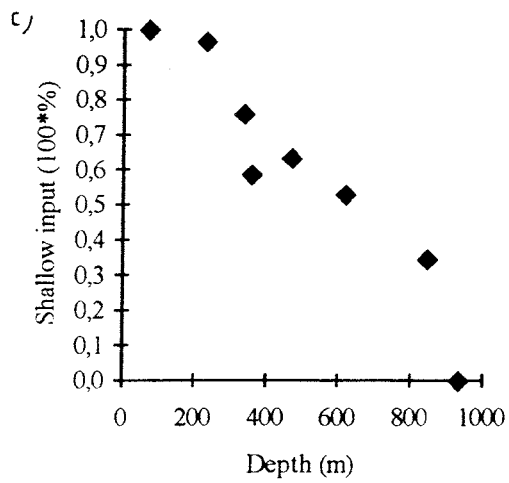
Figure 6.11. Zone EW-1: shallow water input vs. depth.
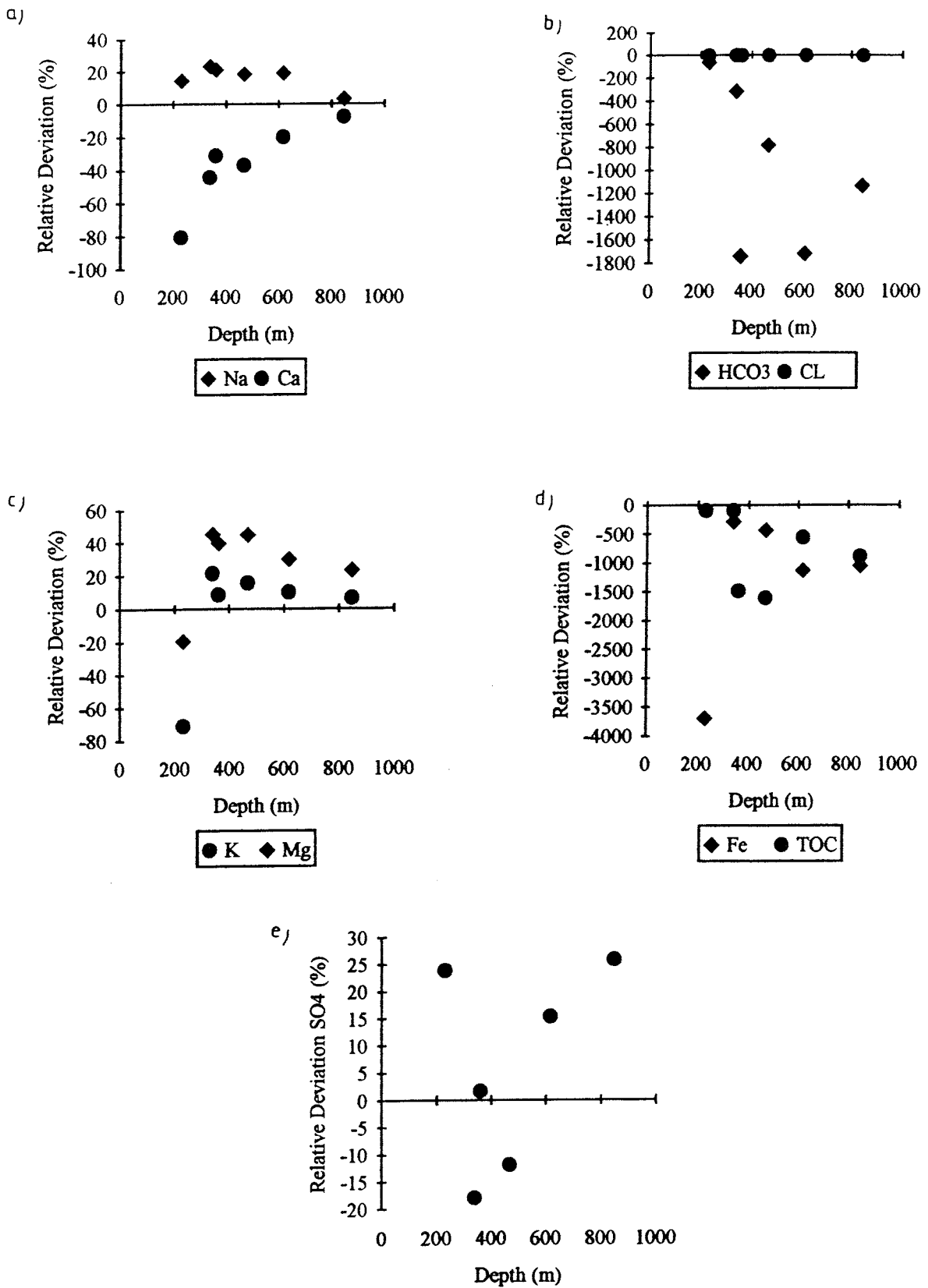
Figure 6.12. Zone EW-1: a) Na, Ca deviation from the two component mixing model, and b) HCO_3 and Cl deviation, c) K and Mg deviation, d) Fe and TOC deviation, and e) SO_4 deviation.

6.3.5. Water/rock Interaction.

As discussed in Section 6.2.2, deviation from the mixing model is believed to be due to water/rock interactions. Little to no deviation from the mixing line indicates conservative behaviour, large deviation indicates an unknown internal source or sink for the particular element. The behaviour of Na, Ca, HCO_3, Cl, K, Mg, Fe, TOC, SO_4, Tr, D and ^{18}O is illustrated in Figure 6.12.

The observed trends in zone EW-1 reflect the general patterns described for the whole area (see Section 6.2.2). The main areas of rock/water interaction fall into three categories; upper 250-300 m where calcite (and the Fe-system) dissolution and precipitation is one of the dominant reactions occurring, together with subordinate ion-exchange; intermediate 300-600 m where most ions show uniform trends which may be due to more limited water/rock interactions taking place as the groundwaters begin to equilibrate (chemically and hydraulically) at greater depths; and greater than 600 m where deep saline groundwaters are mixing at the interface with the intermediate type. Deviations from the mixing line, for example, for HCO_3, may reflect the calcite precipitation/dissolution processes inferred above. The initially high SO_4 deviation may be due to the oxidation of pyrite or gypsum dissolution, although as stated earlier gypsum instability is not considered to play a major role. The marked change of sulphate to a negative deviation around 250-300 m is probably due to bacterial reduction. The iron content in groundwaters from 0-50 m generally show high (>2 mg/L) values resulting from oxidation and weathering of Fe-minerals such as biotite, chlorite and sporadically pyrite. Thereafter, with increasing depth there is normally a steady decrease in iron content. These reactions essentially reflect, for example, the changing groundwater redox conditions leading to the precipitation of amorphous Fe-oxyhydroxides which commonly line some of the fracture surfaces. This precipitation (and probably also sorption processes) can explain some of the relative deviation patterns observed for Fe.

Some of the deviations around the mixing line may be artificially induced by the pumping and sampling activities in the various boreholes which may result in changes of pH and Eh. In particular calcite precipitation can result when groundwaters, oversaturated or near-equilibrated with calcite, are pulled into contact with similar groundwaters and mixed. In general, however, rock/water interactions in combination with the mixing of different end-members mostly account for the changes observed in the water chemistry along zone EW-1. This is furthermore supported by preliminary modelling using the NETPATH program (Plummer et al., 1991).

6.3.6. Redox Conditions.

Reliability of in situ Eh Measurements.

Groundwater redox conditions can be described by three characteristics: intensity, capacity and kinetics. The Eh value or the redox potential is an intensity parameter similar to pH. The Eh value defines the potential for a redox reaction to proceed in a certain direction, in the same way as pH does for acid-base reactions. Examples of such reactions are (after Wikberg, 1992):

$$Fe^{2+} \leftrightarrow Fe^{3+} + e^- \quad \text{redox reaction}$$
$$H_2S \leftrightarrow HS^- + H^+ \quad \text{acid-base reaction}$$
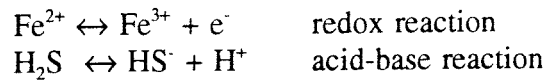
These are only half cell reactions, which means that another half cell reaction is needed in order to balance them.

High Eh values corresponding to oxidising conditions drive the reaction to the right; low Eh values corresponding to reducing conditions drive the reaction to the left. For aqueous solutions the upper and lower limits of Eh are set by the decomposition of water into oxygen and hydrogen respectively, i.e. +815 mV and -414 mV at pH=7 and 25° C. The Eh buffering capacity comes from the concentration of oxidisable and reducible species in the solution and similar species in solid form in contact with the solution. The redox capacity is equivalent to the amount of ferrous iron available for reduction (Wikberg, 1992).

Many authors have compared the measured Eh to the value calculated on the basis of different redox couples. The most extensive work in this context was made by examining the USGS records of Eh data with respect to the redox couples of ferrous and ferric iron, sulphide-sulphur, sulphide-sulphate, nitrogen couples, methane-bicarbonate and a few others. None of the redox couples agreed with the measured Eh values. It was therefore concluded that Eh cannot be measured in natural groundwaters because of a lack of true equilibrium.

However, the experience within the SKB radioactive waste programme points to the contrary. Based on site-specific investigations over a period of several years, a fairly successful method of field Eh measurement has been achieved. Success depends on the following points: a) poorly buffered waters require a long time to obtain stable electrode readings, b) different electrode types give initially different readings, however, after a levelling out period, they stabilise to within a couple of tens of mV, c) flow-through cells at the surface give reasonably accurate readings, even though they are more sensitive to oxygen contamination, and d) only when the readings on all three chosen electrodes agree, is the obtained value a close measurement of groundwater Eh (Wikberg, 1992).

Recently, Grenthe et al. (1992) have modelled all the Eh values measured within the SKB programme. The recorded values reflect equilibrium between the ferrous iron in solution and varying crystalline forms of ferric oxide ($Fe(OH)_3$). Thus, using the $Fe_{(II)}$ content in the groundwater and the measured pH, the measured Eh values can be corrected by using the following formula:

$$Eh = E_0^* - (RT/F) (3pH + \log [Fe^{2+}]) \tag{1}$$

where $E_0^* = 707$ mV and $RT/F = 56$ mV.

The corrected Äspö values are listed in Table 6.5 showing only a moderate deviation. Figure 6.13 compares the measured and calculated Eh values for zone EW-1. The agreement, although far from perfect, nevertheless provides some support for the suggested model of Grenthe et al. (1992).
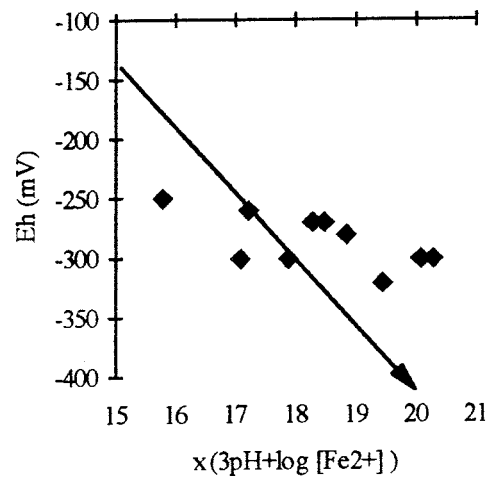
Figure 6.13. The in situ field Eh data plot close to the calculated theoretical values (denoted by arrow) given by equation (1).
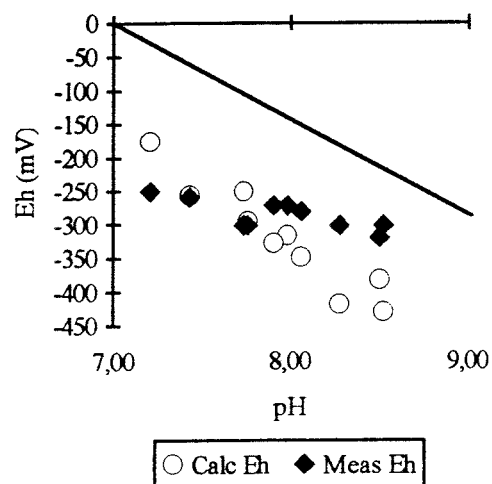
Figure 6.14. Measured Eh (meas) and calculated (calc) vs. measured pH; values are plotted on a simplified stability diagram based on Garrels and Christ (1965). The values plot within the pyrite stability field; above the line is the hematite stability field.

The calculated Eh values plot within the stability field of pyrite (FeS_2); one measured point falls within the stability field of hematite (Fe_2O_3) (Fig. 6.14). Pyrite, however, is relatively rare as a fracture filling phase; as shown by this study, ferric oxyhydroxide is the redox controlling solubility phase. The plotted data can therefore be regarded to fall within the ferric oxyhydroxide stability field, within an area considered to lie partly at equilibrium between pyrite and hematite (Krauskopf, 1967).

Buffering Capacity of the Bedrock.

Swedish groundwaters are all reducing below a depth of 100m, and most of the waters already from a depth of few tens of metres (Wikberg, 1992). The main indicator is generally a high concentration of ferrous iron due to weathering of iron rich minerals. At greater depth the iron content decreases while sulphide contents increase. In general, however, since the contents of iron, sulphide, total organic carbon and manganese in the water are small (Wikberg, 1992; Banwart et. al., 1992), the main redox buffering capacity of the system mostly reflects the chemistry of the bedrock and fracture minerals.

The main reductants in the water are iron and total organic carbon, both of which decrease with depth along zone EW-1 (e.g. Fig. 6.16). The redox potential (Eh) is mainly controlled by the iron system in the water and the rock; sulphate is not believed to be involved in the redox processes.

Despite the shallow water component detected in zone EW-1, coupled with the fact that the zone is hydraulically active, both the measured and calculated low redox potentials indicate how rapid and efficient the redox buffering is. This compares favourably with the results from the redox experiment presently being carried out at shallow depths at Äspö (Banwart et al., 1992). Zone EW-1 is particularly efficient because of the large amounts of iron oxides/hydroxides present along sheared conducting planes in the fault zone. The absence of a magnetite anomaly across the zone is due to the complete and pervasive oxidation of the magnetite to hematite and Fe-oxyhydroxides.

The occurrence of Fe-oxyhydroxide at depth within zone EW-1, whilst often reflecting hydrothermal activity, may also be of low temperature origin (Grenthe et al., 1992). This is thought to result from the decreasing solubility of $Fe_{(III)}$ at high pH and low carbonate groundwater conditions common at increased depths.

6.4. Isotopic geochemistry and origin of the Äspö groundwaters.

From chemical considerations, the Äspö groundwaters seem to represent the mixing product of different waters from different origins. The mixing models support two main sources: near-surface derived meteoric water (with a modern Baltic seawater component) and highly saline deep waters.

6.4.1. Stable Isotopes.

Using a plot of $\delta^{18}O$ versus δD, the Äspö groundwaters, together with near-surface fresh/brackish waters from both Äspö and Laxemar and present day Baltic seawater for comparison, are related to the global meteoric water line (Fig. 6.15). The numbers alongside the samples relate to Table 6.3, where (1) represents the uppermost shallow level, and the other numbers systematically represent the different sampled levels at increasing depth. Although all the samples plot below the global meteoric line, and there is a large spread of isotopic values ($\delta^{18}O$ from -15.8 to -7.2‰ and δD from -124 to -62‰), the groundwaters are clearly meteoric related in origin. The position of the samples below the global meteoric line, i.e. indicating small enrichments in $\delta^{18}O$ or depletions in δD, is often interpreted as indicating surface water evaporation effects, for example, in enclosed basins or inland seas (e.g. Gascoyne et al., 1987). Similar isotopic trends have been reported from other areas in Fennoscandia (e.g. Kankainen, 1986; Smellie and Wikberg, 1991; Pitkänen et al., 1992).

At first glance the Äspö stable isotopic data appear to lack any kind of overall consistency. Some samples show a degree of affinity with modern Baltic waters (KAS06:3,4, and HAS13), other with near-surface fresh/brackish waters (KAS04:1, and KAS06:2), and of the remainder, the deep saline varieties (KAS02:6,7 and KAS03:7,8) tend to cluster around the -13.2 to -12.5‰ $\delta^{18}O$ interval and also closer to the global meteoric line; observations also noted by Tullborg et al. (1990). Within the same cluster area, but showing a slight shify to heavier $\delta^{18}O$ signatures, are less saline and shallower waters which have been sampled using low pump extraction rates and could therefore be considered "representative" of the rockmass in the immediate vicinity of the sampled location (e.g. KAS02:2,3,4,5).

Borehole KAS03 shows a quite regular trend to lighter isotopic values with decreasing depth (KAS03:6,5,4,3,2,1). All these samples lie either within or adjacent to the major recharging EW-1 zone and the isotopic scatter reflects degrees of groundwater mixing, some probably explained by the generally high extraction pump rates used for sampling purposes. This enhanced mixing during pumping may be through hydraulic connections with shallower levels (fresh/brackish source) or to the adjacent EW-1 zone (recharging mixing source). The light isotopic signatures for KAS03:1 (low extraction rates), and to a lesser extent KAS03:2,3 (higher extraction rates), suggest a sizeable cold climate recharge component of very ancient origin (low pmc giving apparent ages of > 20 000 years). This shows that away from the recharging EW-1 zone, pockets of ancient waters within the top 200-250 m of bedrock have apparently been largely isolated from any major mixing with younger recharge waters. The increase towards a heavier signature at greater depths within and closely adjacent to zone EW-1 indicates increasing mixing of light $\delta^{18}O$ waters with deep heavier $\delta^{18}O$ saline waters.
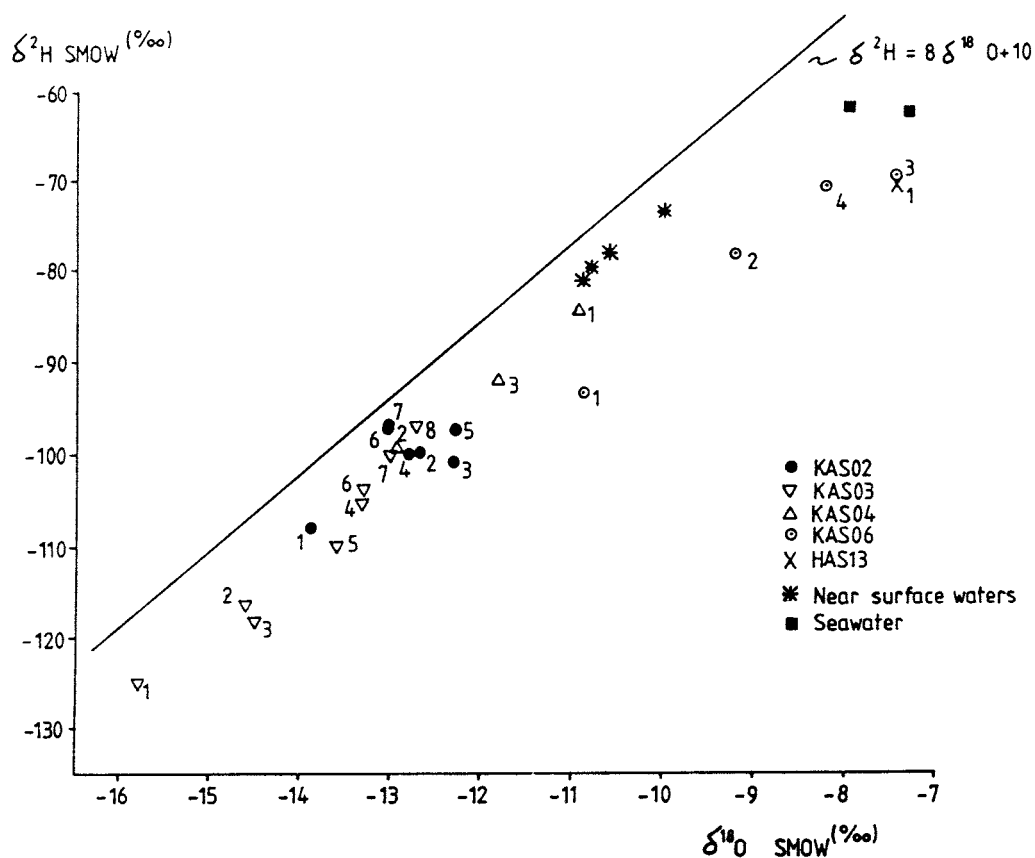
Figure 6.15. Stable isotope compositions of the Äspö groundwaters.

Because of high extraction rates and the recharging nature of zone EW-1, most of the KAS03 waters below 250 m are considered to represent typical "fracture matrix" compositions (i.e. mainly associated with zone EW-1 or other conducting zones intersecting EW-1), rather than compositions typical for the adjacent "bedrock mass". The former explanation is preferred because if these compositions were more typical for the adjacent, more competent bedrock mass, then the waters should have shown a closer affinity to the KAS02 waters which all plot (with the exception of KAS02:1 which lies with the upper 250 m of the bedrock and shows mixing with lighter $\delta^{18}O$ waters in common with the shallower KAS03 samples) in a small cluster together with the most saline varieties.

The influence of modern Baltic and modern near-surface fresh/brackish waters is more apparent in the KAS04 samples (KAS04:1 in particular with 4.3 TU, KAS04:3 less so), where there is an increasing trend to a more near-surface fresh/brackish water composition. Based on this trend, however, sample KAS04:2 plots towards a much lighter isotopic value than expected. This can be readily explained by the fact that KAS04:2 is interpreted as resulting from short-circuiting a major water component from the EW-1 recharge zone (see Section 4.1.8.2), which in turn would result in a lighter isotopic component in common with the KAS03 samples.

All the sections sampled in KAS06 have been subject to excessive extraction rates and all samples plot towards heavier isotopic compositions, more in common with modern Baltic meteoric water. Mixing of Baltic water with mainly near-surface fresh/brackish waters is apparent from the isotopic trends. KAS06:1 is located near zone EW-3 which is recharging in character and may account for some cold climate recharge mixing to give lighter isotopic signatures. Modern water mixing is supported by the presence of tritium (3.8 TU).

In contrast to the other boreholes described, KAS06 is located close to the periphery of Äspö island with potential access to the surrounding Baltic waters. The dominance of the Baltic component in most of the KAS06 samples is best explained by the bedrock hydraulics, where short-circuiting to Baltic compositions has probably occurred. Generally, short-circuiting has contributed to the general mixing of different groundwater types during sampling.

6.4.2. Radiocarbon.

In terms of relative age, the Baltic seawater/near-surface fresh/brackish waters should represent the most recent, youngest water components, the deep saline waters should be among the oldest, and the remainder should be of intermediate age due to the natural hydraulic and imposed mixing processes. Although not many radiocarbon data are available, there are enough to generally support these trends. Important exceptions, however, do occur. The upper part of KAS03, which records salinities of only 1300 to 3000 mg/L Cl, in comparison to the deep saline waters (>12 000 mg/l Cl) has anomalously light stable isotopic signatures and also contains the least amount of percentage modern carbon (2-8%) measured in any of the Äspö groundwaters. As suggested above, the most ready explanation is that these samples represent ancient mixtures of seawaters diluted by cold climate recharge mostly occurring within the upper 200- 250 m of bedrock.

6.4.3. Uranium Decay Series.

Table 6.5 lists the $^{234}U/^{238}U$ activity ratios for the Äspö groundwaters which are high to very high (2.6 to 7.2) showing widespread isotopic disequilibria in the groundwaters due to excess ^{234}U caused by rock/water interaction processes. This ^{234}U excess is caused by the ingrowth of ^{234}U due to the solution of alpha-recoil ^{234}Th at the rock/water interfaces during the permeation of groundwater through the bedrock. The inference, therefore, is that the groundwaters are moving sufficiently slowly through the bedrock so as to allow a ^{234}U excess to accumulate. The high activity ratio values which characterise many of the Äspö groundwaters indicate long residence times thus generally supporting the very old age of some of these waters. This is not only evident in the deep Ca-rich waters, but even fairly near the surface away from major conducting fractures.

<u>Summary.</u>

The Äspö isotopic data indicate five different groupings: a) modern Baltic seawater (0-50 m; recent), b) fresh/brackish near-surface water (0-200 m; recent), c) deep saline water (>800 m; ancient), d) brackish water collected at low extraction rates from less conductive, more massive rock units (100-250 m; ancient), e) water representative of the "fracture

extraction rates coupled with short-circuiting between the sampled borehole section and the surface bedrock horizons. This is in close accordance with the hydrogeochemical data and supported by the groundwater mixing models.

These findings are also in broad agreement with Tullborg and Wallin (1991) who recognised a homogeneous "older" meteoric water below 500 m, an upper heterogeneous "younger" meteoric water (50-500 m), and a near-surface "Baltic" water; this subdivision was based on the stability of the $\delta^{18}O$-values. Attempts were made to correlate the $\delta^{13}C$ and $\delta^{18}O$ values of fracture filling calcites with these groundwater types, but any classification was obscured because of possible crystal zoning (i.e. the sample chosen may reflect several calcite generations of growth, each with a distinctive $\delta^{18}O$ isotopic signature) and/or the mixing of different groundwater types. Even in the uppermost near-surface rock fractures, where isotopic equilibria might have been expected between fracture calcites and modern day Baltic Sea water, no corresponding marine isotopic signatures were measured. This lack of correlation, generally in the upper 500 m of the bedrock, has been attributed in part to the mixing of Baltic Sea water with meteoric water which has influenced the isotopic signatures of the calcites present in hydraulically open fractures. At greater depths, the calcites mostly cluster around the isotopic interval representing calcites in equilibrium with deeper, more stagnant groundwaters (>500 m).

The Äspö stable isotpe data have been compared to some other investigated regions in Fennoscandia (Fig. 6.16). In comparison, there is a great spread of values which include most of the studied areas. This illustrates the great complexity and extent of groundwater mixing at Äspö, with indications that varying proportions of both marine and non-marine groundwaters are involved in their genesis (see discussion below).

6.4.4. Saline Groundwater.

The present status of deep saline groundwaters in Fennoscandia and their origin has been recently reviewed by Smellie and Wikberg (1991), and most of the following details have been extracted from this source. The occurrence of deep saline waters in crystalline basement rocks is not uncommon. Occurrences have been documented from the Canadian and Fennoscandian Shield areas, and from the Carnmenellis granite in S.W. England (see Fritz and Frape, 1982; Hyyppä, 1984; Edmunds et al., 1985; Nordstrom, 1986; Ahlbom et al., 1986, Kankainen, 1986; Frape and Fritz, 1987; Puigdomènech and Nordstrom, 1987; Blomqvist et al., 1989; Nurmi et al., 1988; Pitkänen et al., 1992). The salinity of these waters have been attributed to one or more processes which include: a) relict ancient marine water, b) residual igneous/metamorphic fluids, c) rock/water interactions, d) release of fluids during the mechanical rupture of fluid inclusions, and e) seawater freezing.

A study of Finnish saline groundwater occurrences in the Fennoscandian Shield (Nurmi et al., 1988) recognised four major groups: 1) brackish to saline groundwaters confined to coastal areas and occurring at shallow depths (50-200 m) below the highest postglacial Litorina Sea shore line, 2) brackish to saline groundwaters at depth (300-900 m) occurring beyond the greatest extent of the postglacial Litorina Sea shores, 3) deep (1000-2000 m) saline groundwaters and brines, and 4) very deep (to at least 11 km) brines.
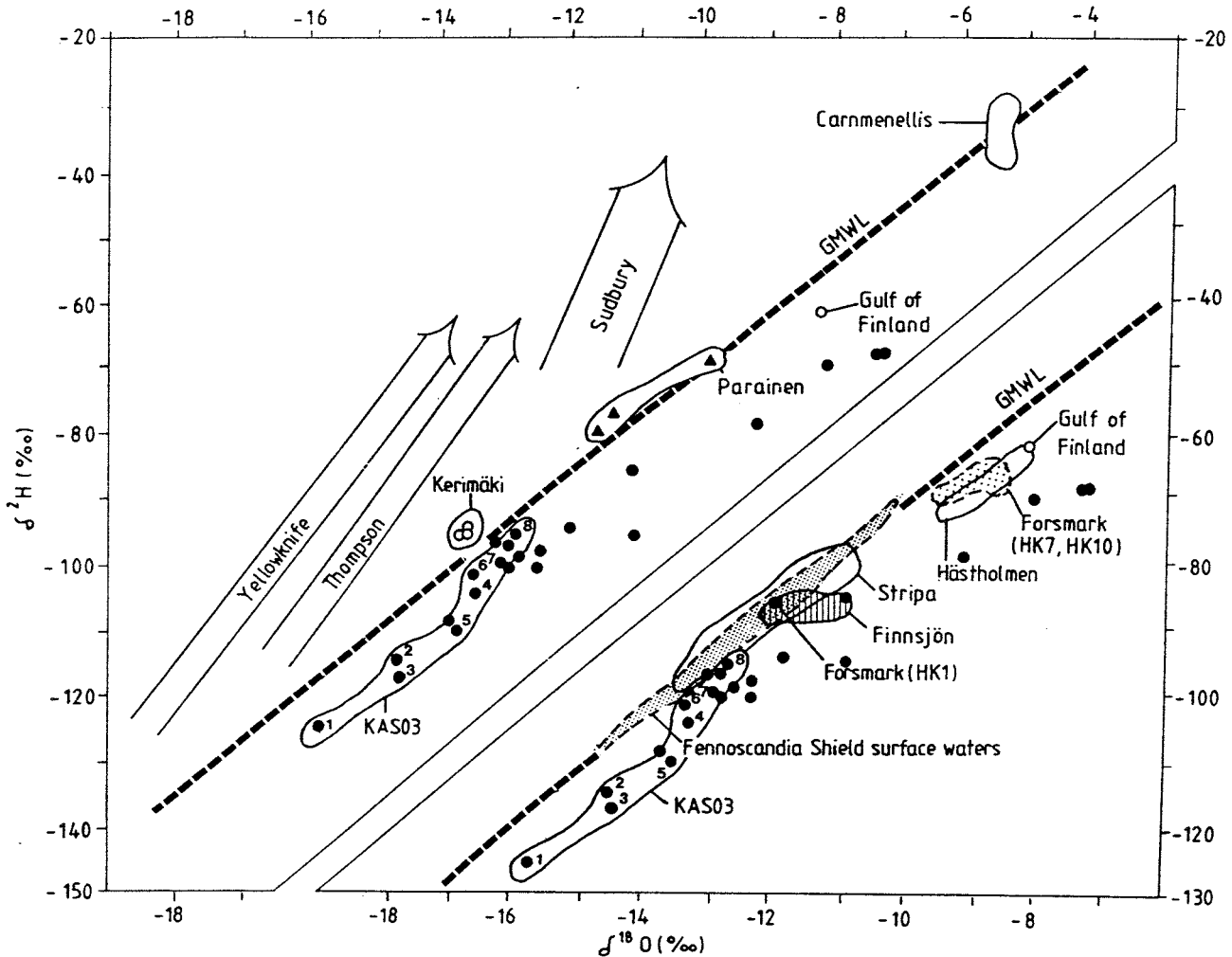
Figure 6.16. Stable isotope composition of the Äspö groundwaters (infilled circles; KAS03 compositions are ringed) compared to other saline groundwater environments in Fennoscandia (modified after Nurmi et al., 1988).

The shallow, coastal brackish and saline groundwaters, occur within a narrow zone bordering the Baltic, demarcated by the maximum extent of the Litorina marine transgressions in the period 7 400-2 500 BP ago. Hästholmen, an island comprising rapakivi granite located off the southeastern coast of Finland, exemplifies such a hydrogeological environment (Hyyppä, 1984; Kankainen, 1986; Nordstrom, 1986). The geochemical and stable isotope data support a seawater origin although somewhat modified by rock/water reactions. The isotope data corresponds to that of present-day seawater in the Gulf of Finland and radiocarbon dating indicates that the mean residence time of the saline water is in the range 4 400-10 000 BP, i.e. considered to be mostly groundwater derived from the Litorina Sea by infiltration, mixed with 15-20% glacial meltwater.

Inland, beyond the influence of the maximum Litorina transgressions, the deeper saline groundwaters lack a marine signature and have been compared to those less brackish waters described from the Stripa area which record apparent ages in excess of 20 000 BP

(Nordstrom et al., 1985). Stable isotope data for the deeper saline groundwaters in Finland fall along the meteoric water line, indicating a meteoric origin, and the present salinity of the waters are believed to mostly reflect rock/water reactions (Nurmi et al., 1988).

In Finland the further sub-division into upper and deeper saline groundwaters is mainly based on differences in salinity and stable isotope signatures. The salinity increases with depth and the isotopic composition changes, plotting consistently above the meteoric water line. The implication is that with increasing depth, mean residence times are considerably longer and that hydrothermal and metamorphic derived waters become more dominant, to the detriment of younger, meteoric-derived waters which characterise the upper horizons.

It is generally accepted that the Br/Cl ratios for saline water is a useful indicator of a marine or non-marine origin because dilution or concentration (by evaporation) of seawater does not markedly affect the ratio of these conservative ions. High Br/Cl ratios are thought to indicate leaching of fluid inclusions, "intergranular salts", or structurally-bound halogens that have a magmatic or hydrothermal origin and are, therefore, distinct from seawater (Gascoyne et al., 1987).
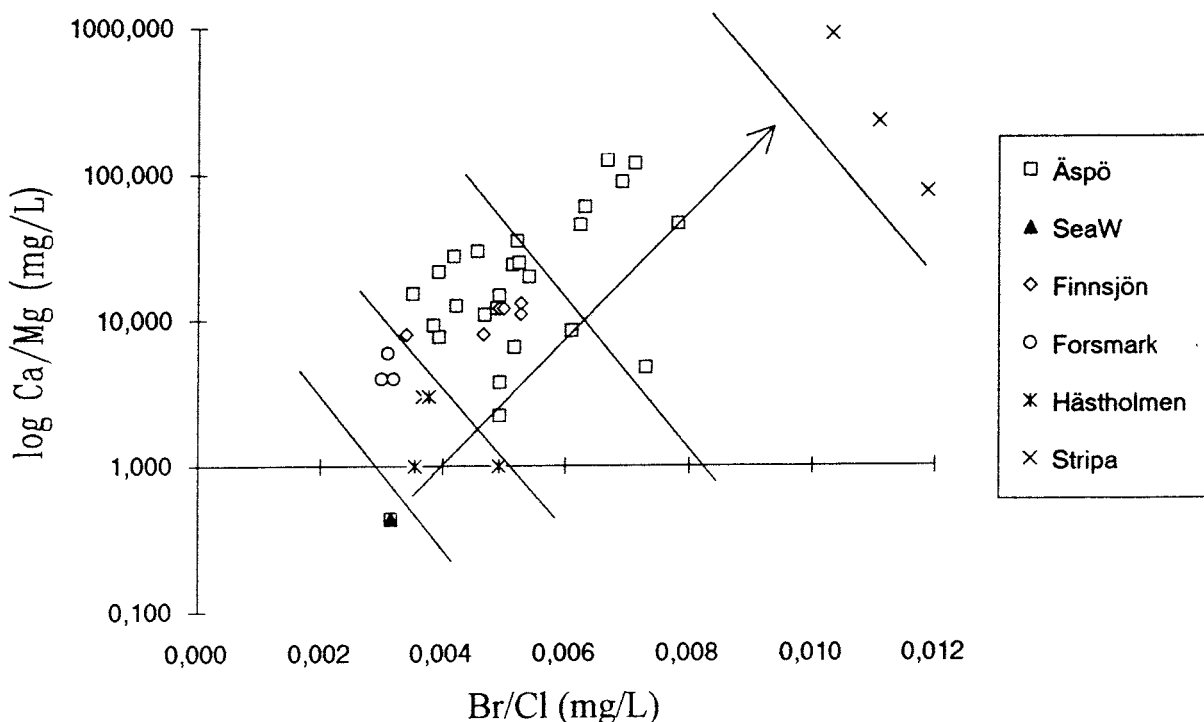
Figure 6.17. Variation of Ca/Mg with Br/Cl (expressed as molecular ratios) for the Äspö groundwaters compared to other Baltic Shield areas.
(Arrow represents increasing non-marine component)

Figure 6.16 shows the variation of Ca/Mg with Br/Cl for the Äspö groundwaters compared to other Baltic Shield areas in Fennoscandia. There is a trend of decreasing marine influence from present-day Baltic seawater through the Forsmark and Hästholmen areas to the main Äspö and Finnsjön groundwater types. The most saline Äspö groundwaters plot intermediate between the Finnsjön and the non-marine Stripa group. The overall impression is that the Äspö groundwaters consist of two distinct saline groundwater groups, a major group with a sizeable marine component with a subordinate component of non-marine derived salts (<0.0062 mg/L Br/Cl), and a minor group with a major non-marine component and marginal marine component (>0.0062 mg/L Br/Cl). This conclusion is in agreement with the sulphur isotope studies which indicate the presence of non-marine groundwaters at depths greater than 500 m (Wallin, 1992).

Marine-derived saline groundwater.

In Fennoscandia, dilution of the non-marine saline groundwaters, particularly at shallow levels by the infiltration of fresh or less saline marine waters through the bedrock from above, should be taken into account, especially when considering the substantial amounts of glacial meltwater available at various times during the period 10 000-20 000 BP ago. Dilution/mixing of such groundwaters can be illustrated by plotting $\delta^{18}O$ as a function of the chloride content (Fig. 6.18). If the Baltic Sea water is considered as diluted ocean water, then it is possible to draw a line connecting a chloride content of 19 000 mg/L
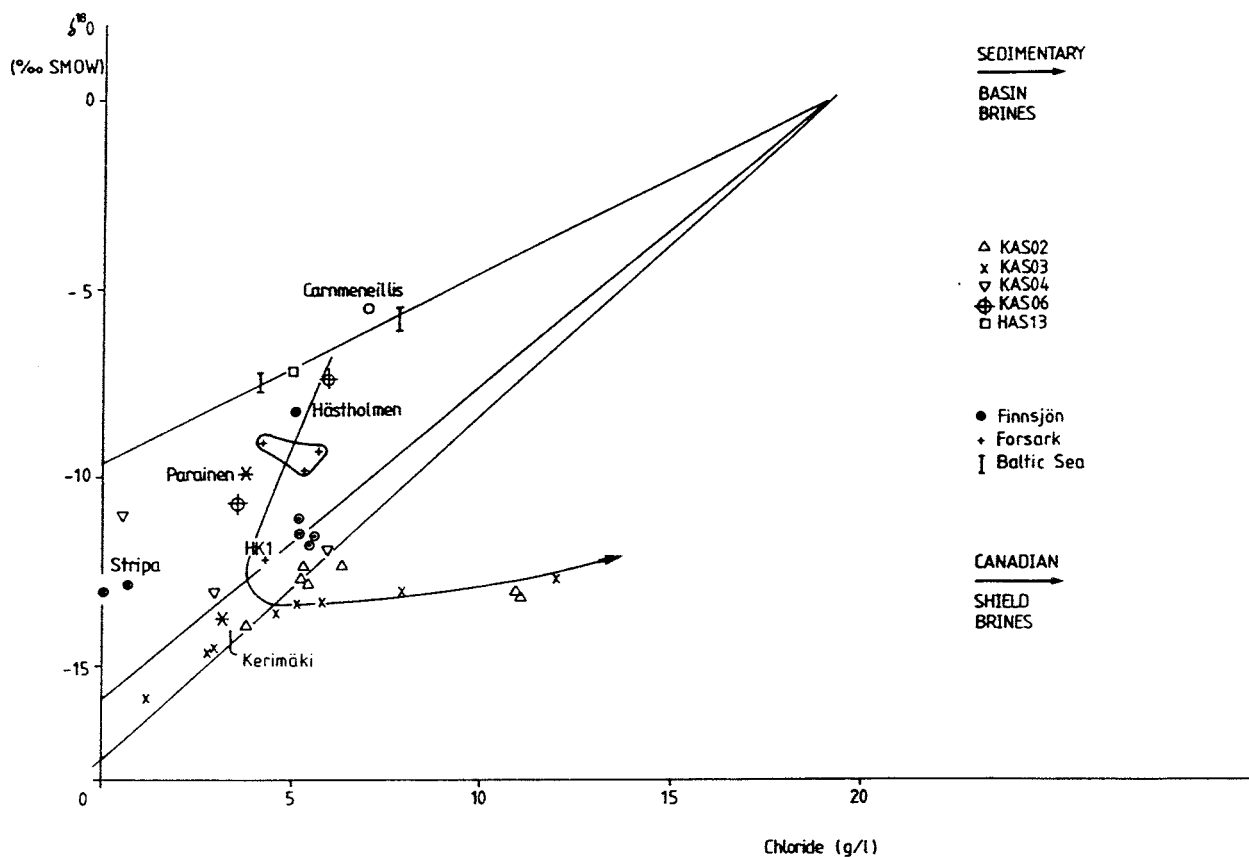
Figure 6.18. ^{18}O versus chloride plot for the Äspö groundwaters; other data from Fennoscandia are plotted for comparison. (Arrow represents groundwaters of increasing age and mixing evolution). (Modified after Smellie and Wikberg, 1991).

(standard world oceanic chloride content and reference for $\delta^{18}O$) through typical Baltic compositions to intersect the $\delta^{18}O$ axis at a chloride content of zero. This $\delta^{18}O$ value should therefore represent non-saline water which has been mixed with the more saline Baltic waters. The obtained intersection value of -9.6 (‰ SMOW) for $\delta^{18}O$ does in fact correlate closely with surface recharge water values for this part of Sweden (Saxena, 1984). With the obvious exception of Carnmenellis (no evidence of a marine component and only included for comparison), all data plot at or below this dilution line.

The Äspö data, however, plot at various positions in the diagram. Most of the KAS02 group, together with two samples from KAS04, of low to medium chloride content (<6 500 mg/L), plot together with the Finnsjön samples; the KAS03 group (<6 000 mg/L) plot slightly below, near to Kerimäki; the single HAS13 sample and one from KAS06 (<6 000 mg/L) plot very close to the Baltic compositions; the remaining three KAS06 samples and one KAS04 sample (<6 000 mg/L) plot between the Baltic and KAS02 groups, similar to Hästholmen and Parainen. A final group, the most saline groundwaters from Äspö (>11 000 mg/L), plot as a distinct anomaly; the KAS03 sample at 8 100 mg/L seems to provide a link with the high saline group, presumably through partial mixing.

In common with almost all the hydrogeochemical parameters investigated in this study, these groupings show a very complex mixing pattern for the Äspö groundwaters. For example, by drawing a line from 19 000 mg/L chloride through the KAS02 Äspö sample group, and including Finnsjön and also HK1 from Forsmark, an $\delta^{18}O$ intersection value of -15.9 (‰ SMOW) is obtained. This indicates that the non-saline water mixed with these saline samples has a much lower $\delta^{18}O$ content than modern day precipitation waters. If the KAS03 group is taken, then this shows an even lower $\delta^{18}O$ content. At the other extreme, there are the samples which have a similar $\delta^{18}O$ content to the Baltic water, and then samples which plot at intermediate positions. Finally there are the high saline waters which are clearly closer to a non-marine, very deep saline end member.

Smellie and Wikberg (1991) interpreted the plotted positions of Forsmark, Hästholmen and Finnsjön as indicating that the non-saline water component has mixed with the saline waters at different times, with Hästholmen and Forsmark being younger than Finnsjön, which conform with the radiocarbon data. Likewise, by comparing the Äspö groundwaters, KAS03 is somewhat older than KAS02, both are older than the Forsmark equivalent samples, and both HAS13 and KAS06 (389-406 m) represent more or less present-day Baltic Sea water. The position of the Carnmenellis waters conforms with the known fact that up to 65% of these waters are believed to be of recent origin. Although the radiocarbon data are incomplete, they support the fact that the KAS03 samples are clearly "older" (ca. 20 000-30 000 BP) than the KAS02 samples (+ KAS06; 304-377 m) which record "younger" apparent ages of ca. 12 000-13 000 BP.

The non-saline water which has mixed with the saline waters has been speculated (amongst others by Kankainen, 1986) as being derived from glacial melt resulting from the Weichselian ice sheet (Phase III some 20 000 BP ago), and subsequently has mixed with the bedrock saline waters of Yoldia-Litorina origin (introduced some 2 500-8 000 BP ago). These dilutions may account for the range of % modern carbon measured in saline groundwaters from these locations (Finnsjön: 19-40 %; Hästholmen: 13-24 %; Äspö:

2-23 %). Mixing may therefore be considered a slow continuous process involving Litorina-derived saline waters in the bedrock and percolating rain/glacial melt water over a long period of time.

These conclusions are generally in line with a recent review by Arad (1991) of some Swedish saline waters. He recognised three chemical end members, fresh, brackish and a Ca-chloride brine, and groundwater evolution followed a two step process in the evolution of the Äspö groundwaters: 1) interaction between shallow fresh water and brackish-marine composition, and 2) dilution of the deep Ca-Cl brine by brackish-marine composition. His conclusions were: a) fresh meteoric water (Ca-Na-HCO$_3$ type) overlies marine and/or altered marine waters, b) salinity stratification results from vertical flushing and dilution of saline water at depth, and c) saline deep waters may contain Ca-Cl brine as an end member. The Na/Cl ratios from 300-400 m downward is in the range of 0.38 to 0.52, accompanied by continuously decreasing Cl/Br ratio.

On the basis of the fissure calcite and groundwater isotopic signatures, Tullborg and Wallin (1991) have postulated three possible scenarios to explain the groundwater salinity at Äspö. These are: "a) overturning of a marine body and later meteoric water input due to the post glacial isostatic movements, b) seawater freezing brine formation as a source of the saline water (after Herut et al., 1990) and later input of meteoric water from above in connection with the post glacial isostatic movements, and c) meteoric water leaching of sediments and salts from nearby sediments due to a vertical as well as a lateral moving meteoric water".

Summary.

For the marine-dominated saline group groundwaters, the geochemical and stable isotopic signatures classify the groundwaters from Hästholmen and Forsmark (excluding HK1) as being coastal marine in origin (i.e. within the maximum extent of the Litorina sea transgressions) with minor modifications resulting from water/rock interactions. Apparent radiocarbon ages for these groundwaters range from 4 400-10 000 BP at Hästholmen (Kankainen, 1986) and from 12 000-15 000 BP at Forsmark. The Finnsjön area also lies below the highest postglacial Litorina Sea shoreline, but further inland. As a result the groundwaters, although still marine in origin, have been modified to a greater extent by water/rock interactions and possibly by other salt water sources (Smellie and Wikberg, 1991); apparent radiocarbon ages range from 9 000-15 000 BP in groundwaters recording below detection levels of tritium. Sample HK1 from Forsmark is anomalous in that isotopically it corresponds closely to the Finnsjön groundwaters. In addition, it is significantly older (ca. 23 000 BP) than the other Forsmark groundwaters. It is believed that HK1, which is artesian and therefore less influenced by contamination and/or natural mixing processes, originates from deeper levels and therefore represents an older and more evolved saline groundwater. In this respect the Finnsjön saline groundwaters should also be expected to be older than Hästholmen and Forsmark. That they are not, is believed to be due to carbon-14 dilution, either due to groundwater mixing during the Holocene, or/and artificially induced during the recent drilling and sampling activities.

With regard to the Äspö groundwaters (those characterised by a dominant marine signature), it is postulated that the majority of the waters to depths of 500 m are similar to

those of Finnsjön, with the possible exception of the KAS03 (130-250 m) waters from alongside zone EW-1, which are similar in age but have anomalously light stable isotope signatures. Younger waters, of greater marine signature and similar to Hästholmen and Forsmark, also occur, but are subordinate. The origin of the waters prior to the Weichselian glacial period of ca. 20 000 BP is unknown, but the salinity may have derived from many possible sources which include accumulated residual igneous/metamorphic fluids, limited fluid/rock interactions, fluid inclusions and other unknown saline sources. These saline waters were then modified by dilution and mixing with infiltrating rain/glacial melt waters prior to, during, and subsequent to the Weichselian ice sheet, and to the more recent Yoldia and Litorina Sea transgressions ca. 10 000 and 7 500 BP ago. Perhaps some seawater freezing has also contributed to increasing salinity during these glacial epochs. In any case, these processes have resulted in a continuous change of groundwater isotopic signatures such as $\delta^{18}O$ and percentage modern carbon. Following isostatic uplift and exposure of Äspö, the near-surface marine water was gradually replaced/flushed out by fresher water (at least within the hydraulically active fracture systems), mostly precipitation, together with some present Baltic Sea water component. The local hydraulic system characterising Äspö is an important control to this mixing and flushing, which are on-going processes occurring coevally with isostatic recovery in the Baltic Shield.

Non marine-derived saline water.

Meteoric-derived groundwaters at Äspö from low conductive bedrock environments or from discharging zones at depth, lack any significant marine signatures and have a general chemistry reflecting water/rock interaction in a near-stagnant environment. Recent mixing and dilution processes (within the last 10 000 BP) have not been a major influence on these groundwaters, unless they have been hydraulically transported upwards into a mixing environment. This is the case of Äspö where the interface between these discharging saline waters and the recharging shallower groundwaters lies around 400-600 m (see Section 6.5). It is believed that these Ca-rich saline waters orginate deep in the bedrock (>1000 m) and chemically represent the large-scale, sub-horizontal regional groundflow direction which is moving very slowly eastwards.

Most reported samples of saline groundwaters seem to represent mixtures of meteoric water with a highly concentrated brine (Pearson, 1987), which may be an ancient relict seawater or fluids genetically linked to geochemical processes occurring from rock/water interactions over long periods of geological time in the bedrock. To date, this description best describes the groundwater types found in much of the Fennoscandia Shield area peripheral to the Baltic Sea. Recently Herut et al. (1990) and Bein and Arad (1992) have forwarded the concept of seawater freezing to explain the Ca-rich brines common to both Canada and Fennoscandia. Laboratory experiments have been linked with field observations to show that by removing H_2O as ice in the primary glacial environment, subsurface brines may be obtained. Experiments show that a decrease in the Na/Cl ratio is caused by the crystallisation of mirabilite ($Na_2SO_4 \cdot 10H_2O$), supplemented by hydrohalite ($NaCl \cdot 2H_2O$); sulphate is removed both in mirabilite and by bacterial reduction (Herut et al., 1990). This freezing model does not by itself account for the high Ca/Mg ratios found in natural brines, as neither Ca or Mg are directly involved in the sequence of mineral precipitation during freezing. However, during migration into the subsurface bedrock

rock/water modifications take place which affect the Ca/Mg ratio but leave the Na/Cl ratio intact (Bein and Arad, 1992).

Bein and Arad (op. cit.) have applied the freezing model concept to groundwaters from the Fennoscandian Shield, including Äspö, and have advocated that this mechanism plays an important role. Whilst there appears to be general support that such a mechanism can occur, for example lake waters peripheral to glaciers in Antartica show compositions predicted by such a freezing model, there is more uncertainty regarding the extent of such a process. This uncertainty is reflected by the complexity of glacial hydraulics, both at the galcier/bedrock contact and in the bedrock subsurface, which can be influenced down to depths of at least one kilometre. Bein and Arad (op. cit.) propose that the saline waters produced from Baltic freezing will penetrate deep into the bedrock underlying, at that point in time, a considerable thickness of ice cover. At our present level of understanding in Fennoscandia, this is considered unlikely. On the other hand, it can be speculated that maximum penetration to the bedrock will occur whilst these saline waters are being produced by freezing, but will soon stop when the Baltic completely freezes, which is expected to occur quite quickly. When ice thicknesses increase, being fed from the NW and moving southeastwards, the critical melting point is exceeded at the glacier/bedrock interface resulting, eventually, in large volumes of glacial melt (and melted saline water) being continuously flushed out towards the glacier margins.

Until glacial hydraulics are known with greater confidence, the deep penetration of the saline waters (resulting from freezing) which is necessary to produce the Ca-rich brines through rock/water modification, is not at all certain to happen. It is perhaps more likely that concentrations of such freezing-derived waters are locally produced in small pockets on the Baltic seafloor, and only penetrate to a superficial extent into the bedrock before being flushed out, together with a large Baltic marine water component, during glacial melt and isostatic uplift. It is even more unlikely that such a mechanism can explain inland occurrences of such brines (which incidently also contain Na-rich varieties), as this would require a major change in hydraulic gradient towards the landmasses from the Baltic.

6.5. Conceptual groundwater flow model.

Figure 6.19. presents the Äspö hydraulic fracture conceptual model as presented by Wikberg et al. (1991). Figure 6.20 shows a NNW-SSE trending vertical profile (AB in Fig. 6.19) through the investigated site, showing the approximate positions of the major fracture zones which control the rate and direction of groundwater flow in the Äspö area. Indicated alongside the sampled borehole sections are points (denoted by arrows) of increased Cl concentration or dilution as derived from the two component mixing model. Figure 6.21. presents some conceptual ideas on groundwater flow illustrated along the vertical profile. The conceptual flow model is mainly based on borehole geochemical trends and detailed observations from individual borehole sections investigated in this report. Little detailed hydraulic data exist in the published literature on groundwater flow directions from the Äspö area apart from some restricted "regional" studies around Äspö (G. Gustafson et al., 1989) and some large-scale numerical modelling by Svensson (1991); discussions with I. Rhén (VBB VIAK) and E. Gustafsson (Geosigma AB) were therefore greatly appreciated.

Regionally, the Äspö area lies within a dominant WNW-ESE trending hydraulic gradient determined by the topography of the mainland, along a profile extending several kilometres to the WNW (Voss and Andersson, 1991). This regional groundwater flow gradient mainly accesses Äspö by two major EW-trending fracture or shear zones (EW-1 and NE-1) which extend westwards to the mainland. Other less important EW-trending fracture zones include NE-2, EW-3 and NE-3,4. Cross-cutting these fractures, and producing a grid-type fracture pattern, is a series of gently dipping discontinuous fractures (20-30°N) which comprise the EW-5/EW-X fracture zones. Located behind the constructed vertical profile are a series of vertical to subvertical NNW-SSE-trending fractures (Fig. 6.19).

Essentially, as this regional groundwater flow approaches Äspö, subsidiary flow directions are established up, down, around and through the fracture grid system, the local directions being determined by the hydraulic properties of the individual fractures, but with the dominant regional groundwater flow direction continuing eastwards. Because of the topography at Äspö, and assuming steady state and porous conditions, two water bodies exist superimposed on the deep regional groundwaters. These consist of a marine-derived water and a floating lens of fresh (to brackish) water, with a narrow dispersion zone at the interface. The thickness of the fresh water (presently approx. 50 m) is dependent on the topography and density variations in groundwater salinity. It has been calculated (Laaksoharju, 1990a) that an increase of 50 cm in groundwater level would produce an increase of 100 m in the thickness of the fresh water layer. In reality, however, conditions are not steady state and porous, but rather more dynamic and fracture controlled. As a result, the aerial extent and thickness of the fresh water layer is variable and greatly influenced by the local hydrology of the upper 100-150 m of bedrock.

Figure 6.21 illustrates a diagramatic representation of possible groundwater flow directions and a series of isohalines obtained from Cl values recorded from the sampled borehole sections. Four groundwater types have been selected; <1 000 mg/L, 1 000-5 000 mg/L), 5 000-10 000 mg/L and >10 000 mg/L Cl. It can be readily seen that a "fresh" or brackish water lens occupies most of the upper 50 m of the island, and that more saline waters (marine-derived) extend to some considerable depth, on average to 300-500 m, but extending further to around 400-500 m in zone EW-1.
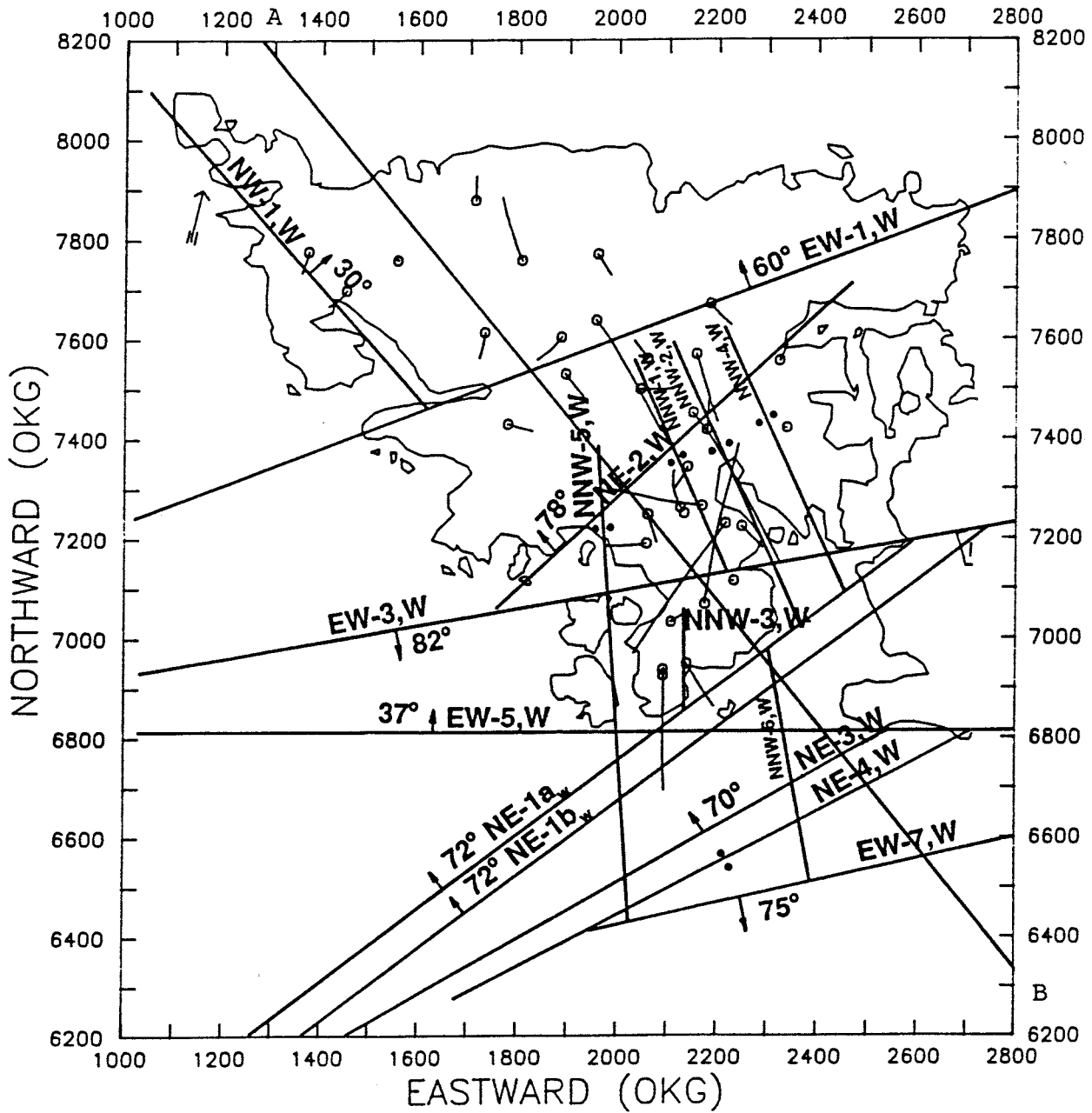
Figure 6.19. Conceptual model of water conducting fractures characterising Äspö.
(after Wikberg et al., 1991)
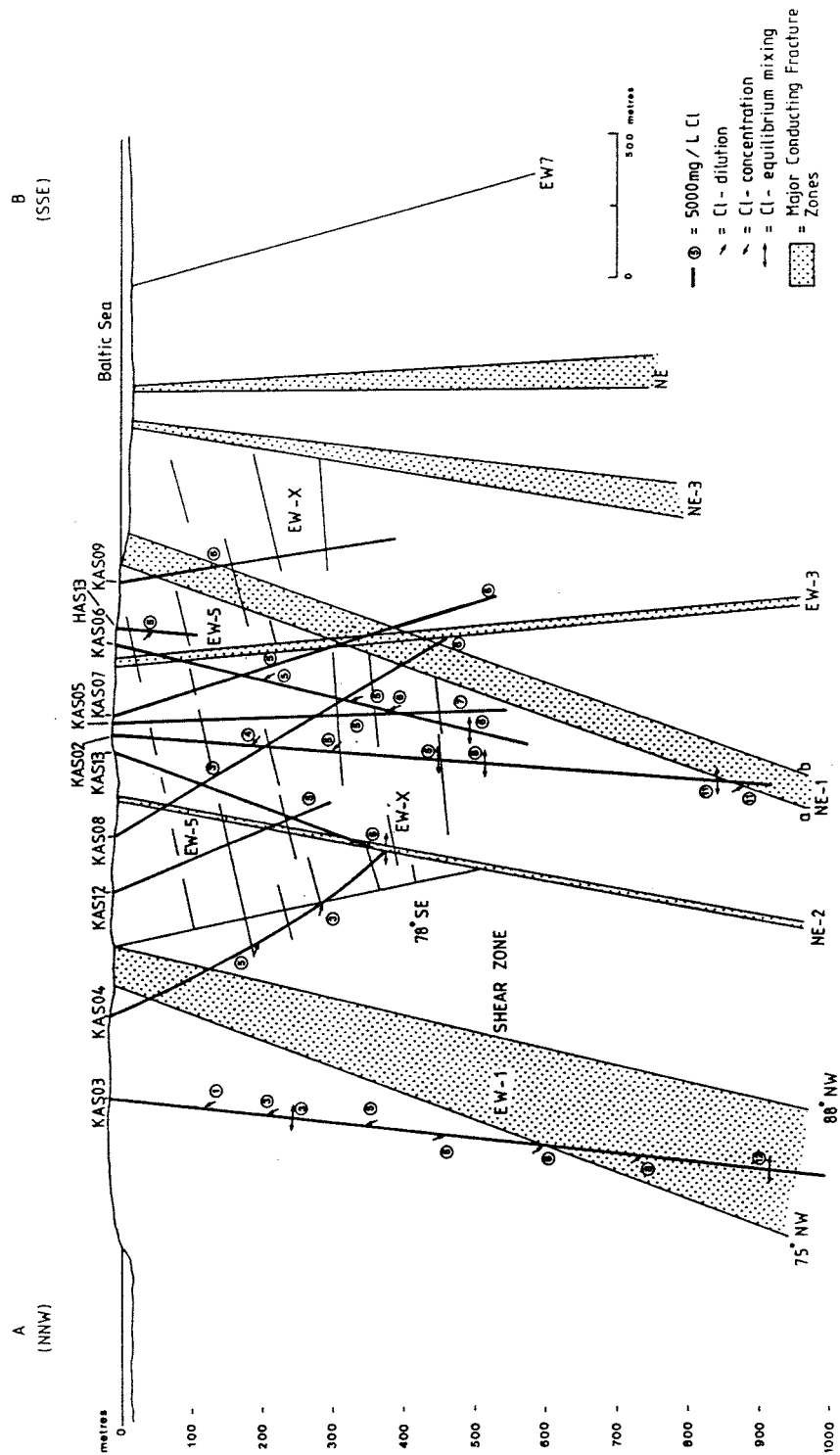
Figure 6.20. Vertical profile (AB in Fig. 6.19) through the Äspö area showing the points of increased Cl concentration or dilution (arrow directions) as determined from a simple two component groundwater mixing model. Also shown are the levels of salinity measured from the borehole sections.

Figure 6.21. Conceptual groundwater flow model for the Äspö area.
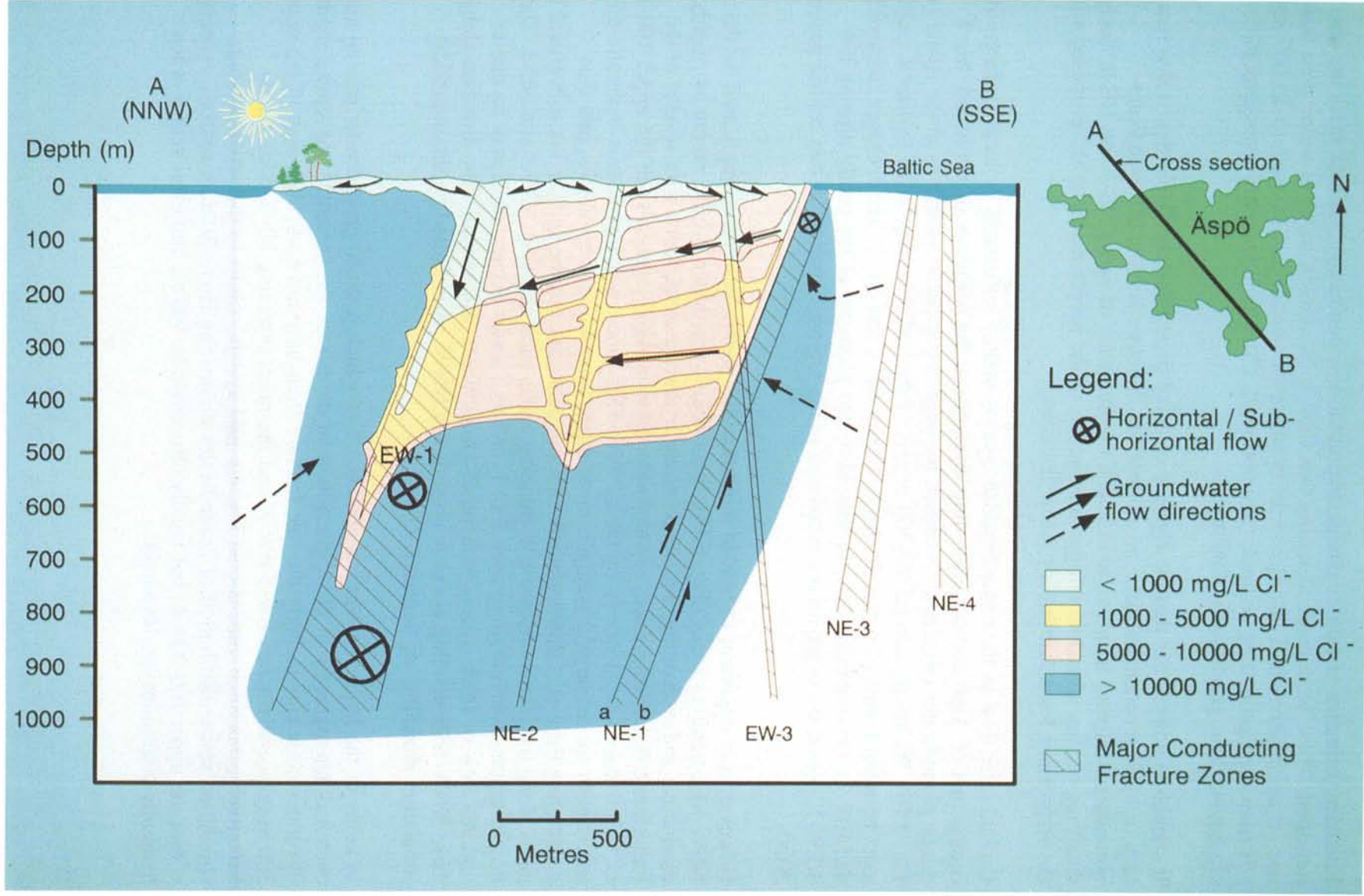
223

Educated estimates of salinity characterising the low conductive bedrock mass are also indicated. These were made assuming that some migration/diffusion of saline pore water has occurred since uplift in order to differentiate the central part of Äspö (5-10 000 mg/L Cl) from the surrounding bedrock (>10 000 mg/L Cl) which generally represents more closed, stagnant groundwater conditions.

It should be pointed out that the absence of detail underlying the Baltic Sea is due to a lack of hydrogeochemical data; no attempt has therefore been made to indicate groundwater mixing trends or to establish the influence of zones NE-3 and NE-4. Such data may become available during construction of the access tunnel to the proposed site of the Äspö Hard Rock Laboratory below the island.

Groundwater flow in the upper brackish layer is mainly influenced by local recharge in the central part of Äspö and corresponding discharge at the periphery of the island. More minor groundwater circulation is caused by small topographic variations in the island (see Fig. 4.7b). Within the central, 50-500 m part of the bedrock, large scale hydraulic gradients exist between points of major discharge (zones NE-1 and NE-2) and recharge (zones EW-1 and EW-3). Groundwater flow, facilitated by the geometry of the gently dipping EW-5/EW-X zones, therefore occurs transverse to the regional gradient in this central part of Äspö.

However, it is important to bear in mind that this pattern has been complicated by the NNW-SSE-trending zones (Fig. 6.19), lying behind the drawn profile, which are highly conductive and recharging, and show strong hydraulic connections with several of the important EW-trending zones. Groundwater flow in Äspö, especially in the upper 100-150 m, is influenced considerably by these NNW-SSE zones, which provide a hydraulic driving mechanism for recharging younger, more dilute waters to greater depths, and then discharging them (i.e. down-gradient in a regional scale) to the surface via subvertical flow paths along the interconnected EW-trending zones such as EW-1, EW-3 and NE-1. The deep dilution observed along zone EW-1, and to a lesser extent NE-2, may be due to regional flow of fresh "recent recharged" groundwater. The overall flow direction along these NNW-SSE trending zones is towards the NNW, as indicated by the numerical simulation modelling of Svensson (1991).

In terms of the hydrogeochemical studies, all of which point to groundwater mixing and chemical heterogeneity in the upper 500 m of the island, the presented conceptual model illustrates quite convincingly the role fracture frequency and hydraulics play in the upper 500 m (especially zones EW-5/EW-X and the interconnecting NNW-SSE zones). Effectively, this three dimensional fracture grid system results in the active mixing, circulation and redistribution of groundwater originating from different sources, especially within the upper 100-200 m, but locally also down to 400 m, and even deeper when hydraulic conditions are favourable.

6.6. Inorganic colloids, other related studies and gases.

Investigations of the quantity, chemical character and radionuclide binding properties of colloids, humic substances and bacteria in groundwaters, have been investigated at Äspö and other localities within the SKB radioactive waste research programme (Allard et al., 1991). An integral part of this programme has also been the sampling and analyses of dissolved gases. The description presented below concerns the present status of such studies related to all existing Swedish site studies excluding, at the moment, Äspö; these stuies are on-going and insufficient data are presently available for full evaluation. Reference to Äspö data is made when possible.

6.6.1. Colloids.

The GEOTAB database contains 305 observations of inorganic colloids collected from 22 deep (maximum 860 m) boreholes at 9 different study sites. At Äspö KAS02, KAS03, KAS04 and KAS06 have been sampled by using column filtering (50-450nm). The average values from those locations are expressed in ppb, and the average values from all the sites are given in parenthesis: Al= 6.0 (29.6), Si= 2.6 (4.4), Ca= 319 (133), S= 25.6 (14), Fe= 1.8 (214) and Mn= 0.6 (2.2) (Laaksoharju and Degueldre, 1992). At Äspö Al and Si are generally lower than at other locations indicating reduced drilling debris contamination. The Ca value, however, shows an increase, indicating possible calcite precipitation during sampling. The S content seems to be higher whilst Fe and Mn are lower than the average for other sites.

The filtered values of Swedish colloids have been classified as representing shallow and deep groundwater systems using multivariate statistics (Mardia et al., 1979). It was found that deep groundwaters with high Cl (>50 mg/L) contained different element concentrations, when compared to the shallow groundwaters with low Cl (<50 mg/L). The Ca content is generally higher in the deep systems, whereas the converse is true for concentrations of Al, Fe and Mn which are greater in the shallow systems. For S and Si the picture is more diffuse. Concentrations generally show an increase in the deep system despite some sporadic high values in the shallow groundwater (Laaksoharju and Degueldre, 1992).

For the colloid calculations the following correlation was used; Ca with calcite (calcium carbonate), Fe with goethite (iron hydroxide), S with troilite (iron sulphide), Si with quartz (silica oxide), Mn with pyrolusite (manganese oxide) and Al with pyrophyllite (clay mineral). The calculated median concentration in the deep and shallow systems is then 415 and 352 ppb respectively. If 89% of the observations have an increased calcium content due to sampling, and this effect is removed from the initial concentration, then the median particle concentration is 222 ppb. If the same type of correction is made for the shallow groundwater, then the Ca values are increased erroneously by 7 %. The median particle concentration in the shallow groundwater is then 249 ppb.

Increased concentrations can also be due to drilling debris and oxidation. A more thorough examination of the possible effects and corrected final concentrations are presently underway. Large colloids (> 30 μm) are assumed to consist mainly of clay minerals, iron hydroxides and manganese oxides. Small colloids (< 30 μm) seem to be mainly

represented by calcite, quartz and troilite (Laaksoharju and Degueldre, 1992). Direct colloid concentration calculations using the Äspö data have not yet been performed, but the element values seem to indicate a lower total concentration of around 100 ppb.

As might be exoected, the pump rate seems to be critical for some elements during colloid sampling. The effect of different pump rates on colloid concentration has recently been tested in Finland in collaboration with TVO; in particular, the effect of contamination from the drilling debris. The pump flow was adjusted to three levels; 0.5 L/min for 9 days, 1.5 L/min. for 12 days and 3.3 L/min. for 9 days. The Al and Si contents appeared to increase, especially at the beginning of each pumping period. The greatest Si content corresponded to the highest pump rate, while Al was greatest at the beginning of the second period. The other measured elements (S, Ca and Mn) are not affected by changes in the pump rate. The Fe-content increased towards the end of the second period, which indicated inflow of shallow water due to a hydraulic connection to a higher level in a nearby borehole (Laaksoharju et al., 1992).

6.6.2. Other Related Studies.

As a very brief up-date on recent activities involving colloids, organics and microbes, the following points are illustrated:

1) Laboratory sorption tests indicated sorption of Pm on silica colloids which was highly dependent on the colloid concentration; this resulted in K_d values ranging from 0.6 to 10 m^3/Kg with a decrease of 100 in colloid concentration. For Cs no such effect could be observed (Sätmark and Albinson, 1990).

2) Careful analyses of organic content in deep groundwaters show that only a small percentage consists of complex-forming humic and fulvic acids. The remainder consists partly of natural yet simple organic compounds and partly of contaminants such as organic "bleeding" from plastic material with low tendencies to form complexes. According to experience in isolating humic substances from deep groundwaters, concentrations are generally well below 0.1 mg/L (Allard et al., 1991).

3) The selected value for bacteria concentration in Swedish groundwater, which was used in a recent performance assessment analysis relating to the disposal of spent fuel (SKB-91), was 10^{-5} kg/m^3 (Pedersen, 1989; 1990).

4) The colloids collected from Poços de Caldas, Brazil, as part of a natural analogue study, were found to have taken up significant fractions of thorium and rare-earth elements and minor amounts of uranium. However, the particulate matter was demonstrated to be immobile and it was concluded that colloid transport was insignificant (Chapman et al., 1990).

6.6.3. Gases.

The gas contents in groundwaters at Äspö have been measured on a regular basis for: H_2, He, CO_2, N_2, CH_4 and CO. The average content consists of 31068 ppb N_2, 8103 ppb H_2, 2055 ppb He, 1124 ppb CO_2 and 40 ppb CH_4. The origin and source can vary. In some cases they may be a migration product from the mantle, and this may possibly concern He, CO_2, CO, CH_4 and H_2, although He is less certain as it can also result from natural radionuclide decay in the granite bedrock. Furthermore, it must be borne in mind that some of the above-mentioned gases can also be generated in the soil or be derived from atmospheric input (e.g. CO_2, N_2). Caution must therefore be employed before any far-reaching conclusions of potential gas accumulations can be assessed.

In Äspö the gas content is generally higher in the deeper waters than at shallower depths. The reason is believed to be two fold: 1) gases are generated in the deeper parts, and 2) deep waters can contain more gas because of higher hydraulic pressure. Carbon ($\delta^{13}C$) isotope analyses on calcite from fracture fillings show a heavy isotopic ratio which indicates a deep inorganic origin for the CH_4 gas (Tullborg and Wallin, 1991). The shallow waters at Äspö generally contain more CO_2 gas than deep water which is taken as an indication of soil input to produce the gas. Calcite weathering or TOC decay have also been discussed as possible sources. The general content of the gases in Äspö is generally low; in some cases contents increase due to atmospheric contamination during analyses (P. Wikberg pers. comm. 1991).

The low content for most of the gases, combined with a low reactivity for N_2 and He (probably also with radionuclides), make these gases less interesting as a possible radionuclide transport medium. The gases can break down rapidly in contact with catalysators, i.e. substances containing elements with different oxidation states, which radionuclides probably can form. The reactivity and mobility of a gas can then change (i.e. H_2 transforms to H_2O) and the radionuclide transport can then be delayed or inhibited.

7. Acknowledgements.

8. References.

Ahlbom, K., Andersson, P., Ekman, L., Gustafsson, E., Smellie, J. and Tullborg, E-L., 1986. Preliminary investigations of fracture zones in the Brändan area, Finnsjön study site. SKB Tech. Rep. (TR 86-05), Stockholm.

Allard, B., Arsenie, I., Borén, H., Ephraim, J., Gårdhammar, G., and Pettersson, C., 1990. Isolation and characterization of humics from natural waters. SKB Tech. Rep. (TR 90-27), Stockholm.

Allard, B. Karlsson, F. and Neretnieks I., 1991. Concentrations of particulate matter and humic substances in deep groundwaters and estimated effects on the adsorption and transport of radio nuclides. SKB Tech. Rep. (TR 91-50), Stockholm.

Almén, K-E. et al., 1986b. Site investigation equipment for geological, geophysical, hydrogeological and hydrochemical characterization. SKB Tech. Rep. (TR 86-16), Stockholm.

Almén, K-E. and Zellman, O., 1991. Äspö Hard Rock Laboratory. Field investigation methodology and instruments used in the pre-investigation phase, 1986-1990. SKB Tech. Rep. (TR 91-21), Stockholm.

Andersson, J-E., 1991. Evaluation of pumping test LPT-2 in KAS06 at Äspö. Geosigma AB Int. Rep., GRAP 91002.

Andrews, J.N. and Kay, R.L.F., 1983. The U-contents and $^{234}U/^{238}U$ activity ratios of dissolved uranium in groundwaters from some Triassic sandstones in England. Isotpe Geoscience, 1, 101-117.

Arad, A., 1991. Salinity origin of groundwater in 8 sites-Sweden. SKB Stat. Rep. (AR 91-09), Stockholm.

Axelsen, K., Wikberg, P., Andersson, L., Nederfelt, K- G., Lund, J., Sjöström, T. and Andersson, O., 1986. Equipment for deep groundwater characterisation: calibration and test run in Fjällveden. SKB Stat. Rep. (AR 86-14), Stockholm.

Barnwart, S., Laaksoharju, M., Nilsson, A-C, Tullborg, E-L. and Wallin, B., 1992. The large-scale redox experiment: Initial characterization of the fracture zone. SKB HRL Prog. Rep. (25-92-04), Stockholm.

Bein, A. and Arad, A. 1992. Saline groundwaters in the Baltic region: Diluted brines formed during glacial periods through freezing of seawater. Unpubl.

Bjarnason, B,. Klasson, H., Leijon, B., Strindell, L. and Öhman, T., 1989. Rock stress measurements in boreholes KAS02, KAS03 and KAS05 on Äspö. SKB HRL Prog. Rep. (25-89-17), Stockholm.

Blomqvist, R., Lahermo, P.W., Lahtinen, R. and Halonen, S., 1989. Geochemical profiles of deep groundwater in Precambrian bedrock in Finland. In: Proceedings of Exploration '87. Third Decennial International Conference on Geophysical and Geochemical Exploration for Minerals and Groundwater (Ed. G. Garland), Ontario Geol. Surv. Spec. Vol. 3, 746-757.

Bruno, J., Forsythe, R. and Werme, L., 1984. Spent UO_2-fuel dissolution: Tentative modelling of experimental apparent solubilities. In: Scientific Basis for Nuclear Waste Management VIII (eds. C.M. Jantzen, J.A. Stone, and R.C. Ewing). Boston.

Carlsten, S., 1989. Results from borehole radar measurements in KAS05, KAS06, KAS07 and KAS08 at Äspö - Interpretation of fracture zones by including radar measurements from KAS02 and KAS04. SGAB, Uppsala. SKB HRL Prog. Rep. (25-89-10), Stockholm.

Carlsten, S., 1990. Borehole radar measurements at Äspö. Boreholes KAS09, KAS10, KAS11, KAS12, KAS13 and KAS14 SGAB, Uppsala. SKB HRL Prog. Rep. (25-90-05).

Carlsten, S., Lindqvist, L. and Olsson, O., 1989. Comparison between radar data and geophysical, geological, and hydrological borehole parameters by multivariate analysis of data. SKB Tech. Rep. (TR 89-15), Stockholm.

Chapman, N. A., McKinley, I. G., Shea, M. E. and Smellie, J. A. T., 1990. The Pocos de Caldas Project: Summary and implications for radioactive waste management. SKB Tech. Rep. (TR 90-24), Stockholm, Nagra Tech. Rep. (NTB 90-33), Baden and UK DOE Tech. Rep. (WR 90-055), London.

Cosma, C., Heikkinen, P., Keskinen, J. and Kormonen, R., 1990. VSP-Survey including 3-D interpretation in Äspö, Sweden. Borehole KAS07. SKB HRL Prog. Rep. (25-90-07), Stockholm.

Craig, H., 1961. Isotope variations in meteoric waters. Science, 133, 1702-1703.

Edmunds, W.M., Andrews, J.N., Burgess, W.G., Kay, R.L.K and Lee, D.J., 1984. The evaluation of saline and thermal ground waters in the Carnmenellis granite. Mineral. Mag., 48(3), 407-424.

Ephraim, J., Mathuthu, A. and Marinsky, J., 1990. Complex forming properties of natural organic acids. Part 2. Complexes with iron and calcium. SKB Tech. Rep. (TR 90-28), Stockholm.

Eriksson, E. and Sehlstedt, S., 1991. Description of background data in the SKB database GEOTAB. Version 2. SKB Tech. Rep. (TR 91-06), Stockholm.

Eriksson, E., Johansson, B., Gerlach, M., Magnusson, S., Nilsson, A-C., Sehlstedt, S. and Stark, T., 1992. GEOTAB: Overview. SKB Tech. Rep. (TR 92-01), Stockholm.

Frape, S.K. and Fritz, P., 1987. Geochemical trends for groundwaters from the Canadian Shield. Geological Association of Canada Special Paper, 33, 19-38.

Fritz, P. and Frape, S.K., 1982. Saline ground waters in the Canadian Shield - a first overview. Chem. Geol., 36, 179-190

Garrels, R. M. and Christ, C. M., 1965. A chemical model for seawater at 25°C and one atmosphere total pressure. Am. J. Sci. 260, 57-66.

Gascoyne, M., Davidson, C.C., Ross, J.D. and Pearson, R., 1987. Saline groundwaters and brines in plutons in the Canadian shield. Geological Association of Canada Special Paper, 33, 53-68.

Gentzschein, B. and Andersson, J-E., 1988a. Transienta mellanhålstester i borrhål KAS02, Äspö. Fältdata och preliminär utvärdering (SGAB), IRAP 88295, Uppsala.

Gentzschein, B. and Andersson, J-E., 1988b. Transienta mellanhålstester i borrhål KAS03, Äspö. Fältdata och preliminär utvärdering (SGAB), IRAP 88277, Uppsala.

Giblin, A.M., Batts, B.D. and Swaine, D.J., 1981. Laboratory simulation studies of uranium mobility in natural waters. Geochim. Cosmochim. Acta, 45, 699-709.

Grenthe, I., Stumm, W., Laaksoharju, M., Nilsson, A-C. and Wikberg, P., 1992. Redox potentials and redox reactions in deep groundwater systems. Applied Geology (In press).

Grundfelt, B., Lindbom, B., Liedholm, M. and Rhen, I., 1990. Predictive groundwater flow modelling of a long time pumping test (LPT1) at Äspö. SKB HRL Prog. Rep. (25-90-04), Stockholm.

Gustafson, G., Liedholm, M., Lindbom, B. and Lundblad, K., 1989. Groundwater flow calculations on a regional scale at the Swedish Hard Rock Laboratory. SKB HRL Prog. Rep. (25-88-17), Stockholm.

Gustafsson, E., 1984. Beräkning av grundvattenflödet i en sprickzon med hjälp av utspädningsteknik, en metodstudie. KBS Stat. Rep. (AR 84-06), Stockholm.

Gustafsson, E., 1986. Bestämmning av grundvattenflödet med utspädningsteknik. Modifiering av utrustning och kompletterande fältmätningar. SKB Stat. Rep. (AR 86-21), Stockholm.

Gustafsson, E. and Andersson, P., 1989. Groundwater flow conditions in a low-angle fracture zone at Finnsjön, Sweden. SKB Tech. Rep. (TR 89-19), Stockholm.

Gustafsson, E. and Andersson, P., 1991. Groundwater flow conditions in a low-angle fracture zone at Finnsjön, Sweden. J. Hydrol. 126, 79-111.

Gustafsson, E., Andersson, P., Ittner, T. and Nordqvist, R., 1991. Large scale three dimensional tracer test at Äspö. Geosigma AB Int. Rep. (GRAP 91001), Uppsala.

Herut, B., Starinsky, A. Katz, A. and Bein, A., 1990. The role of seawater freezing in the formation of subsurface brines. Geochim. Cosmochim. Acta, 54, 13-21.

Hyyppä, J., 1984. Geochemistry of the ground waters of the bedrock on Hästholmen, Loviisa. Nucl. Waste Comm. Finn. Power Co., Rep. (YJT-84-05), Helsinki (in Finnish with English summary).

Ittner, T., Gustafsson, E., Andersson, P. and Eriksson, C-O., 1991. Groundwater flow measurements at Äspö with the dilution method. SKB HRL. Prog. Rep. (25-91-18), Stockholm.

Jarl, L-G. and Johansson, Å., 1988: U-Pb zircon ages of granitoids from the Småland-Värmland granite-porphyry belt, southern and central Sweden. GFF, 110, 21-28.

Kankainen, T., 1986. On the age and origin of groundwater from the rapakivi granite at the island of Hästholmen. Nucl. Waste Comm. Finn. Power Co. Rep. (YJT 86-29), Helsinki.

KBS-3, 1983. Final storage of spent nuclear fuel - KBS-3. SKBF/KBS, Stockholm (5 volumes).

Kornfält, K-A. and Wikman, H., 1987a. Description of the map of solid rocks around Simpevarp. SKB HRL Prog. Rep. (25-87-02), Stockholm.

Kornfält, K.-A. and Wikman, H., 1987b. Description to the map (No 4) of solid rocks of 3 small areas around Simpevarp. SKB HRL Prog. Rep. (25-87-02a), Stockholm.

Krauskopf, K.B., 1967. Intoduction to geochemistry, McGraw-Hill Book Co., New York, 721 p.

Laaksoharju, M., 1988. Shallow groundwater chemistry at Laxemar, Äspö and Ävrö. SKB HRL Prog. Rep. (25-88-04), Stockholm.

Laaksoharju, M. and Nilsson, A-C., 1989. Models of groundwater composition and of hydraulic conditions based on chemometrical and chemical analyses of deep groundwater at Äspö and Laxemar. SKB HRL Prog.Rep. (25-89-04), Stockholm.

Laaksoharju, M., 1990a. Measured and predicted groundwater chemistry at Äspö. SKB HRL Prog. Rep. (25-90-13), Stockholm.

Laaksoharju, M., 1990b. Colloidal particles in deep Swedish granitic groundwater. SKB Stat. Rep. (AR 90-37), Stockholm.

Laaksoharju, M. and Degueldre, C., 1992. Colloids from the Swedish granitic groundwater. SKB Tech. Rep. (In prep.), Stockholm.

Laaksoharju, M., Vuorinen, U., Allard, B. etc., 1992. Artifacts and measured colloid concentrations. TVO/SKB Tech. Rep. (In prep), Stockholm.

Langmuir, D. and Whittemore, 1971. Variation in the stability of precipitated ferric oxyhydroxides. Proc. Symo. Nonequilibrium Systems in Natural Water Chem. Editor J.D. Hem, Advances in Chemistry Series No. 106, American Chemical Society, Washington, D.C., 209-234.

Langmuir, D., 1978. Uranium solution-mineral equilibria at low temperatures. Geochim. Cosmochim. Acta, 42, 547-569.

Liedholm, M., 1989. Combined evaluation of geological, hydrogeological and geophysical information. SKB HRL Prog. Rep. (25-89-03), Stockholm.

Liedholm, M., 1990. General geological, hydrogeological and hydrochemical information. Technical notes 18-32. SKB HRL Prog. Rep. (25-90-16b), Stockholm.

Lindahl, H., 1989. Framtagning av översiktligt underlag för bedömning av förutsättningarna för grundvattenbildning i Äspö-området. SKB TPM (25-89-008), Stockholm.

Lindberg, R.D. and Runnels, D.D., 1984. Groundwater redox reactions: An analysis of equilibrium state applied on Eh measurements and geochemical modelling. Science, 225, 925- 927.

Mardia, K.V., Kent, J.T. and Bibby, J.M., 1979. Multivariate Analysis. Academic Press. 518p.

Marinsky, J., Reddy, M., Ephraim, J. and Mathuthu, A., 1988. Ion binding by humic and fulvic acids: a computational procedure based on functional site heterogeneity and the physical chemistry of polyelectrolyte solutions. SKB Tech. Rep. (TR 88-04), Stockholm.

McKinley, I.G., West, J.M. and Grogan, H.A., 1985. An analytical overview of the consequences of microbial activity in a Swiss Low/Intermediate-level waste repository. Nagra Tech. Rep. (NTB 85-45), Baden.

Miekeley, N., Coutinho de Jesus, Porto da Silveira, and Degueldre, C., 1991. Chemical and physical characterisation of suspended particles and colloids in waters from the Osamu Utsumi mine and Morro do Ferro analogue study sites, Poços de Caldas, Brazil. SKB Tech. Rep. (TR 90-18), Stockholm, Nagra Tech. Rep. (NTB 90-27), Baden and UK DOE Tech. Rep. (WR 90-49), London.

Nilsson, A-C., 1989. Chemical characterization of deep groundwater on Äspö 1989. SKB HRL Prog. Rep. (25-89-14), Stockholm.

Nilsson, A-C., 1991. Groundwater chemistry monitoring at Äspö during 1990. SKB HRL Prog. Rep. (25-91-04), Stockholm.

Nilsson, L., 1988. Hydraulic tests. Pumping tests at Laxemar. SKB HRL Prog. Rep. (25-87-11b), Stockholm.

Nilsson, L., 1989. Hydraulic tests at Äspö and Laxemar. Evaluation. SKB HRL Prog. Rep. (25- 88-14), Stockholm.

Nilsson, L., 1990. Hydraulic tests at Äspö KAS05-KAS08, HAS13-HAS17. Evaluation. SKB HRL Prog. Rep. (25-89-20), Stockholm.

Nisca, D., 1987. Aeromagnetic interpretation. SKB HRL Prog. Rep. (25-87-23), Stockholm.

Nisca, D., 1988. Geophysical laboratory measurements on core samples from Klx01, Laxemar and Kas02, Äspö. SKB HRL Prog. Rep. (25-88-06), Stockholm.

Niva, B. and Gabriel, G., 1988. Borehole radar measurements at Äspö and Laxemar - Boreholes Kas02, Kas03, Kas04, Klx01, Has02 and Hav07. SKB HRL Prog. Rep. (25-87-22), Stockholm.

Nordstrom, D.K. and Ball, J.W., 1984. Chemical models, computer programs and metal complexation in natural waters. In: Complexation of trace metals in natural waters (Eds. C.J.M. Kramer and J.C. Duinker); Martinus Nijhoff/Dr. J.W. Junk Publishers, 149-164.

Nordstrom, D.K., 1985. Editor: Hydrogeological and hydrogeochemical investigations in boreholes - Final report of the phase I geochemical investigations of the Stripa groundwaters. Stripa Project Tech. Rep. (TR 85-06), Stockholm.

Nordstrom, D.K., 1986. Hydrogeochemical interpretation of the groundwater at the Hästholmen site, Finland. Nucl. Waste Comm. Finn. Power Co. Rep. (YJT 86-32), Helsinki.

Nordstrom, D.K., 1989. Application of a cation exchange mass-balance model to the interpretation of saline groundwater chemistry evolved from Holocene seawater entrapped in rapakivi granite at Hästholmen, Finland. Proceedings of the 6th International Symposium on Water-rock Interaction, Malvern 1989.

Nurmi, P.A., Kukkonen, I.T. and Lahermo, P.W., 1988. Geochemistry and origin of saline ground waters in the Fennoscandian Shield. Appl. Geochem., 3: 185-203.

Ogilvi, N.A., 1958. An electrolytical method of determining the filtration velocity of underground waters (in Russian), Bull. Sci-Tech. Inf., 4 (16), Gosgeoltekhizdat, Moscow.

Parkhurst, D.L., Thorstenson, D.C. and Plummer, L.N., 1980, PHREEQE-A computer program for geochemical calculations: U.S. Geological Survey Water-Resources Investigation Report (80-96), 210p.

Pearson, F.J., 1987. Models of mineral controls on composition of saline groundwaters of the Canadian Shield. Geological Association of Canada Special Paper, 33, 39-52.

Pedersen, K., 1988. Preliminary investigations of deep ground water microbiology in Swedish granitic rock. SKB Tech. Rep. (TR 88-01), Stockholm.

Pedersen, K., 1989. Deep ground water microbiology in Swedish granitic rock and it's relevance for radionuclide migration from a Swedish high-level nuclear waste repository. SKB Tech. Rep. (TR 89-23), Stockholm.

Pedersen, K., 1990. Potential effects of bacteria on radionuclide transport from a Swedish high-level nuclear waste repository. SKB Tech. Rep. (TR 90-05), Stockholm.

Pedersen, K. and Albinsson Y., 1990. The effect from the number of cells, pH and lanthanide concentration on the sorption of promethium on gram negative bacterium. SKB Tech. Rep. (TR 90-26), Stockholm.

Pettersen, C., Ephraim, B., Allard, B. and Borén, H., 1990. Characterization of humic substances from deep groundwaters in granitic bedrock in Sweden. SKB Tech. Rep. (TR 90-29), Stockholm.

Plummer, L.N., Jones, B.F. and Truesdell, A.H., 1976, WATEQF-A FORTRAN IV version of WATEQ, a computer program for calcualting chemical equilibria of natural waters: U.S. Geological Survey Water Resources Investigations Report (76-13).

Plummer, L.N., Prestemon, E.C and Parkhurst, D.L., 1991. An interactive code (Netpath) for modeling Net geochemical reactions along a flow path. U.S. Geological Survey Water Resources Investigations Report (91-4078).

Pitkänen, P., Snellman, M., Leino-Forsman, H. and Front, K., 1992. Ground water chemistry and water-rock interaction at Olkiluoto. Nucl. Waste Comm. Finn. Power Co. Rep. (YJT 92-02), Helsinki.

Puigdomènech, I. and Nordström, D.K., 1987. Geochemical interpretation of ground waters from Finnsjön, Sweden. SKB Tech. Rep. (TR 87-15), Stockholm.

Puigdomènech, I. and Bruno, J., 1988. Modelling uranium solubilities in aqueous solutions: Validation of a thermodynamic data base for the EQ3/6 geochemical codes. SKB Tech. Rep. (TR 88-21), Stockholm.

Rhén, I., 1987 Compilation of geohydrological data. SKB HRL Prog. Rep. (25-87-10), Stockholm.

Rhén,I., 1988. Swedish Hardrock Laboratory transient interference tests on Äspö 1988. Evaluation. SKB, HRL Prog. Rep. (25-88-13), Stockholm.

Rhén, I., 1989. Transient interference tests on Äspö 1988. SKB HRL Prog. Rep. (25-88-13), Stockholm.

Rhén, I., Forsmark, T. and Nilsson, L., 1991. Hydraulic tests on Äspö, Bockholmen and Laxemar, 1990, in KAS09, KAS11-14, HAS18-20, KBH01-02 and KLX01. Evaluation. SKB HRL Prog. Rep. (25-91-01), Stockholm.

Saxena, R.K., 1984. Surface and ground water mixing and identification of local recharge-discharge zones from seasonal fluctuations of oxygen-18 in ground water in fissured rock. In: Proc. Hydrochemical Balances of Freshwater Systems. IAHS, September 1984, Uppsala, 150, 419-428.

Sehlstedt, S. and Triumf, C-A., 1988. Interpretation of geophysical logging data from KAS02 - KAS04 and HAS08 - HAS12 at Äspö and KLX01 at Laxemar. SKB HRL Prog. Rep. (25-88-15), Stockholm.

Sehlstedt, S. and Stråhle, A., 1989. Geological core mapping and geophysical bore hole logging in the bore holes KAS05 - KAS08 at Äspö. SKB HRL Prog. Rep. (25-89-09), Stockholm.

Sehlstedt, S., Stråhle, A. and Triumf, C-A., 1990. Geological core mapping and geophysical borehole logging in the boreholes KBH02, KAS09, KAS11 - KAS14 and HAS18 - HAS20 at Äspö. SKB HRL Prog. Rep. (25-90-06), Stockholm.

Smellie, J., Larsson, N-Å., Wikberg, P. and Carlsson, L., 1985. Hydrochemical investigations in crystalline bedrock in relation to existing hydraulic conditions. Experience from the SKB test-sites in Sweden. SKB Tech. Rep. (TR 85-11), Stockholm.

Smellie, J., Larsson, N-Å., Wikberg, P., Puigdomènech, I. and Tullborg, E-L., 1987. Hydrochemical investigations in crystalline bedrock in relation to existing hydraulic conditions: Klipperås test-site, Småland, Southern Sweden. SKB Tech. Rep (TR 87-21), Sweden.

Smellie, J.A.T.. and Wikberg, P., 1989. Hydrochemical investigations at Finnsjön, Sweden. J. Hydrol., 126, 129-158.

Smellie, J.A.T.. and Wikberg, P., 1991. Hydrochemical investigations at Finnsjön, Sweden. SKB Tech. Rep. (TR 89-19), Stockholm.

Smellie, J.A.T. and Laaksoharju, M., 1991. Hydrogeochemical investigations in relation to existing geologic and hydraulic conditions. SKB HRL Prog. Rep. (25-91-05), Stockholm.

Stanfors, R., 1988. SKB Hard Rock Laboratory. Geological borehole description KAS02, KAS03, KAS04, KLX01. SKB HRL Prog. Rep. (25-88-18), Stockholm.

Stråhle, A. 1988. Drillcore investigation in the Simpevarp area. Boreholes KAS02, KAS03, KAS04 and KLX01. SKB HRL Prog. Rep. (25-88-07), Stockholm.

Stråhle, A. 1989. Drill core investigation in the Äspö area, Oskarshamn, Sweden. SKB, Prog. Rep. (25-88-07), Stockholm.

Stråhle, A. and Fridh, B., 1989. Orientation of selected drillcore sections from the boreholes KAS05 and KAS06 Äspö, Sweden. A televiewer investigation in small diameter boreholes. SKB HRL Prog. Rep. (25-89-08), Stockholm.

Svensson, T., 1987. Hydrological conditions in the Simpevarp area. SKB HRL Prog. Rep. (25- 87-09), Stockholm.

Svensson, U., 1988. Numerical simulations of seawater intrusion in fractured porous media. SKB HRL Prog. Rep. (25-88-09), Stockholm.

Svensson, U. 1990a. The island of Äspö. Numerical calculations of natural and forced groundwater circulation. SKB Prog. Rep. (25-90-03), Stockholm.

Svensson, U., 1990b. Numerical prediction of tracer trajectories during a pumptest. SKB HRL Prog. Rep. (25-90-10), Stockholm.

Svensson, U., 1991. Groundwater flow at Äspö and changes due to excavation of the laboratory. SKB HRL Prog. Rep. (25-91-03), Stockholm.

Sätmark, B. and Albinsson, Y., 1990. Sorption of radionuclides on silica and granite colloids, and stability of colloids from natural occurring minerals. SKB Stat. Rep. (AR 90-20), Stockholm.

Talbot, C., Riad, L. and Munier, R., 1988. Structures and tectonic history of Äspö, SE Sweden. SKB HRL Prog. Rep. (25-88-05), Stockholm.

Tirén, S., Beckholmen, M. and Isaksson, H., 1987. Structural analysis of digital terrain models, Simpevarp area. Southeastern Sweden. Method study EBBA 11. SKB HRL Prog. Rep. (25-87-21), Stockholm.

Tirén, S. and Beckholm, M., 1987. Structural analysis of countoured maps. Äspö and Ävrö, Simpevarp area, Southeastern Sweden. SKB HRL Prog. Report (25-87-22), Stockholm.

Tullborg, E-L., 1988. Fracture fillings in the drillcores from Äspö and Laxemar. In: Wikman, H., Kornfält, K-A., Riad, L., Munier, R. and Tullborg, E-L., 1988. SKB Status Rep. (AR 88-11), Stockholm.

Tullborg, E-L., 1989. Fracture fillings in the drillcores KAS05-KAS08 from Äspö, Southeastern Sweden. SKB HRL Prog. Rep. (25-89-16), Stockholm.

Tullborg, E-L., Wallin, B. and Landström, O., 1990. Hydrochemical studies of fracture minerals from water conducting fractures and deep groundwaters at Äspö. SKB HRL Prog. Rep. (25-90-01), Stockholm.

Tullborg, E-L. and Wallin, B., 1991. Syable isotope studies of calcite fracture fillings ($\delta^{18}O$, $\delta^{13}C$) and groundwaters ($\delta^{18}O$, δD). SKB HRL Prog. Rep. (25-90-01), Stockholm.

Voss, C.I. and Andersson, J., 1991. Some aspects of regional flow of variable-density groundwater in crystalline basement rock of Sweden. Swedish Nuclear Power Inspectorate (SKI), Tech. Rep. (TR 91-9), Stockholm.

Vuorinen, U., 1987. A review on colloidal systems in general and in respect of nuclear disposal. TVO Tech. Rep. (YJT 87-06), Helsinki.

Wallin, B., 1990. Carbon, oxygen and sulfur isotope signatures for groundwater classification at Laxemar, SE Sweden. SKB HRL Prog. Rep. (25-90-12), Stockholm.

Wallin, B., 1992. Sulphur and oxygen isotope evidence from dissolved sulphates in groundwater and sulphide sulphur in fissure fillings at Äspö, southeastern Sweden. SKB HRL Prog. Rep. (25-92-08), Stockholm.

Wikberg, P., 1987. The chemistry of deep groundwaters in crystalline rocks. Ph.D. Thesis: Department Inorganic Chemistry, KTH, Stockholm.

Wikberg, P., Axelsen, K. and Fredlund, F., 1987. Deep groundwater chemistry. SKB Tech. Rep. (TR 87-07), Stockholm.

Wikberg, P., Gustafson, G., Rhén, I. and Stanfors, R., 1991. Äspö Hard Rock Laboratory. Evaluation and conceptual modelling based on the pre-investigations 1986-1990. SKB Tech. Rep. (TR 91-22), Stockholm.

Wikberg, P., 1992. Laboratory Eh simulations in relation to the redox conditions in natural granitic groundwaters. Presented at a Workshop on Sorption Processes, Interlaken (October, 1991).

Wikman, H., Kornfält, K-A., Riad, L., Munier, R. and Tullborg, E-L., 1988. Detailed investigation of the drillcores KAS02, KAS03 and KAS04 on Äspö island and KLX01 at Laxemar. SKB HRL Prog. Rep. (25-88-11), Stockholm.

Wikström, A., 1984. A possible relationship between augen gneisses and postorogenic granites in SE Sweden. J. Struct. Geol., 6, 409-415.

Wikström, A. and Aaro, S., 1986. The Finspång augen gneiss massif - geology, geophysics and relationship to postorogenic granites. SGU Series C. 813.

Wikström, A., 1989. General geological-tectonic study of the Simpevarp area with special attention to the Äspö island. SKB HRL Prog. Rep. (25-89-06), Stockholm.

Wold, S., 1987. Principal component analyses. Chemometric and Intelligent Laboratory Systems, 2, 35-37.

APPENDIX 1

Multivariant analysis: outline of approach used in this study.

Appendix 1.

Multivariant Analyses.

Multivariate analyses (MV) are used to identify or model the character of analytical data; the strength of this approach is that several or all variables in a data matrix can be examined simultaneously. The character of the data in a general data matrix is therefore more easily identified than using univariate analysis, where only one variable is compared at a time (Wold, 1987). With multivariate analysis, data can be explored, minimised, structured, classified and correlated. This technique is especially designed for evaluation and interpretation.

MV deals with Objects (samples) described by Variables (chemical quantities), and searches to establish the relationship between objects, between variables, and between objects and variables.

Objects can be:	equal	Variables can be:	equal
	similar		similar
	dissimilar		dissimilar
	proportional		proportional
	mixtures		linear comb

MV attempts to address the following: that objects 1, 2 and 3 are equal or similar, that objects 4 and 5 are equal or similar, but dissimilar from objects 1, 2 and 3. These objects can be assigned to various categories and this is accomodated by using classification analyses. Linear or complex relationships are possible between one variable and some other variables, or between some variables and some other variables; these relationships are expressed by a Correlation analysis. The variables need not all to be of the same type, for example, variables Cl, Na, Ca, K are continuous variables, water flow is a discrete variable and the sampling method and rock type are considered discrete variables.

Initial modelling using multivariant analysis concentrated on classifying or categorising the groundwaters by simplifying the available Äspö analytical data. The questions posed were: a) which are the most useful chemical variables?, b) which variables are insignificant?, c) can the groundwaters be correctly/realistically classified?, d) can unknown categories of groundwater chemistry be predicted? (Mardia et al. 1979) and e) can the method be used for quality control of the samples? During the modelling of Äspö the following MV-techniques were found to be useful:

Scaling Transformation.

Information derived from comparing variables measured using different techniques can be problematical. To overcome this, various scaling transformation methods whereby each variable is allocated a unit variance, thus eliminating the arbitrary choice of scale.

Principal Component Analyses.

The resolution of some variables can also be different (because of different measuring techniques) or the importance of some variables can be greater than others. It may be necessary, therefore, to evaluate them differently and to search for linear combinations (weighted sum) which is in some sense optimal. If all the objects fall into one group, then Principal Component Analysis and Factor Analysis are two techniques which can help to answer such questions.

Instead of just using the overall mean, that is a linear combination, principal component analyses seek out the original variables which have maximal variance. More generally, principal component analysis seeks linear combinations which can be used to summarise the data, losing in the process as little information as possible. This attempt to reduce dimensionality can be described as "parsimonious summarisation" of the data. Water information, for example, can then be summarised by using, say , two linear combinations. If it is possible, the dimensionality would be reduced from p=5 to p=2. The percentage loss of information can also be detected by rejecting different variables. An adequate number of components to explain 90% of the total variation should be used.

One problem is that principal components are not scale-invariant. This means that problems can be caused by using the depth, which is expressed in metres, and comparing this with chemical data. However, some scaling techniques are available even for this eventuality.

The reduction of dimensions afforded by principal component analyses can be used graphically. Thus, if the first two components, say Cl and HCO_3, explain "most" of the variance, then a scatter diagram showing the distribution of the objects on these two dimensions will often give a fair indication of the overall distribution of the data.

Factor Analyses.

Factor analysis is a mathematical model which attempts to explain the correlation between a large set of variables in terms of a small number of underlying factors. A major assumption of factor analysis is that it is not possible to observe these factors directly; the variables depend upon the factors but are also subject to random errors.

In this study, principal factor analysis were used together with a second method maximum likelihood factor analysis. Principal factor analysis is closely related to principal component analysis. Both methods attempt to explain a set of data in a smaller number of dimensions (p) than initially.

First, principal component analysis is merely a transformation of the data. No assumptions are made about the nature of the covariance matrix from which the data come from, i.e. a well-defined model. If this premise is not met, then factor analysis may give spurious results. Second, in principal component analyses the emphasis is on a transformation from the observed variables to principal components, whereas in factor analysis the emphasis is on a transformation from the underlying factors to the observed variables. Of course, the principal component transformation is invertible, and if it is decided to retain the first k components, then x can be approximated by these components. Thus, if the factor model holds and if the specific variances are small, principal component analysis and factor analysis would be expected to give similar results.

Maximum likelihood factor analysis is used when the data are assumed to be normally distributed, and enables a significance test to be made about the validity of the k-factor model. Factor analysis (unlike principal component analysis) is unaffected by a re-scaling of the variables.

Canonical Correlation.

In some cases the objects can fall into more then one group or classes. In such situations it may be required to investigate the use of linear combinations within each group separately. The idea of taking linear combinations is an important one in multivariate analysis, and this leads to the method known as canonical correlation analysis.

Canonical correlation analysis involves partitioning a collection of variables into two sets, an x-set and a y-set. The objective is to find linear combinations and the largest possible correlation. Such linear combinations can give insight into the relationship between two sets of variables.

Canonical correlation analysis has certain maximal properties similar to those of principal component analysis. However, whereas principal component analysis considers relationships within a set of variables, the focus of canonical correlation is on the relationship between two groups of variables.

On way to view canonical correlation analysis is an extension of multiple regression. Canonical correlation analysis can also be applied to qualitative data which is especially useful when data are a mixture of qualitative and quantitative characteristics. The qualitative data can be represented by dummy zero-one values.

Discriminant Analyses.

If new objects are examined and analysed, discriminate analyses can show which category it belongs to. If no categorisation has been made, the population can be subdivided into groups using cluster analysis.

Discriminant analyses consider population or groups of data. The objective of this analysis is to allocate a new individual to one or several groups of data on the basis of its measured values. Of course it is desirable to make as few "mistakes" as possible in this classification. There are two cases:

1)   Discrimination when populations are known. This situation occurs when the samples are large enough (all the Swedish groundwaters).

2)   Discrimination during estimation. This situation often occurs when data are new and limited; subsequently, the classification may be changed. In this analysis the probabilities of a classification failure are indicated.

Some of the variables can be discarded during this analysis according to the following rule: "As the number of variables increase, then information carried by any one variable, not carried by the other variables, tends to decrease".

Multivariate Control Charts.

Multivariate quality control operations can handle slight simultaneous shifts in several variables, which may not attract attention unless all variables are considered together. The MV Control Charts procedure allows you to construct control charts for multivariate samples in which different measurements can be correlated. The procedure is based on Hotelling's T-squared and assumes that the data come from a multivariate normal distribution. Essentially, the procedure transforms the original correlated variables into new variables that are independent and then constructs a single statistic based on the new variables. The system then plots the multivariate observations on a single control chart with an upper limit; observations beyond the limit are not considered.

The Used Computer Codes.

Parvus (Forina, 1988), consisting of 50 small programs written in Basic, are relatively easy to learn and use with a well written manual. The program comes with the source code so that changes or applications can therefore be made. Sophisticated statistical analyses, such as discriminant, factor and principal component analyses, are included.

STATGRAFICS (1991) version 5.0 from STSC is a menu-driven software package that integrates data transformation and generation capabilities, a wide variety of uni

and multivariate statistical and mathematical analyses, and high-resolution colour graphics.

<u>References.</u>

Mardia, K.V., Kent J.T. and Bibby J.M., 1979. Multivariate Analysis. Academic press.
518 p.

Forina, M., Leardi, R. and Lanteri, S., 1988. PARVUS, an extendable package of programs for data exploration, classification and correlation. Elsevier Scientific Software. Amsterdam. 260 p.

Statgrafics (1991). Software for statistical mathematical modelling. STSC, Inc.

APPENDIX 2

Drilling operations: chemical analyses of Äspö groundwaters.

Borehole	KAS05	KAS05	KAS05	KAS05
Section (m)	155-388	387-550	387-550	387-550
Sample no	1	1	2	3
Sampling method	SDD	SDD	SDD	SDD
Date Collected	890203	890228	890228	890228
Drilling water %	39.80	38.40	33.40	28.40
Cond. mS/m	1460	1680	1724	1804
Density g/ml	-	1.0041	1.0045	1.0049
pH	6.9	6.7	6.6	6.4
Alkalinity (mg/l HCO_3)	29	33	28	15

Element	mg/l			
Na	1525	2000	2000	2080
K	12.5	15.2	14.2	13.5
Ca	1380	1800	1880	1980
Mg	55	60	55	44
Cl	5400	6080	6330	6680
SO_4	270	445	490	535
SiO_2-Si	3.3	3.0	3.1	2.9

Borehole	KAS06	KAS06	KAS06	KAS06	KAS06	KAS06	KAS06	KAS06	KAS06	KAS06
Section (m)	106-217	106-217	217-317	217-317	319-396	319-396	396-505	396-505	505-602	505-602
Sample no	1	2	1	2	1	2	1	2	1	2
Sampling method	SDD	SDD	SDD	SDD	SDD	SDD	SDD	SDD	SDD	SDD
Date Collected	890107	890107	890111	890111	890114	890114	890125	890125	890202	890202
Drilling water %	5.96	31.60	33.90	25.00	1.73	0.93	1.38	0.77	13.28	8.40
Cond. mS/m	1484	1476	1430	1390	1464	1484	1708	1700	1560	1710
Density g/ml	1.0028	1.0028	1.0028	1.0027	1.0030	1.0032	1.0044	1.0043	1.0033	1.0041
pH	7.5	7.4	7.6	7.6	7.3	7.1	7.4	7.4	7.4	7.2
Alkalinity(mg/l HCO_3)	98	87	74	61	53	44	55	55	83	48

Element					mg/l					
Na	1850	1778	1650	1570	1600	1740	2175	2190	2000	2100
K	33.0	34.0	26.0	21.0	11.0	9.3	14.0	11.0	23.0	17.0
Ca	1040	1022	1200	1220	1480	1430	1525	1523	1390	1720
Mg	205	213	133	115	78	70	157	158	163	100
Cl	5600	5410	5150	5000	5400	5410	6300	6300	5800	6300
SO_4	153	152	155	130	234	240	440	440	285	450
SiO_2-Si	3.3	2.5	3.9	3.6	5.3	5.4	5.3	5.6	3.2	3.7

Borehole	KAS07	KAS07	KAS07	KAS07	KAS07	KAS07	KAS07	KAS07
Section (m)	106-212	106-212	212-304	212-304	372-604	372-604	462-604	462-604
Sample no	1	2	1	2	1	2	1	2
Sampling method	SDD	SDD	SDD	SDD	SDD	SDD	SDD	SDD
Date Collected	890106	890106	890110	890110	890219	890219	890219	890219
Drilling water %	6.12	22.60	54.20	8.76	38.00	41.40	36.60	43.80
Cond. mS/m	413	390	480	975	2280	2290	2550	2350
Density g/ml	0.9981	0.9980	0.9985	1.0008	1.0077	1.0076	1.0088	1.0078
pH	7.9	8.0	8.0	7.6	7.2	7.0	6.9	7.0
Alkalinity (mg/l HCO_3)	237	231	212	78	12	11	13	14

Element	mg/l							
Na	540	460	580	1055	2590	2500	2700	2550
K	5.7	8.2	9.1	10.3	12.1	11.2	12.7	13.4
Ca	289	244	328	868	2825	2820	3206	2860
Mg	19	20	33	57	70	100	45	75
Cl	1160	1100	1450	3220	8700	8700	9560	8950
SO_4	120	136	137	125	510	505	500	500
SiO_2-Si	5.4	3.6	3.7	4.2	1.9	2.3	1.1	1.9

APPENDIX 3

Monitoring operations: chemical analyses of Äspö groundwaters

Borehole	KAS05	KAS05	KAS05	KAS05	KAS05	KAS05
Section (m)	320-380	320-380	320-380	440-549	440-549	440-549
Sample no	1659	1675	1684	1660	1674	1685
Sampling method	MONIT.	MONIT.	MONIT.	MONIT.	MONIT.	MONIT.
Date Collected	900530	900606	900613	900530	900606	900613
W.flow ml/m	250	290	290	290	290	300
Drilling water %	29.00	22.00	2.40	20.00	7.70	2.00
Cond.mS/m	-	1550	1530	-	1970	1930
pH	7.3	7.3	7.4	7.1	7.4	7.5
Alkalinity (mg/l HCO_3)	24.1	23.8	21.2	14.0	12.0	10.8
Charge Balance %	-2.33	-2.11	-2.20	-2.33	-1.72	-3.25

Element		mg/l			mg/l	
Na	1730	1700	1700	2240	2250	2180
K	-	8.0	8.2	-	11.4	10.7
Ca	1430	1410	1400	1950	1960	1900
Mg	51.7	54.6	55.5	40.5	41.0	41.4
Sr	24.9	24.5	24.0	33.6	33.5	32.5
Mn	0.41	0.42	0.40	0.30	0.27	0.25
Li	0.87	0.86	0.81	1.22	1.20	1.17
Fe(tot)	0.80	0.49	0.37	0.4	0.19	0.15
Cl	5350	5270	5270	6950	6900	6900
F	1.6	1.6	1.5	1.9	1.7	1.8
S(ICP)	116.00	110.00	108.00	191.00	195.00	195.00
SO_4^{2-} (calc)	348	330	324	573	585	585
SiO_2-Si	3.8	4.1	4.1	2.8	3.4	3.3

Borehole	KAS07	KAS07	KAS07	KAS07	KAS07	KAS07
Section (m)	191-290	191-290	191-290	191-290	191-290	191-290
Sample no	1639	1642	1648	1654	1673	1690
Sampling method	MONIT.	MONIT.	MONIT.	MONIT.	MONIT.	MONIT.
Date Collected	900503	900509	900514	900528	900606	900613
w.flow ml/m	290	230	250	240	250	240
Drilling water %	0.18	0.16	0.17	0.22	0.24	0.08
Cond. mS/m	-	-	-	-	1420	1460
Density g/ml	-	-	-	-	-	-
pH	7.8	8.0	7.9	7.8	7.5	7.4
Alkalinity (mg/l HCO_3)	251.0	129.0	120.0	108.0	97.4	83.0
Charge Balance %	-2.22	-2.24	-2.54	-2.17	-1.18	-2.69

Element				mg/l		
Na	1370	1590	1600	1600	1570	1570
K	-	-	8.5	-	8.6	8.2
Ca	1020	1220	1250	1260	1220	1240
Mg	73.0	98.0	92.0	89.0	85.0	85.0
Sr	17.5	20.4	21.1	21.7	20.7	21.3
Mn	0.49	0.63	0.73	0.69	0.76	0.79
Li	0.5	0.54	0.55	0.59	0.58	0.60
Fe(tot)	<0.005	0.11	0.06	-	0.9	0.41
Cl	4150	4940	5030	4990	4760	4950
F	1.1	1.3	1.4	1.8	1.5	1.5
S(ICP)	15.3	54.00	58.00	62.00	67.00	70.50
SO_4^{2-} (calc)	46	162	174	186	201	212
SiO_2-Si	2.0	3.2	3.4	4.0	4.1	4.4

Borehole	KAS07	KAS07	KAS07	KAS07	KAS07	KAS07
Section (m)	501-604	501-604	501-604	501-604	501-604	501-604
Sample no	1638	1641	1649	1655	1672	1689
Sampling method	MONIT.	MONIT.	MONIT.	MONIT.	MONIT.	MONIT.
Date Collected	900503	900509	900514	900528	900606	900613
W.flow ml/m	300	270	300	300	290	340
Drilling water %	0.23	0.18	0.20	0.20	0.34	0.11
Cond. mS/m	-	-	-	-	1740	1690
Density g/ml	-	-	-	-	-	-
pH	7.8	8.0	7.8	7.8	7.2	7.3
Alkalinity (mg/l HCO_3)	24.0	22.0	26.0	23.8	22.0	18.3
Charge Balance %	-2.49	-2.82	-2.53	-2.58	-1.59	-2.98

Element				mg/l		
Na	1950	1940 (1928)	1950	1980	1980	1940
K	-	10.6 (10.2)	10.4	-	10.3	9.5
Ca	1600	1620 (1770)	1600	1610	1620	1580
Mg	59.0	58.0 (55.6)	59.0	59.1	60.2	58.7
Sr	27.2	28.1 (30.2)	27.7	28.2	28.0	27.7
Mn	0.19	0.22 (0.20)	0.28	0.26	0.35	0.35
Li	0.98	1.03 (1.20)	1.01	1.03	1.02	1.03
Fe(tot)	0.74	0.58 (0.51)	0.41	-	0.54	0.42
Cl	6060	6100	6060	6110	6010	6040
F	1.9	1.8	1.8	1.7	1.7	1.6
S(ICP)	118.00	133.00 (135.4	125.00	132.00	135.00	137.00
SO_4^{2-}(calc)	354	399	375	396	405	411
SiO_2-Si	2.7	2.9 (2.6)	2.6	2.8	3.7	4.1

Borehole	KAS08	KAS08	KAS08	KAS08	KAS08	KAS08
Section (m)	140-200	140-200	140-200	503-601	503-601	503-601
Sample no	1663	1670	1683	1664	1671	1682
Sampling method	MONIT.	MONIT.	MONIT.	MONIT.	MONIT.	MONIT.
Date Collected	900530	900606	900613	900530	900606	900530
W.flow ml/m	310	320	330	300	310	310
Drilling water %	5.40	9.00	5.40	9.00	5.00	2.10
Cond. mS/m	-	990	997	-	1770	1770
Density g/ml	-	-	-	-	-	-
pH	7.7	7.4	7.5	7.2	7.2	7.3
Alkalinity (mg/l HCO_3)	164	82.0	77.5	37.5	49.4	52.5
Charge Balance %	-1.11	-1.75	-2.70	-2.19	-1.35	-2.28

Element		mg/l			mg/l	
Na	930	1130	1140	2140	2200	2160
K	7.90	7.60	7.20	-	13.2	12.1
Ca	496	711	730	1400	1390	1350
Mg	49.3	60.8	63.1	146	160	163
Sr	8.5	11.8	11.8	22.9	21.6	21.1
Mn	0.25	0.46	0.47	0.78	0.87	0.90
Li	0.21	0.26	0.27	0.60	0.55	0.55
Fe(tot)	0.05	0.72	0.65	1.32	1.32	1.27
Cl	2380	3160	3280	6160	6170	6160
F	1.4	1.4	1.5	1.6	1.7	1.7
S(ICP)	21.2	44.00	46.00	142.00	144.00	144.00
SO_4^{2-}(calc)	64	132	138	426	432	432
SiO_2-Si	4.6	3.5	3.3	4.6	5.0	4.8

Borehole	KAS09	KAS09	KAS09
Section (m)	116-150	116-150	116-150
Sample no	1662	1665	1686
Sampling method	MONIT.	MONIT.	MONIT.
Date Collected	90530	900606	900613
W.flow ml/m	410	370	390
Drilling water %	0.28	0.05	0.10
Cond. mS/m	-	1660	1620
Density g/ml	-	-	-
pH	7.2	7.2	7.2
Alkalinity (mg/l HCO_3)	270	270	269
Charge Balance %	-2.24	-2.66	-3.77

Element		mg/l	
Na	2350	2330 (2200)	2250
K	-	40.0	45.3
Ca	730	730 (686)	700
Mg	251	250 (233)	250
Sr	11.6	11.6 (11.3)	11.2
Mn	1.80	1.80(1.48)	1.71
Li	0.28	0.29(0.30)	0.27
Fe(tot)	3.41	2.88(2.60)	2.74
Cl	5680	5690	5680
F	1.6	1.6	1.5
S(ICP)	34.00	36.20(33.50	35.10
SO_4^{2-}(calc)	102	109 (100)	105
SiO_2-Si	4.3	5.2 (4.4)	4.0

Borehole	KAS12	KAS12	KAS12	
Section (m)	279-330	279-330	279-330	
Sample no	1658	1668	1680	
Sampling method	MONIT.	MONIT.	MONIT.	
Date Collected	900530	900606	900613	
W.flow ml/m	310	300	320	
Drilling water %	0.34	0.22	0.19	
Cond. mS/m	-	1570	-	
Density g/ml	-	-	-	
pH	7.7	7.4	7.4	
Alkalinity (mg/l HCO_3)	37.2	45.6	46.7	
Charge Balance %	-1.8	-2.14	-2.18	

Element		mg/l		
Na	1860	1840	1840	(1860)
K	-	-	10.5	(10.3)
Ca	1310	1310	1310	(1320)
Mg	110	113	116	(115)
Sr	22.3	21.8	21.6	(22.8)
Mn	0.71	0.80	0.81	(0.72)
Li	0.46	0.50	0.50	(0.57)
Fe(tot)	0.26	0.73	0.67	(0.69)
Cl	5480	5480	5500	
F	1.8	1.7	1.6	
S(ICP)	100.00	105.00	106.40	(99.30)
SO_4^{2-}(calc)	300	315	319	(298)
SiO_2-Si	2.9	4.1	3.6	(3.8)

List of SKB reports

Annual Reports

1977-78
TR 121
KBS Technical Reports 1 – 120
Summaries
Stockholm, May 1979

1979
TR 79-28
The KBS Annual Report 1979
KBS Technical Reports 79-01 – 79-27
Summaries
Stockholm, March 1980

1980
TR 80-26
The KBS Annual Report 1980
KBS Technical Reports 80-01 – 80-25
Summaries
Stockholm, March 1981

1981
TR 81-17
The KBS Annual Report 1981
KBS Technical Reports 81-01 – 81-16
Summaries
Stockholm, April 1982

1982
TR 82-28
The KBS Annual Report 1982
KBS Technical Reports 82-01 – 82-27
Summaries
Stockholm, July 1983

1983
TR 83-77
The KBS Annual Report 1983
KBS Technical Reports 83-01 – 83-76
Summaries
Stockholm, June 1984

1984
TR 85-01
Annual Research and Development Report 1984
Including Summaries of Technical Reports Issued during 1984. (Technical Reports 84-01 – 84-19)
Stockholm, June 1985

1985
TR 85-20
Annual Research and Development Report 1985
Including Summaries of Technical Reports Issued during 1985. (Technical Reports 85-01 – 85-19)
Stockholm, May 1986

1986
TR 86-31
SKB Annual Report 1986
Including Summaries of Technical Reports Issued during 1986
Stockholm, May 1987

1987
TR 87-33
SKB Annual Report 1987
Including Summaries of Technical Reports Issued during 1987
Stockholm, May 1988

1988
TR 88-32
SKB Annual Report 1988
Including Summaries of Technical Reports Issued during 1988
Stockholm, May 1989

1989
TR 89-40
SKB Annual Report 1989
Including Summaries of Technical Reports Issued during 1989
Stockholm, May 1990

1990
TR 90-46
SKB Annual Report 1990
Including Summaries of Technical Reports Issued during 1990
Stockholm, May 1991

1991
TR 91-64
SKB Annual Report 1991
Including Summaries of Technical Reports Issued during 1991
Stockholm, April 1992

Technical Reports
List of SKB Technical Reports 1992

TR 92-01
GEOTAB. Overview
Ebbe Eriksson[1], Bertil Johansson[2],
Margareta Gerlach[3], Stefan Magnusson[2],
Ann-Chatrin Nilsson[4], Stefan Sehlstedt[3],
Tomas Stark[1]
[1]SGAB, [2]ERGODATA AB, [3]MRM Konsult AB
[4]KTH
January 1992

TR 92-02
Sternö study site. Scope of activities and main results
Kaj Ahlbom[1], Jan-Erik Andersson[2], Rune Nordqvist[2], Christer Ljunggren[3], Sven Tirén[2], Clifford Voss[4]
[1]Conterra AB, [2]Geosigma AB, [3]Renco AB, [4]U.S. Geological Survey
January 1992

TR 92-03
Numerical groundwater flow calculations at the Finnsjön study site – extended regional area
Björn Lindbom, Anders Boghammar
Kemakta Consultants Co, Stockholm
March 1992

TR 92-04
Low temperature creep of copper intended for nuclear waste containers
P J Henderson, J-O Österberg, B Ivarsson
Swedish Institute for Metals Research, Stockholm
March 1992

TR 92-05
Boyancy flow in fractured rock with a salt gradient in the groundwater – An initital study
Johan Claesson
Department of Building Physics, Lund University, Sweden
February 1992

TR 92-06
Characterization of nearfield rock – A basis for comparison of repository concepts
Roland Pusch, Harald Hökmark
Clay Technology AB and Lund University of Technology
December 1991

TR 92-07
Discrete fracture modelling of the Finnsjön rock mass: Phase 2
J E Geier, C-L Axelsson, L Hässler, A Benabderrahmane
Golden Geosystem AB, Uppsala, Sweden
April 1992

TR 92-08
Statistical inference and comparison of stochastic models for the hydraulic conductivity at the Finnsjön site
Sven Norman
Starprog AB
April 1992

TR 92-09
Description of the transport mechanisms and pathways in the far field of a KBS-3 type repository
Mark Elert[1], Ivars Neretnieks[2], Nils Kjellbert[3], Anders Ström[3]
[1]Kemakta Konsult AB
[2]Royal Institute of Technology
[3]Swedish Nuclear Fuel and Waste Management Co
April 1992

TR 92-10
Description of groundwater chemical data in the SKB database GEOTAB prior to 1990
Sif Laurent[1], Stefan Magnusson[2], Ann-Chatrin Nilsson[3]
[1]IVL, Stockholm
[2]Ergodata AB, Göteborg
[3]Dept. of Inorg. Chemistry, KTH, Stockholm
April 1992

TR 92-11
Numerical groundwter flow calculations at the Finnsjön study site – the influence of the regional gradient
Björn Lindbom, Anders Boghammar
Kemakta Consultants Co., Stockholm, Sweden
April 1992

TR 92-12
HYDRASTAR – a code for stochastic simulation of groundwater flow
Sven Norman
Abraxas Konsult
May 1992

TR 92-13
Radionuclide solubilities to be used in SKB 91
Jordi Bruno[1], Patrik Sellin[2]
[1]MBT, Barcelona Spain
[2]SKB, Stockholm, Sweden
June 1992

TR 92-14
Numerical calculations on heterogeneity of groundwater flow
Sven Follin
Department of Land and Water Resources, Royal Institute of Technology
June 1992

TR 92-15
Kamlunge study site.
Scope of activities and main results
Kaj Ahlbom[1], Jan-Erik Andersson[2],
Peter Andersson[2], Thomas Ittner[2],
Christer Ljunggren[3], Sven Tirén[2]
[1]Conterra AB
[2]Geosigma AB
[3]Renco AB
May 1992

TR 92-16
Equipment for deployment of canisters
with spent nuclear fuel and bentonite
buffer in horisontal holes
Vesa Henttonen, Miko Suikki
JP-Engineering Oy, Raisio, Finland
June 1992

TR 92-17
The implication of fractal dimension in
hydrogeology and rock mechanics
Version 1.1
W Dershowitz[1], K Redus[1], P Wallmann[1],
P LaPointe[1], C-L Axelsson[2]
[1]Golder Associates Inc., Seattle, Washington, USA
[2]Golder Associates Geosystem AB, Uppsala,
Sweden
February 1992

TR 92-18
Stochastic continuum simulation of
mass arrival using a synthetic data set.
The effect of hard and soft conditioning
Kung Chen Shan[1], Wen Xian Huan[1], Vladimir
Cvetkovic[1], Anders Winberg[2]
[1] Royal Institute of Technology, Stockholm
[2] Conterra AB, Gothenburg
June 1992

TR 92-19
Partitioning and transmutation.
A review of the current state of the art
Mats Skålberg, Jan-Olov Liljenzin
Department of Nuclear Chemistry,
Chalmers University of Technology
October 1992

TR 92-20
SKB 91
Final disposal of spent nuclear fuel.
Importance of the bedrock for safety
SKB
May 1992

TR 92-21
The Protogine Zone.
Geology and mobility during the last
1.5 Ga
Per-Gunnar Andréasson, Agnes Rodhe
September 1992

TR 92-22
Klipperås study site.
Scope of activities and main results
Kaj Ahlbom[1], Jan-Erik Andersson[2],
Peter Andersson[2], Tomas Ittner[2],
Christer Ljunggren[3], Sven Tirén[2]
[1]Conterra AB
[2]Geosigma AB
[3]Renco AB
September 1992

TR 92-23
Bedrock stability in Southeastern
Sweden. Evidence from fracturing in
the Ordovician limestones of Northern
Öland
Alan Geoffrey Milnes[1], David G Gee[2]
[1]Geological and Environmental Assessments
(GEA), Zürich, Switzerland
[2]Geologiska Institutionen, Lund, Sweden
September 1992

TR 92-24
Plan 92
Costs for management of the
radioactive waste from nuclear power
production
Swedish Nuclear Fuel and Waste Management Co
June 1992

TR 92-25
Gabbro as a host rock for a nuclear
waste repository
Kaj Ahlbom[1], Bengt Leijon[1], Magnus Liedholm[2],
John Smellie[1]
[1]Conterra AB
[2]VBB VIAK
September 1992

TR 92-26
Copper canisters for nuclear high level
waste disposal. Corrosion aspects
Lars Werme, Patrik Sellin, Nils Kjellbert
Swedish Nuclear Fuel and Waste Management
Co, Stockholm, Sweden
October 1992

TR 92-27
Thermo-mechanical FE-analysis of butt-welding of a Cu-Fe canister for spent nuclear fuel

B L Josefson[1], L Karlsson[2], L-E Lindgren[2],
M Jonsson[2]
[1]Chalmers University of Technology, Göteborg,
Sweden
[2]Division of Computer Aided Design, Luleå
University of Technology, Luleå, Sweden
October 1992

TR 92-28
A rock mechanics study of Fracture Zone 2 at the Finnsjön site

Bengt Lijon[1], Christer Ljunggren[2]
[1]Conterra AB
[2]Renco AB
January 1992

TR 92-29
Release calculations in a repository of the very long tunnel type

L Romero, L Moreno, I Neretnieks
Department of Chemical Engineering,
Royal Institute of Technology, Stockholm, Sweden
November 1992

TR 92-30
Interaction between rock, bentonite buffer and canister. FEM calculations of some mechanical effects on the canister in different disposal concepts

Lennart Börgesson
Clay Technology AB, Lund Sweden
July 1992